An Effective-One-Body Description of Spinning Binaries

Dissertation

zur

Erlangung der naturwissenschaftlichen Doktorwürde

(Dr. sc. nat.)

vorgelegt der

Mathematisch-naturwissenschaftlichen Fakultät

der

Universität Zürich

von

Simone Balmelli

von

Paradiso TI

Promotionskomitee

Prof. Dr. Philippe Jetzer (Vorsitz und Leitung)
Prof. Dr. Gino Isidori
Dr. Alessandro Nagar

Zürich, 2016

To my grandfather Luigi.
In the first memory that I have of him, we were both walking through the woods near home, the rain pouring down softly.
In the last memory, I had just begun the course in General Relativity, and his eyes were shining, full of curiosity.

Summary

Gravitational waves are retardation effects in the geometry of spacetime, that were firstly predicted by Einstein in 1918. Although almost hundred years are passed since then, no direct detection of gravitational waves has been accomplished yet. Their interaction with matter is very weak, and spacetime is deformed by an almost infinitesimal fraction under the passage of a gravitational wave. Nevertheless, thanks to recent advances in interferometry techniques, a first direct detection is expected to occur soon. Interferometric ground-based detectors are currently looking for the brightest sources of gravitational waves in the sky, among which are coalescing black hole (or neutron star) binaries. Future detectors (such as the space-born eLISA) will be able to observe, for instance, the merger of supermassive black hole at cosmological distances, thus opening an entire new window to astronomy. Gravitational wave detection would also provide the first tests of General Relativity in the strong-field regime, allowing for example a direct probe of the Kerr metric.

In order to extract signal from noise, and to allow parameter estimation of the sources, it is necessary to provide a very accurate theoretical modeling of the waveforms, which in turns requires an excellent description of the general relativistic two-body dynamics. In Chapter 2, we expose some basic features of the Arnowitt-Deser-Misner formalism, a method allowing to cast Einstein's equation into a canonical form. In particular, we discuss some aspects of the canonical description of spin, and give then an overview of the center-of-mass reduced, post-Newtonian expanded Hamiltonian in ADM coordinates at 3.5PN accuracy and up to quadratic order in the spins.

In Chapter 3, we introduce the effective-one-body (EOB) approach, the currently only existing semi-analytical method being able to accurately describe the complete waveform emitted by a coalescing process. We focus the attention onto the conservative sector, and discuss how the Hamiltonian in ADM coordinates can be reformulated into an EOB model.

The author's own scientific contribution begins with Chapter 4, where an inclusion of next-to-leading order (NLO) spin-spin effects into an EOB Hamiltonian is proposed, however only for the special case of aligned spins and equatorial orbits. In Chapter 5, the model is generalized to arbitrarily oriented, precessing spins. Remarkably enough, the number of coefficient being necessary to reproduce the NLO spin-spin coupling shrinks down from 25 (in the ADM case) to 12 (in the EOB). The EOB Hamiltonian of chapters 4 and 5 is however a rather complicated function of the momenta.

A new, improved model is proposed in Chapter 6. This EOB that has a much simpler momentum dependency than the previous EOB Hamiltonian, and encodes the whole NLO spin-spin coupling into only 9 independent coefficients. This Hamiltonian is the main result of the thesis.

Finally, in Chapter 8 we also apply the EOB model (endowed with a description of tidal effects, as discussed Chapter 7) to study the merger of neutron star binaries, and use it to derive some quasi-universal properties that may be useful to constrain the equation of state of nuclear matter. The results are confirmed by Numerical Relativity simulations.

Zusammenfassung

Gravitationswellen sind Retardierungseffekte in der Raumzeit, die von Einstein in 1918 vorhergesagt wurden. Obwohl fast 100 Jahre seit damals vergangen sind, ist bis jetzt noch keine direkte Messung von Gravitationswellen durchgeführt worden. Die Wechselwirkung mit der Materie ist nämlich sehr schwach, und die Krümmung in der Raumzeit, die einer Gravitationswelle entspricht, ist winzig. Heutzutage, dank bedeutender technischer Fortschritte in der Interferometerie, ist eine erste Detektion in Kürze zu erwarten. Die existierenden Detektoren sind auf der Suche nach den stärksten Quellen von Gravitationswellen im All, und insbesondere nach Systemen, die aus zweier rotierenden, zusammenstossenden Schwarzen Löcher oder Neutronensterne bestehen. Zukünftliche Detektoren (wie die geplante Satellitenmission eLISA) werden in der Lage sein, superschwere Schwarze Löcher in kosmologischen Abstände zu beobachten, was einer Revolutionierung der Astronomie entsprechen würde. Mit einer Detektion von Gravitationswellen würde auch erstmals möglich sein, die Vorhersagen der Allgemeinen Relativitätstheorie unter extremen Gravitationsfeldern zu überprüfen.

Um das Signal einer Gravitationswelle aus dem Rauschen herausziehen zu können, wird eine sehr genaue theoretische Modellierung der Wellenform benötigt. Dies impliziert, dass eine präzise Beschreibung des Zweikörperproblems in der Allgemeinen Relativitätstheorie von grosser Wichtigkeit ist. Im Kapitel 2 werden die Grundlagen des Arnowitt-Deser-Misner Formalismus beschrieben, der erlaubt, die Einstein-Hilbert Aktion in kanonische Form zu bringen. Die kanonische Formulierung des Spins in der ADM Theorie wird hier sorgfältig behandelt. Am Schluss werden explizite Resultate für die Hamiltonfunktion in der post-Newton'schen (PN) expandierten Form gesammelt, bis zur 3.5PN Ordnung und bis zur quadratischen Kopplung in den Spins.

Vergangene Studien haben gezeigt, dass der "effective-one-body approach" der beste Formalismus anbietet, um Ergebnisse aus der PN Theorie auf das Zweikörperproblem anzuwenden. Heutzutage ist die EOB die einzige semianalytische Methode, welche die ganze Wellenform aus dem relativistischen Zusammenstoss zweier Körper beschreiben kann. Im Kapitel 3 wird das EOB Formalismus eingeführt, und insbesondere wird diskutiert, wie eine EOB Hamiltonfunktion aus einer Hamiltonfunktion in ADM Koordinaten konstruiert werden kann.

Die eigene wissenschaftliche Arbeit des Authors wird ab Kapitel 4 behandelt. Hier wird eine Inklusion der "next-to-leading" Ordnung (NLO) Spin-Spin Kopplung in eine EOB Hamiltonfunktion vorgeschlagen, für den Spezialfall von parallelen Spins und äquatorialer Orbits. Eine Verallgemeinerung dieses Verfahren zu beliebigen Spinorientierungen ist im Kapitel 5 zu finden. Eine bemerkenswerte Eigenschaft ist die Tatsache, dass die 25, die NLO Spin-Spin ADM Hamiltonfunktion definierenden Koeffizienten nur auf 12 EOB Koeffizienten reduziert werden. Das Ergebnis ist aber ein EOB Modell, welches eine komplizierte Abhängigkeit von den Impulsvariablen enthält.

Dieses Modell wird im Kapitel 6 verbessert. Die neue EOB Hamiltonfunktion ist eine viel einfachere Funktion der Impulsvariablen, und ausserdem beschreibt die ganze NLO Spin-Spin Kopplung mittels 9 unabhängigen Koeffizienten (statt 12 wie in der vorherigen Version). Diese Hamiltonfunktion ist das Hauptergebnis der Dissertation.

Am Schluss wird eine Anwendung der EOB Methode auf Neutronensterne diskutiert. Die EOB

wird benüzt, um quasiuniverselle Eigenschaften der Verschmelzung zweier Neutronensternen herzuleiten, die für das Studium der Zustandsgleichung der Kernmaterie hilfreich sein können. Diese Erfindungen wurden durch numerische Simulationen bestätigt.

Acknowledgements

I would like to thank, first of all, all people involved with the University of Zürich who have contributed, more or less directly, to this thesis.

My supervisor Philippe Jetzer has provided me with the opportunity of writing this thesis. To him I owe the initial, fundamental input of directing my study onto the effective-one-body approach. During the four years spent by me at the University of Zürich, he has always been open for scientific discussions, and ready to give advice when needed. I especially appreciated the trust he has always put on his own students, which contributed to create a very positive atmosphere in our research group.

I also would like to thank Gian Michele Graf, my Master Thesis supervisor at the ETHZ, who helped me to establish a contact with Thibault Damour, and with the IHÉS in general; and Prasenjit Saha, for having transmitted to me, thanks to his vast knowledge, a lot of fascination for astrophysics.

I also thank Esther Meier and Regina Schmid, who are very kind and positive persons, always ready to give help.

I furthermore thank all of my past and present colleagues. Starting from the very beginning, the office colleagues Andreas Bleuler, Sebastian Elser and Aurel Schneider supported my early months at the University, offering me coffee, and helping me to understand the UNIX basics, by which I was really scared at that time. Yannick Boetzel, Ruxandra Bondarescu, Flavio Lanfranconi, Andrew Lundgren, Sergey Mirzoyan, Rizwana Kausar, have all been (group and/or office) colleagues with whom I enjoyed the stay at the university.

Furthermore, I would like to thank Rafael Küng, Lionel Philippoz and Andreas Schärer for the very nice company during the second half of my PhD, and especially during some conferences abroad. They contributed to make our research group a great place, where the relationships could definitely go beyond the formal level between working colleagues.

A very special thank goes to Davide Fiacconi, Cédric Huwyler, Mario Lubini and Crescenzo Tortora for having been very important reference points during my PhD. They provided me advice under many aspects of my research, allowing me to develop skills and enlarge my knowledge. But, most of all, they are friends with whom I shared some of the best moments.

From the scientific point of view, no other place has been relevant for my thesis as the *Institut des Hautes Études Scientifiques* (IHÉS) in Bures-sur-Yvette. The IHÉS has provided the alpha and omega for my work. The effective-one-body approach has been invented, and mostly developed there, together with the half of the scientific results that are collected in this thesis. Alessandro Nagar has been responsible for my first invitation at the IHÉS. To him I owe my profound gratitude. He has been the main reference person at the IHÉS; he made me truly aware of being engaged in a research activity of great interest, and made me involved in a side project, together with Sebastiano Bernuzzi, that led to a publication on Physical Review Letters. His deep knowledge of both numerical and analytical aspects of General Relativity makes him a very admirable researcher to my view.

My staying at the IHÉS has been an outsdanding experience under many points of view. Among the persons which contributed to make it a great time, there are Donato Bini, who I met at the IHÉS several times, and with whom I had interesting discussions during the breaks; and Enno Harms, with whom I

shared the condition of being a PhD student in visit at the IHÉS. I also received precious inputs from the already mentioned Sebastiano Bernuzzi, although I never had the possibility to meet him personally;

If the IHÉS has been fundamental for my work, this is due to no other person than Thibault Damour, the inventor of the EOB approach. I first met him, during the second year of my thesis, at the ETH Zürich, where he was invited to give a talk. Before that meeting, I was concerned with all possible doubts about my own work; in the time span of a few minutes, Damour got the point of my work, explained me what was wrong (and what was "horrible"), and at the same time gave me the key to resolve the problem. This conversation gave the right input to the development of my research, that I could take on, since then, with much more confidence. Later on, at the IHÉS, I had the possibility of collaborating closer with Damour, and of appreciating his outstanding knowledge of General Relativity and of theoretical physics in general, as well as his crystal clear way of reasoning. His contribution to the development of my own scientific methodology has been huge.

I would also like to thank some people which are not connected with the institutions where I conducted my research, and in particular, friends and family.

With my friends Marwan Kilani, Alberto Paganini and Claudio Sibilia, I often had the opportunity for discussing and exchanging ideas. Furthermore, there is one person whose positioning in these acknowledgements is in principle not well defined. This is Lorenzo de Vittori, who has been a friend and school colleague since our first year in the high school, and with whom I even shared the office during these four years of PhD. After thirteen years of studying and working together, our professional careers separate now. I think that this is the right moment to wish him all the best for the future.

Finally, I would like to express my deepest thanks to my family; to my grandmother Ester, who has always transmitted to me positivity and joy for life. To my parents Ermes e Katia, who do not only provided me with the opportunity of studying. They supported all choices I made, and have been a clear and solid reference point since my birth. There are no words to describe what parents really do for a son.

This thesis does not only belong to me, but also to my girlfriend Daniela. She has been with me in every moment of these four years, sustained my humor swings, gave me comfort. Almost every emotion that is behind this thesis was empathetically shared with her. I owe her my deepest gratitude.

Simone Balmelli Zürich, 13.11.2015

Table of Contents

1 Introduction **3**

2 The ADM formalism **9**

2.1 Introduction to the ADM formalism 9

2.1.1 Self-gravitating point masses 13

An example: derivation of the Newtonian dynamics 14

2.1.2 ADM four-momentum and Poincaré invariance 15

2.2 Spin couplings 17

2.2.1 Fermi transport of a gyroscope 18

2.2.2 Multipole expansion of the energy-momentum tensor 19

2.2.3 ADM Hamiltonians with spin 21

Symmetry generator approach 21

Other methods 24

Reduced center-of-mass Hamiltonians 24

3 The Effective-one-body approach **29**

3.1 Motivation 29

3.2 The EOB energy mapping 33

3.3 Canonical transformations 36

3.4 The EOB Hamiltonian 39

3.4.1 Extension to higher orders of accuracy 40

Padé-resummation 42

3.5 The full EOB formalism 43

3.6 An EOB Hamiltonian for spinning black-hole binaries 45

3.6.1 A ν-deformed, separable Kerr metric 46

3.6.2 Including the LO spin-spin coupling 48

3.6.3 The spin-orbit sector 49

Including the NLO and NNLO spin-orbit coupling in DJS gauge 50

Brief summary: the spinning EOB Hamiltonian 52

3.6.4 Preview of chapters 4 and 5: a possible NLO spin-spin inclusion 53

3.7 A new EOB Hamiltonian for spinning, nonprecessing black hole binaries 54

Appendices **59**

3.A The quadrupole formula and the 22-spherical mode 59

4 EOB Hamiltonian with NLO spin-spin terms for aligned spins **63**

4.1 Introduction 64

4.2 NLO, spin-spin Hamiltonian in ADM coordinates 66

4.3 Transformation from ADM to EOB coordinates 68

4.4 PN Expansion of the EOB Hamiltonian 69

4.5 Including the NLO spin-spin coupling 72

4.6 Discussion 76

4.7 Conclusion 80

4.8 Appendix: Existence of equatorial orbits 81

5 EOB Hamiltonian with NLO spin-spin terms **83**

5.1 Introduction 84

5.2 Summary of the previous work 85

5.3 Including NLO spin-spin terms into the EOB for general orbits 87

5.3.1 The prescription 87

5.3.2 The general solution 89

5.3.3 Gauge fixing 92

5.4 Discussion: "full" and "partial" inclusion 94

5.5 Conclusion 96

6 A new EOB Hamiltonian with NLO spin-spin coupling **99**

6.1 Introduction 99

6.2 A new NLO Hamiltonian with NLO spin-spin coupling 101

6.2.1 Structure of the Kerr Hamiltonian in Cartesian-like coordinates 101

6.2.2 The Effective-One-Body orbital Hamiltonian 103

6.2.3 Canonical transformation from ADM to EOB 105

6.2.4 Gauge choice 107

6.2.5 Resummation options 113

6.2.6 The quadratic forms 114

6.3 The spin-orbit sector and the last stable circular orbit 117

6.4 Conclusions 122

6.5 Appendix: On the hidden "symmetry" of the NLO spin-spin coupling 123

7 A few things about neutron stars **125**

7.0.1 Equation of state and maximal mass of degenerate matter 125

7.0.2 Tidal effects in the EOB 127

8 Quasiuniversal properties of neutron star mergers **129**

8.1 Introduction 129

8.2 EOB and the LSO 130

8.3 κ_ℓ^T-universal relations 131

8.4 Comparison with NR 133

8.5 Outlook 134

9 Conclusions **137**

References **139**

Curriculum Vitae **149**

CHAPTER 1

Introduction

The process leading to scientific knowledge is made of two opposite mechanisms: deduction and induction. Deduction constitutes the largest part of the scientific work, and allows to extend the network of causal connections relating theory with experiment. For instance, analyzing the predictions of a theory, with the aim of finding a correspondence with the measured data, is a deductive procedure. In the inductive part, the scientist follows a path that is more difficult to describe, and where some kind of *creativity* is involved. He focuses his own attention onto some particular propositions, which, on the basis of his physical intuition, are felt by him to have a particularly deep relation with Nature. Generalizing the range of validity of these propositions to a larger domain may be the basis for the development of a new theory. Induction is often a leap in the dark, and the vast majority of speculations about the laws or physics are unmercifully confuted by the experiment. In some cases, however, they are not, and continue to be valid (at least at some degree of approximation) at the present time. This is probably the most fascinating aspect of theoretical physics, where the subjectivity of the theoretician seems to have grasped some very intimate aspects of Nature. Among the most notable cases, there are of course Newton's dynamical laws and its theory of gravitation, Maxwell' equations for the classical electromagnetism, as well as Schrödinger's and Dirac's quantum mechanical equations.

One hundred years ago, the formulation of a new theory of gravitation, which fully deserves to be included in the above list, was being completed. It was Einstein's General Relativity, often recognized as one of the most elegant theories in physics. Its formalism unifies the concepts of space, time and gravity in a unique mathematical object: spacetime, a four-dimensional Lorentzian manifold describing gravity by its own curvature. At the basis of General Relativity there is the equivalence principle, which identifies the gravitational mass of a body with its inertial mass.

Before Eddington's experimental verification of light deflection, accomplished in 1919, General Relativity had strenuous competitors. In particular, the Finnish physicist Gunnar Nordstöm had developed a different theory of gravity having the same ultimate goal of Einstein's, that is, to make gravitation consistent with the findings of Special Relativity. According to the model of Nordstöm, the equivalence principle was violated in the relativistic regime, however at a degree that was difficult, if not impossible, to measure at that time. There may be no better example to highlight the role of subjectivity and intuition during the formulation of a new theory, than the

following words, successively written by Einstein in 1933, and concerning his own reaction to the proposal of Nordström [1]:

> This did not fit with the old experimental fact that all bodies have the same acceleration in a gravitational field. This law, which may also be formulated as the law of the equality of inertial and gravitational mass, was now brought to me in all its significance. I was in the highest degree amazed at its existence and guessed that in it must lie the key to a deeper understanding of inertia and gravitation. I had no serious doubts about its strict validity even without knowing the results of the admirable experiments of Eötvös, which - if my memory is right - I only came to know later.

In principle, there was no fully rational reason that could have prevented Einstein to reject the "old experimental fact" (i.e., Galileo's experiment about the universality of free fall), since relativistic corrections to it (like in Nordström theory) would have stayed well below the experiment's accuracy level. Nevertheless, Einstein had the feeling that the equivalence principle was "the key to a deeper understanding of inertia and gravitation". And, in the end, it turned out that he was right.

Since its birth, General Relativity has been successful under many points of view. At the time of its formulation, it was the only gravity theory able to account for Mercury perihelion precession and for light deflection. More recent measurements have confirmed other implications of the theory, such as time dilation in a gravitational field and geodetic precession of a gyroscope; moreover, the validity of the equivalence principle has been verified at extremely high accuracies. Cosmology models are among the most important results it led to: the Friedmann-Lemaître models, which date back to the 20's, and still constitute the basics of standard cosmology, are particular solutions of Einstein's equations.

Furthermore, the most reasonable answer to the problem of a massive star's collapse has been provided so far by General Relativity. If the mass M is sufficiently large, the remaining object (a black hole) is described (in the simplest, nonrotating case) by the Schwarzschild metric

$$ds^2 = -\left(1 - \frac{2GM}{c^2 R}\right)c^2 dt^2 + \frac{1}{1 - \frac{2GM}{c^2 R}} dR^2 + R^2\left(d\theta^2 + \sin^2\theta\, d\varphi^2\right). \tag{1.1}$$

This corresponds to an extreme curvature in spacetime, with an horizon building up at a distance $R = 2M$ from the center, and marking the boundary with an interior region lying at future infinity with respect to the external world. Starting from the 1915 derivation of the Schwarzschild metric as an exact solution of Einstein's equations, the study of black holes have long been a field of pure speculation. First in the 60's, with the discovery of quasars, i.e., distant astrophysical objects emitting enormous amounts of electromagnetic radiation, the General Relativity picture for black holes has seriously been taken into consideration by the astrophysical community. At the present time, the black hole problem remains one of the most important unanswered questions in astrophysics. Although compact objects with incredibly large masses are known to exist (for instance, in correspondence of the radiation source SgrA* at the center of our galaxy), it has not been possible to directly probe the Schwarzschild (or, more generally, the Kerr) metric yet.

At least one more element must be added to the mosaic of General Relativity we have presented so far. Shortly after the formulation of its theory, Einstein realized that gravity must exhibit, similarly to electromagnetism, retardation effects. His 1918 paper *Über Gravitationswellen* [2] posed the basis for a new sub-branch of physics, concerning the generation and propagation of gravitational waves. The emission of gravitational waves can be modeled, in the simplest case,

within the framework of linearized gravity. Considering the gravitational field, described by the metric $g_{\mu\nu}$, as a small perturbation of the Minkowski (flat) metric $\eta_{\mu\nu}$, we may write

$$g_{\mu\nu} = \eta_{\mu\nu} + h_{\mu\nu}, \tag{1.2}$$

with $|h_{\mu\nu}| \ll 1$, and work linearly in the reformulation $\overline{h}_{\mu\nu} \equiv h_{\mu\nu} - \frac{1}{2}\eta_{\mu\nu}h^{\sigma}{}_{\sigma}$ of the tensor $h_{\mu\nu}$ (where we have used the Einstein sum convention on the index σ). Imposing, in analogy with electrodynamics, the (transverse) Lorentz gauge $\partial^{\nu}\overline{h}_{\mu\nu} = 0$, the Einstein equations reduce to

$$\left(\Delta - \frac{1}{c^2}\frac{\partial^2}{\partial_t^2}\right)\overline{h}_{\mu\nu} = -\frac{16\pi G}{c^4}T_{\mu\nu}, \tag{1.3}$$

where Δ is the Laplace operator, and $T_{\mu\nu}$ the stress-energy tensor. This is nothing but a wave equation: if the matter (or energy) source $T_{\mu\nu}$ changes in time following, say, an oscillatory motion governed by a frequency ω, then $\overline{h}_{\mu\nu}$ will describe a wave propagating at the speed of light and containing frequency modes which are multiples of ω. A source with a nonvanishing mass-quadrupole moment Q_{ij} (where i and j denote spatial indices) emits *quadrupolar radiation* as a dominant effect. It is described by the formula [2]

$$h_{ij}^{TT} = \frac{1}{D}\frac{2G}{c^4}\ddot{Q}_{ij}^{TT}, \tag{1.4}$$

where D is the distance from the source. Here, the label "TT" denotes a particular choice of coordinates, the so-called transverse-traceless gauge, that can be obtained by using an appropriate projector[1]. We come to the essential point: dynamical mass configurations are, in principle, sources of gravitational waves. The strongest emitters are systems where huge masses are involved. A binary system of self-gravitating, coalescing black holes is among the best systems to look at in the search for gravitational radiation, no matter if intergalactic, or even cosmological distances separates it from the Earth. Nevertheless, the amplitude of the waves in question is extremely small, being of the order of magnitude $|h_{\mu\nu}| \sim 10^{-21}$ for standard astrophysical sources.

As a consequence, an observation of gravitational waves has long believed to be impracticable. The only true result obtained so far has been the verification of the formula describing the quadrupolar radiation flux. This has been done thanks to the 1974-discovered binary pulsar PSR B1913+16, which is a system of two neutron stars (actually the first-ever discovered binary of this type), gravitating one around the other with a period of about eight hours. Russell Hulse and Joseph Taylor, the researchers that had discovered the binary, accomplished then careful measurements of the orbital frequency, and found an excellent agreement with the quadrupole radiation formula (1.4), which predicts a steady increase in the frequency due to the orbital energy- and angular momentum losses.

Starting from the 80's, and in spite of the elusive character of gravitational waves, the first prospects for building interferometric gravitational wave detectors began to be elaborated. The first instruments were constructed in the 90's and early 2000's. At the present time, a first detection is expected to occur soon. In particular, the Advanced LIGO network, in the United States, is currently searching for possible sources at an unprecedented sensitivity. At its maximal performance capability, that will be reached in a few years, the estimated event rate of incoming waves makes the possibility of a detection very realistic. Other detectors are Virgo, in Italy, which is undergoing and upgrade to an advanced configuration, the smaller GEO600, in Germany, and the Japanese detector KAGRA, which is still under construction. Among the future projects, the

[1] We refer the reader to [3] for a detailed but simple introduction to the theory of gravitational waves.

space-born detector eLISA may be the most notable one. Unlike the ground based interferometers (whose sensitivity is in the range of $10^2 - 10^3$ Hz, and is thus limited to the final stages of the coalescence of neutron stars, and small black hole binaries), eLISA will be able to measure frequencies down to $10^{-4} - 10^{-5}$ Hz, which are the realm of supermassive coalescing black holes.

Gravitational wave detection would be a crucial step for the development of physics. It would open an entire new window to astronomy, allowing unprecedented tests of strong-field features of General Relativity, and creating a completely new interplay between fundamental theories, astrophysics and cosmology. For the first time, black holes could be observed directly, and the Kerr metric probed. Neutron stars could be studied under a new perspective, and some key informations about their internal structure could be gained. Finally, eLISA will be able to observe the merger of supermassive black holes at enormous cosmological distances (up to redshift ~ 20), thus providing a fundamental contribution to the (currently very incomplete) understanding of black hole formation and evolution, which is intimately linked to galactic evolution models.

For both ground-based and space-born detectors, in order to extract the gravitational waves signal from noise, it is necessary to provide very accurate templates of the expected waveform, which needs a very large theoretical effort. Einstein's equations are a system of ten coupled, second-order, non-linear partial differential equations, and hoping to find an exact solution for the general relativistic two-body problem is illusory. Post-Newtonian (PN) theory, the most important approximation method for the general relativistic dynamics, is a perturbative scheme in the small parameter $\epsilon \sim (v/c)^2 \sim GM/(c^2R)$, where v is the reciprocal velocity of the binary, and R the separation between the two bodies[2]. When the orbiting bodies are close enough from one another, and the wave amplitude is approaching a maximal value, thereby making the signal stronger and better detectable, PN theory ceases to be accurate.

In order to overcome the problems, Buonanno and Damour proposed an improved approach to the two-body dynamics [4], that reformulates PN results by resumming them in a particular, simpler way. This method is known with the name of Effective-One-Body (EOB) approach. At the present time, more than fifteen years after it first formulation, the EOB is the only semi-analytical method able to generate the complete waveform a coalescing process. When completed with some parameters calibrated against Numerical Relativity waveforms, the EOB is almost as accurate as Numerical Relativity itself. In this thesis, the main argument of discussion is the inclusion of spin couplings in the EOB model. The importance for an accurate description of spin can motivated, using a basic argument, by the fact that every astrophysical object is in principle expected to have a non vanishing angular momentum. In particular, black hole configurations with large, aligned spins seem to be favored by disk accretion mechanisms [5], and generate a wave signal up to 2 times stronger than in the nonspinning case [6].

Later on, there will be place to discuss a lot of technical details concerning the EOB. Let us, instead, end this introductory section touching a more general aspect. To make things clear, although we are going to speak of EOB and PN theory as if they where two competing approaches, we stress that the EOB is *not* an alternative approximation method to solve Einstein equations. Its starting point are PN results, and it could not exist without them.

However, while PN theory is "minimal", in the sense that it develops the equation of motions up to the order at which they are known, setting to zero all higher-order terms, the EOB is not. It contains, in the form of a *resummation*, some speculation about the missing terms. In other words, taking into account our limited knowledge of the dynamics of General Relativity, PN theory and EOB are equivalent; but in the domain where analytic knowledge is still missing, and where PN

[2]Notice that, because of the virial theorem, $(v/c)^2$ and $GM/(c^2R)$ can be assumed to be of the same order of magnitude.

theory falls silent, the EOB tries to make a guess. The reader will have the possibility to verify that this guess is not, of course, made in a random way. Each development of the model is done pursuing simplicity and formal elegance above all.

At this point, it shall have become clear that PN theory is a deductive methodology: assuming General Relativity to be true, it constructs a logical chain of connections leading to the result. By contrast, what makes the EOB unique and intriguing is its particular inductive character. Some aspects of its construction, and in particular the pursuit of beauty (in a sense very close to simplicity), may call to mind the process leading to the formulation of great theories. The EOB is of course not a theory, nor pretends to be one. It is rather a substructure: as General Relativity is a model aiming at representing Nature and its essence, the EOB is a model hoping to grasp the essential aspects of General Relativity, though only for what concerns the two-body problem. In the process leading to both General Relativity and the EOB, the primary role is played by subjective rules and intuition.

CHAPTER 2

The ADM formalism applied to the general relativistic two-body problem

For a long time since the birth of General Relativity, there has been no substantial need of pushing the knowledge of the dynamics of self-gravitating systems at high accuracies. The 1PN equations of motion (first correctly derived by Einstein, Infeld and Hoffmann [7]), were sufficiently precise to satisfactorily match all observations at the level of the solar system. Only with the observation of the first relativistic binary systems (such as the 1974 discovery of the Hulse-Taylor binary pulsar [8]), it emerged the necessity of an (at least) 2.5PN accurate description of the two-body problem (see e.g. [9]), which could account for the leading-order radiation-reaction effects. More recently, under the prospect of a forthcoming gravitational wave detection, the full 3PN (see e.g. [10–13]) and even 4PN dynamics [14, 15] have been derived. The majority of these contributons are based upon the canonical formulation of General Relativity developed 1963 by Arnowitt, Deser and Misner (ADM) in Ref. [16], which has also proven to be very useful for post-Newtonian calculations involving spins. In this chapter, an outlook of the ADM formalism is given. In Sec 2.1, following the thread of the original ADM paper, we discuss the canonical formulation of the Einstein-Hilbert action, also mentioning the coupling with matter variables, while Sec 2.2 will be devoted to the description of spinning systems in the ADM formulation. Throughout this chapter, we use units with $c \equiv 1$, $4\pi G \equiv 1$.

2.1 Introduction to the ADM formalism

Diffeomorphism covariance has often led to difficulties in the study of the dynamics of General Relativity. Covariance of a theory under some changes of coordinates means that the theory itself contains a given number of redundant parameters, and therefore the dynamics is not described by a minimal set of independent variables. At the beginning of the 60's, Arnowitt, Deser and Misner [16] have been able to cast the Einstein equations (under the assumption of asymptotically flat spacetimes) into a canonical form. In such a way, the dynamics is not only expressed in terms of independent parameters, but is also written in a very standard and well-studied way. The idea beyond the work of ADM was motivated by already known "parametrization properties" of the action principle. In practice, the action of a system with n degrees of freedom

$$I = \int dt \left(\sum_{i=1}^{n} p_i \dot{q}_i - H(p,q) \right) \tag{2.1}$$

may be rewritten in "parametrized form", i.e., describing the time as a new, redundant coordinate q_{n+1} depending on an arbitrary parameter τ. Moreover, the new Hamiltonian can be set to zero if one defines the canonical momentum p_{n+1} associated to q_{n+1} such as to satisfy

$$p_{n+1} = -H. \tag{2.2}$$

This condition can be inserted into the action by means of a Lagrange multiplier $N(\tau)$ and a constraint $\mathcal{H}(p_{n+1}, q, p)$, whose simple root satisfies Eq. (2.2). The action in parametrized form reads

$$I = \int d\tau \left(\sum_{i=1}^{n+1} p_i \frac{dq_i}{d\tau} - N\mathcal{H} \right). \tag{2.3}$$

Since N must solve the Lagrange equations for any choice of τ as a parameter, it is clear that it transforms according to $N(\tau)d\tau = N'(\tau')d\tau'$ under an arbitrary redefinition $\tau'(\tau)$. As a consequence, the action (2.3) is generally covariant under reparametrizations of τ. One has then, in accordance with the above remarks, a covariant theory expressed in terms of redundant variables.

The procedure for recovering the original, non-parametrized form (2.3) can be sketched as follows:

i) Solve the *constraint equation* $\mathcal{H} = 0$.

ii) Apply a gauge choice, i.e., define a *coordinate condition* $q_{M+1}(\tau)$.

iii) The Hamiltonian is obtained with the variation $H = -\delta I / \delta q_{M+1}$.

The same discussion can be made in a field theory like General Relativity, with the four-coordinates x^μ instead of τ and with fields $\gamma_{ij}(x^\mu)$, $\pi_{ij}(x^\mu)$ instead of the phase-space variables. We have mentioned that the parametrized action (2.3), just as General Relativity, exhibits a general covariance. The main result due to Arnowitt, Deser and Misner, was actually to show that the Einstein-Hilbert action can be written into a parametrized form (analogous to (2.3)), and to cast it into a fully reduced, canonical form corresponding to (2.1). We proceed now summarizing these findings.

At first, since time plays the role of a parameter in the canonical equations of motion, it is necessary to perform some kind of "3+1" splitting of spacetime. Given the four-metric $g_{\mu\nu}$, a three-covariant spatial metric γ_{ij} is simply obtained by restricting it to the space-like components,

$$\gamma_{ij} \equiv g_{ij}. \tag{2.4}$$

This allows to define intrinsic quantities on the three-dimensional surface, like a Riemann tensor, a Ricci tensor and a scalar curvature R. The contravariant γ^{ij} is defined so that $\gamma_{ik}\gamma^{kj} = \delta_i{}^j$, and is used to raise and lower three-indices. The remaining four elements of the full metric elements can be rewritten according to

$$N \equiv \left(g^{00} \right)^{-1/2}, \qquad N_i \equiv g_{0i}, \tag{2.5}$$

that are related with the unit vector $n_\mu = (-N, 0, 0, 0)$, $n^\mu = 1/N(1, -N^i)$ lying perpendicular to the surfaces of constant time t. It is also necessary to introduce some quantities plaing the role of momenta. It is natural to assume that the momenta shall be somehow related to the time evolution of the surfaces of constant time. More precisely, one may expect them to be extrinsic of the surfaces, i.e., to depend on the embedding of the surfaces in time. One may thus consider the second fundamental form $K_{ij} \equiv -n_{(i;j)}$ (also called "extrinsic curvature") of the three-surfaces , which is a measure of the local curvature in time, as a possible candidate for representing the field momentum. The choice made by ADM, ultimately motivated by the appropriateness for reaching a canonical structure, has been that of defining the momenta as

$$\pi^{ij} = -\sqrt{\gamma}\left(K^{ij} - \gamma^{ij}K\right). \tag{2.6}$$

With these definitions, the Einstein-Hilbert action takes the parametrized form

$$I = \int d^4x \left(\pi^{ij}\gamma_{ij,0} - N\mathcal{H}^{\text{field}} + N^i\mathcal{H}_i^{\text{field}} + (\text{td})\right), \tag{2.7}$$

where (td) denotes a divergence and a total time derivative, which obviously do not affect the action, and where $\mathcal{H}^{\text{field}}$ and $\mathcal{H}_i^{\text{field}}$ are explicit functions of γ_{ij} and of π^{ij},

$$\mathcal{H}^{\text{field}} = -\sqrt{\gamma}^{-1}\left(\gamma R - \gamma_{ij}\gamma_{kl}\pi^{ik}\pi^{jl} + \frac{1}{2}\left(\gamma_{ij}\pi^{ij}\right)^2\right) \tag{2.8}$$

$$\mathcal{H}_i^{\text{field}} = 2\gamma_{ij}\pi^{jk}_{;k}. \tag{2.9}$$

A variation of γ_{ij} and π^{ij} leads to their time-evolution equations, whose solution is unique if the initial values for γ_{ij}, π^{ij}, N and N_i are specified. The set of allowed initial values is however limited by the constraint equations $\mathcal{H}^{\text{field}} = 0$ and $\mathcal{H}_i^{\text{field}} = 0$, that are obtained by independent variations of N and N^i. As shown by ADM, the maintenance in time of the constraint equations is guaranteed by the Bianchi identities.

Notice that there is no equation determining the time-evolution of N and of N^i, which is therefore left arbitrary. However, this is not meant to be a problem, since N and of N^i merely describe the continuation of coordinates at different times. The fact that fixing N and N^i actually correspond to a choice of coordinates can be understood performing a δp_{n+1}-variation of the action (2.3), which leads to the equation of motion

$$\frac{dq_{n+1}}{d\tau} = -N\frac{\partial\mathcal{H}}{\partial p_{n+1}}. \tag{2.10}$$

It is then clear that N fixes the coordinate condition $q_{n+1}(\tau)$.

The twelve dynamical variables γ_{ij} and π^{ij} reduce to eight by virtue of the constraint equations. Furthermore, imposing the coordinate conditions shrinks the number of independent variables to four, which corresponds to a system with two degrees of freedom. There is of course no unique canonical choice of coordinates. Anyway, it is useful to perform an orthogonal decomposition of the symmetric tensors γ_{ij} and π^{ij}, so as to isolate the transverse-traceless parts h_{ij}^{TT} and $\pi^{ij\text{TT}}$ of γ_{ij} and of the momentum tensor, respectively, from the remaining (non-traceless) transverse and longitudinal components [16].

ADM showed that, fixing the gauge according to

$$\pi^{ii}_{,jj} - \pi^{ij}_{,ij} \equiv 0 \tag{2.11a}$$

$$\gamma_{ij,j} \equiv 0, \tag{2.11b}$$

and after solving the constraint equations, the action (2.7) can be brought into the form

$$I = \int d^4x\, \pi^{ij\mathrm{TT}} h^{\mathrm{TT}}_{ij,0} - \int dt\, E. \tag{2.12}$$

The ADM energy E is constructed analogously to H in point iii) above[1] . It is expressed as the volume integral[2]

$$E = -\int d^3x\, \gamma_{jj,ii} = -\int dS_i\, \gamma_{jj,i}, \tag{2.13}$$

where the element dS_i denotes a surface integral at spatial infinity. We may finally add a vanishing term to obtain

$$E = \int dS_i \left(\gamma_{ij,j} - \gamma_{jj,i}\right). \tag{2.14}$$

This expression has been proven to be independent of the choice of coordinates (see also [18]), under the assumptions of asymptotically flat spacetimes and provided that Lorentz boosts are not performed[3]. By virtue of the constraint equations and of the coordinate conditions, E can solely be expressed in terms of the transverse-traceless variables. This fact, together with the structure of the action (2.12), clearly means that h^{TT}_{ij} and $\pi^{ij\mathrm{TT}}$ actually are a (minimal) set of canonical variables. The field dynamics is therefore described by the Hamiltonian

$$H_{\mathrm{ADM}}\left(h^{\mathrm{TT}}_{ij}, \pi^{ij\mathrm{TT}}\right) \equiv E \tag{2.15}$$

according to

$$\partial_t \gamma^{\mathrm{TT}}_{ij} = \frac{\delta H_{\mathrm{ADM}}}{\delta \pi^{ij\mathrm{TT}}} \qquad\qquad \partial_t \pi^{ij\mathrm{TT}} = -\frac{\delta H_{\mathrm{ADM}}}{\delta h^{\mathrm{TT}}_{ij}}. \tag{2.16}$$

For applications to the the two-body problem, the most used gauge, called ADM tranverse-traceless (ADMTT), is slightly different from the one discussed above. Following e.g. [19], it is obtained requiring

[1] More concretely, the gauge condition (2.11) provides a relation of the type $x^\mu(\gamma_{ij}, \pi^{ij})$ for the four-coordinates x^μ. Consequently, the explicit meaning acquired by the time coordinate $t \equiv x^0$ allows to extract a term $\delta I = -E\delta t$ from the variation $\delta \int \pi^{ij}\gamma_{ij,0}$ of the full kinetic part.

[2] Here, we are following the arguments used in the original ADM paper, which however involve a not fully clear non-cancellation of a total divergence. ADM motivated this fact stating that "the integrands [...] are *not* divergences when expressed as functions of the canonical variables", see Footnote 14 in Ref. citearn:62. This problematic issue was clarified, e.g., by Regge and Teitelboim [17]. Without imposing the ADM gauge condition exposed above, but requiring some "physically reasonable" asymptotic behaviors of the field (and in particular a finite total mass), they rederived Eq. (**??**) below in a more proper way.

[3] These assumptions are equivalent to require that any two allowed coordinate frames converge towards the same Minkowskian coordinates at spatial infinity.

$$\partial_j\left(\gamma_{ij} - \frac{1}{3}\gamma_{kk}\delta_{ij}\right) = 0, \tag{2.17}$$

$$\pi^{ii} = 0. \tag{2.18}$$

The first condition means that the traceless part of γ_{ij} must also be transverse (it will be denoted as h_{ij}^{TT}). The remaining trace component $\frac{1}{3}\gamma_{kk}\delta_{ij}$ can be expressed in terms of a scalar function φ so that

$$\gamma_{ij} = \left(1 + \frac{\varphi}{8}\right)^4 \delta_{ij} + h_{ij}^{\mathrm{TT}}. \tag{2.19}$$

On the other hand, the traceless π^{ij} can be decomposed in the sum of a traceless-transverse part $\pi^{ij\mathrm{TT}}$ and of a traceless-longitudinal part $\tilde{\pi}^{ij}$, which is derivable from a vector potential $\tilde{\pi}^{i}$[4].

This gauge turns out to be canonical as well. One can easily verify that, since both combinations $\pi^{ij}\delta_{ij}\,(1+\varphi/8)^4_{,0}$ and $\tilde{\pi}^{ij}h^{\mathrm{TT}}_{ij,0}$ vanish, the full kinetic term $\pi^{ij}\gamma_{ij,0}$ of Eq. (2.7) simply reduces to $\pi^{ij\mathrm{TT}}h^{\mathrm{TT}}_{ij,0}$. Furthermore, because of the invariance of the ADM Hamiltonian under coordinate transformations, the expression (2.14) for the ADM energy is still valid. The only important difference with respect to the previous gauge lies in the constraint equations, that must now be solved for $\varphi\left(h_{ij}^{\mathrm{TT}}, \pi^{ij\mathrm{TT}}\right)$ and for $\tilde{\pi}^{i}\left(h_{ij}^{\mathrm{TT}}, \pi^{ij\mathrm{TT}}\right)$ (however, because of non-linearity, a solution can normally only be found in some approximation scheme, such as the post-Newtonian one). The reduced Hamiltonian in ADMTT gauge can now be written as

$$H_{\mathrm{ADM}}\left(h_{ij}^{\mathrm{TT}}, \pi^{ij\mathrm{TT}}\right) = -\int d^3x\, \Delta\varphi. \tag{2.20}$$

2.1.1 Self-gravitating point masses

Let us first consider a test particle with mass m moving in an external gravitational field. The corresponding parametrized action can be written as

$$I_{\mathrm{M}} = \int d\tau\left[p_\mu u^\mu - \tilde{N}\left(p_\mu p^\mu + m^2\right)\right], \tag{2.21}$$

with a Lagrange-multiplier $\tilde{N}$ that ensures the mass-shell constraint $p_\mu p^\mu + m^2$ to be satisfied . The constraint may be solved in terms of $p_0(p^i, g_{\mu\nu})$. In analogy to the simple system discussed at the beginning of Sec. 2.1, one may choose the coordinate $t \equiv x^0(\tau) \equiv \tau$, so that the Hamiltonian is

$$H_{\mathrm{M}} = -p_0 \tag{2.22}$$

In the special case of a a static metric, time can be set orthogonally to the spatial directions. Then, the solution $p_0(p^i, g_{\mu\nu})$ is immediate, and reads $p_0 = -\sqrt{m^2 + p_i p^i}$. For more general situations we make use of the 3+1 splitting introduced in Sec. 2.1, which leads to

$$H_{\mathrm{M}} = N\sqrt{m^2 + p_i p^i} - N^i p_i. \tag{2.23}$$

[4]See the original ADM paper for more details about the orthogonal decomposition into transverse and longitudinal elements.

Notice that N, N^i, and γ_{ij} are nothing but given functions of the canonical coordinates r^i and of time. However, it is worth to remark that we have ended up with a structure that recalls the constraint equations for the metric fields. This is the key that allows to describe, in the ADM approach, the interaction of dynamical fields with matter. In other words, we have so far just solved the matter constraint of the total system, and it still remains to consider the field as a dynamical variable. More concretely, one first has to introduce the matter-Hamiltonian densities $\mathcal{H}^M$ and $\mathcal{H}_i^M$:

$$\mathcal{H}^M \equiv \sqrt{m^2 + \gamma^{ij} p_i p_j}\, \delta(\boldsymbol{x} - \boldsymbol{r}), \qquad \mathcal{H}_i^M \equiv p_i\, \delta(\boldsymbol{x} - \boldsymbol{r}). \tag{2.24}$$

At this intermediate stage, the total action $I_{\rm tot} = I_{\rm M} + I$ (where I is the Enstein-Hilbert action discussed in Sec. 2.1) has the "partially parametrized" form

$$I_{\rm tot} = p_i r^i_{,0} + \int d^4x \Big[\pi^{ij} \gamma_{ij,0} - N \left(\mathcal{H}^{\rm field} + \mathcal{H}^{\rm M} \right) + N^i \left(\mathcal{H}_i^{\rm field} + \mathcal{H}_i^{\rm M} \right) \Big]. \tag{2.25}$$

The whole information describing the coupling between field and matter is therefore fully included the constraint equations

$$\mathcal{H}^{\rm field} + \mathcal{H}^{\rm M} = 0, \qquad \mathcal{H}_i^{\rm field} + \mathcal{H}_i^{\rm M} = 0, \tag{2.26}$$

that are now solved (in the ADMTT gauge) by $\varphi\left(h_{ij}^{\rm TT}, \pi^{ij\rm TT}, r^i, p_i\right)$ and $\tilde{\pi}^i\left(h_{ij}^{\rm TT}, \pi^{ij\rm TT}, r^i, p_i\right)$. The ADM energy is still given by Eq. (2.20), and aquires the meaning of an Hamiltonian when expressed in terms of all (field an matter) canonical variables.

An example: derivation of the Newtonian dynamics

To give a concrete example, we can check the formalism by computing the LO and the NLO contribution to the two-body relativistic Hamiltonian. The perturbative expansion is performed by introducing an appropriate post-Newtonian counting for the involved quantities and variables. In powers of c^{-1}, consistent rules are given by $m_a \sim c^{-2}$, $p_a^i \sim c^{-3}$, $\varphi \sim c^{-2}$, $h_{ij}^{\rm TT} \sim c^{-4}$, $\tilde{\pi}^{ij} \sim c^{-3}$, and $\pi^{ij\rm TT} \sim c^{-5}$ (see, e.g., Ref. [20]). The index $a = 1, 2$ simply labels the two bodies.

Let us now consider the constraint equation $\mathcal{H}^{\rm field} + \mathcal{H}^{\rm M} = 0$. The momentum-dependent part of $\mathcal{H}^{\rm field}$ (2.8) is quadratic in π^{ij}, and is therefore of order $\sim c^{-6}$. By contrast, the "static" part $\sqrt{\gamma}R$ is quadratic in the derivatives of γ_{ij}, and is thus expected to contain terms of type $\partial_i \partial_j \varphi \sim c^{-2}$ and $\partial_i \varphi\, \partial_j \varphi \sim c^{-4}$. For our purpose, we can thus assume that $\mathcal{H}^{\rm field} = -\sqrt{\gamma}R$, neglecting all π^{ij}. Similarly, the lowest-order term of the matter Hamiltonian $\mathcal{H}^{\rm M}$ is equal to $m_1\delta_1 + m_2\delta_2 \sim c^{-2}$, while the next contribution is of type $p_a^i p_a^j \delta_a / m_a \sim c^{-4}$. It is thus clear that the constraint equation is $\sim c^{-2}$ at LO and $\sim c^{-4}$ at NLO. After expanding the scalar curvature R, the first constraint

$$-\sqrt{\gamma}R + \sqrt{m_1^2 + \gamma^{ij} p_{1\,i} p_{1\,j}}\, \delta_1 + \sqrt{m_2^2 + \gamma^{ij} p_{2\,i} p_{2\,j}}\, \delta_2 = 0 \tag{2.27}$$

turns into

$$-\Delta \varphi_{\rm LO} = m_1 \delta_1 + m_2 \delta_2 \tag{2.28}$$

$$-\Delta \varphi_{\rm NLO} = \frac{p_1^i p_1^i}{2m_1} \delta_1 + \frac{p_2^i p_2^i}{2m_2} \delta_2 - \frac{1}{8} \varphi_{\rm LO} \left(m_1 \delta_1 + m_2 \delta_2 \right). \tag{2.29}$$

Notice that we do not need to solve any other equation. Although the three remaining constraints $\mathcal{H}_i^{\text{field}} + \mathcal{H}_i^{\text{M}} = 0$ actually start at order $\mathcal{O}(c^{-3})$, which is dominant with respect to Eq. (2.29), their contribution to the energy density $-\Delta\varphi$ only enters at higher orders.

A volume integration of Eq. (2.28) trivially leads to

$$H_{\text{LO}}^{\text{ADM}} = m_1 + m_2, \tag{2.30}$$

the rest mass-energy of the system. Furthermore, we calculate φ_{LO} with a Poisson integral,

$$\varphi_{\text{LO}} = \frac{1}{4\pi}\left(\frac{m_1}{|\boldsymbol{x}-\boldsymbol{r}_1|} + \frac{m_2}{|\boldsymbol{x}-\boldsymbol{r}_2|}\right), \tag{2.31}$$

and insert it into Eq. (2.29). One immediately realizes that this procedure is affected by a serious problem, since the integral of $\Delta\varphi_{\text{NLO}}$ involves the divergent terms

$$m_a \frac{\delta(\boldsymbol{x}-\boldsymbol{z_a})}{|\boldsymbol{x}-\boldsymbol{r}_a|}. \tag{2.32}$$

This issue arises from the assumption of particles as point masses. If the mass distribution were taken to be a smooth function ρ_a, the corresponding "extended body" solution $\varphi_{a,\,\text{LO}}^{\text{ext}}$ would be smooth and well-defined even inside the support of ρ_a. Instead of a divergent integral, one would then simply end up with the finite, constant term $\int d^3x\ \varphi_{a,\,\text{LO}}^{\text{ext}}(\boldsymbol{x}-\boldsymbol{r}_a)\,\rho_a(\boldsymbol{x}-\boldsymbol{r}_a)$, that obviously does not affect the Hamiltonian dynamics. This argument suggests that the ill-defined terms $m_a\delta(\boldsymbol{x}-\boldsymbol{z_a})/|\boldsymbol{x}-\boldsymbol{r}_a|$ should simply be set to zero before evaluating the integral, which is nothing but a *regularization* procedure. For higher-order calculations, the problem becomes more subtle, and a rigorous regularization prescription must be developed (in particular, Hadamard *partie finie* and Riesz regularization methods have successfully been applied to post Newtonian calculations, see e.g. [21]).

Inserting the gravitational constant $G = (4\pi)^{-1}$, the result is the Newtonian Hamiltonian

$$H_{\text{NLO}}^{\text{ADM}} = -\int d^3x\ \Delta\varphi_{\text{NLO}} = \frac{\boldsymbol{p}_1^2}{2\,m_1} + \frac{\boldsymbol{p}_2^2}{2\,m_2} - \frac{G m_1 m_2}{|\boldsymbol{r}_1-\boldsymbol{r}_2|}. \tag{2.33}$$

2.1.2 ADM four-momentum and Poincaré invariance

The ADM approach is of course not generally covariant, since it involves certain gauge choices separating, for instance, time from space. For the same reason, it is also not manifestly Poincaré invariant: although space translations and rotations do not alter the form of the ADM Hamiltonian, Lorentz boosts do. Nevertheless, for asymptotically flat spacetimes, the underlying Poincaré invariance of general relativity can be brought into evidence in some restricted sense.

The ADM energy E can be viewed as the 0-th component of a four-momentum vector P^μ, with

$$P^i = -2\int dS_j\ \pi^{ij}, \tag{2.34}$$

that is constructed from the ADM action as the generator of space and time translations. As for the energy, the integration is performed over a surface at spatial infinity. All components of P^μ are unique in the sense they are invariant under arbitrary, local changes of coordinates and under space translations. They are also constant in time, and therefore, once expressed in terms of the

canonical variables, the Poisson Bracket $\{P^\mu, P^\nu\} = 0$ must hold. There is thus a certain analogy with the total four-momentum of a system in Special Relativity, more generally, one may expect the existence of a set of symmetry generators P^μ and $J^{\mu\nu}$ (expressed in terms of the canonical variables) satisfying the Poincaré algebra (see e.g. [12])

$$\{P^\mu, P^\nu\} = 0 \tag{2.35}$$
$$\{P^\mu, J^{\rho\sigma}\} = -\eta^{\mu\rho} P^\sigma + \eta^{\mu\sigma} P^\rho \tag{2.36}$$
$$\{J^{\mu\nu}, J^{\rho\sigma}\} = -\eta^{\nu\rho} J^{\mu\sigma} + \eta^{\mu\rho} J^{\nu\sigma} + \eta^{\sigma\mu} J^{\rho\nu} - \eta^{\sigma\nu} J^{\rho\nu}. \tag{2.37}$$

An equivalent, 3+1 formulation of the above commutators can be introduced with $J^i \equiv 1/2\, \epsilon^{ijk} J_{jk}$ and $J^{0i} \equiv G^i - t\, P^i$ (notice that any $J^{\mu\nu}$ fulfilling the Poincaré algebra is necessarily antisymmetric), and decomposes into the spatial translation

$$\{P^i, P^j\} = 0, \tag{2.38}$$

conservation laws

$$\{P^i, E\} = 0, \qquad \{J^i, E\} = 0, \tag{2.39}$$

infinitesimal rotations

$$\{J^i, P^j\} = \epsilon^{ijk} P^k, \qquad \{J^i, J^j\} = \epsilon^{ijk} J^k, \qquad \{J^i, G^j\} = \epsilon^{ijk} G^k, \tag{2.40}$$

and, finally, into the identities

$$\{G^i, E\} = P^i, \qquad \{G^i, P^j\} = E\, \delta^{ij}, \qquad \{G^i, G^j\} = -\epsilon^{ijk} J^k. \tag{2.41}$$

Under the assumption of some asymptotic behaviors of the fields, Regge and Teitelboim [17] introduced the ADM angular momentum

$$J^{ij} = -2 \int dS_k \left(x^i \pi^{jk} - x^j \pi^{ik} \right) \tag{2.42}$$

as the generator of infinitesimal spatial rotations. When expressed in terms of canonical variables, it satisfies Eqs. (2.38)-(2.40). On the other hand, showing the existence of a functional G^i satisfying the required rules is a more complex task. For the two-body problem, G^i has explicitly been constructed at some given post-Newtonian approximation orders (see [12] for 3PN, where the requirement of Poincaré invariance also helped to fix an ambiguity due to different regularization methods, [15] for 4PN, and, e.g., [19] for some spin-dependent results up to 3PN). These results have important implications, that will turn out to be very helpful for the purposes of this chapter. To prepare the ground for the following sections, we sketch them here.

i) First of all, the conservation in time of $J^{i0} = G^i - tP^i$ allows to choose a reference frame where $J^{i0} = 0$ for every t. This is simply achieved setting $G^i = 0$. It is then clear that $P^i = 0$ holds at any time as well, thereby suggesting to call this coordinate system "center-of-mass frame". As in the Newtonian case, the existence of such a privileged frame allows to strongly simplify the description of the two-body dynamics, and opens the doors to the EOB approach.

ii) Secondly, the generators of the Poincaré group may be used to introduce the concept of *spin* in General Relativity. In order to introduce it, we may proceed as follows. At first, we associate to G^i the spatial coordinate $\tilde{X}^i = G^i/E$, that could be interpreted as the center-of-mass position. We define the antisymmetric spin tensor $\tilde{S}^{\mu\nu}$ as the angular momentum tensor $J^{\mu\nu}$ measured in the center-of-mass frame $G^i = 0$. More concretely, with $\tilde{X}^0 \equiv t$, it must hold that

$$J^{\mu\nu} = \tilde{X}^\mu P^\nu - \tilde{X}^\nu P^\mu + \tilde{S}^{\mu\nu}. \tag{2.43}$$

By definition of $\tilde{X}^i$, the condition $\tilde{S}^{i0} = 0$ holds, and can be interpreted as the mass-dipole of the system being equal to zero when observed from the center-of-mass frame. This is a particular version of the so-called *spin supplementary condition*. The spin tensor is not unique: because of the invariance of $J^{\mu\nu}$ and P^i, it transforms as

$$\tilde{S}^{\mu\nu} \to \tilde{S}^{\mu\nu} - \delta\tilde{X}^\mu P^\nu + \delta\tilde{X}^\nu P^\mu \tag{2.44}$$

under a change $\tilde{X}^i \to \tilde{X}^i + \delta\tilde{X}^i$. In the new coordinate frame, the shifted reference position leads to a mass-dipole with the non-vanishing components $-\delta X^i E$. Nevertheless, there must exist an independent observer crossing the center of the new coordinate frame with four-velocity f_ν and measuring, in that precise moment, a mass-dipole equal to zero. The supplementary condition of the transformed spin tensor $S^{\mu\nu}$ can accordingly be formulated as

$$S^{\mu\nu} f_\nu = 0. \tag{2.45}$$

We finally come to a crucial point. Thanks to the Poincaré algebra, Eq. (2.43) provides a rule for the transformation of $\tilde{S}^{\mu\nu}$ under Poisson brackets. In the same way, one can reconstruct the Poisson brackets of a spin tensor transformed according to (3.86). Therefore, an appropriate choice of the supplementary condition should ultimately allow to build a spin tensor that satisfies the canonical rules[5]

$$\{S^{ij}, S^{kl}\} = \delta_{ik}S^{jl} - \delta_{il}S^{jk} + \delta_{jl}S^{ik} - \delta_{jk}S^{il} \tag{2.46}$$

$$\{S^{ij}, X^k\} = 0 \tag{2.47}$$

$$\{S^{ij}, P^l\} = 0. \tag{2.48}$$

2.2 Spin couplings

The pioneering work of Mathisson [23], together with the successive contributions of Papapetrou [24] (one and a half decades later), Pirani [25], Tulczyjew [26] and Dixon [27] opened the doors to a large number of studies concerning the dynamics of spinning bodies in General Relativity.

In the post-Newtonian approximation scheme, after the preliminary works [28] and [29], the first derivation of the complete LO spin-orbit and spin-spin coupling has been provided by Barker and O'Connell [30, 31] by virtue of a quantum mechanical formalism. Their results were later confirmed by calculations in a classical framework (see e.g. [32]).

There has been a gap of thirty years between these LO formulations and their extension to the next post-Newtonian order. The first full derivation of the NLO spin-orbit coupling was performed in

[5] As discussed in [22], the existence of canonical spin variables is a consequence of Darboux theorem.

harmonic coordinates by Faye, Blanchet and Buonanno [33], and by Blanchet, Buonanno and Faye [34]. An Hamiltonian formulation of the same spin-orbit interaction has been then provided by Damour, Jaranowski and Schäfer [22] in ADM coordinates. Subsequently, basing on the canonical formalism developed in [35, 36], the ADM approach has been used by Hartung and Steinhoff [37] to push the knowledge of the spin-orbit sector to NNLO. Meanwhile, the breakthrough of a new approximation method based on Effective-Field-Theory (EFT) techniques, developed by Goldberger and Rothstein [38] (occasionally named, perhaps somewhat confoundingly, "non-relativistic General Relativity"), allowed an independent derivation of the NLO coupling in the almost simultaneous works of Porto [39] and Levi [40] (see also the publication of Perrodin [41]). Recently, thanks to the formalism developed in [42], EFT methods have also been able to recover the NNLO spin-orbit interaction [43].

Shortly after the EFT approach had been proposed to calculate the dynamics of gravitating objects, and before the just mentioned NLO spin-orbit calculations, the EFT was extended to spinning bodies by Porto [44], who also calculated the NLO spin-spin potential for the first time [45]. This led to the first derivation of the NLO spin-spin coupling for black holes, which is due to Porto and Rothstein [46, 47]. In the same year, the above mentioned ADM formalism allowed an Hamiltonian (and therefore canonical) derivation of the same spin-spin interaction. The spin-squared terms can be found collecting the contributions of Hergt and Schäfer [48] and of Steinhoff, Hergt and Schäfer [49], while the spin(1)-spin(2) terms are given by Ref. [50]. A discrepancy between the spin(1)-spin(2) dynamics of Porto and Rothstein and the one derived within the ADM formalism was clarified in [51, 52].

An extension of the NLO spin-squared coupling to general binaries, including e.g. neutron stars (whose spin-induced quadrupolar deformations differs from the one of black holes) has been performed in Ref. [53] within the ADM formalism. The corresponding EFT result is found in the paper of Levi and Steinhoff [42]. Finally, we mention that spin(1)-spin(2) terms have been pushed to NNLO within the ADM formalism by Hartung and Steinhoff [37], followed by the corresponding EFT results obtained by Levi [54], while a derivation of the NNLO spin-spin coupling has only been performed within the EFT method, and still needs work to be formulated into an Hamiltonian; this results are due to Levi and Steinhoff [55]. The equivalence between the ADM and the EFT approaches at the NNLO spin(1)-spin(2) level was shown in Ref. [56].

In this section, we introduce the concept of spin in General Relativity, and make use of the ADM formalism discussed above to give an idea of the methods that have been employed to derive the complicated spin dynamics in the post-Newtonian approximation scheme. Besides of continuity with respect to the previous section, the reason why we prefer to emphasize the ADM method rather than EFT is simply that the former is more naturally related to the EOB, insofar as it directly provides an Hamiltonian (and canonical) formulation of spin. By contrast, the EFT formalism does not imply canonical equations of motion (for instance, the EFT potential involves higher-order derivatives of the spin) and needs a nontrivial reformulation in order to be brought into an Hamiltonian form [56].

2.2.1 Fermi transport of a gyroscope

In Sec 2.1.2 we have provided, within the context of the ADM formalism, a possible definition of spin in terms of the generators of the Poincaré group. Starting from this definition, we aim now at building a connection towards a more geometrical (and perhaps more intuitive) approach. Let us consider a point particle endowed with an intrinsic angular momentum $S^{\mu\nu}$ and moving with four-velocity u_μ in an external gravitational field. Because of the arguments exposed in Sec 2.1.2, we can assume the spin supplementary condition $S^{0\nu} = 0$ to be satisfied in the center-of-mass

frame of the particle. This equation can be covariantly generalized according to $S^{\mu\nu}u_\nu = 0$, which is called the Mathisson-Pirani supplementary condition. Let us now introduce the four-vector

$$S_\mu \equiv \frac{1}{2}\sqrt{-g}\epsilon_{\mu\nu\rho\sigma}u^\nu S^{\rho\sigma}, \tag{2.49}$$

where ϵ is the Levi-Civita symbol. [Here, although the four-vector S_μ is constructed from an antisymmetric tensor with six components, no information has got lost in the process. Indeed, the above equation can be inverted according to

$$S^{\mu\nu} = \frac{1}{\sqrt{-g}}\epsilon^{\mu\nu\rho\sigma}u_\rho S_\sigma, \tag{2.50}$$

whose validity is made possible by the Mathisson-Pirani supplementary condition.] Switching once again to the rest frame of the particle, we are left with a purely spatial angular momentum vector $S^\mu = (0, \boldsymbol{S})$ (with $\boldsymbol{S} = \frac{1}{2}\sqrt{-g}\epsilon^{ijk}S^{jk}$), that we may call a gyroscope. Notice that one is not allowed to consider the particle as being free-falling, and consequently its rest frame is non-Minkowskian. However, provided that the particle does not contain higher-order multipolar deformations, we can assume the gyroscope to be unaffected by the gravitational field, which translates into the equation $\frac{d\boldsymbol{S}}{dt} = 0$.

In an arbitrary frame moving with four-velocity u_μ, the gyroscope vector S^μ must satisfy the covariant identity $S^\mu u_\mu = 0$ (which follows from $S^\mu = (0, \boldsymbol{S})$ in the rest frame), while the covariant generalization of the time evolution equation takes the form (see e.g. [57])

$$\frac{DS^\mu}{d\tau} = S^\nu \frac{Du_\nu}{d\tau}u^\mu. \tag{2.51}$$

The latter equation is just the Fermi transport[6] $\frac{D_F}{d\tau}S^\mu = 0$ of S^μ under the condition $S^\mu u_\mu = 0$.

2.2.2 Multipole expansion of the energy-momentum tensor

For a proper formulation of the dynamics of a spinning particle, we must refer to the sequence of papers having started with the work of Mathisson [23] that was mentioned at the beginning of this chapter. The great contribution of Mathisson was connected with the idea of reducing the extremely complicated dynamics of an extended body (in principle, only a body of finite size can account for the existence of an intrinsic angular momentum) to the description of a point particle equipped with a given number of multipoles $m^{\mu\nu}$, $m^{\alpha\mu\nu}$, and so on. His method, harbinger of distribution theory, consisted in the use of an arbitrary symmetric "test" tensor $\varphi_{\mu\nu}$ with compact

[6] We remind the reader that the Fermi-Walker connection D_F along an observer curve with velocity u_μ is defined by

$$\frac{D_F}{d\tau}X^\mu = \frac{DX^\mu}{d\tau} + X^\nu u_\nu \frac{Du^\mu}{d\tau} - X^\nu \frac{Du_\nu}{d\tau}u^\mu, \tag{2.52}$$

and thus differs from the covariant derivative only when performed along non-geodesic curves. Given the orthogonal projectors P_t and P_S onto the time and space directions of the observer, the Fermi-Walker connection is uniquely determined by the property

$$\frac{D_F}{d\tau}X = \left(P_t\frac{D}{d\tau}P_t + P_S\frac{D}{d\tau}P_S\right)X \tag{2.53}$$

(where the covariant derivative $\frac{D}{d\tau}$ has to be understood as an operator multiplying the projectors). It is now clear why the Fermi-Walker connection is appropriate for determining the evolution of a gyroscope: a Fermi-transported spatial vector, unlike a parallel transported one, remains spatial even along non-geodesic curves.

support, so that the energy-momentum tensor $T^{\mu\nu}$ of the particle satisfies

$$\int d^4x\,\sqrt{-g}\,T^{\mu\nu}\varphi_{\mu\nu} = \int d\tau\left(m^{\mu\nu}\varphi_{\mu\nu} + m^{\alpha\mu\nu}\varphi_{\mu\nu;\alpha} + ...\right), \tag{2.54}$$

where the integration on the right hand side extends over the particle worldline. Tulczyjew [26] was the first to provide a fully covariant description of the dynamics of a pole-dipole particle. Exploiting the conservation law $T^{\mu\nu}{}_{;\nu} = 0$, he showed that there is an antisymmetric tensor $S^{\mu\nu}$ satisfying the Mathisson-Pirani condition

$$S^{\mu\nu}u_\nu = 0, \tag{2.55}$$

such that

$$\sqrt{-g}\,T^{\mu\nu} = \int d\tau\left(m\,u^\mu u^\nu\delta - (S^{\alpha(\mu}u^{\nu)}\delta)_{;\alpha}\right), \tag{2.56}$$

where δ denotes the four-dimensional delta function centered at the particle position. Applying the conservation law on this specific tensor, the Mathisson-Papapetrou equations

$$\frac{DS^{\mu\nu}}{d\tau} = 0, \qquad m\frac{Du^\mu}{d\tau} = -\frac{1}{2}R^\mu{}_{\nu\alpha\beta}u^\nu S^{\alpha\beta} \tag{2.57}$$

are obtained. The association of $S^{\mu\nu}$ with a spin tensor is quite natural. First of all, it is expected that the intrinsic angular momentum of a particle (being of dipole character) appears in the second term of the above multipole expansion, and specifically, it is clear that a spin tensor must be contracted with the four-velocity in order to get the right dimension. The correct rescaling $S^{\mu\nu} \to \lambda S^{\mu\nu}$ can be fixed by requiring correspondence with a non-relativistic system. For instance, an homogeneous extended body with mass density ρ and angular momentum density $s^i = \rho\,\epsilon^{ijk}r^j v^k$ has the energy-momentum components $T^{0i} = \rho\,v^i = -s^{ij}_{\ ,j}$, where, as usually, $s^{ij} \equiv \epsilon^{ijk}s^k$. On the other hand, setting $u^\mu \equiv (1,\mathbf{0})$ and $\tau \equiv t$, the non-relativistic limit of Eq. (2.56) yields $T^{0i} = S^{ij}\delta(\boldsymbol{x}-\boldsymbol{r})_{,i}$, which is nothing but the distribution-theory analogous of $-s^{ij}_{\ ,j}$, and thus we need no rescaling ($\lambda = 1$).

We conclude this introductory discussion about the spin by checking that the precession equation (2.57), toghether with the supplementary condition (2.55), is equivalent to the Fermi transport of a gyroscope discussed in Sec. 2.2.1. We already know that an antisymmetric tensor satisfying the Mathisson-Pirani condition, when used to construct a four-vector S^μ according to Eq. (2.49), yields the "gyroscope condition" $S^\nu u_\nu = 0$. Now, the Fermi transport equation (2.51) is recovered applying the first Mathisson-Papapetrou equation (2.57) to Eq. (2.49), and then inserting the inverse relation (2.50).

It is of course not necessary to remain in the Mathisson-Pirani spin gauge. The momentum p^μ can be considered as a separated variable in the energy-momentum tensor (2.56), which then becomes

$$\sqrt{-g}\,T^{\mu\nu} = \int d\tau\left(p^{(\mu}u^{\nu)}\delta - (S^{\alpha(\mu}u^{\nu)}\delta)_{;\alpha}\right), \tag{2.58}$$

with the first MP equation

$$\frac{DS^{\mu\nu}}{d\tau} = 2p^{[\mu}u^{\nu]}. \tag{2.59}$$

A modification of the spin gauge allows to change the relation between u^μ and p^μ. In particular, a different spin supplementary condition $\hat{S}^{\mu\nu} f_\nu = 0$ can be imposed, and using Eq. (2.59) to evaluate $\frac{D}{dt}(\hat{S}^{\mu\nu} f_\nu) = 0$, it leads to a new defintion $p^\mu(u^\nu, \hat{S}^{\nu\rho}, f^\nu)$ of the momentum.

In order to calculate spin-orbit and the spin(1)-spin(2) coupling, a pole-dipole approximation like the one given by Eq. (2.58) is sufficient. However, spin-squared terms need a quadrupolar approximation of the energy-momentum tensor. Tulczyjew's results can be formulated with the help of a quadrupolar tensor $J^{\alpha\beta\mu\nu}$, sharing the same symmetries of the four-dimensional Riemann tensor $R^{\alpha\beta\mu\nu}$, so that

$$\sqrt{-g}\, T^{\mu\nu} = \int d\tau \left(p^{(\mu} u^{\nu)} \delta - (S^{\alpha(\mu} u^{\nu)} \delta)_{;\alpha} + \frac{1}{3} J^{\alpha\beta\rho(\mu} R_{\alpha\beta\rho}{}^{\nu)} \delta - \frac{2}{3} \left(J^{\mu\alpha\beta\nu} \delta \right)_{;(\alpha\beta)} \right). \tag{2.60}$$

The tensor $J^{\alpha\beta\mu\nu}$ should then be further decomposed (see, e.g. Ref. [58]) in such a way to isolate those components that can actually be associated to a quadrupolar deformation due to spin.

2.2.3 ADM Hamiltonians with spin

We consider now a two-body system of spinning objects, labeled by the index $a = 1, 2$, with momenta $\tilde{p}_a^\mu$, four-velocities $\tilde{u}_a^\mu$ and spins $\tilde{S}_a^{\mu,\nu}$ in the Mathisson-Pirani gauge. Once the energy-momentum tensor of the system is known at the desired multipolar order (see, in addition to the work of Tulczyjew, the contributions of Dixon [27, 59, 60] for a formalism beyond the quadrupole, and Ref. [61] for a recent derivation due to Steinhoff and Puetzfeld), the procedure for calculating spin-couplings in the post-Newtonian approximation can be sketched as follows:

i) Introduce appropriate gauge choices, together with a spin supplementary condition, in order to identify a canonical set of variables.

ii) Iteratively solve the post-Newtonian expanded constraint equations, and express the ADM energy as a function of the canonical variables.

Point i) is the main subject of the already cited works of Hartung, Hergt, Schäfer and Steinhoff. When the canonical variables are found, point ii) is conceptually straightforward (up to possible issues arising from the regularization procedure), but is more demanding at the level of algebraic computations. We try now to summarize the main features related to the computation of the spin-orbit and the spin-spin couplings, with some details about point i). To this purpose, some elements of the symmetry generators approach [19, 35] will now be exposed.

Symmetry generator approach

The multipolar information contained in energy-momentum tensor $T^{\mu\nu}$ must be encoded into the ADM constraint equations (2.26). To this purpose, we reconsider the Einstein-Hilbert action in parametrized form (2.7). Under a variation of metric components N and N^i, the action yields a subset of the Einstein equations $G^{\mu\nu} = 0$, and namely their projection into the n_μ direction, which takes the form of the constraint equations $\mathcal{H}^{\text{field}} = 0$ and $\mathcal{H}_i^{\text{field}} = 0$. In the same way, the constraints (2.26), obtained varying of the total (field+matter) Lagrangian, must be equivalent to the n_μ-projection of the nonvacuum Einstein equations. Concretely, a separation of matter from fields leads to the identifications

$$\mathcal{H}^{\rm M} = N\sqrt{-g}T^{00} \qquad \mathcal{H}_i^{\rm M} = \sqrt{-g}T^0_{\ i}. \tag{2.61}$$

At this stage, $\mathcal{H}^{\rm M}$ and $\mathcal{H}_i^{\rm M}$ are only known as functions of the noncanonical variables $\tilde{u}_a^\mu$, $\tilde{p}_{a,\mu}$, $\tilde{S}^{\mu\nu}$ and γ_{ij}. A first step towards a canonical spin is that of imposing the Newton-Wigner spin-supplementary condition (with n_μ being the ADM unit vector pointing in time direction)

$$\left(n_\mu + \frac{\tilde{p}_{a,\mu}}{m}\right)\hat{S}_a^{\mu\nu} = 0, \tag{2.62}$$

which corresponds to a spin transformation $\tilde{S}_a^{\mu,\nu} \to \hat{S}_a^{\mu,\nu}$, and leads to canonical Poisson Brackets in flat spacetime, as shown in Ref. [62]. In this new gauge, the constancy of the Mathisson-Pirani spin scalar $\tilde{S}_a^{\mu\nu}\tilde{S}^a_{\mu\nu}$ translates into

$$\gamma^{ij}\gamma^{kl}\hat{S}^a_{ik}\hat{S}^a_{jl} \equiv 2s_a^2 = \text{const.} \tag{2.63}$$

Now, a spatial spin tensor $S^a_{(i)(j)}$ with constant magnitude [7]

$$\frac{1}{2}S^a_{(i)(j)}S^a_{(i)(j)} = S^a_{(i)}S^a_{(i)} = s_a^2 \tag{2.64}$$

can be constructed with a dreibein field $e_{ij} = e_{ji}$, according to $\hat{S}^a_{kl} \equiv e_{ki}\,e_{lj}\,S^a_{(i)(j)}$. An explicit expression of the dreibein e_{ij} can be achieved as a perturbation series in terms of the metric elements. The constant euclidean length of the spin vector $S^a_{(i)}$ is of crucial relevance, since a canonical angular momentum can only be (infinitesimally) rotated by the action of a Poisson Bracket, and never undergoes a change in magnitude. We may therefore adopt $S^a_{(i)(j)}$ as the final, canonical spin variables, and accordingly look for a possible definition of the canonical momentum (we recall that the above used $\tilde{p}^\mu$ and $\tilde{x}^\mu$ are *noncanonical*). We are now at the stage where the symmetry generators come into play. The idea is to exploit the fact that the Poincaré group generators (see the standard textbook [63] for a detailed introduction) for the two-body system must be given by

$$P_i = \sum_a p_{a\,i}, \qquad J_{ij} = \sum_a r_a^i\,p_{a\,j} - r_a^j\,p_{a\,i} + S_{a\,(i)(j)}, \tag{2.65}$$

where r_a^i, $p_{a\,j}$ and $S_{a\,(i)(j)}$ are the particle's canonical position, momentum and spin, respectively. Let us now spend few words to justify this statement. It is clear that, if the matter variables individually satisfy the Poincaré algebra, so do P_i and J_{ij} as well. On the other hand, the above expressions can easily be inferred from the generator properties [19]. For example, the generator P_i of an infinitesimal spatial translation $r_a^i \to r_a^i + \epsilon^i$ acts on the coordinate r_a^i as

$$\delta r_a^i = \epsilon^j\{r_a^i, P_j\}. \tag{2.66}$$

It is then clear that $P_i = \sum_a p_{a\,i}$, where $p_{a\,i}$ is the canonical conjugate to r_a^i. Under an infinitesimal rotation $r_a^i \to \omega^{ij}r_a^j$, where ω^{ij} is antisymmetric, we correspondingly have

$$\delta r_a^i = -\frac{1}{2}\omega^{jk}\{r_a^i, J_{jk}\}. \tag{2.67}$$

[7] As usually, we use the notation $S_{(i)} \equiv \epsilon_{ijk}S_{(j)(k)}$, with the Levi-Civita symbol ϵ.

Therefore, $\frac{\partial J_{jk}}{\partial p_{ai}} = -\delta_{ij}\, r_a^k + \delta_{ik} r_a^j$. Moreover, the spin tensor transforms as

$$\omega^{ik} S_{a(k)(j)} + \omega^{jk} S_{a(i)(k)} = \delta S_{a(i)(j)} = -\frac{1}{2}\omega^{kl}\{S_{a(i)(j)}, J_{kl}\}. \tag{2.68}$$

Since the $S_{a(i)(j)}$ is canonical (we recall the rule (2.46)), the Poisson Bracket $-\frac{1}{2}\omega^{kl}\{S_{a(i)(j)}, S_{a(k)(l)}\}$ exactly yields the left hand side of the above equation. By the above arguments, putting together orbital and spin degrees of freedom, Eq. (**??**) immediately follows. The consistency conditions obtained equating Eqs. (2.65) with Eqs. (2.34) and (2.42) eventually lead to an identification of the canonical variables r_a^i and p_{ai}, so that one can express (before solving the constraint equations) $\mathcal{H}$ and $\mathcal{H}_i$ as functions of γ_{ij}, p_{ai} and $S_{a(i)(j)}$[8]. More concretely, the ADM field momenta

$$P^i = -2\int dS_j\, \pi^{ij}, \qquad J^{ij} = -2\int dS_k \left(x^i \pi^{jk} - x^j \pi^{ik}\right) \tag{2.69}$$

are equivalent, up to second order in the spins and because of the constraint equations, to

$$P^i = \int d^3x\, \mathcal{H}_i^{\mathrm{M}}, \qquad J^{ij} = \int d^3x \left(x^i \mathcal{H}_j^{\mathrm{M}} - x^j \mathcal{H}_i^{\mathrm{M}}\right). \tag{2.70}$$

As discussed in Ref. [19],

$$\mathcal{H}_i^{\mathrm{M}} = \sum_a \left(p_{ai}\delta_a + \frac{1}{2}\left(S_{a(i)(j)}\delta_a\right)_{,j}\right) \tag{2.71}$$

is a solution for which (2.70) is equal to (2.65) (be aware that δ_a denotes here the three-dimensional delta function). It is now clear that this defines a relation between the canonical p_{ai}, the non-canonical p_μ and $S_{a(i)(j)}$, that can be used to define also $\mathcal{H}^{\mathrm{M}}$ in terms of γ_{ij}, p_{ai} and $S_{a(i)(j)}$. At this point, the post-Newtonian expanded constraint equations can be iterated to obtain, in the ADMTT gauge, φ and $\tilde{\pi}^{ij}$ as functions of the canonical variables. Expanded constraint equations valid up to second order in the spin can be found for example in Eqs. (7.4)-(7.6) of Ref. [35]. The sources $\mathcal{H}^{\mathrm{M}}$ and $\mathcal{H}_i^{\mathrm{M}}$ at the dipole approximation level are given by Eqs. (7.9)-(7.17) there, while Eqs. (6.40)-(6.43) of Ref. [19] must be taken into account for the quadrupolar approximation. As already mentioned, sovling the contraint equations may present some non-trivial issues due to regularization procedures (Hadamard *partie fine*, described e.g. in Ref. [10], can be used for both spin-orbit and spin-spin calculations up to NLO, while for the NNLO spin-orbit level a regularization based on the Riesz formula has been employed [37]). As in the Newtonian case discussed in Sec. 2.1.1, a volume integration of $\Delta\varphi$ leads to the ADM Hamiltonian $H^{\mathrm{ADM}}\left(r_a^i, p_{ai}, S_{a(i)(j)}, h_{ij}^{\mathrm{TT}}, \pi^{ij\,\mathrm{TT}}\right)$.

The reduction to a matter-only dynamics is performed by appropriately removing the independent field degrees of freedom h_{ij}^{TT} and $\pi^{ij\,\mathrm{TT}}$ under the requirement that no gravitational radiations is incoming from outwards. As explained e.g. in Ref. [10], this can done by solving the equation of motion for h_{ij}^{TT} and $\pi^{ij\,\mathrm{TT}}$, and by inserting the result into a Routhian reformulation of the ADM Hamiltonian. As a final result, one is simply lefft with the matter-only ADM Hamiltonian $H^{\mathrm{ADM}}\left(r_a^i, p_{ai}, S_{a(i)(j)}\right)$.

The method we have summarized here has been explicitly used to calculate the NLO spin-orbit and NLO spin(1)-spin(2) Hamiltonians [35]. Its underlying idea may also be used, in principle,

[8] Notice that for higher spin effects, the field momentum π^{ij} (and possibly also the metric γ_{ij}) shall be modified in order to incorporate spin terms, see Eq. (4.18) of Ref. [19].

to obtain the NLO spin-squared contribution, or even higher-order spin effects (although more consistency conditions will be necessary [19]). However, the first derivations of these Hamiltonians followed somewhat different paths, so that it is difficult to expose them here in a unified way. The calculation of the NLO spin-squared Hamiltonian [48, 49] was performed thanks to an ansatz for the source Hamiltonians $\mathcal{H}^{\mathrm{M}}$ and $\mathcal{H}_i^{\mathrm{M}}$, fixed imposing the Poincaré algebra. By contrast, the formalism used for the NNLO spin-orbit Hamiltonian [36, 37] constructs a rather explicit Lagrangian from which the equations of motion are derived.

Other methods

We briefly discuss the approach followed by Damour, Jaranowski and Schäfer [22]. Their method shall not be regarded as an alternative procedure for identifying the canonical variables, which may still have to be found with a method like the one exposed in the previous section. It rather provides a different way to construct the Hamiltonian, directly evaluating the Mathisson-Papapetrou equations of motions instead of solving the constraint equations to obtain the ADM energy. The approach, as it is formulated for the spin-orbit [22] and spin(1)-spin(2) [35] level, consists in expressing the first MP equation in the 3+1-decomposed form

$$\frac{d}{dt}S_{a(i)} = \epsilon_{ijk}\Omega_{aj}S_{a(k)}, \tag{2.72}$$

where $\Omega_{ai} \equiv \Omega_{ai}\left(N, N_j, \gamma_{jk}, u^j, S_{b(j)}\right)$. Once the Ω_{ai} are known in terms of the canonical variables at the requested order[9] , the spin-orbit, or spin(1)-spin(2) Hamiltonian immediately follows as

$$H_{\mathrm{so,s_1s_2}} = \sum_a S_{a(i)}\,\Omega_{ai}\left(x_a^j, p_{aj}, S_{b(j)}\right). \tag{2.73}$$

In the spin-orbit case, Ω_{ai} is of course meant to be spin-independent.

We finally mention the "action approach", where an appropriate ansatz for the Lagrangian is constructed and then fixed requiring particular conditions to be satisfied. A rederivation of the LO and NLO spin-orbit, as well as the LO spin-spin Hamiltonian has been possible within this framework, whereas the calculations for the NLO spin-spin coupling have never been truly tackled. We refer the reader to the detailed description in Ref. [19] for what concerns this particular method.

Reduced center-of-mass Hamiltonians

Thanks to the formalism sketched in this chapter, spin-dependent (conservative) Hamiltonians can thus be calculated in the post-Newtonian approximation. We expose here the results up to the highest order so far reached in the ADM formalism, i.e., as already mentioned, the NNLO spin-orbit and NLO spin-spin level. These Hamiltonians will depend, apart from the canonical variables $\boldsymbol{r}_a \equiv (r_a^1, r_a^2, r_a^3)$, $\boldsymbol{p}_a \equiv (p_{a1}, p_{a2}, p_{a3})$ and $\boldsymbol{S}_a \equiv (S_{a(1)}, S_{a(2)}, S_{a(3)})$, also on the individual masses m_1 and m_2 as external parameters. The existence of a center-of-mass G_i (that has been proven for all orders at which the ADM Hamiltonian has been calculated) allows a great simplification of the formulas. As discussed in Sec 2.1.2, it is then possible to define a center-of-mass momentum $\boldsymbol{P} \equiv \boldsymbol{p}_1 = -\boldsymbol{p}_2$. Because of the invariance under spatial translations and rotations,

[9] To do this, it may actually be necessary to solve the constraint equations, but at a lower spin-order than in the symmetry generator approach, for instance.

the Hamiltonians are then of the simple type $H(\boldsymbol{R},\boldsymbol{P},\boldsymbol{S}_1,\boldsymbol{S}_2)$, where $\boldsymbol{R}\equiv\boldsymbol{r}_1-\boldsymbol{r}_2$. A further simplification is introduced considering the dimensionless $\hat{H}\equiv H/\mu$, $\boldsymbol{r}\equiv\boldsymbol{R}/M$, $r\equiv|\boldsymbol{r}|$, $\boldsymbol{n}\equiv\boldsymbol{r}/r$ and $\boldsymbol{p}\equiv\boldsymbol{P}/\mu$, where $\mu=m_1\,m_2/M$ is the reduced mass and $M\equiv m_1+m_2$ the total mass of the system. The spins can accordingly be reduced to $\boldsymbol{\chi}_a=\boldsymbol{S}_a/m_a^2$, whose euclidean length reaches a maximal value of 1 for extremal black holes. The dependency on the individual masses will then also be encoded in a dimensionless way. The peculiar symmetry of the mass-centered two-body system is fully exploited introducing the symmetric mass-ratio $\nu\equiv\mu/M$, that ranges from 0, in the extreme mass-ratio limit, to 1/4 in the equal-mass case. To describe spin-dependent terms, where a formal asymmetry due to the separated variables $\boldsymbol{\chi}_1$ and $\boldsymbol{\chi}_2$ remains, one could also make use of the mass-ratios m_a/m_b, as in Chapter 4, 5, or $X_a\equiv m_a/M$, as in Chapter 6. However, if one fixes the labels so that, for instance, $m_1\geq m_2$, every dimensionless combination of the two masses is ultimately a function of ν:

$$\frac{m_1}{m_2}=\frac{1}{2\nu}\left(1+\sqrt{1-4\nu}\right)-1,\qquad \frac{m_2}{m_1}=\frac{1}{2\nu}\left(1-\sqrt{1-4\nu}\right)-1, \tag{2.74}$$

and

$$X_1=\frac{1}{2}\left(1+\sqrt{1-4\nu}\right),\qquad X_2=\frac{1}{2}\left(1-\sqrt{1-4\nu}\right). \tag{2.75}$$

The reduced purely orbital Hamiltonian reads, up to 3PN:

$$\hat{H}_{\rm N}=\frac{\boldsymbol{p}^2}{2}-\frac{1}{r} \tag{2.76}$$

$$\hat{H}_{\rm 1PN}=\frac{1}{8}(3\nu-1)\boldsymbol{p}^4-\frac{1}{2}(3+\nu)\frac{\boldsymbol{p}^2}{r}-\frac{\nu}{2}\frac{(\boldsymbol{n}\cdot\boldsymbol{p})^2}{r}+\frac{1}{2}\frac{1}{r^2} \tag{2.77}$$

$$\begin{aligned}\hat{H}_{\rm 2PN}=&\frac{1}{16}(1-5\nu+5\nu^2)\boldsymbol{p}^6+\frac{1}{8}(5-20\nu-3\nu^2)\frac{\boldsymbol{p}^4}{r}-\frac{\nu^2}{4}\frac{(\boldsymbol{n}\cdot\boldsymbol{p})^2\boldsymbol{p}^2}{r}\\&-\frac{3}{8}\nu^2\frac{(\boldsymbol{n}\cdot\boldsymbol{p})^4}{r}+\frac{1}{2}(5+8\nu)\frac{\boldsymbol{p}^2}{r^2}+\frac{3}{2}\nu\frac{(\boldsymbol{n}\cdot\boldsymbol{p})^2}{r^2}-\frac{1}{4}(1+3\nu)\frac{1}{r^3}\end{aligned} \tag{2.78}$$

$$\begin{aligned}\hat{H}_{\rm 3PN}=&\frac{1}{128}\left(-5+35\nu-70\nu^2+35\nu^3\right)\boldsymbol{p}^8+\frac{1}{16}\Bigg[\left(-7+42\nu-53\nu^2-5\nu^3\right)\frac{\boldsymbol{p}^6}{r}\\&+(2-3\nu)\,\nu^2\frac{\boldsymbol{p}^4(\boldsymbol{n}\cdot\boldsymbol{p})^2}{r}+3(1-\nu)\nu^2\frac{\boldsymbol{p}^2(\boldsymbol{n}\cdot\boldsymbol{p})^4}{r}-5\nu^3\frac{(\boldsymbol{n}\cdot\boldsymbol{p})^6}{r}\Bigg]\\&+\frac{1}{16}(-27+136\nu+109\nu^2)\frac{\boldsymbol{p}^4}{r^2}+\frac{1}{16}(17+30\nu)\nu\frac{\boldsymbol{p}^2(\boldsymbol{n}\cdot\boldsymbol{p})^2}{r^2}\\&+\frac{1}{12}(5+43\nu)\nu\frac{(\boldsymbol{n}\cdot\boldsymbol{p})^4}{r^2}+\left(-\frac{25}{8}+\left(\frac{\pi^2}{64}-\frac{335}{48}\right)\nu-\frac{23}{8}\nu^2\right)\frac{\boldsymbol{p}^2}{r^3}\\&+\left(-\frac{85}{16}-\frac{3\pi^2}{64}-\frac{7}{4}\nu\right)\nu\frac{(\boldsymbol{n}\cdot\boldsymbol{p})^2}{r^3}+\left(\frac{1}{8}+\left(\frac{109}{12}-\frac{21\pi^2}{32}\right)\nu\right)\frac{1}{r^4}.\end{aligned} \tag{2.79}$$

The spin-orbit coupling is most conveniently described through the spin combinations

$$\boldsymbol{\chi}\equiv\left(\frac{m_1}{m_2}\boldsymbol{\chi}_1+\frac{m_2}{m_1}\boldsymbol{\chi}_2\right),\qquad \boldsymbol{\chi}^*\equiv(\boldsymbol{\chi}_1+\boldsymbol{\chi}_2). \tag{2.80}$$

The center-of-mass result can be written as

$$\hat{H}_{\rm so} = \frac{\nu}{r^2}(\boldsymbol{n}\times\boldsymbol{p})\cdot\left(g_{\chi}^{\rm ADM}\boldsymbol{\chi} + g_{\chi^*}^{\rm ADM}\boldsymbol{\chi}^*\right), \tag{2.81}$$

where the post-Newtonian expansion of the so-called gyro-gravitomagnetic ratios $g_{\chi}^{\rm ADM}$ and $g_{\chi^*}^{\rm ADM}$ reads, up to NNLO, (see e.g. Ref. [64])

$$\begin{aligned} g_{\chi}^{\rm ADM} = 2 &+ \left[\frac{19}{8}\nu\boldsymbol{p}^2 + \frac{3}{2}\nu(\boldsymbol{n}\cdot\boldsymbol{p})^2 - (6+2\nu)\frac{1}{r}\right] + \left[-\frac{9}{8}\nu\left(1-\frac{22}{9}\nu\right)\boldsymbol{p}^4 - \frac{3}{4}\nu\left(1-\frac{9}{4}\nu\right)\boldsymbol{p}^2(\boldsymbol{n}\cdot\boldsymbol{p})^2\right. \\ &\left. + \frac{15}{16}\nu^2(\boldsymbol{n}\cdot\boldsymbol{p})^4 - \frac{157}{8}\nu\left(1+\frac{39}{314}\nu\right)\frac{\boldsymbol{p}^2}{r} - 16\nu\left(1+\frac{45}{256}\nu\right)\frac{(\boldsymbol{n}\cdot\boldsymbol{p})^2}{r} + \frac{21}{2}(1+\nu)\frac{1}{r^2}\right] \end{aligned} \tag{2.82}$$

$$\begin{aligned} g_{\chi^*}^{\rm ADM} = \frac{3}{2} &+ \left[\left(-\frac{5}{8}+2\nu\right)\boldsymbol{p}^2 + \frac{3}{4}\nu(\boldsymbol{n}\cdot\boldsymbol{p})^2 - (5+2\nu)\frac{1}{r}\right] + \left[\frac{1}{16}(7-37\nu+39\nu^2)\boldsymbol{p}^4\right. \\ &+ \frac{9}{16}\nu(2\nu-1)\boldsymbol{p}^2(\boldsymbol{n}\cdot\boldsymbol{p})^2 + \frac{1}{8}\left(27-129\nu-\frac{39}{2}\nu^2\right)\frac{\boldsymbol{p}^2}{r} - 6\nu\left(1+\frac{15}{32}\nu\right)\frac{(\boldsymbol{n}\cdot\boldsymbol{p})^2}{r} \\ &\left.+\left(\frac{75}{8}+\frac{41}{4}\nu\right)\frac{1}{r^2}\right]. \end{aligned} \tag{2.83}$$

The LO spin-spin Hamiltonian is given by

$$\hat{H}_{\rm ss}^{\rm LO} = \frac{1}{2r^3}\left(3(\boldsymbol{n}\cdot\boldsymbol{\chi}_0)^2 - \boldsymbol{\chi}_0^2\right), \tag{2.84}$$

with the spin combination $\boldsymbol{\chi}_0 \equiv X_1\boldsymbol{\chi}_1 + X_2\boldsymbol{\chi}_2$. Finally, the NLO spin-spin Hamiltonian is equal to

$$\begin{aligned} \hat{H}_{\rm ss}^{\rm NLO} = &\frac{3\nu}{4r^3}\left[\left(\nu+\frac{m_1}{m_2}(\nu-1)\right)\boldsymbol{p}^2\boldsymbol{\chi}_1^2 + \left(\frac{\nu}{2}-\frac{m_1}{m_2}\nu\right)(\boldsymbol{n}\cdot\boldsymbol{p})^2\boldsymbol{\chi}_1^2 + \left(-\frac{7}{2}\nu+\frac{m_1}{m_2}3(1-\nu)\right)\boldsymbol{p}^2(\boldsymbol{n}\cdot\boldsymbol{\chi}_1)^2\right. \\ &+ \frac{m_1}{m_2}5\nu(\boldsymbol{n}\cdot\boldsymbol{p})^2(\boldsymbol{n}\cdot\boldsymbol{\chi}_1)^2 + \frac{\nu}{3}(\boldsymbol{p}\cdot\boldsymbol{\chi}_1)^2 - \left(\nu+\frac{m_1}{m_2}2\nu\right)(\boldsymbol{n}\cdot\boldsymbol{p})(\boldsymbol{n}\cdot\boldsymbol{\chi}_1)(\boldsymbol{p}\cdot\boldsymbol{\chi}_1)\Big] \\ &+ \frac{\nu}{2r^4}\left[\left(\nu+\frac{m_1}{m_2}(5+\nu)\right)\boldsymbol{\chi}_1^2 - \left(5\nu+\frac{m_1}{m_2}(9+5\nu)\right)(\boldsymbol{n}\cdot\boldsymbol{\chi}_1)^2\right] + \frac{3\nu}{4r^3}\left[\left(\nu+\frac{m_2}{m_1}(\nu-1)\right)\boldsymbol{p}^2\boldsymbol{\chi}_2^2\right. \\ &+ \left(\frac{\nu}{2}-\frac{m_2}{m_1}\nu\right)(\boldsymbol{n}\cdot\boldsymbol{p})^2\boldsymbol{\chi}_2^2 + \left(-\frac{7}{2}\nu+\frac{m_2}{m_1}3(1-\nu)\right)\boldsymbol{p}^2(\boldsymbol{n}\cdot\boldsymbol{\chi}_2)^2 + \frac{m_2}{m_1}5\nu(\boldsymbol{n}\cdot\boldsymbol{p})^2(\boldsymbol{n}\cdot\boldsymbol{\chi}_2)^2 \\ &+ \frac{\nu}{3}(\boldsymbol{p}\cdot\boldsymbol{\chi}_2)^2 - \left(\nu+\frac{m_2}{m_1}2\nu\right)(\boldsymbol{n}\cdot\boldsymbol{p})(\boldsymbol{n}\cdot\boldsymbol{\chi}_2)(\boldsymbol{p}\cdot\boldsymbol{\chi}_2)\Big] + \frac{\nu}{2r^4}\left[\left(\nu+\frac{m_2}{m_1}(5+\nu)\right)\boldsymbol{\chi}_2^2\right. \\ &\left.- \left(5\nu+\frac{m_2}{m_1}(9+5\nu)\right)(\boldsymbol{n}\cdot\boldsymbol{\chi}_2)^2\right] + \frac{3\nu}{r^3}\left[-\left(\frac{1}{2}+\frac{\nu}{3}\right)\boldsymbol{p}^2(\boldsymbol{\chi}_1\cdot\boldsymbol{\chi}_2) + \left(1-\frac{\nu}{4}\right)(\boldsymbol{n}\cdot\boldsymbol{p})^2(\boldsymbol{\chi}_1\cdot\boldsymbol{\chi}_2)\right. \\ &+ \left(\frac{1}{2}+\frac{3}{4}\nu\right)\boldsymbol{p}^2(\boldsymbol{n}\cdot\boldsymbol{\chi}_1)(\boldsymbol{n}\cdot\boldsymbol{\chi}_2) + \frac{5}{2}\nu(\boldsymbol{n}\cdot\boldsymbol{p})^2(\boldsymbol{n}\cdot\boldsymbol{\chi}_1)(\boldsymbol{n}\cdot\boldsymbol{\chi}_2) + \left(\frac{1}{2}+\frac{\nu}{6}\right)(\boldsymbol{p}\cdot\boldsymbol{\chi}_1)(\boldsymbol{p}\cdot\boldsymbol{\chi}_2) \\ &s - \left(1+\frac{\nu}{4}-\frac{\nu}{2}\frac{m_1}{m_2}\right)(\boldsymbol{n}\cdot\boldsymbol{p})(\boldsymbol{n}\cdot\boldsymbol{\chi}_1)(\boldsymbol{p}\cdot\boldsymbol{\chi}_2) - \left(1+\frac{\nu}{4}-\frac{\nu}{2}\frac{m_2}{m_1}\right)(\boldsymbol{n}\cdot\boldsymbol{p})(\boldsymbol{p}\cdot\boldsymbol{\chi}_1)(\boldsymbol{n}\cdot\boldsymbol{\chi}_2)\Big] \\ &+ \frac{\nu}{r^4}\Big[6(\boldsymbol{\chi}_1\cdot\boldsymbol{\chi}_2) - 12(\boldsymbol{n}\cdot\boldsymbol{\chi}_1)(\boldsymbol{n}\cdot\boldsymbol{\chi}_2)\Big]. \end{aligned} \tag{2.85}$$

In order to avoid confusion, the dynamics of these Hamiltonians is better formulated by reintroducing the physical variables $H = \mu H$, $\boldsymbol{R} = Mr$, $\boldsymbol{P} = \mu p$ and $\boldsymbol{S}_a = m_a^2 \boldsymbol{\chi}_a$. We recall that the canonical Poisson Brackets for $\boldsymbol{R}$, $\boldsymbol{P}$ and $\boldsymbol{S}_1$, $\boldsymbol{S}_2$ are given by

$$\{R^i, P^j\} = \delta^{ij}, \qquad \{S_a^i, S_b^j\} = \delta_{ab}\epsilon^{ij}S_a^k, \tag{2.86}$$

while all others are zero. It follows that the equations of motion defined by the Hamiltonian are

$$\frac{d\boldsymbol{R}}{dt} = \{\boldsymbol{R}, H\} = \frac{\partial H}{\partial \boldsymbol{P}}, \qquad \frac{d\boldsymbol{P}}{dt} = \{\boldsymbol{R}, H\} = -\frac{\partial H}{\partial \boldsymbol{R}} \tag{2.87}$$

$$\tag{2.88}$$

for the orbital degrees of freedom and

$$\frac{d\boldsymbol{S}_a}{dt} = \{\boldsymbol{S}_a, H\} = \frac{\partial H}{\partial \boldsymbol{S}_1} \times \boldsymbol{S}_a \tag{2.89}$$

for the spins $\boldsymbol{S}_1$ and $\boldsymbol{S}_2$. From the last equation, it is clear that the spin magnitudes $|\boldsymbol{S}_a|$ are conserved. It is also possible to verify, with the above Poisson Brackets, that the total angular momentum $\boldsymbol{J} \equiv \boldsymbol{L} + \boldsymbol{S}_1 + \boldsymbol{S}_2$ is conserved, where $\boldsymbol{L} \equiv \boldsymbol{R} \times \boldsymbol{P}$ is the orbital angular momentum. In general, however, neither the spin vectors $\boldsymbol{S}_1$, $\boldsymbol{S}_2$, nor the the orbital angular momentum $\boldsymbol{L}$ are individually conserved: this leads to the *precession* of spins and of the orbital plane. [See the appendix of Chapter 4 for a discussion about the nonprecessing case, where spins and angular momentum are (and stay) aligned during the evolution.]

These properties remain true in the EOB dynamics. In the next chapters, we will investigate how the ADM Hamiltonians collected here can be reformulated into an EOB framework.

CHAPTER 3

The Effective-one-body approach

In this chapter, the reader is introduced to the EOB formalism [64–81]. In particular, the construction of the EOB Hamiltonian is followed step-by-step. We shall remark that, after a common origin [65–69], two branches of the EOB have developed in a rather separate way; we may call the first branch the "IHÉS model" [64, 70–73, 78, 79, 81] and the second one the "Maryland model" [74–77, 80]; without entering into details, we simply state here that the performance of both approaches is comparable (see, e.g, [82–92] for comparisons with numerical simulations). This thesis belongs to the IHÉS lineage. For simplicity reasons, we will later speak of the EOB as if it where an unique model, avoiding, most of the time, to discuss the differences with respect to the other existing version. Throughout this chapter, we use units with $G \equiv c \equiv 1$.

3.1 Motivation

Let us start with a qualitative description of the coalescence of two black holes according to the current picture. The *inspiral* phase of a coalescing process is characterized by a slow but steady increase in both the wave frequency and amplitude, that is well-described by post-Newtonian (PN) theory. During this phase, the system typically moves along a sequence of quasi-circular orbits, each characterized by a specific value of the angular momentum L. As the waves carry away energy and angular momentum, the orbits begin to shrink more and more rapidly until the radial velocity $\dot{r}$ can no longer be considered small with respect to the orbital frequency ω. This means that the orbits deviate from quasi-circularity, and the gravitating objects *plunge* into their reciprocal gravitational field. In correspondence of the *merger*, the wave amplitude reaches a maximum, and then suddenly drops. This is the *ringdown* phase, where the emitted wave modes are exponentially damped in the amplitude, so that the system asymptotically relaxes towards a stationary configuration.

We wish now to investigate, using very basic arguments, the breakdown of PN theory in describing the post-inspiral waveform of a coalescing process. In particular, the aim is to bring into evidence, with a purely conservative approach (and without solving the equations of motion) the bad strong-field behavior of PN theory. We believe that the approach we are going to illustrate, despite its low accuracy, allows to understand that the problem of PN theory is already present

at the conservative level. Since this entire work is ultimately devoted to Hamiltonian dynamics, we think that this is a good point to start in order to introduce the EOB approach.

In practice, we shall simply consider circular orbits as they are described by the conservative dynamics up to 3PN accuracy, and compute the quadrupolar (Newtonian) radiation produced in correspondence of each of these orbits. Given a center-of-mass Hamiltonian $H(R, P_R, L)$ in polar variables, circular orbits are simply defined by

$$\frac{\partial}{\partial R} H(R, P_R = 0, L) \equiv 0 \tag{3.1}$$

and are parametrized by the separation radius R, in the sense that the angular momentum for circular orbits is given by $L_{\rm circ} = L_{\rm circ}(R)$. The orbital frequency $\omega_{\rm circ}$ of circular orbits is then simply given by

$$\omega_{\rm circ}(R) = \frac{\partial}{\partial L} H(R, P_R = 0, L)\Big|_{L=L_{\rm circ}}. \tag{3.2}$$

Depending on the considered model, circular orbits may cease to exist below a given separation radius, thereby defining a last stable orbit (LSO)[1] (this happens, as we shall see, for the 1PN ADM dynamics). Beyond the LSO, our simple approach for the evaluation of the dynamics needs a different strategy: we fix energy and angular momentum as given at the LSO ($E \equiv E_{\rm LSO}$, $L \equiv L_{\rm LSO}$) and model the subsequent infall as and *adiabatic plunge*. Concretely, in the region $R < R_{\rm LSO}$, we calculate the radial velocity vector $P_R^{\rm plg}(R)$ so that

$$H(R, P_R^{\rm plg}, L_{\rm LSO}) = E_{\rm LSO} = H(R_{\rm LSO}, P_R = 0, L_{LSO}). \tag{3.3}$$

This allows to calculate the (adiabatic) angular frequency during the plunge according to

$$\omega_{\rm plg}^{\rm ad}(R) = \frac{\partial}{\partial L} H(R, P_R^{\rm plg}, L)\Big|_{L=L_{\rm LSO}}. \tag{3.4}$$

During a nonadiabatic (and more realistic) plunge, modeled by considering radiation reaction effects, the orbital angular momentum L gets reduced with respect to the adiabatic $L = L_{\rm LSO}$ because of angular-momentum radiation. By thinking in terms of the Newtonian angular momentum $L_{\rm Newt} \equiv \mu R^2 \omega$, it is therefore reasonable to suppose that the "non-adiabatic" frequency $\omega_{\rm plg}^{\rm nad}$ during plunge is smaller than $\omega_{\rm plg}^{\rm ad}$ when compared at the same separation radius R,

$$\omega_{\rm plg}^{\rm nad}(R) \lesssim \omega_{\rm plg}^{\rm ad}(R) \tag{3.5}$$

We will come again to this point later.

Let us consider an equal-mass ($m_1 = m_2 \equiv M/2$) binary system moving on the $\theta = \pi/2$ plane. For quasi-circular orbits[2] , $\dot{R} \ll \omega$, the $l = m = 2$ (Newtonian) spherical mode reads (see Sec (3.A) for more details)

$$h^{22} = -8\frac{M}{D}\sqrt{\frac{\pi}{5}}(R\omega)^2 e^{-2i\varphi}. \tag{3.6}$$

[1] Here we use the notation $R_{\rm LSO}$, $L_{\rm LSO}$ and $E_{\rm LSO}$ for indicating the radius, angular momentum and energy at the LSO.

[2] We must recall that, however, the orbits sensibly deviate from circularity during the plunge. The effect of next-to-quasi-circular terms during the plunge and merger in the EOB description is shown, e.g. in Fig. 9 of Ref. [91], and is clearly that of reducing the amplitude of the waveform during plunge and merger.

The existence of a maximum in the wave amplitude is therefore the result of a subtle interplay between the (shrinking) radius R and the (increasing) orbital frequency ω. A too large ω may prevent the maximum to build up. We plot in Fig 3.1 the distance-normalized amplitude $|h^{22}|D/M$ calculated with the above prescription, for the Newtonian (N) and post-Newtonian Hamiltonians up to 3PN (see Eqs. (2.76)-(2.79)), as a function of the reciprocal radius $u \equiv M/R$. More precisely, the curve N is built taking the Hamiltonian $H \equiv H_N$, Eq. (2.76); the curve 1PN is obtained with $H \equiv H_N + H_{1PN}$, Eqs. (2.76)-(2.77), and analogously for the 2PN and 3PN Hamiltonians.

Because of Kepler's 3rd law, $\omega^2 R^3 = M$, the Newtonian curve is simply a linear function of u. The 1PN Hamiltonian is the only one, among the Hamiltonians considered here, that presents an LSO, which is reached for $r \approx 9.9M$, $u \approx 0.10$ and is marked by a small circle on the plot. We stress that the 1PN curve is calculated with $\omega = \omega_{\rm circ}(u)$ until the LSO, and is continued to the right by $\omega = \omega^{\rm ad}_{\rm plg}(R)$, while all other curves N, 2PN and 3PN are just calculated with $\omega = \omega_{\rm circ}(R)$. The 1PN curve is stopped as soon as $P_R^{\rm plg}/\mu$ becomes of order unity. We notice (i) a bad strong-field convergence of PN terms, since the predictions are very different depending on the PN order taken into account, and (ii) the absence of a maximum in the Newtonian, 2PN and 3PN wave amplitudes. It is therefore clear that PN theory (at least up to the considered order) is not able to describe the plunge and merger. Due to this high strong-field unreliability, in the data-analysis of PN-generated waveforms the inspiral process is typically truncated in correspondence of the Schwarzschild LSO, $R^{\rm Schw}_{\rm LSO} = 6M$, $u^{\rm Schw}_{\rm LSO} \approx 1.67$ (see e.g. [93]). In the past, the most common answer to the failure of PN theory was that of invoking Numerical Relativity as the only tool able to accurately describe the complete waveform of a comparable-mass system (this was, just to mention an influent personality, the point of view of Kip Thorne, see e.g. [94]). Numerical Relativity methods have experienced a breakthrough in 2005 thanks to Pretorius [95], Campanelli, Lousto, Marronetti and Zlochower [96], and Baker, Centrella, Choi, Koppitz and van Meter [97], and have since then greatly improved, producing a large number of waveforms (see, in particular, the public catalog [98] of the Caltech-Cornell-CITA Simulating eXtreme Spacetimes collaboration). The generation of an high-resolution waveform, however, still needs days to months of supercomputing time.

As early as 1999, Buonanno ad Damour [65], motivated by a strong confidence in analytical methods, proposed the effective-one-body approach, which essentially is a reformulation (and *resummation*) of PN results into a new, refined model, as an attempt to push the analytical description of coalescing binaries beyond the inspiral phase. There will be time, starting from the next section, to discuss the details of the EOB. Let us now just reveal in advance some of its features. The (nonspinning) EOB Hamiltonian has the form [65]

$$H_{\rm EOB}(R, P_R, L) = M\sqrt{1 + 2\nu\left(\frac{1}{\mu}\sqrt{A(R,\nu)\left(\mu^2 + \frac{1}{B(R,\nu)}P_R^2 + \frac{L^2}{R^2} + Q_4\right)} - 1\right)}, \tag{3.7}$$

where $A(R,\nu)$ and $B(R,\nu)$ are specific EOB functions (see the next sections) that encode the PN couplings up to a given order (currently known up to 3PN for B and 4PN for A), and Q_4 is a quartic-in-momenta 3PN term, $Q_4 = 2(4-3\nu)\nu P_R^4/r^2$. In particular, since the contributions due to B and Q_4 are vanishing under the assumption of circular orbits, the EOB *radial potential* $A(R,\nu)$ plays the most important role.

This Hamiltonian, unlike the expanded Newtonian, 2PN and 3PN ones, predicts the existence of an LSO. We show in Fig (3.2) a plot analogous to Fig (3.1), but with the EOB Hamiltonian instead of the PN expanded one, where the distance-normalized (Newtonian) wave amplitude $|h^{22}|R/M$

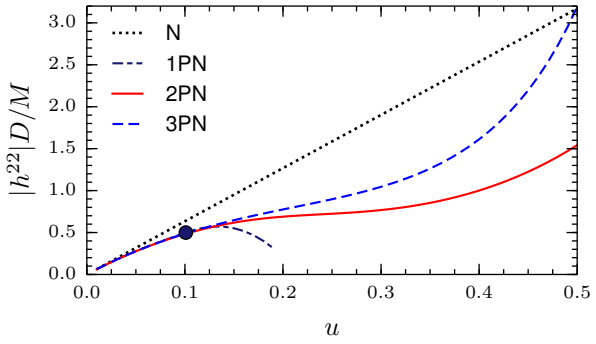

Figure 3.1: *Distance-normalized (Newtonian) wave amplitude $|h^{22}|D/M$ as a function of the reciprocal, dimensionless radial separation $u = M/R$, for the Newtonian (N), 1PN, 2PN and 3PN conservative dynamics. See the main text for details about the approach used to evaluate the dynamics. The small circle correspond to the 1PN LSO.*

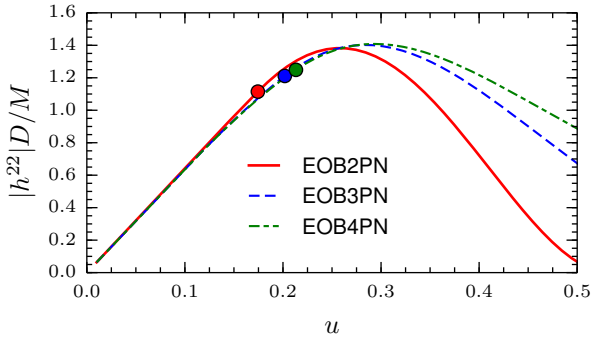

Figure 3.2: *Distance-normalized (Newtonian) wave amplitude $|h^{22}|D/M$ as a function of the reciprocal, dimensionless radial separation $u = M/R$, for the EOB conservative dynamics at the 2PN, 3PN and 4PN accuracy level. See the main text for details about the approach used to evaluate the dynamics. The small circles mark the LSO.*

is plotted against the EOB reciprocal radius[3] u. The curves corresponding to the EOB dynamics at 2PN, 3PN and 4PN order are plotted. As for the curve 1PN in Fig (3.1), at the left of the LSO (which is marked by a dot) the orbital frequency is taken for circular orbits, $\omega = \omega_{\rm circ}$, while ad the right of the LSO we model it according to the adiabatic plunge, $\omega = \omega^{\rm ad}_{\rm plg}$.

We can immediately notice that the EOB predicts, at all order plotted here, a peak of the waveform amplitude at $R \approx 3M$. This is a strong hint that the EOB may actually be able to describe the dynamics beyond the inspiral phase. We can define this peak as the *moment of merger* in the EOB description. This feature, which is related, as discussed above, to an orbital frequency ω that does not increase too much, can be imputed to the particular behavior of the EOB radial potential $A(R,\nu)$, since $\omega \propto A(R,\nu)L/r^2$. In fact, as we will see later, $A(R,\nu)$ is a *ν-deformed* version of the Schwarzschild radial potential $A^{\rm Schw}(R) \equiv 1 - 2M/R$, which is zero for $R = 2M$. As we shall see, $A(R,\nu)$, similarly to $A^{\rm Schw}(R)$, is small in the crucial region regulating the merger.

[3] Be careful that the EOB canonical variables differ from the PN ones by a canonical transformation at subleading order. For this reason, although the wave-amplitude plotted on the y-axis is gauge invariant, the radial coordinate at the x-axis is not, and therefore Fig (3.2) cannot be compared one-to-one with Fig (3.1). This fact does not alter, however, a qualitative discussion about the existence of a maximum of the wave amplitude.

Because of some remarks that we have made above, (see Eq. (3.5), and Footnote 2), we *a priori* expect that both the inclusion of radiation-reaction effects into the equations of motion, and of next-to-quasi-circular effects into the waveform, have the effect of reducing the wave amplitude in the post-inspiral stages, thereby preserving the existence of a peak.

The simple arguments discussed here, though quite representative in showing a fundamental difference between EOB approach and PN theory, cannot go beyond the qualitative level. It would be *naïve* to sing the praises of the EOB Hamiltonian for the only reason that it predicts the existence of a peak in the wave amplitude. A serious analysis requires, of course, a quantitative comparison between EOB- and Numerical Relativity generated waveforms. Current (tuned) EOB models are able to generate complete waveforms, in the case of non spinning binaries, with a final phase difference with respect to Numerical Relativity that does not exceed the numerical error of the simulation itself, see e.g. [90–92]. This is an extremely accurate performance, and should be considered as the strongest argument in favor of the EOB.

3.2 The EOB energy mapping

The EOB approach finds its birth with the already mentioned work of Buonanno and Damour [65]. Let us consider a gravitating (nonspinning) binary system with masses m_1 and m_2, described by the action (see Sec. 2.1.1)

$$I_{\rm tot}[R_1^\mu, R_2^\mu, g_{\mu\nu}] = -\int m_1 ds_1 - \int m_2 ds_2 + I[g_{\mu\nu}], \tag{3.8}$$

with the matter contributions[4] $ds_a = \sqrt{-g_{\mu\nu} dR_a^\mu dR_a^\nu}$ and the Einstein-Hilbert action $I[g_{\mu\nu}]$ (i.e., the interaction term). Here, according to what we have exposed in Chapter 2, we consider a matter-only dynamics, which is ultimately described by the Hamiltonians that are collected – up to 3PN – in Sec 2.2.3. [we recall that these Hamiltonians are obtained, within a PN-expansion framework, by (i) an ADM-canonicalization of the total (field + matter) action and (ii) setting to zero the independent field degrees of freedom (representing incoming gravitational-wave radiation).] Let $H(\boldsymbol{r}, \boldsymbol{p})$ be the PN-expanded Hamiltonian reproducing the dynamics (3.8) up to 2PN, see Eqs. (2.76)-(2.78)[5]. For later convenience, we define H such as to also involve the (constant) rest-mass contribution $M = m_1 + m_2$,

$$H \equiv M + \mu(\hat{H}_{\rm N} + \hat{H}_{\rm 1PN} + \hat{H}_{\rm 2PN}). \tag{3.9}$$

The purpose of the EOB approach is to *map* the matter-only part of the two-body dynamics defined by Eq. (3.8) to the geodesic motion of a single particle of mass m_0 in an effective metric $g^{\rm eff}_{\mu\nu}$,

$$I_{\rm eff}[R^\mu_{{\rm eff},0}] = -\int m_0 \, ds_0^{\rm eff}, \tag{3.10}$$

with $ds_0^{\rm eff} = \sqrt{-g^{\rm eff}_{\mu\nu} dR^\mu_{{\rm eff},0} dR^\nu_{{\rm eff},0}}$ denoting the line element along the trajectory of the effective particle. By exploiting some consistency conditions, we will now constrain the effective problem

[4] Notice that $-\sum_a \int m_a ds_a \equiv I_M$ in the notation of Sec. 2.1.1.

[5] In order to fix the EOB energy mapping, it is actually sufficient to consider the 2PN dynamics, as in Ref. [65]. Higher-order PN terms will then be inserted into the EOB without modifying the basic EOB structure we are exposing here.

up to some degree. First of all, since the two-body Hamiltonian $\hat{H}(\boldsymbol{r},\boldsymbol{p})$ is invariant under time translations and spatial rotations, the effective metric is required to be static and spherically symmetric. Assuming a Schwarzschild-type gauge[6] one can make the general ansatz

$$g^{\rm eff}_{\mu\nu}dR^\mu_{\rm e}\,dR^\nu_{\rm e} = -A(R_{\rm e},m_1,m_2)dt^2_{\rm e} + B(R_{\rm e},m_1,m_2)dR^2_{\rm e} + R^2_{\rm e}\left(d\theta^2_{\rm e}+\sin^2\theta_{\rm e}\,d\varphi^2_{\rm e}\right), \tag{3.11}$$

with some functions $A(R_{\rm e},m_1,m_2)$ and $B(R_{\rm e},m_1,m_2)$ that are still to be determined. In Eq. (3.11), we have introduced the effective coordinates $t_{\rm e}$, $R_{\rm e}$, $\theta_{\rm e}$ and $\varphi_{\rm e}$ ("e" is a shorthand for "eff") in which the effective problem is described. The metric $g^{\rm eff}_{\mu\nu}$ is expected to behave, in the weak field regime, like a Newtonian field. We may thus introduce a second mass parameter $M_0(m_1,m_2)$, and require that A and B expand as

$$A(R_{\rm e},m_1,m_2) \approx 1 - \frac{2M_0}{R_{\rm e}} + \mathcal{O}\left(\frac{M_0^2}{R_{\rm e}^2}\right) \tag{3.12}$$

$$B(R_{\rm e},m_1,m_2) \approx 1 + \mathcal{O}\left(\frac{M_0}{R_{\rm e}}\right). \tag{3.13}$$

The dynamics defined by the effective metric (3.11)-(3.13), when taken at Newtonian order, is equivalently described by the Hamiltonian

$$H^{\rm eff}_{\rm N} = \frac{\boldsymbol{P}^2_{\rm e}}{2m_0} - \frac{M_0\,m_0}{R_{\rm e}}. \tag{3.14}$$

It is then very natural to define a "mass mapping" $m_1,\,m_2 \to m_0,\,M_0$ between the two-body and the effective system according to

$$m_0 \equiv \mu = \frac{m_1\,m_2}{m_1+m_2}, \qquad M_0 \equiv M = m_1+m_2, \tag{3.15}$$

so that (3.14) becomes identical to the Newtonian Hamiltonian. Notice the obvious, but important fact that both combinations μ and M are *symmetric* under exchange of the particle labels 1 and 2, thereby respecting the formal symmetry of the two-body problem. At higher PN orders this symmetry must be satisfied as well, and the effective metric, which may no longer be a function of the total mass M alone, should also depend, say, on the symmetric mass ratio $\nu \equiv \mu/M$. We might thus introduce the dimensionless variable $u \equiv M/R_{\rm e}$, and revisit the functional dependence of the A and B potentials by writing $A(u,\nu) \equiv A(R_{\rm e},m_1,m_2)$ and $B(u,\nu) \equiv A(R_{\rm e},m_1,m_2)$.

Now that we have refined the notation, we can make a further step and require that, in the test particle limit $\nu \to 0$, the effective metric reduces to the Schwarzschild metric

$$A(u,\nu=0) = 1-2u \qquad B(u,\nu=0) = \frac{1}{1-2u}. \tag{3.16}$$

Let us remark that the Newtonian limit (3.12)-(3.13) implies that, at the orders $\mathcal{O}(1)$ and $\mathcal{O}(u)$, there can be no ν-deformation of the Schwarzschild structure (3.16).

Up to now, we have only made the simplest part of the work. In order to associate (at 2PN accuracy) the two-body dynamics (3.8) with the effective one (3.10), we need to follow more closely the discussion of the original paper [65], which tackles the problem using an Hamilton-Jacobi formalism. Consider again the two-body ADM dynamics: since, as mentioned, $H(\boldsymbol{R},\boldsymbol{P})$

[6] Here, under "Schwarzschild-type gauge" we mean the particular choice of the radial coordinate $R_{\rm e}$ for which the angular line element is equal to $d\Omega^2_{\rm e} = R^2_{\rm e}\left(d\theta^2_{\rm e}+\sin^2\theta_{\rm e}\,d\varphi^2_{\rm e}\right)$.

(Eq. (3.9)) is invariant under time translations and space rotations, $E \equiv H(\boldsymbol{R},\boldsymbol{P})$ and $\boldsymbol{L} \equiv \boldsymbol{R}\times\boldsymbol{P}$ are both conserved quantities. Then, the Hamilton-Jacobi equation defined by $H(\boldsymbol{R},\boldsymbol{P})$,

$$H\left(\boldsymbol{R}, \frac{\partial S}{\partial \boldsymbol{R}}\right) + \frac{\partial S}{\partial t} = 0 \tag{3.17}$$

can be separated according to

$$S = -E\,t + l\,\varphi + S_R(R,E,L), \tag{3.18}$$

where we have used the polar representation $\boldsymbol{R} \equiv (R\cos\varphi, R\sin\varphi, 0)$, and with $L \equiv |\boldsymbol{L}|$. The radial action variable[7]

$$I_R(E,L) \equiv \mu M \frac{2}{2\pi}\int_{R_{\min}}^{R_{\max}} dR \frac{dS_R}{dR}(R,E,L) \tag{3.19}$$

allows to obtain a gauge-invariant relation between the energy E, the orbital angular momentum $L \equiv \mu M\, l$, and the Delaunay action variable $\mathcal{N} \equiv I_R + L$. At 2PN accuracy, the result is of the form [99]

$$\frac{E(\mathcal{N},L)}{\mu} = \frac{M}{\mu} - \frac{(\mu M)^2}{2\mathcal{N}}\left(1 + (\mu M)^2\left(\frac{c_{3,1}}{\mathcal{N}L} + \frac{c_{4,0}}{\mathcal{N}^2}\right) + (\mu M)^4\left(\frac{c_{3,3}}{\mathcal{N}L^3} + \frac{c_{4,2}}{\mathcal{N}^2L^2} + \frac{c_{5,1}}{\mathcal{N}^3L} + \frac{c_{6,0}}{\mathcal{N}^4}\right)\right), \tag{3.20}$$

where $c_{i,j}$ are ν-dependent coefficients. Notice that this result is formally equivalent to the energy-level formula for the Bohr-Sommerfeld atom model, with $\mathcal{N}/\hbar$, $L/\hbar$, and the two body gravitational coupling constant $\mu M = m_1 m_2$ playing the role of the principal quantum number, the angular momentum quantum number and the fine-structure constant, respectively.

The effective problem can be formulated in a very similar way. The (geodesic) Hamilton-Jacobi equation[8] related to $g^{\rm eff}_{\mu\nu}$ (we recall the associations $m_0 \equiv \mu$, $M_0 \equiv M$),

$$g^{\mu\nu}_{\rm eff}\frac{\partial S_{\rm eff}}{\partial R^\mu_{\rm e}}\frac{\partial S_{\rm eff}}{\partial R^\nu_{\rm e}} + \mu^2 = 0, \tag{3.21}$$

must be solved for a principal function of the type

$$S_{\rm eff} = -E_{\rm e}\,t_{\rm e} + L_{\rm e}\,\varphi_{\rm e} + S_{{\rm e},R}(R_{\rm e}, E_{\rm e}, l_{\rm e}), \tag{3.22}$$

where $E_{\rm e}$ and $L_{\rm e}$ are the (conserved) effective energy and angular momentum. The Hamilton-Jacobi equation admits energy levels of the formal type

$$\frac{E_{\rm e}(\mathcal{N}_{\rm e}, L_{\rm e})}{\mu} = 1 - \frac{(\mu M)^2}{2\mathcal{N}_{\rm e}}\left(1 + (\mu M)^2\left(\frac{c^{\rm e}_{3,1}}{\mathcal{N}_{\rm e}L_{\rm e}} + \frac{c^{\rm e}_{4,0}}{\mathcal{N}^2_{\rm e}}\right) + (\mu M)^4\left(\frac{c^{\rm e}_{3,3}}{\mathcal{N}_{\rm e}L^3_{\rm e}} + \frac{c^{\rm e}_{4,2}}{\mathcal{N}^2_{\rm e}L^2_{\rm e}} + \frac{c^{\rm e}_{5,1}}{\mathcal{N}^3_{\rm e}L_{\rm e}} + \frac{c^{\rm e}_{6,0}}{\mathcal{N}^4_{\rm e}}\right)\right), \tag{3.23}$$

[7] A complete solution of the Hamilton-Jacobi equation would require an indefinite integral over R, so as to explicitly calculate $S_R(R,E,L)$. Here, however, we do not need to fully solve the equations of motion, and the action variable $I_R(E,L)$ (which is more easily obtained than S_R) turns out to be sufficient.

[8] The reader may be confused by the different formulations of the Hamilton-Jacobi equation Eq. (3.17), which is in 3+1 form, and Eq. (3.21), which is in covariant form. We remark that the covariant Hamilton-Jacobi equation (3.21) can be cast into the 3+1 formulation $H^{\rm eff}\left(\boldsymbol{R}_{\rm e}, \frac{\partial S_{\rm eff}}{\partial \boldsymbol{R}_{\rm e}}\right) + \frac{\partial S_{\rm eff}}{\partial t_{\rm e}} = 0$ for the Hamiltonian $H_{\rm eff} = N_{\rm eff}\sqrt{\mu^2 + \gamma^{ij}_{\rm eff}P_{{\rm e},i}P_{{\rm e},j}} + N^i_{\rm eff}P_{{\rm e},i}$, Eq. (2.23).

with coefficients $c^{\rm e}_{i,j}$ depending on the structure of $A(u,\nu)$ and of $B(u,\nu)$. A comparison of the formulae (3.20) and (3.23) is the key to an EOB formulation of the two-body dynamics. By thinking in terms of the quantum correspondence principle, according to which $\mathcal{N}$ and L are quantized in terms of $\hbar$, Buonanno and Damour found very natural to identify the two-body action variables $\mathcal{N}$ and L with the effective ones $\mathcal{N}_{\rm e}$ and $L_{\rm e}$, i.e. to set

$$\mathcal{N}_{\rm e} \equiv \mathcal{N}, \qquad L_{\rm e} \equiv L. \tag{3.24}$$

It is also evident, however, that the rest-mass contributions to Eq. (3.20) and Eq. (3.23) differ from one another by a factor ν, and that this issue cannot be corrected by any relativistic, subleading-order modification of the "mass mapping" (3.15). In order to establish a correspondence between the two formalisms, a nontrivial "energy mapping"

$$E \to E_{\rm e} \tag{3.25}$$

must be defined as well. [Notice that a redefinition of the energy can be understood as a different gauge choice for the time coordinate. In particular, since $E \equiv -\delta I/(\delta t)$ (see e.g. Eq. (2.12)), (3.25) corresponds to a "time mapping" $t \to t_{\rm e}$ satisfying $dE/dE_{\rm e} = dt_{\rm e}/dt$.] The result found by Buonanno and Damour is remarkable: the weak-field and test-mass lmits (3.12), (3.13) and (3.16)[9] , together with the identification of the effective masses (3.15) and of the action variables $\mathcal{N}$ and L (3.24), uniquely lead to the relation

$$\frac{E_{\rm e}}{\mu} = \frac{E^2 - m_1^2 - m_2^2}{2m_1 m_2}, \tag{3.26}$$

which is of an astonishing simplicity and elegance[10]. Furthermore, the PN expansion of the potentials $A(u,\nu)$ and $B(u,\nu)$ is uniquely defined up to 2PN, and reads

$$A(u,\nu) = 1 - 2u + 2\nu u^3 + \mathcal{O}(u^4) \tag{3.27}$$

$$B(u,\nu) = 1 + 2u + (4 - 6\nu)u^2 + \mathcal{O}(u^3). \tag{3.28}$$

We have here a second remarkable feature: the 11 independent terms composing the 1PN and 2PN Hamiltonians in ADM coordinates, Eqs. (2.77)-(2.78), reduce, in the EOB, to 2 ν-dependent terms only. In particular, the radial potential $A(u,\nu)$ does not involve any ν-deformation at 1PN accuracy. The dramatic reduction of coefficients with respect to the ADM case is one of the most spectacular features of the EOB approach.

3.3 Canonical transformations

At this point, one can solve the Hamilton-Jacobi equation (3.21) for the effective problem and map, according to Eq. (3.26), the effective Hamiltonian into a "real" one. We leave however this task for the next section, and first discuss the formalism describing the relations between the ADM and EOB coordinates, that will turn out to be very useful later. For simplicity, and for

[9] More precisely, instead of Eqs. (3.12)-(3.13), (3.16), it is sufficient to constrain the expanded form of A and B according to $A(u,\nu) \equiv 1 - 2u + \mathcal{O}(u^2)$ and $B(u,\nu) \equiv 1 + 2u + \mathcal{O}(u^2)$, which is a weaker requirement.

[10] Quoting [65], if we consider two-particle scattering states $E^2 = (p_1^\mu + p_2^\mu)^2$, the function $E_{\rm e}(E^2)$ given by (3.26) is «the most natural symmetric function of the asymptotic 4-momenta p_1^μ, p_2^μ of a two-particle system which reduces, in the test-mass limit $m_1 \ll m_1$, to the energy of m_2 in the rest frame of m_1».

continuity with respect to the previous section, we consider the ADM and EOB Hamiltonians as being equivalent at the 2PN accuracy level. Anyway, one should keep in mind that the formalism discussed here can be generalized to higher orders in a rather straightforward way.

In Sec (3.2), the two-body dynamics has been associated to the effective one by means of the gauge invariant relations (3.20) and (3.23). The ADM *phase-space coordinates* $\boldsymbol{R}$ and $\boldsymbol{P} \equiv (\partial S)/(\partial \boldsymbol{R})$, however, are not the same of the effective (or EOB) phase-space coordinates $\boldsymbol{R}_{\rm e}$ and $\boldsymbol{P}_{\rm e} \equiv (\partial S_{\rm eff})/(\partial \boldsymbol{R}_{\rm e})$ (that are rather of Schwarzschild type). Since both ADM and EOB descriptions are Hamiltonian (see Sec 3.4 for an explicit formulation of the EOB Hamiltonian $H_{\rm EOB}(\boldsymbol{R}_{\rm e}, \boldsymbol{P}_{\rm e})$) and equivalent to each other up to 2PN accuracy level, their respective phase-space coordinates must be related to each other by a corresponding canonical transformation. Denoting by $H_{\rm EOB}(\boldsymbol{R}_{\rm e}, \boldsymbol{P}_{\rm e})|_{\rm 2PN}$ the PN expansion of $H_{\rm EOB}(\boldsymbol{R}_{\rm e}, \boldsymbol{P}_{\rm e})$ up to 2PN, it must hold that

$$\boldsymbol{P}_{\rm e}\, d\boldsymbol{R}_{\rm e} - H_{\rm EOB}(\boldsymbol{R}_{\rm e}, \boldsymbol{P}_{\rm e})|_{\rm 2PN} dt = \boldsymbol{P}\, d\boldsymbol{R} - H(\boldsymbol{R}, \boldsymbol{P}) dt + d\tilde{G}, \tag{3.29}$$

where $d\tilde{G}$ is the total differential of a phase-space function $\tilde{G}(\boldsymbol{R}, \boldsymbol{R}_{\rm e}, t)$, which is called the ("type-1") *generating function* of the canonical transformation. In the EOB formalism, we rather consider a "type-2" generating function $\tilde{G}_2(\boldsymbol{R}, \boldsymbol{P}_{\rm e}, t) \equiv \boldsymbol{R}_{\rm e} \cdot \boldsymbol{P}_{\rm e} + \tilde{G}(\boldsymbol{R}, \boldsymbol{R}_{\rm e}, t)$, that is related to $\tilde{G}(\boldsymbol{R}, \boldsymbol{R}_{\rm e})$ by a Legendre transformation changing the functional dependence from $\boldsymbol{R}_{\rm e}$ to $\boldsymbol{P}_{\rm e} \equiv -(\partial \tilde{G})/(\partial \boldsymbol{R}_{\rm e})$. With

$$d\tilde{G}(\boldsymbol{R}, \boldsymbol{R}_{\rm e}, t) = \frac{\partial \tilde{G}_2}{\partial \boldsymbol{R}} d\boldsymbol{R} - \boldsymbol{P}_{\rm e} d\boldsymbol{R}_{\rm e} + \frac{\partial \tilde{G}_2}{\partial t} dt + \left(\frac{\partial \tilde{G}_2}{\partial \boldsymbol{P}_{\rm e}} - \boldsymbol{R}_{\rm e} \right) d\boldsymbol{P}_{\rm e}, \tag{3.30}$$

we obtain the transformation rules

$$\boldsymbol{R}_{\rm e} = \frac{\partial \tilde{G}_2(\boldsymbol{R}, \boldsymbol{P}_{\rm e})}{\partial \boldsymbol{P}_{\rm e}}, \qquad \boldsymbol{P} = -\frac{\partial \tilde{G}_2(\boldsymbol{R}, \boldsymbol{P}_{\rm e})}{\partial \boldsymbol{R}}, \quad \text{and} \tag{3.31}$$

$$H_{\rm EOB}|_{\rm 2PN}(\boldsymbol{R}_{\rm e}, \boldsymbol{P}_{\rm e}) = H(\boldsymbol{R}, \boldsymbol{P}) + \frac{\partial \tilde{G}_2}{\partial t}(\boldsymbol{R}, \boldsymbol{P}_{\rm e}). \tag{3.32}$$

Notice that the first identity is simply the definition of the variable $\boldsymbol{R}_{\rm e}$ according to the Legendre transformation from $\tilde{G}_2$ to $\tilde{G}$. Moreover, as it will be pointed out in Sec 3.4, $H_{\rm EOB}$ is defined in such a way that $H_{\rm EOB}|_{\rm 2PN} = H$, and thus $(\partial \tilde{G}_2)/(\partial t) = 0$.[11]

Let us reintroduce, for a while, the usage of c as a simple label accounting for the PN order, yet maintaining its numerical value equal to 1. We already know, from the Newtonian limit (3.14), that there is no difference between $\boldsymbol{R}$,$\boldsymbol{P}$ and $\boldsymbol{R}_{\rm e}$,$\boldsymbol{P}_{\rm e}$ at the Newtonian level of accuracy. We can thus model $\tilde{G}_2$ as describing a *small* transformation

$$\boldsymbol{R}_{\rm e} \approx \boldsymbol{R} + \frac{1}{c^2}\delta\boldsymbol{R}_{\rm 1PN} + \frac{1}{c^4}\delta\boldsymbol{R}_{\rm 2PN} \qquad \boldsymbol{P}_{\rm e} \approx \boldsymbol{P} + \frac{1}{c^2}\delta\boldsymbol{P}_{\rm 1PN} + \frac{1}{c^4}\delta\boldsymbol{P}_{\rm 2PN} \tag{3.33}$$

near the identity, according to

$$\tilde{G}_2 \equiv \boldsymbol{R} \cdot \boldsymbol{P}_{\rm e} + \frac{1}{c^2} G_{\rm 1PN}(\boldsymbol{R}, \boldsymbol{P}_{\rm e}) + \frac{1}{c^4} G_{\rm 2PN}(\boldsymbol{R}, \boldsymbol{P}_{\rm e}). \tag{3.34}$$

[11] Loosely speaking, we can say that the time-dependent part of the transformation is already encoded in $H_{\rm EOB}$ by the energy mapping (3.26).

In the above equation, $G_{2,\mathrm{id}}(\boldsymbol{R},\boldsymbol{P}_\mathrm{e}) \equiv \boldsymbol{R}\cdot\boldsymbol{P}_\mathrm{e}$ is the type-2 generating function corresponding to the identity transformation $\boldsymbol{R} \to (\partial G_{2,\mathrm{id}})/(\partial \boldsymbol{P}_\mathrm{e}) = \boldsymbol{R}$, $\boldsymbol{P} \to (\partial G_{2,\mathrm{id}})/(\partial \boldsymbol{R}) = \boldsymbol{P}$, while $G_{1\mathrm{PN}}(\boldsymbol{R},\boldsymbol{P}_\mathrm{e})$ and $G_{2\mathrm{PN}}(\boldsymbol{R},\boldsymbol{P}_\mathrm{e})$ are type-2 generating functions of 1PN and 2PN order, respectively. Introducing the Poisson Brackets

$$\{f,g\} \equiv \sum_{i=1}^{3} \frac{\partial f}{\partial R^i}\frac{\partial g}{\partial P_{\mathrm{e},i}} - \frac{\partial f}{\partial P_{\mathrm{e},i}}\frac{\partial g}{\partial R^i} \tag{3.35}$$

we can rewrite the coordinate transformation (3.31) as

$$\boldsymbol{R}_\mathrm{e} = \boldsymbol{R} + \frac{1}{c^2}\{\boldsymbol{R}, G_{1\mathrm{PN}}(\boldsymbol{R},\boldsymbol{P}_\mathrm{e})\} + \frac{1}{c^4}\{\boldsymbol{R}, G_{2\mathrm{PN}}(\boldsymbol{R},\boldsymbol{P}_\mathrm{e})\} + \mathcal{O}\left(\frac{1}{c^6}\right) \tag{3.36}$$

$$\boldsymbol{P}_\mathrm{e} = \boldsymbol{P} + \frac{1}{c^2}\{\boldsymbol{P}_\mathrm{e}, G_{1\mathrm{PN}}(\boldsymbol{R},\boldsymbol{P}_\mathrm{e})\} + \frac{1}{c^4}\{\boldsymbol{P}_\mathrm{e}, G_{2\mathrm{PN}}(\boldsymbol{R},\boldsymbol{P}_\mathrm{e})\} + \mathcal{O}\left(\frac{1}{c^6}\right). \tag{3.37}$$

The generating function $\tilde{G}$ also define the rules (at least in a perturbative way) for the transformation

$$H_{\mathrm{EOB}}|_{2\mathrm{PN}}(\boldsymbol{R}_\mathrm{e},\boldsymbol{P}_\mathrm{e}) = H(\boldsymbol{R}_\mathrm{e},\boldsymbol{P}_\mathrm{e}) + \frac{1}{c^2}\delta H_{1\mathrm{PN}}(\boldsymbol{R}_\mathrm{e},\boldsymbol{P}_\mathrm{e}) + \frac{1}{c^4}\delta H_{2\mathrm{PN}}(\boldsymbol{R}_\mathrm{e},\boldsymbol{P}_\mathrm{e}) + \mathcal{O}\left(\frac{1}{c^6}\right) \tag{3.38}$$

of the Hamiltonian. We insert, in the numerical identity $H_{\mathrm{EOB}}|_{2\mathrm{PN}}(\boldsymbol{R}_\mathrm{e},\boldsymbol{P}_\mathrm{e}) = H(\boldsymbol{R},\boldsymbol{P})$ (Eq. (3.32)), the transformation rules (3.36)-(3.37). The part of the transformation which is *linear* in $G_{\mathrm{PN}} \equiv G_{1\mathrm{PN}} + G_{2\mathrm{PN}} + ...$ is most easily computed. At linear order in G_{PN}, indeed, we can set $\boldsymbol{P} = \boldsymbol{P}_\mathrm{e} - \{\boldsymbol{P}_\mathrm{e}, G_{\mathrm{PN}}(\boldsymbol{R}_\mathrm{e},\boldsymbol{P}_\mathrm{e})\}$, $\boldsymbol{R} = \boldsymbol{R}_\mathrm{e} - \{\boldsymbol{R}_\mathrm{e}, G_{\mathrm{PN}}(\boldsymbol{R}_\mathrm{e},\boldsymbol{P}_\mathrm{e})\}$ [12], and

$$H_{\mathrm{EOB}}|_{2\mathrm{PN}}(\boldsymbol{R}_\mathrm{e},\boldsymbol{P}_\mathrm{e}) = H\Big(\boldsymbol{R}_\mathrm{e} - \{\boldsymbol{R}_\mathrm{e}, G_{\mathrm{PN}}\},\ \boldsymbol{P}_\mathrm{e} - \{\boldsymbol{P}_\mathrm{e}, G_{\mathrm{PN}}\}\Big) + \mathcal{O}(G_{\mathrm{PN}}^2) \tag{3.39}$$

$$= H(\boldsymbol{R}_\mathrm{e},\boldsymbol{P}_\mathrm{e}) - \{H, G_{\mathrm{PN}}\}(\boldsymbol{R}_\mathrm{e},\boldsymbol{P}_\mathrm{e}) + \mathcal{O}(G_{\mathrm{PN}}^2), \tag{3.40}$$

where the last equality is obtained by a linear-order Taylor expansion of H around $\boldsymbol{R}_\mathrm{e}$ and $\boldsymbol{P}_\mathrm{e}$. This leads, for instance, to the identity

$$H_{\mathrm{EOB}}|_{1\mathrm{PN}} = H_{1\mathrm{PN}} + \{G_{1\mathrm{PN}}, H_\mathrm{N}\}. \tag{3.41}$$

By contrast, in order to find the 2PN relation between H_{EOB} and H, one must evaluate, besides of the terms linear in $G_{2\mathrm{PN}}$, also the terms *quadratic* in $G_{1\mathrm{PN}}$, which imply a more complicated transformation (see Sec VI of Ref. [65]). The 2PN-accurate mapping between ADM and EOB formalism discussed in Sec 3.2 uniquely defines the generating functions $G_{1\mathrm{PN}}$ and $G_{2\mathrm{PN}}$. The leading-order transformation is given by

$$G_{1\mathrm{PN}}(\boldsymbol{R},\boldsymbol{P}) = \boldsymbol{R}\cdot\boldsymbol{P}\left(-\frac{\nu}{2}\boldsymbol{P}^2 + \left(1+\frac{\nu}{2}\right)\frac{1}{|\boldsymbol{R}|}\right), \tag{3.42}$$

see [65], and see Eqs. (6.19), (6.20) in the same reference for $G_{2\mathrm{PN}}$. The Hamiltonian transformations given by the linear equation (3.40), together with quadratic, and possibly higher-order effects, will play a central role for further developments of the EOB Hamiltonian. For instance, at the 3PN level, one is free to choose a new generating function $G_{3\mathrm{PN}}$, entering linearly at the

[12] Notice that the Poisson Brackets only involve, now, the "new" coordinates $\boldsymbol{R}_\mathrm{e}$, $\boldsymbol{P}_\mathrm{e}$, and are thus of type $\{f,g\}(\boldsymbol{R}_\mathrm{e},\boldsymbol{P}_\mathrm{e})$ rather than $\{f,g\}(\boldsymbol{R},\boldsymbol{P}_\mathrm{e})$ as in Eq. (3.35).

3PN level according to (3.40) (and obviously leaving the lower-orders untouched), that can be used to rearrange the ADM Hamiltonian in a more suitable form before encoding into an EOB Hamiltonian. In the EOB approach, we call *gauge freedom* the possibility of choosing an *ad hoc* canonical transformation for fixing the Hamiltonian at a given PN order.

3.4 The EOB Hamiltonian

It is well-known that the Hamiltonian of a system which is invariant under time translations is conserved. As described, for instance, by the Hamilton-Jacobi equation (3.17) with the separation ansatz (3.18), the two-body Hamiltonian is numerically equal to the relativistic energy (i.e., with the rest-mass contribution), $H(\boldsymbol{R},\boldsymbol{P}) = E$. Similarly, $H^{\rm eff}(\boldsymbol{R}_{\rm e},\boldsymbol{P}_{\rm e}) = E_{\rm e}$ for the effective problem.

[This is the right moment to introduce a change in notation. Starting from now, the label "e" will always be omitted from the EOB (or effective) coordinates, so that, unless differently specified, $\boldsymbol{R}$ and $\boldsymbol{P}$ will denote the EOB coordinates. We will also make use of the dimensionless variables $\boldsymbol{r} \equiv \boldsymbol{R}/M$, $r \equiv |\boldsymbol{r}|$, $\boldsymbol{n} \equiv \boldsymbol{r}/r$, and $\boldsymbol{p} \equiv \boldsymbol{P}/\mu$, that can be useful to simplify the notation in some cases.]

By inverting the energy mapping (3.26), we can thus define a new Hamiltonian $H_{\rm EOB} = E$, the *EOB Hamiltonian*, describing the *real* problem in an effective way. More specifically,

$$H_{\rm EOB}(\boldsymbol{R},\boldsymbol{P}) = M\sqrt{1+2\nu\left(\frac{H^{\rm eff}(\boldsymbol{R},\boldsymbol{P})}{\mu}-1\right)}. \tag{3.43}$$

The effective Hamiltonian $H^{\rm eff}$ can be obtained from the Hamilton-Jacobi equation (3.21) with the metric (3.11) and the separation ansatz (3.22). With $P_R \equiv (\partial S)/(\partial R)$, $L \equiv (\partial S)/(\partial\varphi)$, the Hamilton-Jacobi equation reads

$$-\frac{E_{\rm e}^2}{A}+\frac{P_R^2}{B}+\frac{L}{R^2}+\mu^2 = 0, \tag{3.44}$$

and is solved for the Hamiltonian $H^{\rm eff} = E_{\rm e}$ according to

$$H^{\rm eff}_{\rm 2PN}(\boldsymbol{R},\boldsymbol{P}) = \sqrt{A(u,\nu)\left(\mu^2+\frac{(\boldsymbol{n}\cdot\boldsymbol{P})^2}{B(u,\nu)}+\frac{(\boldsymbol{R}\times\boldsymbol{P})^2}{R^2}\right)}, \tag{3.45}$$

where we have made use of the identities $P_R = (\boldsymbol{n}\cdot\boldsymbol{P})$, $L = \boldsymbol{R}\times\boldsymbol{P}$.

Let us now briefly discuss the form of the A and B potentials. Since the two-body ADM dynamics only constrains the PN-expanded form of A and B, see Eqs. (3.27), (3.28), we are in principle free to define them as any functions whose expanded forms satisfy Eqs. (3.27),(3.28). We accordingly say that A and B (and, more generally, the EOB Hamiltonian) *resum* the PN results. Notice that the resummation of the ν-independent part of A and B has already been fixed in Sec 3.2, where it was required to reproduce the Schwarzschild case. In the full, ν-dependent case, one defines

$$A(u,\nu) \equiv 1-2u+2\nu u^3 \tag{3.46}$$

$$B(u,\nu) \equiv \frac{D(u,\nu)}{A(u,\nu)}, \quad \text{with} \quad D(u,\nu) \equiv \frac{1}{1+6\nu u^2}. \tag{3.47}$$

The factorization of $A(u,\nu)^{-1}$ in $B(u,\nu)$ has the goal of maintaining a Schwarzschild-like structure even for $\nu \neq 0$. In particular, this formulation ensures that the simple roots $A(u,\nu) = 0$ and

$B(u,\nu)^{-1} = 0$ coincide, so that the existence of a ν-deformed Schwarzschild horizon is preserved. For the same reason, the factor $D(u,\nu)$ is inversely resummed, so as to prevent the formation of singularities in $B(u,\nu)^{-1}$.

3.4.1 Extension to higher orders of accuracy

After the final fixation of the 3PN dynamics [12] (whose main part had already been derived by Jaranowski and Schäfer [10]), Damour, Jaranowski and Schäfer tackled the problem of including the complicated 3PN coupling into the EOB [67]. They had to choose among the two following options: i) to keep the description of the effective dynamics as a geodesic motion in an effective metric (or in other words, to maintain the fulfillment of the Hamilton-Jacobi equation (3.21)), but at the price of introducing a subleading-order modification of the energy mapping formula (3.26), and of compromising the Schwarzschild-type resummation of the B-potential; or ii) to relax the Hamilton-Jacobi equation with the introduction of non-geodesic terms into the dynamics, saving both the "standard" energy mapping and the Schwarzschild structure of the B-potential.

Renouncing at the condition of geodesic motion did not seem unaffordable to the authors, and option ii) was chosen, further motivated by the simplicity of the results it led to. This choice has two main implications on the structure of the EOB Hamiltonian:

- First of all, the relation (4.20) between $H_{\rm EOB}$ and $H^{\rm eff}$,

$$H_{\rm EOB} = M\sqrt{1 + 2\nu\left(\hat{H}^{\rm eff} - 1\right)},$$

  is now taken to be valid at all orders, and is no longer considered as a mere 2PN approximation of a more complicated function.

- Relaxing the Hamilton Jacobi equation means that there is more flexibility in including new couplings into the EOB. In particular, direct modifications at the level of $H^{\rm eff}$ are allowed, and not only at the level of the effective metric $g^{\rm eff}_{\mu\nu}$.

Exploiting the gauge freedom carried by a 3PN generating function $G_{\rm 3PN}$ (which is composed, in the most general case, by 7 independent coefficients, see Eq. (3.7) in Ref. [67]), the 11 coefficients that define the 3PN Hamiltonian (2.79) can in principle be reduced to $11 - 7 = 4$ according to the transformation rule

$$H^{\rm ADM}_{\rm 3PN} \to H^{\rm ADM}_{\rm 3PN} + \{G_{\rm 3PN}, H_{\rm N}\}. \tag{3.48}$$

[To be more precise, we recall that the 3PN Hamiltonian $H^{\rm ADM}_{\rm 3PN}$ in ADM coordinates must also be transformed according to the already fixed 1PN and 2PN canonical transformations, involving linear couplings of $G_{\rm 2PN}$, as well as linear, quadratic and cubic couplings of $G_{\rm 1PN}$.] After having performed all necessary transformations from ADM to EOB, it turns out that a suitable choice of $G_{\rm 3PN}$ leads to an effective Hamiltonian which, once squared (in order to remove the square root), and taken at 3PN in Taylor-expanded form, is of the type

$$\left(\hat{H}^{\rm eff}\right)^2|_{\rm 3PN} = c_1\frac{(\boldsymbol{n}\cdot\boldsymbol{p})^4}{r^2} + c_3\frac{(\boldsymbol{n}\cdot\boldsymbol{p})^2}{r^3} + c_4\frac{1}{r^4}. \tag{3.49}$$

Because of an *a priori* unexpected cancellation, due to an implicit relation between the 3PN coefficients (see Eq. (4.33) of Ref. [67]), the remaining terms can thus be reduced to only 3 instead of 4, which is a remarkable result. A possible option for resumming (3.49) might be to add first term $\propto u^4$ to $A(u,\nu)$, a second one $\propto u^3$ to $D(u,\nu)$, and to insert a third (non-geodesic) term $\propto u^2(\boldsymbol{n}\cdot\boldsymbol{P})^4$

somewhere else in the effective Hamiltonian. We summarize here the results, also including, without discussing it, the 4PN correction to the A-potential calculated by Bini and Damour [79]. The effective Hamiltonian is given by

$$H^{\rm eff}(\boldsymbol{R},\boldsymbol{P}) = \sqrt{A(u,\nu)\left(\mu^2 + \frac{(\boldsymbol{n}\cdot\boldsymbol{P})^2}{B(u,\nu)} + \frac{(\boldsymbol{R}\times\boldsymbol{P})^2}{R^2} + Q_4\right)}, \tag{3.50}$$

with the non-geodesic quartic-in-momenta 3PN term

$$Q_4 = 2(4-3\nu)\nu\frac{(\boldsymbol{n}\cdot\boldsymbol{P})^4}{r^2}. \tag{3.51}$$

The (PN-expanded) potential A, involving both 3PN ($\propto u^4$) and 4PN ($\propto u^5$) terms, is equal to

$$A_{\rm 4PN}(u,\nu) = 1 - 2u + 2\nu u^3 + \nu\left(\frac{94}{3} - \frac{41}{32}\pi^2\right)u^4 + \nu\left(a_5^{\rm c}(\nu) + a_5^{\rm ln}(\nu)\ln u\right)u^5, \tag{3.52}$$

with

$$a_5(\nu) = \left(-\frac{4237}{60} + \frac{2275}{512}\pi^2 + \frac{256}{5}\ln 2 + \frac{128}{5}\gamma + \left(-\frac{221}{6} + \frac{41}{32}\pi^2\right)\nu\right), \qquad a_5^{\rm ln} = \frac{64}{5}, \tag{3.53}$$

where γ is Euler's constant. As a nice corollary notice that, while the 3PN ADM Hamiltonian (2.79) encodes quadratic and cubic ν-dependences, only terms linear in ν survive in the EOB A-potential.

Recent EOB models make use of an A-potential equipped with some 5PN information. In particular, the 5PN logarithmic contribution [100–102] to $A(u,\nu)$ is known, and is given by a term

$$\nu\, a_6^{\rm ln}(\nu)\ln u\, u^6, \quad \text{with} \qquad a_6^{\rm ln}(\nu) = -\frac{7004}{105} - \frac{144}{5}\nu. \tag{3.54}$$

The still unknown non-logarithmic 5PN term $\nu\, a_6^{\rm c}(\nu)u^6$ entering the A-potential can be estimated, in an empirical way, by a comparison with Numerical Relativity waveforms. The last version of the coefficient $a_6^{\rm c}(\nu)$ (which has been calibrated for the spinning EOB model that will be exposed in Sec 3.7) is given by [92]

$$a_6^{c({\rm NR})}(\nu) = 3097.3\nu^2 - 1330.6\nu + 81.38, \tag{3.55}$$

where we we have used the label "NR" to stress that this is not an exact result, and may change for different EOB versions. The 5PN-calibrated is given by

$$A_{\rm 5PN}(u,\nu) \equiv A_{\rm 4PN}(u,\nu) + \nu\left(a_6^{c({\rm NR})}(\nu) + a_6^{\rm ln}(\nu)\ln u\right)u^6. \tag{3.56}$$

Because of the model-dependence of $a_6^{c({\rm NR})}(\nu)$, in this thesis we will rather take $A_{\rm 4PN}$ (or even $A_{\rm 3PN}$, like in Chapter 4) as the standard PN expanded A-potential. The resummed potential $D(u,\nu)$ factorizing B, see Eq. (3.47), is given up to 3PN order ($\propto u^3$) by

$$D(u,\nu) \equiv \frac{1}{1 + 6\nu u^2 + 2(26-3\nu)\nu u^3}. \tag{3.57}$$

Padé-resummation

Together with the 3PN coupling, an important modification in the resummation of the A-potential is introduced. The 3PN coefficient $a_4 = \left(94/3 - 41\pi^2/32\right) \approx 18.7$ has the problem of being quite large. In the proximity of the Schwarzschild horizon $u = 1/2$, and for $\nu = 1/4$, the 3PN term $\nu\, a_4\, u^4$ is larger than the 2PN one $\nu\, a_3\, u^3 = u^3/2$ by a factor $\gtrsim 4$, leading to a bad convergence in the strong field.

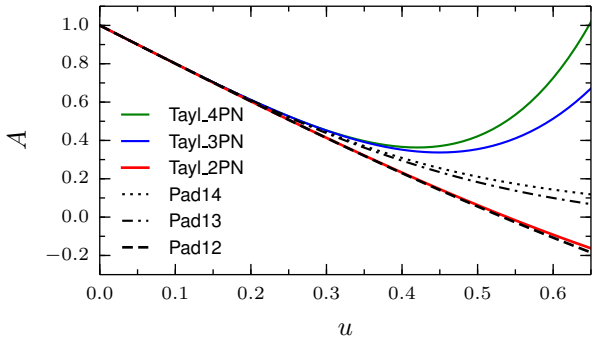

Figure 3.3: *The radial potential $A(u,\nu)$ is plotted versus the reciprocal dimensionless separation radius u in the equal-mass cases $\nu = 1/4$, at 2PN (Tayl_2PN, Pad12), 3PN (Tayl_3PN, Pad13) and 4PN (Tayl_4PN, Pad14) order. Both the Taylor-expanded form (Tayl) and the (1,n)-Padé resummation (Pad1n) are considered. Notice that, for clarity purposes, the plot extends even beyond the Schwarzschild horizon $u = 1/2$.*

In order to overcome this problem, one may explore the possibility of resumming the A-potential in a non-Taylor-expanded form. The most convenient choice, adopted in [67] and then essentially kept invariant up to the most recent models [91, 92], has been that of resumming the (n-th order) A potential by means of a (1,n)-Padé approximant[13] in the variable u around $u = 0$. In practice, denoting by $A_{n\mathrm{PN}}$ the n-th order, Taylor expanded A potential, the corresponding Padéed potential has the form

$$A(u,\nu) \equiv P^1_n\Big[A_{n\mathrm{PN}}(u,\nu)\Big] = \frac{1 + n_1\, u}{1 + d_1\, u + ... + d_n\, u^n}, \tag{3.58}$$

where the coefficients n_1, d_1, ... d_n are uniquely defined by requiring that the n-th order Taylor expansion of $A(u,\nu)$ around $u = 0$ is equal to $A_{n\mathrm{PN}}$. In particular, the radial potential $A(u,\nu)$ entering Eq. (3.50) is the Padé $P^1_4[A_{4\mathrm{PN}}]$ of $A_{4\mathrm{PN}}$, Eq. (3.52). Notice, however, that the logarithm $\ln u$ that is found in $A_{4\mathrm{PN}}$ cannot be consistently Padéed (being singular at $u = 0$), and shall thus be treated as a constant while taking the Padé approximant.

In Fig 3.3, the behavior of the radial potential $A(u,\nu)$ is shown for the equal-mass case, for different PN orders and for both Taylor-expanded form and (1,n)-Padé resummation. The diverging character of the Taylor-expanded 3PN and 4PN curves is clearly visible. By contrast, the Padé-approximants do not diverge, an do not differ too much from one another when the PN order is changed. There is, however, an important topological difference with respect to the Taylor-expanded 2PN case, which is not entirely visible from the figure: while the latter has a Schwarzschild-type structure, with an horizon around $u = 1/2$, the Padé approximants always remain positive, and tend to zero as $u \to \infty$. This is not meant to be a big problem, since the

[13] Notice that a Padé-approach for improving the convergence of the PN dynamics had already been tackled before the EOB was formulated, see e.g. [103].

modeling of an horizon is not strictly necessary for the EOB Hamiltonian (we recall that, after merger, the waveform description is provided by black hole perturbation theory).

3.5 The full EOB formalism

In order to provide a description of the waveform generated by a coalescing binary, the EOB Hamiltonian must be accompanied by

i) An implementation of radiation reaction effects.

ii) A formalism for calculating the waveform generated by the EOB Hamiltonian, together with a prescription to mark the transition to black-hole perturbation theory.

In the past years, there has been a large effort to improve the analytical formalism for i) and ii) using a resummation philosophy similar to the one employed for the EOB Hamiltonian. For the sake of completeness, following essentially Ref. [91], we summarize here *state-of-the-art* of the nonconservative part of the EOB formalism.

Let us consider the EOB Hamiltonian $\hat{H}_{\rm EOB} = H_{\rm EOB}/\mu$, Eq. (4.20), by using polar coordinates $(r\cos\varphi, r\sin\varphi, 0) = \boldsymbol{r}$ on the equatorial plane $\theta \equiv \pi/2$, with the radial $p_r \equiv (\boldsymbol{n}\cdot\boldsymbol{p})$ and angular momentum variable $p_\varphi \equiv L_z = \boldsymbol{r}\times\boldsymbol{p}$. The equations of motion are most conveniently expressed, for numerical purposes, by the "tortoise"[14] radial variable $r_* \equiv \int dr\sqrt{B/A}$ and its associate momentum $p_{r_*} \equiv \sqrt{A/B}\,p_r$ [104]. Radiation reaction effects are added *ad hoc*, in the form of angular momentum and radial energy losses to the Hamiltonian equations defined by $\hat{H}_{\rm EOB}$. Explictly, the equations of motion read

$$\frac{d\varphi}{dt} = \frac{\partial \hat{H}_{\rm EOB}}{\partial p_\varphi}, \qquad \frac{dp_\varphi}{dt} = \hat{\mathcal{F}}_\varphi, \tag{3.59}$$

$$\frac{dr}{dt} = \sqrt{\frac{A}{B}}\frac{\partial \hat{H}_{\rm EOB}}{\partial p_{r_*}}, \qquad \frac{dp_{r_*}}{dt} = -\sqrt{\frac{A}{B}}\frac{\partial \hat{H}_{\rm EOB}}{dr} + \hat{\mathcal{F}}_{r_*}. \tag{3.60}$$

Here, as in the previous sections, we will use the notation $\omega \equiv (d\varphi)/(dt)$ for the orbital angular velocity. Besides of the terms arising from the conservative Hamilton equations, there is an angular momentum flux $\hat{\mathcal{F}}_\varphi$ (which is the most important radiation reaction ingredient, as pointed out in Ref. [66]), and a radial energy flux $\hat{\mathcal{F}}_{r_*}$ [78]. The fluxes are the result of the balance between outward radiation (taken at spatial infinity from the source) and horizon-absorbed radiation. Let us, therefore, first expose the formalism for the waveform resummation. The inspiral-plunge multipolar waveform is factorized as [73, 82, 84]

$$h_{lm} = h_{lm}^{(N,\epsilon)}(v_\varphi)\, S_{\rm eff}^{(\epsilon)}\, \hat{h}_{lm}^{\rm tail}(y)\left(\rho_{lm}(v_\varphi^2)\right)^2 \hat{h}_{lm}^{\rm NQC}, \tag{3.61}$$

whose main ingredient is the Newtonian waveform

$$h_{lm}^{(N,\epsilon)}(v_\varphi) = \frac{M\nu}{D}\, n_{lm}^{(\epsilon)}\, c_{l+\epsilon}(\nu)\, v_\varphi^{l+\epsilon}\, Y^{l-\epsilon,-m}(\pi/2,\varphi), \tag{3.62}$$

[14] As a curiosity, the name "tortoise" actually refers to Zeno's well-known paradox, where a tortoise is engaged in a race against Achilles. In the Schwarzschild spacetime, the horizon $r = 2$ corresponds to a tortoise radius $r_* = -\infty$, and is thus in some sense "never reached", just as Achilles "never reaches" the tortoise according to the paradox.

where the system is assumed to lay on the equatorial plane ($\theta = \pi/2$), with orbital phase φ, and at a distance D from the observer. In the above equations, $\epsilon \equiv \pi(l+m)$ is the parity of the corresponding multipole ($\pi(\cdot)$ denoting the parity operator), i.e., $\epsilon = 0$ for even parity, mass-generated multipoles, and $\epsilon = 1$ for odd-parity, current-generated multipoles. The variable $v_\varphi = r_\omega\,\omega$ is an EOB version of the azimuthal velocity, firstly introduced in [105], and defined in terms of a modified EOB radius r_ω which guarantees that third Kepler's law is satisfied, $1 = \omega^2 r_\omega^3$. Both $n_{lm}^{(\epsilon)}$ and $c_{l+\epsilon}(\nu)$ are numerical coefficients [73] emerging from the multipolar wave-decomposition in spherical harmonics, and from the inclusion of finite mass-ratio effects, respectively (see also [106]).

The Newtonian waveform $h_{lm}^{(N,\epsilon)}(v_\varphi)$ factorizes the whole expression (3.61). The remaining terms are subleading-order corrections of type $1+\mathcal{O}(x)$, where $x \equiv (M\omega)^{2/3}$ is the dimensionless frequency parameter. In particular, $\hat{S}_{\rm eff}^{(\epsilon)}$ is an effective source, with $\hat{S}_{\rm eff}^{(0)} = \hat{H}^{\rm eff}$ and $\hat{S}_{\rm eff}^{(1)} = p_\varphi/(r_\omega v_\varphi)$. The tail factor $\hat{h}_{lm}^{\rm tail}(y) = T_{lm}(y)e^{i\delta_{lm}(y)}$ (where $y \equiv (H_{\rm EOB}\,\omega)^{2/3}$ is an EOB version of the dimensionless frequency parameter) resums an infinite number of logarithms, that are due to the propagation in a curved background (see [73, 82, 84] for more detailed definitions, and [91] for a recent introduction of a Padé resummation of the δ_{lm}'s). PN corrections to the waveform are encoded in the building block $[\rho_{lm}(v_\varphi^2)]^2$, already present in Refs. [82, 84], where it was denoted as f_{lm}, but whose resummation has been improved in Ref. [73]. Finally, $\hat{h}_{lm}^{\rm NQC}$ denotes next-to-quasi-circular corrections to the waveform [91].

Let us now consider the radiation-reaction fluxes. The angular momentum flux is decomposed in the sum of an asymptotic, outwardly radiated flux (labeled by A), and an horizon-absorbed flux (labeled by H), and reads

$$\hat{\mathcal{F}}_\varphi = -\frac{32}{5}\nu r_\omega^4\,\omega^5\left(\hat{f}^A + (1-4\nu+2\nu^2)v_\varphi^4\hat{f}^H\right). \tag{3.63}$$

The functions $\hat{f}^A$ and $\hat{f}^H$ factorize the 22-multipole, and are given by the the ratio

$$\hat{f}^{(A,H)} = \left(\sum_{l=2}^{l_{\rm max}}\sum_{m=1}^{l} F_{lm}^{(A,H,\epsilon)}\right)/F_{22}^{(A,H,\epsilon)} \tag{3.64}$$

for a maximal considered multipole $l = l_{\rm max}$. In the last equation, the asymptotic flux $F_{lm}^{(A,\epsilon)}$ is expressed in terms of Eq. (3.61) [72],

$$F_{lm}^{(A,\epsilon)} = \frac{1}{8\pi}(m\omega)^2|Dh_{lm}^{(\epsilon)}|^2, \tag{3.65}$$

while, for what concerns the horizon-absorbed flux $F_{lm}^{(H,\epsilon)}$, we refer the reader to [107] . Finally, we mention that the radial flux has the form [78]

$$\hat{\mathcal{F}}_{r_*} = -\frac{5}{3}\frac{p_{r_*}}{p_\varphi}\hat{\mathcal{F}}_\varphi(1+c_1(\nu)\,u+c_2(\nu)\,u^2), \tag{3.66}$$

for given coefficients $c_1(\nu)$ and $c_2(\nu)$. However, it must be remarked that current EOB models tend to set the radial flux to zero, because there seems to be, in such a way, a better agreement with NR data (see e.g. [81, 92, 108]). This issue still has to be clarified.

In order to provide a complete waveform, a model describing the ringdown of a perturbed black-hole metric must be attached, in correspondence of the merger, to the inspiral-plunge waveform

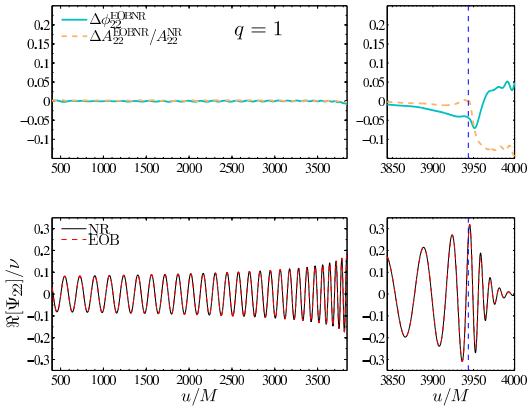

Figure 3.4: *Comparison between the 22-mode of the EOB model of [91] and a NR waveform from the Caltech-Cornell CITA group [109] for mass ratio $q \equiv m_1/m_2 = 1$. Both the phase difference $\Delta\phi$ (in radians) and the fractional amplitude difference $\Delta A/A$ remain below ~ 0.05 (in absolute value) through all inspiral stages and merger. The figure is taken from Ref. [91].*

exposed here [66, 82, 87, 91]. The ringdown waveform is expressed as the sum of quasi-normal modes

$$h_{lm}^{\rm ringdown} = \frac{M}{R}\sum_{n=0}^{N-1} C_n^{lm} e^{-\sigma_n^{+,lm}(t-t_m)}, \tag{3.67}$$

where C_n^{lm} are complex coefficients, and where $\sigma_n^{+,lm}$ is the complex frequency of the (l,m)-mode. The *moment of merger* t_m can be defined as the time at which the orbital frequency described by the EOB dynamics reaches a maximum.

Once all wished analytical information has been inserted into EOB model, the waveform generated by the EOB is finally compared with NR data. As we have already mentioned, the information carried by the NR waveform can be used to further improve, or to *complete*, the EOB model. The idea is to insert, at certain strategic points in the EOB, some parameters that have to be fitted with NR data. The most natural place to insert a calibration parameter is the lowest-order unknown term in the A-potential (which currently is the 5PN order, see also Sec 3.4.1). Additional calibration parameters can also be used in other sectors (for instance, to fix the next-to-quasi-circular corrections of the waveform, see [91]; or in the spin-orbit sector of a spinning EOB model [81, 92]).

The nonspinning EOB model summarized here is currently able to generate waveforms that agree with NR waveforms within the numerical errors of the simulations (see e.g. [91]).

3.6 An EOB Hamiltonian for spinning black-hole binaries

Consider a system of two coalescing black holes, with masses m_1 and m_2, and with *spins* $\boldsymbol{S}_1$ and $\boldsymbol{S}_2$, according to the formalism developed in Chapter 2. The formulation of an EOB Hamiltonian describing the dynamics of this system is the main argument to which this thesis is devoted. The literature we follow here is essentially composed of Refs. [64, 68, 70, 81]. The outline of these papers is the following: in Ref. [68], Damour firstly introduced a spin formalism for the EOB Hamiltonian, which included i) the exact $\nu \to 0$ limit of a test particle in a Kerr background, ii) the LO spin-orbit coupling, and also ii) the LO spin-spin coupling. In the EOB, the spin-orbit coupling where then pushed to NLO by Damour, Jaranowski and Schäfer [70], and to NNLO

by Nagar [64], leaving the basic formalism of [68] almost unchanged. Chapters 4 and 5 will be devoted to the inclusion of NLO spin-spin effects starting from the spinning EOB model of [64, 68, 70]. On the other hand, Damour and Nagar proposed in Ref. [81] an improved spinning EOB model (where part of the results of Chapter 4 are also included). This motivated the author of this thesis, together with Damour, to revisit the NLO spin-spin coupling in the EOB, proposing a new EOB Hamiltonian which is closer to the formalism elaborated in [81]. This will be exposed in Chapter 6.

3.6.1 A ν-deformed, separable Kerr metric

One of the basic ideas that has led, in Sec 3.2, to the construction of the EOB Hamiltonian, has been that of defining the effective dynamics as a ν-deformation of the Schwarzschild Hamiltonian. It is thus natural to tackle the problem of the inclusion of spin in the EOB in an analogous manner, i.e., to look for a ν-deformation of the Kerr metric. In Boyer-Lindquist coordinates, the inverse Kerr metric $g^{\mu\nu}$ is equal to

$$g^{tt} = \frac{1}{\rho^2}\left(a^2\sin^2(\theta) - \frac{\left(a^2+R^2\right)^2}{\Delta(R)}\right), \qquad g^{t\varphi} = \frac{a}{\rho^2}\left(1 - \frac{a^2+R^2}{\Delta(R)}\right), \tag{3.68a}$$

$$g^{RR} = \frac{\Delta(R)}{\rho^2}, \qquad g^{\theta\theta} = \frac{1}{\rho^2}, \qquad g^{\varphi\varphi} = \frac{1}{\rho^2}\left(\frac{1}{\sin^2(\theta)} - \frac{a^2}{\Delta(R)}\right), \tag{3.68b}$$

where

$$\rho^2 \equiv 1 + a^2\cos^2\theta, \quad \text{and} \qquad \Delta \equiv R^2 - 2MR + a^2, \tag{3.69}$$

and where $a \equiv S/M$ is the Kerr parameter, with S being the spin of the Kerr black hole and M its total mass. Let μ be the mass of a test particle moving in the Kerr background. Recovering the formalism used in Sec 3.2, the Hamilton-Jacobi equation for the principal function $S_{\rm K}$ in the Kerr metric can be written as [110]

$$0 = g^{\mu\nu}\frac{\partial S_{\rm K}}{\partial R^\mu}\frac{\partial S_{\rm K}}{\partial R^\nu} + \mu^2 \tag{3.70}$$

$$= \frac{1}{\rho^2}\left[\Delta\left(\frac{\partial S_{\rm K}}{\partial R}\right)^2 + \left(\frac{\partial S_{\rm K}}{\partial\theta}\right)^2 + \frac{1}{\sin^2\theta}\left(\frac{\partial S_{\rm K}}{\partial\varphi} + a\sin^2\theta\frac{\partial S_{\rm K}}{\partial t}\right)^2 - \frac{1}{\Delta}\left((R^2+a^2)\frac{\partial S_{\rm K}}{\partial t} + a\frac{\partial S_{\rm K}}{\partial\varphi}\right)^2\right] + \mu^2. \tag{3.71}$$

Similarly as before, we can make the ansatz $S_{\rm K} = -E\,t + L_z\varphi + S_\theta + S_r$, with the energy E and the momentum in z-direction L_z being constants of motion. Notice that the z-axis is now defined to be the rotational axis of the black-hole, so that we no longer have the right to adjust the coordinate frame so as to impose equatorial ($\theta = \pi/2$) orbits, as we had done in Sec 3.2 for the spherically symmetric Schwarzschild-like metric. As a consequence, the case $p_\theta \neq 0$ cannot be ignored, and introduces an additional degree of freedom in the equations of motion. However, since the third term in Eq. (3.71) is purely θ-dependent, the Hamilton-Jacobi equation turns out to be separable, leading to a new constant of motion, the Carter constant

$$\mathcal{K} \equiv \left(\frac{\partial S_{\rm K}}{\partial\theta}\right)^2 + \frac{1}{\sin^2\theta}\left(L_z - a\,E\sin^2\theta\right)^2 + \mu^2 a^2\cos^2\theta. \tag{3.72}$$

The existence of the Carter constant prevents chaotical behavior of geodesics in Kerr spacetime. Moreover, it allows a qualitative insight on some aspects of the dynamics, such as the presence of a two-parametric family of spherical (i.e., of constant Boyer-Lindquist radius), non equatorial orbits (see, e.g. [111, 112], and [68] for a discussion of quasi-spherical nonequatorial orbits in the two-body problem with an EOB approach). The approach of Damour to the spinning EOB in 2001 has been that of introducing the ν-deformation of the Kerr metric so as to maintain these nice separability properties. More precisely, it was searched a ν-deformed Kerr-like metric that depends on an effective Kerr parameter $a_{\rm eff}$ (which is still to be defined here, but that is expected to be a function of the two spins $\boldsymbol{S}_1$ and $\boldsymbol{S}_2$ of the two individual black holes, together with their masses m_1 and m_2). This effective metric should i) reduce to the Kerr metric (3.68) in the test-mass limit $\nu \to 0$ and for $a_{\rm eff} \to a$; ii) reduce to the nonspinning EOB effective metric for $a_{\rm eff} \to 0$.

To this purpose, consider the function $\Delta(r) = R^2 - 2MR + a^2$ appearing in Eq. (3.71). Setting $a \to 0$ in Eq. (3.71) (and comparing, for instance, with Eq. (3.44)), we immediately observe that the Δ multiplying $(\partial S_{\rm K})/(\partial R)$ corresponds the Schwarzschild potential B^{-1}, whereas the Δ in the second last term of Eq. (3.71) corresponds to the Schwarzschild A-potential. Since we already have, in the EOB, effective versions $A(u,\nu)$ and $B(u,\nu)$ of the Schwarzschild potentials A and B, it is natural to define an effective Kerr-like cometric $g^{\mu\nu}_{\rm eff}$ for the effective problem according to [68]

$$g^{\mu\nu}_{\rm eff} P_\mu P_\nu = \frac{1}{\rho^2}\left[\Delta_r P_R^2 + P_\theta^2 + \frac{1}{\sin^2\theta}\left(P_\varphi + a_{\rm eff}\sin^2 P_t\right)^2 - \frac{1}{\Delta_t}\left((R^2 + a_{\rm eff}^2)P_t + a_{\rm eff}P_\varphi\right)^2\right], \tag{3.73}$$

where Δ_t and Δ_r are ν-deformed and spin-dependent Kerr-like potentials. With the analytical results (3.52), (3.53) in Sec 3.4.1, the Δ_t and Δ_r are defined by[15]

$$\Delta_t = R^2 P_4^1\left[A_{\rm 4PN}(u,\nu) + a_{\rm eff}^2 u^2\right], \qquad \Delta_r = \frac{\Delta_t}{D(u,\nu)}. \tag{3.74}$$

The separability properties are clearly preserved in the effective metric. As discussed in [68], in the adiabatic spin approximation $a_{\rm eff} \approx const$[16] , the separability of the Q_4-modified[17] Hamilton-Jacobi equation

$$g^{\mu\nu}_{\rm eff}\frac{\partial S_{\rm eff}}{\partial R^\mu}\frac{\partial S_{\rm eff}}{\partial R^\nu} + Q_4 + \mu^2 = 0 \tag{3.75}$$

leads to a purely radial equation of the type

$$\Delta_r P_r^2 + C_2 P_r^4 = f(R, E_{\rm eff}, L_{z,\rm eff}, \mathcal{K}_{\rm eff}), \tag{3.76}$$

where $Q_4 = C_2 P_r^4$, and with the effective constants of motion $E_{\rm eff}$, $L_{z,\rm eff}$ and $\mathcal{K}_{\rm eff}$. This in turn implies the existence of a two-parametric family of spherical orbits, defined by $f \equiv \partial f/\partial R \equiv 0$, whose one-parametric boundary $f \equiv \partial f/\partial R \equiv \partial^2 f/\partial^2 R \equiv 0$ describe innermost stable spherical orbits; we may consider this qualitative picture as a nice result obtained thanks to the approach proposed in [68]. In order to write down the Hamiltonian, let us switch to Boyer-Lindquist based,

[15] We recall that, by using these results, we are including PN terms at an hybrid order between 3PN and 4PN. More precisely, the 3PN order is complete, while the 4PN is only complete for circular orbits, and does not include any non-circular correction.

[16] More precisely, it is assumed that the spins $\boldsymbol{S}_1$ and $\boldsymbol{S}_2$ defining the effective spin parameter $a_{\rm eff}$ evolve slowly with respect to the orbital dynamics.

[17] The non geodesic, 3PN term Q_4 (3.51) can indeed be considered as a perturbation of the Hamilton-Jacobi equation [67].

Cartesian-like coordinates $R^x = R\cos\varphi\sin\theta$, $R^y = R\sin\varphi\sin\theta$, $R^z = R\cos\theta$, and accordingly promote $a_{\rm eff}$ to a vectorial Kerr parameter $\boldsymbol{a}_{\rm eff}$. As already discussed in Chapter 2, the 3+1 decomposition

$$N = \frac{1}{\sqrt{-g^{00}_{\rm eff}}}, \qquad N^i = \frac{g^{0i}_{\rm eff}}{g^{00}_{\rm eff}} \qquad \gamma^{ij} = g^{ij}_{\rm eff} - \frac{g^{0i}_{\rm eff} g^{0j}_{\rm eff}}{g^{00}_{\rm eff}} \tag{3.77}$$

allows to extract, from the Hamilton-Jacobi equation (given in this case by Eq. (3.75)), the effective Hamiltonian

$$H^{\rm eff} = N^i P_i + N\sqrt{\mu^2 + \gamma^{ij} P_i P_j + Q_4}. \tag{3.78}$$

Explicitly, the effective Hamiltonian $H^{\rm eff}(\boldsymbol{R}, \boldsymbol{P}, \boldsymbol{a}_{\rm eff}, \nu)$ in Boyer-Lindquist-based, Cartesian-like coordinates reads

$$\begin{aligned} H^{\rm eff} = {} & \frac{\left(R^2 + \boldsymbol{a}^2_{\rm eff} - \Delta_t\right)}{\mathcal{R}^4 + (\boldsymbol{n}\cdot\boldsymbol{a}_{\rm eff})^2\Delta_t} \boldsymbol{L}\cdot\boldsymbol{a}_{\rm eff} \\ & + \left(\frac{\Delta_t}{\mathcal{R}^4 + (\boldsymbol{n}\cdot\boldsymbol{a}_{\rm eff})^2\Delta_t}\right)^{1/2} \left(R^2 + (\boldsymbol{n}\cdot\boldsymbol{a}_{\rm eff})^2\right)^{1/2} \left[1 + \frac{1}{\left(1 + \frac{(\boldsymbol{n}\cdot\boldsymbol{a}_{\rm eff})^2}{R^2}\right)} \left(\boldsymbol{P}^2 + \left(\frac{\Delta_r}{R^2} - 1\right)(\boldsymbol{n}\cdot\boldsymbol{P})^2 \right.\right. \\ & \left.\left. - \frac{1}{\mathcal{R}^4 + (\boldsymbol{n}\cdot\boldsymbol{a}_{\rm eff})^2\Delta_t} \left(2R^2 - \Delta_t + \boldsymbol{a}^2_{\rm eff} + (\boldsymbol{n}\cdot\boldsymbol{a}_{\rm eff})^2\right)((\boldsymbol{n}\times\boldsymbol{P})\cdot\boldsymbol{a}_{\rm eff})^2 \right) + Q_4(\boldsymbol{P}) \right]^{1/2}. \end{aligned} \tag{3.79}$$

3.6.2 Including the LO spin-spin coupling

Although the dominant spin effect is the spin-orbit one, that already starts at the 1.5PN level, we leave the treatment of the spin-orbit sector to Sec 3.6.3, and first discuss the LO spin-spin coupling, which is of 2PN accuracy. Consider the individual vectorial spin parameter $\boldsymbol{a}_i \equiv \boldsymbol{S}_i/m_i \equiv \boldsymbol{\chi}_i m_i$ of the two black holes $i = 1, 2$, where $\boldsymbol{S}_i$ is the spin vector, and $\boldsymbol{\chi}_i$ the dimensionless spin vector as introduced in Sec 2.2.3. In ADM coordinates we have, Eq. (2.84),

$$H^{\rm LO}_{\rm ss} = \frac{\mu M}{2R^3}\left(3(\boldsymbol{n}\cdot\boldsymbol{a}_0)^2 - \boldsymbol{a}_0^2\right), \tag{3.80}$$

where

$$\boldsymbol{a}_0 \equiv \boldsymbol{a}_1 + \boldsymbol{a}_2 = \frac{\boldsymbol{S}_1}{m_1} + \frac{\boldsymbol{S}_2}{m_2} \tag{3.81}$$

is a combination of the two individual spins. On the other hand, the LO spin-spin coupling described (in Boyer-Lindquist-based coordinates) by the EOB Hamiltonian $H_{\rm EOB} = M\sqrt{1 + 2\nu(H^{\rm eff}/\mu - 1)}$, with $H^{\rm eff}$ given by Eqs. (3.73), (3.77), (3.78), is equal to

$$H_{\rm EOB}|_{\rm LOss} = \mu M\left[\left(\frac{(\boldsymbol{n}\cdot\boldsymbol{P})^2}{R^2} - \frac{1}{2}\frac{\boldsymbol{P}^2}{R^2}\right)\boldsymbol{a}^2_{\rm eff} + \frac{1}{2}\frac{(\boldsymbol{P}\cdot\boldsymbol{a}_{\rm eff})^2}{R^2} - \frac{(\boldsymbol{n}\cdot\boldsymbol{P})(\boldsymbol{P}\cdot\boldsymbol{a}_{\rm eff})(\boldsymbol{n}\cdot\boldsymbol{a}_{\rm eff})}{R^2} + \frac{(\boldsymbol{n}\cdot\boldsymbol{a}_{\rm eff})^2}{R^3}\right]. \tag{3.82}$$

[Notice, in passing, that the energy mapping (3.26) is equal to the identity at the LO spin-spin accuracy level, so that the LO spin-spin terms of the EOB and effective Hamiltonian actually

correspond, $H_{\rm EOB}|_{\rm LOss} = H^{\rm eff}|_{\rm LOss}$.] We may now wonder whether it is possible to define the effective vectorial Kerr parameter $\boldsymbol{a}_{\rm eff}$ as a function of $\boldsymbol{a}_1$ and $\boldsymbol{a}_2$ so that (3.80) and (3.82) are canonically equivalent.

The result is easily found by considering the test-mass limit $m_2/m_1 \to 0$, where the only surviving spin effect is proportional to the square $\boldsymbol{a}_1^2$ of the central spin parameter $\boldsymbol{a}_1$, and therefore $\boldsymbol{a}_0 \to \boldsymbol{a}_1$, $\boldsymbol{a}_{\rm eff} \to \boldsymbol{a}_1$[18]. In this limit, Eqs. (3.80), (3.82) are nothing but two canonically equivalent, LO spin-spin descriptions of the Kerr dynamics, in ADM and Boyer-Lindquist coordinates, respectively. Since, in ADM coordinates, the LO spin-spin Kerr Hamiltonian has the same formal structure of the two-body one (it suffices to replace $\boldsymbol{a}_1$ by $\boldsymbol{a}_0$), we understand that defining

$$\boldsymbol{a}_{\rm eff} \equiv \boldsymbol{a}_0 \tag{3.83}$$

allows to also reproduce the full LO spin-spin coupling in the EOB Hamiltonian[19]. The corresponding canonical transformation can be calculated explicitly, and reads (according to the formalism of Sec 3.3),

$$H_{\rm EOB}|_{\rm LOss} = H^{\rm LO}_{\rm ss} + \{G^{\rm LO}_{\rm ss}, H_{\rm N}\}, \tag{3.84}$$

with the spin-dependent generating function [75]

$$G^{\rm LO}_{\rm ss} = -\frac{\mu M}{2R}\Big((\boldsymbol{n}\cdot\boldsymbol{P})\boldsymbol{a}_0^2 - (\boldsymbol{n}\cdot\boldsymbol{a}_0)(\boldsymbol{P}\cdot\boldsymbol{a}_0)\Big). \tag{3.85}$$

Under a general, spin-dependent transformation G_s, besides of the orbital variables $\boldsymbol{R}$, and $\boldsymbol{P}$, also the spins $\boldsymbol{S}_1$ and $\boldsymbol{S}_2$ are transformed. The corresponding rule is given by

$$\boldsymbol{S}_a \to \boldsymbol{S}_a + \{G_s, \boldsymbol{S}_a\} = \boldsymbol{S}_a + \frac{\partial G_s}{\partial \boldsymbol{S}_a}\times \boldsymbol{S}_a, \tag{3.86}$$

where the last equality is a consequence of the Poisson Bracket for canonical spin variables, that is,

$$\{S_a^i, S_b^j\} = \delta_{ab}\,\epsilon^{ijk}\,S_a^k, \tag{3.87}$$

see Eq. (2.46). It is important to remark that Eq. (3.86) describes an infinitesimal rotation $\delta\boldsymbol{S} = \boldsymbol{\Omega}\times\boldsymbol{S}$, and as a such it does not affect the spin magnitude (just as the time evolution preserves the spin length, see the discussion in Sec 2.2.3). Notice also that, in the case of $G^{\rm LO}_{\rm ss}$, the aligned-spins and equatorial-orbits configuration $(\boldsymbol{n}\cdot\boldsymbol{S}_a) = 0$, $(\boldsymbol{P}\cdot\boldsymbol{S}_a) = 0$ and $\boldsymbol{S}_a \parallel \boldsymbol{S}_b$ is not destroyed by the rotation. It is easy to show that, more generally, no even-in-spin generating function can rotate the spins away from the aligned-spins and equatorial configuration.

3.6.3 The spin-orbit sector

In this section, following Refs. [64, 68, 70], we discuss a possible inclusion of the spin-orbit effects (2.80)-(2.83) into the EOB. We start from the LO spin-orbit coupling, which in ADM coordinates reads

[18] We recall that, for a fixed $\boldsymbol{a}_1 \neq 0$ and in the limit $m_2/m_1 \to 0$, the spin ratio $\boldsymbol{a}_2/\boldsymbol{a}_1 \to 0$, since the spin parameters are bounded in length by the mass of their bodies ($|\boldsymbol{a}_i| \leq m_i$).

[19] The original derivation in [68] followed another, though not very dissimilar argument. There, the NLO spin-spin coupling of the EOB Hamiltonian is calculated in ADM coordinates starting from the formula describing the quadrupole deformation of the Kerr-metric [113].

$$H_{\rm so}^{\rm LO} = \frac{1}{R^3}\boldsymbol{L}\cdot\Big(2\,\boldsymbol{S}+\frac{3}{2}\boldsymbol{S}^*\Big), \tag{3.88}$$

with the angular momentum $\boldsymbol{L}\equiv(\boldsymbol{R}\times\boldsymbol{P})$ and with the spin combinations

$$\boldsymbol{S}\equiv\boldsymbol{S}_1+\boldsymbol{S}_2=m_1\boldsymbol{a}_1+m_2\boldsymbol{a}_2, \qquad \boldsymbol{S}^*\equiv\frac{m_2}{m_1}\boldsymbol{S}_1+\frac{m_1}{m_2}\boldsymbol{S}_2=m_2\boldsymbol{a}_1+m_1\boldsymbol{a}_2, \tag{3.89}$$

that are related to the dimensionless $\boldsymbol{\chi}$ and $\boldsymbol{\chi}^*$ in Eq. (2.80) by $\boldsymbol{S}=M\mu\boldsymbol{\chi}$ and $\boldsymbol{S}^*=M\mu\boldsymbol{\chi}^*$. In the effective Hamiltonian (3.78) (again in Boyer-Lindquist-based coordinates, and furthermore with the LO spin-spin inclusion $\boldsymbol{a}_{\rm eff}\equiv\boldsymbol{a}_0\equiv\boldsymbol{a}_1+\boldsymbol{a}_2$), all couplings that are odd in the spins are entailed in the "shift-part"

$$N^i\,P_i=\frac{\big(R^2+\boldsymbol{a}_0^2-\Delta_t\big)}{\mathcal{R}^4+(\boldsymbol{n}\cdot\boldsymbol{a}_0)^2\Delta_t}\boldsymbol{L}\cdot\boldsymbol{a}_0, \tag{3.90}$$

where $\mathcal{R}^4\equiv R^4+R^2\boldsymbol{a}_0^2+2M\,R\,\boldsymbol{a}_0^2$. After PN expanding the above expression, the LO spin-orbit coupling (which remains unaltered under the mapping $H^{\rm eff}\to H_{\rm EOB}$) is simply given by

$$H_{\rm EOB}|_{\rm LOso}=\frac{2\,M}{R^3}\boldsymbol{L}\cdot\boldsymbol{a}_0, \tag{3.91}$$

where the factor $2M$ comes from the second term expansion $\Delta_t^{\rm PN}=R^2(1-\frac{2M}{R}+\frac{\boldsymbol{a}_0^2}{R^2}+...)$. The fact that $M\,\boldsymbol{a}_0=\boldsymbol{S}+\boldsymbol{S}^*$ seems to be quite fortunate, since Eq. (3.91) already reproduces the correct $\boldsymbol{S}$-coupling of Eq. (3.88). However, the $\boldsymbol{S}^*$-couplings of Eq. (3.91) and of Eq. (3.88) differ by a factor 3/4 from one another, and one might therefore decide to modify the effective Hamiltonian by adding a spin-orbit correcting term

$$N^i\,P_i\to N^i\,P_i+\Delta H_{\rm so}\equiv\frac{\big(R^2+\boldsymbol{a}_0^2-\Delta_t\big)}{2\,M(\mathcal{R}^4+(\boldsymbol{n}\cdot\boldsymbol{a}_0)^2\Delta_t)}\boldsymbol{L}\cdot\Big(g_S^{\rm eff,\,LO}\boldsymbol{S}+g_{S^*}^{\rm eff,\,LO}\boldsymbol{S}^*\Big), \tag{3.92}$$

with the LO gyro-gravitomagnetic factors

$$g_S^{\rm eff,\,LO}=2, \qquad g_{S^*}^{\rm eff,\,LO}=\frac{3}{2}. \tag{3.93}$$

This Hamiltonian modification can also be viewed as a redefinition $\boldsymbol{a}_0\to\boldsymbol{a}_0-\boldsymbol{S}^*/(4M)$ of the *linear* effective spin parameter entering the metric elements $g_{\rm eff}^{0i}$, that neither violates the separability properties of the effective metric, nor introduces additional nongeodesic terms into the EOB Hamiltonian. However, as we are going to discuss, the effective Hamiltonian must be modified in a nongeodesic way in order to include higher-order spin-orbit effects.

Including the NLO and NNLO spin-orbit coupling in DJS gauge

At the NLO spin-orbit order, the ADM Hamiltonian has the formal structure

$$H_{\rm so}^{\rm NLO}\sim\sum_{a=1,2}\frac{1}{R^3}\Big(\boldsymbol{P}^2+(\boldsymbol{n}\cdot\boldsymbol{P})^2+\frac{1}{R}\Big)\boldsymbol{L}\cdot\boldsymbol{S}_a, \tag{3.94}$$

and similarly, at NNLO,

$$H_{\rm so}^{\rm NNLO}\sim\sum_{a=1,2}\frac{1}{R^3}\Big(\boldsymbol{P}^4+\boldsymbol{P}^2(\boldsymbol{n}\cdot\boldsymbol{P})^2+(\boldsymbol{n}\cdot\boldsymbol{P})^4+\frac{\boldsymbol{P}^2}{R}+\frac{(\boldsymbol{n}\cdot\boldsymbol{P})^2}{R}+\frac{1}{R^2}\Big)\boldsymbol{L}\cdot\boldsymbol{S}_a, \tag{3.95}$$

see Eqs. (2.82), (2.83). It is clear that a momentum-dependence of this type cannot be reproduced by any effective metric term $N^i P_i$ (which can only produce a coupling $\boldsymbol{L}\cdot\boldsymbol{S}_a$). Consequently, the most natural procedure may be that of introducing subleading-order modifications of the effective gyro-gravitomagnetic factors $g_S^{\rm eff}$ and $g_{S^*}^{\rm eff}$ (whose LO contribution is given by Eq. (3.93)), by adding to them a momentum dependence similar to the one exhibited in the ADM case. This is a direct modification of the effective Hamiltonian and, similarly to the inclusion of Q_4 at the 3PN orbital level, it is of nongeodesic character. In practice, it is sufficient to calculate the transformation $g_S^{\rm ADM}, g_{S^*}^{\rm ADM} \to g_S^{\rm eff}, g_{S^*}^{\rm eff}$ under the ADM $\to$ EOB change of coordinates (see Refs. [64, 70]), and to apply the result on the spin-orbit part of the effective Hamiltonian. However, as already discussed, there is the freedom to perform an additional (and in this case spin-dependent) canonical transformation, acting linearly at the considered order, that reduces the number of involved terms. The most general generating functions acting at the NLO and NNLO spin-orbit level are of the formal type

$$G_{\rm so}^{\rm NLO} \sim \frac{(\boldsymbol{R}\cdot\boldsymbol{P})}{R^3}\sum_{a=1,2}\boldsymbol{L}\cdot\boldsymbol{S}_a, \tag{3.96}$$

$$G_{\rm so}^{\rm NNLO} \sim \frac{(\boldsymbol{R}\cdot\boldsymbol{P})}{R^3}\sum_{a=1,2}\left(\boldsymbol{P}^2+(\boldsymbol{n}\cdot\boldsymbol{P})^2+\frac{1}{R}\right)\boldsymbol{L}\cdot\boldsymbol{S}_a, \tag{3.97}$$

and act according to

$$H_{\rm so}^{\rm NLO} \to H_{\rm so}^{\rm NLO} + \{G_{\rm so}^{\rm NLO}, H_N\}, \tag{3.98}$$

$$H_{\rm so}^{\rm NNLO} \to H_{\rm so}^{\rm NNLO} + \{G_{\rm so}^{\rm NNLO}, H_N\} + \{G_{\rm so}^{\rm NLO}, H_{1PN}\}. \tag{3.99}$$

In principle, we can use the 2 degrees of freedom introduced by $G_{\rm so}^{\rm NLO}$ to reduce the 6 coefficients of $H_{\rm so}^{\rm NLO}$ to 4, and correspondingly, the 12 coefficients of $H_{\rm so}^{\rm NNLO}$ should shrink down to 6 under suitable action choice of $G_{\rm so}^{\rm NNLO}$. To get an idea of type of transformation we are dealing with, consider the following Poisson brackets:

$$\left\{\frac{(\boldsymbol{R}\cdot\boldsymbol{P})}{R^3}\boldsymbol{L}\cdot\boldsymbol{S}_a, H_{\rm N}\right\} = \left(\frac{\boldsymbol{P}^2}{R^3} - 3\frac{(\boldsymbol{n}\cdot\boldsymbol{P})^2}{R^3} - \frac{1}{R^4}\right)\boldsymbol{L}\cdot\boldsymbol{S}_a \tag{3.100}$$

$$\left\{\frac{(\boldsymbol{R}\cdot\boldsymbol{P})}{R^4}\boldsymbol{L}\cdot\boldsymbol{S}_a, H_{\rm N}\right\} = \left(\frac{\boldsymbol{P}^2}{R^4} - 4\frac{(\boldsymbol{n}\cdot\boldsymbol{P})^2}{R^4} - \frac{1}{R^5}\right)\boldsymbol{L}\cdot\boldsymbol{S}_a \tag{3.101}$$

$$\left\{\frac{(\boldsymbol{R}\cdot\boldsymbol{P})\boldsymbol{P}^2}{R^3}\boldsymbol{L}\cdot\boldsymbol{S}_a, H_{\rm N}\right\} = \left(\frac{\boldsymbol{P}^4}{R^3} - 3\frac{\boldsymbol{P}^2(\boldsymbol{n}\cdot\boldsymbol{P})^2}{R^3} - \frac{\boldsymbol{P}^2}{R^4} - 2\frac{(\boldsymbol{n}\cdot\boldsymbol{P})^2}{R^4}\right)\boldsymbol{L}\cdot\boldsymbol{S}_a, \tag{3.102}$$

the first one corresponding to a NLO spin-orbit Hamiltonian transformation, and the other two to a NNLO one. From Eqs. (3.100)-(3.102), it is clear that a suitable choice of $G_{\rm so}^{\rm NLO}$ and of $G_{\rm so}^{\rm NNLO}$ allows to remove all couplings of the type $\sim \boldsymbol{P}^2$ and $\sim \boldsymbol{P}^4$, so that the resulting Hamiltonian reduces to a simple momentum-independent potential in the case of circular orbits $(\boldsymbol{n}\cdot\boldsymbol{P}) = 0$. The gauge is uniquely fixed by requiring that also the terms $\sim \boldsymbol{P}^2(\boldsymbol{n}\cdot\boldsymbol{P})^2$ must vanish, which can be obtained with a strategy very similar to the one discussed so far. We may call this choice the Damour-Jaranowski-Schäfer (DJS) gauge, since it was firstly applied, at least in the spinning EOB framework,[20] in Ref. [70].

[20] Notice that the spin term $\boldsymbol{L}\cdot\boldsymbol{S}_a$ is actually irrelevant in Eqs. (3.100)-(3.102), and therefore the discussion done here is also valid, essentially, for the nonspinning case.

In order to write down the results found in [64, 70], one should be careful with the notation. We *define* the higher-order generalization of the effective gyro-gravitomagnetic ratios

$$g_S^{\rm eff} \equiv g_S^{\rm eff,\,LO} + g_S^{\rm eff,\,NLO} + g_S^{\rm eff,\,NNLO} + ... \tag{3.103}$$
$$g_{S^*}^{\rm eff} \equiv g_{S^*}^{\rm eff,\,LO} + g_{S^*}^{\rm eff,\,NLO} + g_{S^*}^{\rm eff,\,NNLO} + ... \tag{3.104}$$

so that the PN expansion of the effective spin-orbit Hamiltonian $H_{\rm so}^{\rm eff}$ is equal to

$$H_{\rm so}^{\rm eff,\,PN} = \frac{1}{R^3}\boldsymbol{L}\cdot\left(g_S^{\rm eff}\boldsymbol{S} + g_{S^*}^{\rm eff}\boldsymbol{S}^*\right). \tag{3.105}$$

There is actually a subtlety, which is due to the fact that the prefactor of $\boldsymbol{L}\cdot\left(g_S^{\rm eff,\,LO}\boldsymbol{S} + g_{S^*}^{\rm eff,\,LO}\boldsymbol{S}^*\right)$ in Eq. (3.92) contains terms of the type

$$\frac{1}{R^3}\left(1 - \nu\frac{M}{R} + ...\right) \tag{3.106}$$

emerging from the PN expansion of Δ_t. Therefore, in order to have (3.105) at NNLO spin accuracy, the effective spin-orbit Hamiltonian must be defined as

$$\frac{\left(R^2 + \boldsymbol{a}_0^2 - \Delta_t\right)}{2M(\mathcal{R}^4 + (\boldsymbol{n}\cdot\boldsymbol{a}_0)^2\Delta_t)}\boldsymbol{L}\cdot\left(\tilde{g}_S^{\rm eff}\boldsymbol{S} + \tilde{g}_{S^*}^{\rm eff}\boldsymbol{S}^*\right), \tag{3.107}$$

with NNLO-modified gyro-gravitomagnetic ratios $\tilde{g}_S^{\rm eff}$ and $\tilde{g}_{S^*}^{\rm eff}$ defined as

$$\tilde{g}_{S,S^*}^{\rm eff,\,NNLO} = g_{S,S^*}^{\rm eff,\,NNLO} + \nu\frac{M}{R}g_{S,S^*}^{\rm eff,\,NLO}. \tag{3.108}$$

By using the dimensionless variables $\boldsymbol{p} \equiv \boldsymbol{P}/\mu$, $r \equiv R/M$, the "non-tilded" gyro-gravitomagnetic ratios read [64, 70]

$$g_S^{\rm eff} = 2 - \frac{27}{8}\nu(\boldsymbol{n}\cdot\boldsymbol{p})^2 - \frac{5\nu}{8}\frac{1}{r} + \frac{5}{8}\nu(1+7\nu)(\boldsymbol{n}\cdot\boldsymbol{p})^4 + \left(-\frac{21}{2}\nu + \frac{23}{8}\nu^2\right)\frac{(\boldsymbol{n}\cdot\boldsymbol{p})^2}{r} - \left(\frac{51}{4}\nu + \frac{\nu^2}{8}\right)\frac{1}{r^2} \tag{3.109}$$

$$g_{S^*}^{\rm eff} = \frac{3}{2} - \left(\frac{9}{4}\nu + \frac{15}{8}\right)(\boldsymbol{n}\cdot\boldsymbol{p})^2 - \left(\frac{9}{8} + \frac{3}{4}\nu\right)\frac{1}{r} + \left(\frac{35}{16} + \frac{5}{2}\nu + \frac{45}{16}\nu^2\right)(\boldsymbol{n}\cdot\boldsymbol{p})^4 + \left(\frac{69}{16} - \frac{9}{4}\nu + \frac{57}{16}\nu^2\right)\frac{(\boldsymbol{n}\cdot\boldsymbol{p})^2}{r} - \left(\frac{27}{16} + \frac{39}{4}\nu + \frac{3}{16}\nu^2\right)\frac{1}{r^2}. \tag{3.110}$$

We now have enough elements to expose the main formalism of the spinning EOB Hamiltonian in a unified way, summarizing the results obtained so far.

Brief summary: the spinning EOB Hamiltonian

Given the total mass $M = m_1 + m_2$ and the reduced mass $\mu = m_1 m_2/M$ of the binary system, and denoting with $\nu \equiv \mu/M$ the symmetric mass-ratio, the spinning EOB Hamiltonian

$$H_{\rm EOB} = M\sqrt{1 + 2\nu\left(\frac{H^{\rm eff}}{\mu} - 1\right)} \tag{3.111}$$

is expressed in terms of the effective Hamiltonian $H^{\rm eff}$, that further decomposes in an orbital (i.e., even in the spins) part $H^{\rm eff}_{\rm orb}$ and a spin-orbit (odd in the spins) part $H^{\rm eff}_{\rm so}$, according to

$$H^{\rm eff} = H^{\rm eff}_{\rm orb} + H^{\rm eff}_{\rm so}. \tag{3.112}$$

The orbital sector depends on the spin combination $\boldsymbol{a}_0 = \boldsymbol{a}_1 + \boldsymbol{a}_2$ (where $\boldsymbol{a}_1$ and $\boldsymbol{a}_2$ are the individual vectorial spin parameters of the two bodies), and is given by

$$H^{\rm eff}_{\rm orb} = \left(\frac{\Delta_t}{\mathcal{R}^4 + (\boldsymbol{n}\cdot\boldsymbol{a}_0)^2\Delta_t}\right)^{1/2} \left(R^2 + (\boldsymbol{n}\cdot\boldsymbol{a}_0)^2\right)^{1/2} \left[1 + \frac{1}{\left(1+\frac{(\boldsymbol{n}\cdot\boldsymbol{a}_0)^2}{R^2}\right)}\left(\boldsymbol{P}^2 + \left(\frac{\Delta_r}{R^2} - 1\right)(\boldsymbol{n}\cdot\boldsymbol{P})^2 \right.\right.$$
$$\left.\left. - \frac{1}{\mathcal{R}^4 + (\boldsymbol{n}\cdot\boldsymbol{a}_0)^2\Delta_t}\left(2R^2 - \Delta_t + \boldsymbol{a}_0^2 + (\boldsymbol{n}\cdot\boldsymbol{a}_0)^2\right)((\boldsymbol{n}\times\boldsymbol{P})\cdot\boldsymbol{a}_0)^2\right) + Q_4(\boldsymbol{P})\right]^{1/2}. \tag{3.113}$$

Here, $\mathcal{R}^4 = R^4 + R^2\boldsymbol{a}_0^2 + 2MR\,\boldsymbol{a}_0^2$, Q_4 can be found in Eq. (3.51), and

$$\Delta_t = R^2 P_4^1\left[A_{\rm 4PN}(u,\nu) + a_{\rm eff}^2 u^2\right], \qquad \Delta_r = \frac{\Delta_t}{D(u,\nu)}, \tag{3.114}$$

with $u = M/R$, while A and D are given by Eqs.(3.52),(3.57). Finally, the spin-orbit part $H^{\rm eff}_{\rm so}$ is given by

$$H^{\rm eff}_{\rm so} = \frac{\left(R^2 + \boldsymbol{a}_0^2 - \Delta_t\right)}{2M(\mathcal{R}^4 + (\boldsymbol{n}\cdot\boldsymbol{a}_0)^2\Delta_t)}\boldsymbol{L}\cdot\left(\tilde{g}^{\rm eff}_S\boldsymbol{S} + \tilde{g}^{\rm eff}_{S^*}\boldsymbol{S}^*\right), \tag{3.115}$$

where $\tilde{g}^{\rm eff}_S$ and $\tilde{g}^{\rm eff}_{S^*}$ are the NNLO-modifed gyro-gravitomagnetic factors, obtained by Eqs. (3.109), (3.110) with the NNLO adjustment (3.108).

The conservative orbital evolution is calculated applying the canonical equations of motion (see, for instance, the last paragraphs of Sec 2.2.3) to the EOB Hamiltonian.

3.6.4 Preview of chapters 4 and 5: a possible NLO spin-spin inclusion

Chapters 4 and 5 are based on the spinning EOB model exposed so far, and discuss an option for including the NLO spin-spin coupling (2.85) in to the EOB Hamiltonian. In Chapter 4, only the case of aligned spins and circular orbits is considered. The idea is that of redefining the effective squared spin $\boldsymbol{a}_0^2$ entering the effective metric, by introducing a subleading-order modification of the formal type

$$\boldsymbol{a}_0^2 \to \boldsymbol{a}_0^2 + \sum_{i,j=1,2}\left(\boldsymbol{p}^2 + (\boldsymbol{n}\cdot\boldsymbol{p})^2 + \frac{1}{r}\right)(\boldsymbol{a}_i\cdot\boldsymbol{a}_j). \tag{3.116}$$

This procedure is extended, in Chapter 5, to the case of general spin orientations. The proposal is to make a distinction, in the EOB Hamiltonian, between all different scalar products that involve quadratic spin variables, which can be of the type $(\boldsymbol{\chi}_i\cdot\boldsymbol{\chi}_j)$, $(\boldsymbol{n}\cdot\boldsymbol{\chi}_i)(\boldsymbol{n}\cdot\boldsymbol{\chi}_j)$, $(\boldsymbol{p}\cdot\boldsymbol{\chi}_i)(\boldsymbol{p}\cdot\boldsymbol{\chi}_j)$, and $(\boldsymbol{n}\cdot\boldsymbol{\chi}_i)(\boldsymbol{p}\cdot\boldsymbol{\chi}_j)$, and to separately modify each of them by a subleading-order deformation similar to the one given by Eq. (3.116). A gauge fixing will reduce the 25 coefficients defining the ADM NLO spin-spin Hamiltonian to only 12. However, no DJS-type could be imposed, and furthermore, the effective Hamiltonian becomes now a very complicated function of the momenta. There is still place to refine the model, and actually an improved Hamiltonian with NLO spin-spin coupling will be proposed in Chapter 6.

In the next section, we introduce the spinning EOB Hamiltonian proposed by Damour and Nagar in 2014 [81], which constitutes the starting point for the NLO spin-spin developments of Chapter 6.

3.7 A new EOB Hamiltonian for spinning, nonprecessing black hole binaries

An improved EOB Hamiltonian for black holes with aligned, nonprecessing spins has been proposed in Ref. ([81]). This Hamiltonian, accompanied by an appropriate implementation of the radiative sector, has been calibrated against Numerical Relativity and is now very accurate [81, 92]. As an example, Fig 3.5 (taken from [92]) shows the corresponding waveform prediction for equal mass and nearly extremal spins, as compared with a NR waveform.

In this section, we make an overview of the main innovations introduced by [81] at the Hamiltonian level. The inspiration for the new developments comes from a revisitation of the Kerr Hamiltonian. Taking, for instance, the $\nu \to 0$ limit of Eq. (3.79), and switching to Boyer-Lindquist coordinates (with $\theta \equiv \pi/2$), it easily checked that the Kerr Hamiltonian has the form (with a being the Kerr parameter)

$$H^{\rm Kerr}_{\rm eq}(R,P_r,P_\varphi,a) = \sqrt{A^{\rm Kerr}_{\rm eq}(R,a)\left(\mu^2 + \frac{P_r^2}{B^{\rm Kerr}_{\rm eq}(R,a)} + \frac{P_\varphi^2}{R_c^2}\right)} + \frac{2}{R R_c^2} M a P_\varphi, \tag{3.117}$$

with the equatorial potentials

$$A^{\rm Kerr}_{\rm eq}(R,a) = \left(1 - \frac{2M}{R_c}\right)\frac{1+\frac{2M}{R_c}}{1+\frac{2M}{R}}, \qquad B^{\rm Kerr}_{\rm eq}(R,a) = (A^{\rm eq})^{-1}\frac{R^2}{R_c^2}, \tag{3.118}$$

and with the *centrifugal radius*

$$R_c^2 = R^2 + a^2 + \frac{2Ma^2}{R}. \tag{3.119}$$

More generally, $R_c(R,a)$ can be defined by requiring that the centrifugal energy has the structure $\sim \mu^2 + P_\varphi^2/R_c^2$, and is therefore a *gauge invariant* quantity. The usage of R_c to parametrize the Kerr Hamiltonian is very convenient. For example, the equatorial radial potential $A^{\rm Kerr}_{\rm eq}(R,a)$ takes a zero at the fixed value $R_c = 2M$, independently of the spin magnitude, while the Boyer-Lindquist radius R oscillates from $R = 2M$, in the Schwarzschild case, to $R = M$, for an extremal black hole. Moreover, Ref. [81] has shown that R_c is very efficient in parametrizing $A^{\rm Kerr}_{\rm eq}$, in the sense that the pure a-dependency in the plot of $A^{\rm eq}$ versus R_c is very weak (see Fig 1 there). For these reasons, one may be tempted to take R_c as the new radial canonical variable instead of R. However, the inverse relation $R(R_c,a)$ (that must be evaluated both in $A^{\rm Kerr}_{\rm eq}$ and in $B^{\rm Kerr}_{\rm eq}$, as well as in the spin-orbit part) turns out to be a very complicated function, see Eq. (17) in Ref. [81], and consequently this idea should rather be abandoned.

In view of these considerations, and starting from the limiting case of the Kerr Hamiltonian, Damour and Nagar developed an EOB model in which an EOB centrifugal radius $R_c(R,a_1,a_2)$ plays a privileged role, however maintaining the Boyer-Lindquist-like coordinate R as the true, canonical variable. Following the EOB model developed in the last section, it is clear that the EOB centrifugal radius must be defined as

$$R_c^2 \equiv R^2 + \boldsymbol{a}_0^2 + \frac{2M\boldsymbol{a}_0^2}{R}, \tag{3.120}$$

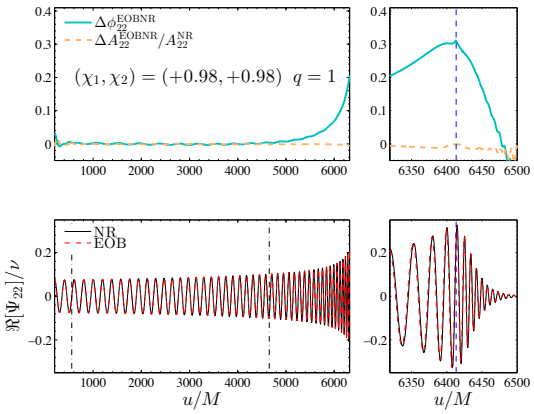

Figure 3.5: *Comparison between the 22-mode of the spinning EOB model of Ref. [81] (whose Hamiltonian part has been exposed in this section) and a NR waveform from the SXS catalog [98] for mass ratio $q \equiv m_1/m_2 = 1$, and for aligned, nearly extremal spins $\chi_1 \equiv \chi_2 \equiv a_i/m_{\equiv}0.98$, $i = 1, 2$. The deviation of both the phase ϕ reaches a maximal value ~ 0.3 in correspondence of the merger, which is much smaller than the uncertainty $\Delta\phi^{(NR)} \sim 2$ rad of the simulation itself. The figure is taken from Ref. [92].*

with the already discussed vectorial spin parameter $\boldsymbol{a}_0 = \boldsymbol{a}_1 + \boldsymbol{a}_2$. [For simplicity, we maintain the same notation R_c that we have used for the Kerr case. From now on, however, R_c will strictly denote the EOB centrifugal radius (3.120).]

The factorization of a Schwarzschild-type potential $(1-2M/R_c)$ in $A_{\rm eq}^{\rm Kerr}$, which is nothing but the Newtonian limit of the nonspinning EOB potential $A_{\rm 4PN}(u_c,\nu)$, Eq. (3.52), evaluated at $u_c \equiv M/R_c$ instead of u, motivates the following definition for the EOB potentials with spin:

$$A_{\rm eq}(R,\nu,\boldsymbol{a}_1,\boldsymbol{a}_2) \equiv P_4^1\Big[A_{\rm 4PN}(u_c,\nu)\Big]\frac{1+\frac{2M}{R_c}}{1+\frac{2M}{R}}, \tag{3.121}$$

$$B_{\rm eq}(R,\nu,\boldsymbol{a}_1,\boldsymbol{a}_2) = \frac{D(u_c,\nu)}{A_{\rm eq}}\frac{R^2}{R_c^2}, \tag{3.122}$$

where the functional form of $D(u_c,\nu)$ can be taken from Eq. (3.57). To be more explicit, with $A_{\rm 4PN}(u_c,\nu)$ and $D(u_c,\nu)$ we mean the potentials as $A_{\rm 4PN}(u_c,\nu) \approx 1 - 2u_c + 2\nu u_c^3 + ...$ and $D(u_c,\nu) = 1/(1 + 6\nu\, u_c + 2(26-3\nu)\nu u_c^3)$, that are obtained from $A_{\rm 4PN}(u,\nu)$ and $D(u,\nu)$ by replacing u by u_c. Leaving for the moment the spin-orbit part unspecified, the orbital effective Hamiltonian is defined in full analogy with Eq. (3.117), namely

$$H_{\rm eq}^{\rm eff}(R,P_r,P_\varphi,\nu,\boldsymbol{a}_1,\boldsymbol{a}_2) = \sqrt{A_{\rm eq}(R,\boldsymbol{a}_0)\left(\mu^2 + \frac{P_r^2}{B_{\rm eq}(R,a)} + \frac{P_\varphi^2}{R_c^2}\right)} + H_{\rm so}^{\rm eff}. \tag{3.123}$$

As discussed in Sec 3.6.2, an effective Hamiltonian reproducing the two-body LO spin-spin coupling is simply obtained from the Kerr Hamiltonian by taking the spin combination $\boldsymbol{a}_0^2$ as the squared spin parameter entering the Kerr metric. For this reason, it is clear that the LO spin-spin coupling described by (3.123) is correct. Moreover, since $1/R = 1/R_c + \mathcal{O}(\boldsymbol{a}_0^2/R^3)$, it is also clear that the spin-independent terms in the PN expansion of $A_{\rm eq}(R,\nu,\boldsymbol{a}_1,\boldsymbol{a}_2)$ and of $B_{\rm eq}(R,\nu,\boldsymbol{a}_1,\boldsymbol{a}_2)$ are equal to the PN expansion of the non spinning potentials $A(u,\nu)$ and $B(u,\nu)$, and consequently, the purely orbital dynamics described by $H^{\rm eff}$ in Eq. (3.123) is consistent with the one described by the previous EOB model. On the other hand, the usage uf u_c instead of u in the ν-deformed part of the effective potentials has the effect of modifying the higher order spin-spin couplings

that are resummed in the EOB. For example, the 2PN term $2\nu u_c^3$ in $A_{\rm eq}(R,\nu,\boldsymbol{a}_1,\boldsymbol{a}_2)$ introduces, at a first approximation, an additional NNLO spin-spin coupling $\sim \mu\nu M^3\boldsymbol{a}_0^2/R^5$.

In Ref. [81], the EOB spin-orbit sector is revisited as well. We recall that the quite complicated 4PN Padéed potential Δ_t is involved in the definition of the previous EOB spin-orbit Hamiltonian, given by Eq. (3.107). Beyond this particular spin-orbit structure, there was the will of keeping an effective dynamics that mainteins the separability properties of the ν-deformed Kerr-like metric.

By contrast, the separability requirement is relaxed in Ref. [81], where the priority is given to the simplicity of the EOB formulation. The new idea is that of defining $H_{\rm so}^{\rm eff}$ in a minimal way, with the only requirement of i) reproducing the NNLO spin-orbit coupling and ii) maintaining the exact purely Kerr, $\nu=0$ coupling. More concretely, we have

$$H_{\rm so}^{\rm eff} = 2u\,u_c^2\hat{G}_S\boldsymbol{L}\cdot\boldsymbol{S} + \frac{3}{2}u_c^3\hat{G}_{S^*}\boldsymbol{L}\cdot\boldsymbol{S}^*. \tag{3.124}$$

In the limit $\nu\to 0$, the first term $2u\,u_c^2\hat{G}_S\boldsymbol{L}\cdot\boldsymbol{S}$ reduces to the Kerr spin-orbit coupling, while the second one vanishes, since $\boldsymbol{S}^*\to 0$ (provided that the Kerr bound $|\boldsymbol{S}_a|\leq m_a^2$ is hold to be true). The functions $2\hat{G}_S$ and $\frac{3}{2}\hat{G}_{S^*}$ are a resummed version of the gyro-gravitomagnetic factors (3.109), (3.110), together with the inclusion of some higher-order couplings[21]. In order to prevent the bad strong-field behavior of the Taylor-expanded gyro-gravitomagnetic factors, which can change in sign at sufficiently low radii (see also the discussion in Chapter 6), they have the inversely-resummed structure (here written at the 4.5PN accuracy level)

$$\hat{G}_{S^{(*)}} = \frac{1}{1+c_{10}^{(*)}u_c+c_{20}^{(*)}u_c^2+c_{30}^{(*)}u_c^3+c_{02}^{(*)}p_{r_*}^2+c_{12}^{(*)}u_cp_{r_*}^2+c_{04}^{(*)}u_cp_{r_*}^2}, \tag{3.125}$$

where the coefficients c can be found in Eqs. (44)-(56) in Ref. [81]. The differences with respect to (3.109), (3.110), apart from the extra 4.5PN and 5.5PN terms, and from the inverse resummation, are the usage of u_c instead of u (which leads to a change in the couplings that are odd, and at least cubic in the spins), and the usage of the dimensionless tortoise momentum $p_{r_*}\equiv P_r\sqrt{A^{\rm eq}/B^{\rm eq}}/\mu$.

As a last thing, we remark that Ref. [81] also proposes a circular-orbit reformulation of the NLO spin-spin terms discussed in [115] (see Chapter 4). More precisely, we can make use of the leading-order 3d Kepler law for circular orbits, that reads $\boldsymbol{p}^2=1/r+\mathcal{O}(1/r^2)$. This can be inserted in the effective spin-squared modification mentioned in Sec 3.6.4, that we shall denote here as

$$\delta\boldsymbol{a}^2 = \sum_{i=1,2}\left(a\,\boldsymbol{p}^2+b\,(\boldsymbol{n}\cdot\boldsymbol{p})^2+c\,\frac{1}{r}\right)(\boldsymbol{a}_i\cdot\boldsymbol{a}_j), \tag{3.126}$$

so as to yield

$$\delta\boldsymbol{a}^2_{\rm circ}(\boldsymbol{R}) = \sum_{i=1,2}(a+c)\frac{M}{R}(\boldsymbol{a}_i\cdot\boldsymbol{a}_j). \tag{3.127}$$

In the case of circular orbits, NLO spin-spin effects can therefore be included into the model of Ref. [81] by redefining the relation between R and R_c according to

$$R_c^2 \equiv R^2+a_0^2+\frac{2M\boldsymbol{a}_0^2}{R}+\delta\boldsymbol{a}^2_{\rm circ}(\boldsymbol{R}). \tag{3.128}$$

[21] In particular, a 4.5PN-level calibration is accompanied by exact ν-independent terms at 4.5PN and 5.5PN accuracy [74, 114].

We notice that, since R_c is a gauge-invariant quantity, this has to be understood as a redefinition of the Boyer-Lindquist-like radial coordinate R. Starting from the spinning EOB model presented here, an inclusion of NLO spin-spin effects for arbitrarily oriented spins will be proposed in Chapter 6. This has to be considered as the culminating point of the present thesis.

Appendix

3.A The quadrupole formula and the 22-spherical mode

In this appendix, we shall spend few words on the multipolar formalism in spherical harmonics, deriving, in particular, Eq. (3.6) from the mass-quadrupole Q_{ij} of an equal-mass binary system.

As already mentioned, in linearized theory, a gravitational wave is described as a small deviation $h_{\mu\nu} = g_{\mu\nu} - \eta_{\mu\nu}$ of the flat metric at a (large enough) distance D from the source. The gauge-fixed transverse-traceless (TT) waveform h_{ij}^{TT} depends on two degrees of freedom, the plus (h_+) and cross ($h_\times$) polarization. Setting, for instance, the z-coordinate along the propagation direction of the wave, $h_{ij}^{\rm TT}$ has the form (see for instance [3])

$$h_{ij}^{\rm TT} = \begin{pmatrix} h_+ & h_\times & 0 \\ h_\times & -h_+ & 0 \\ 0 & 0 & 0 \end{pmatrix}. \tag{3.129}$$

In a first approximation, the emission of a gravitational wave is described by the well-known quadrupole formula [2]

$$h_{ij}^{\rm TT} = \frac{2}{D}\Lambda_{ij,kl}\ddot{Q}_{kl}(t-D). \tag{3.130}$$

The tensor

$$\Lambda_{ij,kl} = (\delta_{ik} - N_i N_k)(\delta_{jl} - N_j N_l) - \frac{1}{2}(\delta_{ij} - N_i N_j)(\delta_{lk} - N_l N_k) \tag{3.131}$$

is the TT projector (with N_i being the unit vector pointing from the source into the direction of the observer), and

$$Q_{ij} = m_1\left(x_1^i x_1^j - \frac{1}{3}|\boldsymbol{x}_1|\delta^{ij}\right) + m_2\left(x_2^i x_2^j - \frac{1}{3}|\boldsymbol{x}_2|\delta^{ij}\right) \tag{3.132}$$

is the symmetric-trace-free (STF) mass-quadrupole moment of the source (assumed here to be a binary system, with x_a^i ($a=1,2$) being the position coordinates of the two individual masses m_a in their center-of-mass frame). In the case of equal masses, and with $\boldsymbol{r} \equiv \boldsymbol{x}_1 - \boldsymbol{x}_2$, $r \equiv |\boldsymbol{r}|$, $M \equiv m_1 + m_2$, we may write

$$Q_{ij} = M\left(r^i r^j - \frac{1}{3} r\, \delta^{ij}\right). \tag{3.133}$$

Beyond the quadrupolar order, the multipole expansion of h_{ij}^{TT} can be made in terms of more complicated (STF) mass-type and current-type moments $\mathcal{U}_{i_1,\ldots,i_l}$ and $\mathcal{V}_{i_1,\ldots,i_l}$, respectively (we use here the notation of Ref. [116], see however [106, 113] for earlier derivations), that are determined by the near-zone multipole moments. It is however also possible to expand the waveform by means of a decomposition in spherical harmonics. In view of this, let us first remind the reader that for every $l = 2, 3, \ldots$ there exists an orthogonal basis $\{\mathcal{Y}^{lm}_{i_1,\ldots i_l} | m = -l, \ldots l\}$ of the STF tensors of rank l, so that the (l,m)-spherical harmonic Y^{lm} satisfies

$$Y^{lm}(\theta,\varphi) = \mathcal{Y}^{lm}_{i_1,\ldots i_l} e^{i_1} \cdots e^{i_l}, \tag{3.134}$$

where $\boldsymbol{e} = (e^1, e^2, e^3)$ is the unit vector with polar angles (θ,φ). One can thus introduce the spherical mass-type multipole moments $\mathcal{U}_{lm}$ so that the (STF) mass-type multipole moment $\mathcal{U}_{i_1,\ldots,i_l}$ can be written as

$$\mathcal{U}_{i_1,\ldots,i_l} = \sum_{m=-l}^{l} \mathcal{U}_{lm} \mathcal{Y}^{lm}. \tag{3.135}$$

In particular, their projection onto the (θ,φ) direction is

$$\mathcal{U}_{i_1,\ldots,i_l} e^{i_1} \cdots e^{i_l} = \sum_{m=-l}^{l} \mathcal{U}_{lm} Y^{lm}(\theta,\varphi). \tag{3.136}$$

Because of the orthogonality of the basis tensors $\mathcal{Y}^{lm}_{i_1,\ldots i_l}$, the above relations can be inverted to yield the spherical moments in terms of the STF ones,

$$\mathcal{U}_{lm} = \frac{4\pi l!}{(2l+1)!!} \mathcal{U}_{i_1,\ldots,i_l} \left(\mathcal{Y}^{lm}_{i_1,\ldots i_l}\right)^*. \tag{3.137}$$

It shall be therefore clear that the multipolar expansion of h_{ij}^{TT} (whose first term, we recall, is given by the quadrupole formula (3.130)), can equivalently be done in terms of the spherical multipoles (see [113] or, for simplicity, Eq. (12) in [116]). A possible connection of the spherical multipole formalism with the "+" and "×" polarizations is provided by the relation

$$h_+ - i\, h_\times = \sum_{l=2}^{\infty} \sum_{m=-l}^{l} h^{lm} Y^{lm}_{-2}(\theta',\varphi'), \tag{3.138}$$

where Y^{lm}_{-2} are the spin-2 weighted spherical harmonics (see e.g. [117]) and where h^{lm} are the multipolar spherical moments of the wave. Neglecting, for simplicity, the current-type multipoles, the h^{lm} are related to the spherical mass-type multipoles $\mathcal{U}_{lm}$ by

$$h^{lm} = \frac{1}{D} \frac{2\sqrt{2}}{l!} \sqrt{\frac{(l+1)(l+2)}{2l(l-1)}} \mathcal{U}_{lm}(t-D). \tag{3.139}$$

In the case of the quadrupolar wave given by Eq. (3.130), only the modes

$$h^{2m} = \frac{\sqrt{6}}{D} Q_{2m}(t-D) \tag{3.140}$$

are non-vanishing (notice that the quadrupolar $\mathcal{U}_{ij}$ is simply equal to the near-zone mass-quadrupole moment Q_{ij}, see Eq. (3.133), and therefore $\mathcal{U}_{2m} \equiv Q_{2m}$). For definiteness, we consider the binary system as laying on the (x,y)-plane, and accordingly associate the polar variables $(\theta = \pi/2, \varphi)$ to the orientation of the binary in space[22]. Then, $h^{2m} = 0$ for $m = -1, 0, 1$, and inserting Eq. (3.133)[23],

$$h^{22} = \frac{\sqrt{6}}{R} \frac{8\pi}{15} \frac{d^2}{dt^2} \left(M r^2 Y^{2\,-2}(\pi/2, \varphi) \right), \tag{3.141}$$

while $h^{2\,-2} = \left(h^{22}\right)^*$. Under the assumption of quasi-circularity, $\dot{r} \ll r\omega$, (with $\omega \equiv \dot{\varphi}$) we end up with the simple expression

$$h^{22} = -8 \frac{M}{D} \sqrt{\frac{\pi}{5}} (r\omega)^2 e^{-2i\varphi}, \tag{3.142}$$

which is used in the main text of this thesis.

[22]The angles (θ, φ) shall not be confused with the "primed" (θ', φ') used in Eq. (3.138), which refer instead to the oscillation direction of the wave modes.

[23]More explicitly, writing Eq. (3.133) as $Q_{ij} = M r^2 (e^i e^j - \frac{\delta^{ij}}{3})$, the $l = m = 2$ case of Eq. (3.137) becomes $Q_{22} \propto r^2 \left(\mathcal{Y}^{22}_{ij} e^i e^j \right)^* = r^2 Y^{2\,-2}$.

CHAPTER 4

Effective-one-body Hamiltonian with next-to-leading order spin-spin coupling for two nonprecessing black holes with aligned spins

S. Balmelli, Ph. Jetzer. *Published in Physical Review D, Volume* **87**, *124036 (2013)*

Abstract

The canonical Arnowitt-Deser-Misner (ADM) Hamiltonian with next-to-leading order (NLO) spin-spin coupling [J. Steinhoff, S. Hergt, and G. Schäfer] is converted into the effective-one-body (EOB) formalism of T. Damour, P. Jaranowski, and G. Schäfer for the special case of spinning black hole binaries whose spins are aligned with the angular momentum. In particular, we propose to include the new terms by adding a dynamical term of NLO to the Kerr parameter squared entering the effective metric. The modified EOB Hamiltonian consistently reduces to the Kerr Hamiltonian as the mass-ratio tends to zero; moreover, it predicts the existence of an innermost stable circular orbit. We also derive, for the general case of arbitrarily oriented spins but in the vanishing mass-ratio limit, a coordinate transformation that maps the NLO spin-spin contribution of the ADM Hamiltonian to the EOB Hamiltonian.

4.1 Introduction

Coalescing black hole binaries (BHBs) are among the most promising gravitational wave (GW) sources for interferometric, ground-based detectors (like the currently operating LIGO, Virgo and GEO) and the planned space-based detector LISA [118]. LIGO and Virgo are going to be upgraded to advanced configurations with a sensitivity improvement of one order of magnitude [119]. The volume of space that can be observed will be enlarged by a factor 1000, making a first detection of GW realistic. In particular, for BHBs with masses of about $10M_{\odot}$, a detection rate of roughly 30 events per year seems to be plausible [119]. The data analysis needed to extract the GW signal from the background noise is mainly based on the so-called matched-filtering technique, which requires a deep theoretical understanding and a very accurate modeling of the waveforms. Since the strongest and most useful signals are emitted in the final stages of the coalescence, a description of the inspiral phase alone (that is already provided with great accuracy by the post-newtonian (PN) theory) is not satisfactory. Up to now, the most precise complete waveforms for coalescing BHBs have been generated by numerical relativity simulations. However, since the waveforms depend on at least eight parameters (2 for the masses and 6 for the two spins), it is not conceivable to cover the parameter space by a sufficient number of simulations. As a consequence, the need has arisen to develop analytical (or semi-analytical) tools to support the results provided by numerical relativity.

Among these methods, the effective-one-body (EOB) approach plays a central role. Proposed for the first time in 1999 [65], it is based on the idea of mapping the dynamics of two gravitationally interacting bodies into the geodesics of a fixed, Schwarzschild-like “effective" metric, that are usually described by an Hamiltonian. The EOB dynamics also includes a dissipative part, that collects the energy and momentum losses of the system and that must be added *ad hoc* into the equations of motion (we refer to [120, 121] for a review of the EOB formalism). EOB models generally involve free parameters that can be calibrated through a comparison with numerical simulations, thus exhibiting a noticeable flexibility. Remarkably enough, the first analytical study of the waveform during inspiral and plunge of non spinning binaries has been accomplished within the EOB formalism [66].

Since then, EOB models have been significantly improved. In the non spinning case, Refs. [71–73, 76, 82–86, 91, 107, 122] have led to increasingly accurate waveforms. Relevant analytical improvements have been made especially in the radiation-reaction sector, with the development of a new formalism for the decomposition of multipolar waveforms [72, 73, 76] and, more recently, with the inclusion of the horizon-absorbed GW flux [91, 107, 122].

By contrast, waveforms from the coalescence of spinning binaries have not reached a comparable accuracy, in particular for rapidly spinning systems, like extremal BHBs (see e.g. Ref. [89]). This may be due simply to the fact that spin effects beyond the leading-order (LO) of the PN expansion series have been derived only in recent years [22, 33, 35, 37, 46, 47, 49, 50, 54, 123, 124], rather than to an intrinsic difficulty of the EOB approach to reproduce the spin interaction. Spin effects of coalescing BHBs have been included for the first time into the conservative part of the EOB formalism in Ref. [68], according to the natural idea of generalizing the Schwarzschild-like metric into a Kerr-like metric. The EOB Hamiltonian proposed there reproduces, when expanded in a PN series, the correct LO spin-orbit and spin-spin couplings. Successively, Ref. [70] extended this model to also reproduce the next-to-leading order (NLO) spin-orbit coupling [22]. More recently, the next-to-next-to-leading order (NNLO) spin-orbit coupling (derived in Ref. [37]) has been included in the same formalism [64].

In parallel to this model, a slightly different approach, based on an analytical result reproducing the exact dynamics of a test spin in curved space-time [74], has been developed in Refs. [75, 77,

89]. When the test spin limit is not valid, this Hamiltonian reproduces the same spin effects of Refs. [64, 70], i.e. the LO spin-spin and the NNLO spin-orbit coupling. Up to now, this is the only spinning EOB Hamiltonian that has been calibrated to numerical relativity waveforms [87, 89], though only in the case of nonprecessing spins. The resulting waveforms are rather accurate, but for nearly extremal black holes (that is, with Kerr parameter $a \gtrsim 0.7M/c^2$) with aligned spin they become unsatisfactory. Indeed, compared to the numerical waveforms, they show a dephasing up to 0.8 rad over the entire evolution, while for mildly rotating ($a \lesssim 0.7M/c^2$) black holes the dephasing does not exceed 0.15 rad [89].

Among the features of both EOB models, it is worth mentioning the existence of an innermost stable circular orbit (ISCO), which gives a measure of the quantity of GWs emitted before the plunge. As in the case of the exact Kerr metric, the ISCO becomes more bounded for larger, aligned spins, and consequently the GW signal gets stronger. In particular, coalescing binaries with aligned, non precessing spins are relevant for GW detection purposes. Indeed, numerical simulations show that BHBs whose spins are aligned with the angular momentum generate a signal 3 times stronger than comparable binaries with spins anti-aligned with respect to the angular momentum and 2 times stronger than comparable non spinning binaries. The observational volume is thus 27 times and 8 times larger, respectively [6]. Moreover, the alignment between spins and angular momentum seems to be favoured by accretion mechanisms in gas-rich environments [5].

NLO spin-spin effects have already been calculated a few years ago [46, 47, 49, 50, 123]. Motivated by the above arguments, this paper attempts to improve the EOB Hamiltonian of Refs. [64, 68, 70] by including the NLO spin-spin coupling in the special case of BHBs whose spins are aligned (or anti-aligned) with the angular momentum. More precisely, we show that it is possible to reproduce the correct NLO spin-spin terms by adding a dynamical NLO term to the square of the Kerr parameter of the effective metric. The price to pay is that an effective spin depending on the dynamical variables may introduce physical inconsistencies like the violation of the Kerr bound. However, we show that this can be avoided by the appropriate introduction of an additional NNLO term to the effective squared spin . Furthermore, the old (variable-independent) effective spin is recovered in the small mass-ratio limit, as required by consistency. Finally, we show that the existence of an ISCO is preserved.

The paper is structured as follows: in Sec. 4.2 we present the PN expanded Hamiltonian provided by the ADM theory, and simplify the NLO spin-spin Hamiltonian of Refs. [49, 50] using the center of mass coordinates and taking into account the alignment constraint. In Sec. 4.3 we discuss the mapping between the ADM and the EOB dynamics, performing the appropriate canonical transformations in the case of rapidly rotating spins. An additional canonical transformation which is quadratic in the spins and of NLO accuracy is introduced. In Sec. 4.4 we summarize the structure of the EOB Hamiltonian as given by Ref. [70] and calculate the corresponding 3PN spin-spin contribution. Sec. 4.5 completes the matching between the ADM and the EOB dynamics, proposing a modification of the spin parameter entering the effective Kerr-like metric in order to reproduce the desired spin-spin coupling. For the general case of arbitrarily oriented spins, we derive the canonical transformation that is needed for ensuring the reduction of a future, complete EOB Hamiltonian with NLO spin-spin coupling to the Kerr Hamiltonian whenever the mass-ratio tends to zero. In Sec. 4.6 we show that the modified Hamiltonian still predicts the existence of an ISCO, and discuss the problems arising from the dependency of the modified effective squared spin on the dynamical variables. Finally, in the Appendix we show that the alignment between spins and total angular momentum is conserved during the dynamical evolution at least at the PN order we are dealing with.

4.2 Next-to-leading order, spin-spin Hamiltonian in ADM coordinates

The PN-expanded ADM Hamiltonian for two gravitationally interacting and spinning point masses can be decomposed as

$$H(\boldsymbol{x},\boldsymbol{p},\boldsymbol{S}_1,\boldsymbol{S}_2) = H_{\rm o}(\boldsymbol{x},\boldsymbol{p}) + H_{\rm so}(\boldsymbol{x},\boldsymbol{p},\boldsymbol{S}_1,\boldsymbol{S}_2) + H_{\rm ss}(\boldsymbol{x},\boldsymbol{p},\boldsymbol{S}_1,\boldsymbol{S}_2) + ..., \tag{4.1}$$

where $H_{\rm o}$ denotes the purely orbital part, while $H_{\rm so}$ and $H_{\rm ss}$ describe the spin-orbit and the spin-spin interaction, respectively.

It may be convenient to introduce the center of mass frame ($\boldsymbol{R} \equiv \boldsymbol{x}_1 - \boldsymbol{x}_2$, $\boldsymbol{P} \equiv \boldsymbol{p}_1 - \boldsymbol{p}_2$) and the corresponding rescaled coordinates $\boldsymbol{r} \equiv \boldsymbol{R}/M$, $\boldsymbol{p} \equiv \boldsymbol{P}/\mu$, where $M \equiv m_1 + m_2$ is the total mass and $\mu \equiv m_1\, m_2/M$ the reduced mass. Moreover, we define the symmetric mass-ratio $\nu \equiv \mu/M$ and use the notation $r \equiv |\boldsymbol{r}|$, $\boldsymbol{n} \equiv \boldsymbol{r}/r$. The spins can be rescaled according to $\hat{\boldsymbol{S}}_a \equiv \boldsymbol{S}_a/(M\mu)$ (but, as discussed below, we will use a different notation). Finally, we rescale the Hamiltonian according to $\hat{H} \equiv H/\mu$ [64, 70]. For simplicity, we use units with $G \equiv 1$. The PN structure of the orbital Hamiltonian is

$$\hat{H}_{\rm o} = \frac{c^2}{\nu} + \hat{H}_{\rm o}^{\rm N} + \hat{H}_{\rm o}^{\rm 1PN} + \hat{H}_{\rm o}^{\rm 2PN} + \hat{H}_{\rm o}^{\rm 3PN} + \mathcal{O}\left(\frac{1}{c^8}\right). \tag{4.2}$$

The Newtonian term is simply

$$\hat{H}_{\rm o}^{\rm N} = \frac{\boldsymbol{p}^2}{2} - \frac{1}{r}, \tag{4.3}$$

while the 1PN one reads

$$\hat{H}_{\rm o}^{\rm 1PN} = \frac{1}{c^2}\left[\frac{(3\nu-1)}{8}\boldsymbol{p}^4 - \frac{(3+\nu)}{2}\frac{\boldsymbol{p}^2}{r} - \frac{\nu}{2}\frac{(\boldsymbol{n}\cdot\boldsymbol{p})^2}{r} + \frac{1}{2r^2}\right]. \tag{4.4}$$

For an explicit expression of the 2PN accurate Hamiltonian see Ref. [99], and for the 3PN accurate one Ref. [10]. The expansion of the spin-dependent part can be written as

$$\begin{aligned} H_{\rm so} &= H_{\rm so}^{\rm LO} + H_{\rm so}^{\rm NLO} + ... = \sum_{a\equiv 1,2} \boldsymbol{S}_a \cdot \left(\boldsymbol{\Omega}_a^{\rm LO} + \boldsymbol{\Omega}_a^{\rm NLO} + ...\right) \\ H_{\rm ss} &= \left(H_{\rm S_1^2}^{\rm LO} + H_{\rm S_2^2}^{\rm LO} + H_{\rm S_1S_2}^{\rm LO}\right) + \left(H_{\rm S_1^2}^{\rm NLO} + H_{\rm S_2^2}^{\rm NLO} + H_{\rm S_1S_2}^{\rm NLO}\right) + ... \equiv H_{\rm ss}^{\rm LO} + H_{\rm ss}^{\rm NLO} + ... \end{aligned} \tag{4.5}$$

The terms composing $H_{\rm so}$ have been derived in Ref. [22] (up to NLO) and in Ref. [37] (at NNLO).

Both $H_{\rm so}$ and $H_{\rm ss}$ formally start at 1PN ($\propto 1/c^2$). However, the real PN order depends on the order of magnitude of the spins. For example, for extremal black holes the spins are proportional to $1/c$, which corresponds to 0.5PN. This implies that the leading order term $H_{\rm so}^{\rm LO}$ of the spin-orbit Hamiltonian is 1.5PN accurate, while $H_{\rm ss}^{\rm LO}$ is 2PN accurate. In this paper, we rescale the spins in such a way that the powers of c^{-1} label the true PN order in the case of extremal black holes. We write

$$\boldsymbol{S}_a = \frac{m_a^2}{c}\boldsymbol{\chi}_a, \tag{4.6}$$

where $|\chi_a| \leq 1$ is dimensionless.

The leading-order spin-spin contribution can be written as [68]

$$\hat{H}^{\rm LO}_{\rm ss} = \frac{1}{2c^4}\frac{3(\boldsymbol{n}\cdot\boldsymbol{\chi}_0)^2 - (\boldsymbol{\chi}_0)^2}{r^3}, \tag{4.7}$$

with the linear combination

$$\boldsymbol{\chi}_0 = \frac{m_1}{M}\boldsymbol{\chi}_1 + \frac{m_2}{M}\boldsymbol{\chi}_2. \tag{4.8}$$

Finally, the next-to-leading order, spin-squared Hamiltonian $H^{\rm NLO}_{\rm S_1^2}$ has been derived explicitly in Ref. [49], and the spin(1)-spin(2) Hamiltonian $H^{\rm NLO}_{\rm S_1S_2}$ in Ref. [50]. After going to the rescaled center of mass coordinates (according to the above prescriptions), they read

$$\begin{aligned}
\hat{H}^{\rm NLO}_{\rm S_1^2} = \;& \frac{\nu}{c^6 r^3}\frac{m_1}{m_2}\Bigg[+ \frac{1}{4}\left(1 - 2\nu - \frac{m_1}{m_2}\nu\right)(\boldsymbol{\chi}_1\cdot\boldsymbol{p})^2 + \frac{3}{8}\left(1 - 4\nu - \frac{m_1}{m_2}\nu\right)\boldsymbol{\chi}_1^2(\boldsymbol{p}\cdot\boldsymbol{n})^2 - \frac{3}{4}\nu\left(1 + \frac{m_1}{m_2}\right)\boldsymbol{\chi}_1^2\boldsymbol{p}^2 \\
& + \frac{3}{8}\left(-1 + 8\nu + 7\frac{m_1}{m_2}\nu\right)(\boldsymbol{\chi}_1\cdot\boldsymbol{n})^2\boldsymbol{p}^2 + \frac{3}{4}\left(-1 + \frac{m_1}{m_2}\nu\right)(\boldsymbol{\chi}_1\cdot\boldsymbol{p})(\boldsymbol{\chi}_1\cdot\boldsymbol{n})(\boldsymbol{p}\cdot\boldsymbol{n}) \\
& + \frac{15}{4}\nu(\boldsymbol{\chi}_1\cdot\boldsymbol{n})^2(\boldsymbol{p}\cdot\boldsymbol{n})^2\Bigg] + \frac{\nu^2}{c^6 r^4}\left(1 + \frac{m_1}{m_2}\right)\left[\left(3 + \frac{5}{2}\frac{m_1}{m_2}\right)\boldsymbol{\chi}_1^2 - \left(7 + \frac{9}{2}\frac{m_1}{m_2}\right)(\boldsymbol{\chi}_1\cdot\boldsymbol{n})^2\right],
\end{aligned} \tag{4.9a}$$

$$\begin{aligned}
\hat{H}^{\rm NLO}_{\rm S_1S_2} = \;& \frac{3\nu^2}{2c^6 r^3}\Bigg[- \left(\frac{5}{2} + \frac{m_2}{m_1} + \frac{m_1}{m_2}\right)\Big((\boldsymbol{p}\wedge\boldsymbol{\chi}_1)\cdot\boldsymbol{n}\Big)\Big((\boldsymbol{p}\wedge\boldsymbol{\chi}_2)\cdot\boldsymbol{n}\Big) + 5(\boldsymbol{\chi}_1\cdot\boldsymbol{n})(\boldsymbol{\chi}_2\cdot\boldsymbol{n})(\boldsymbol{p}\cdot\boldsymbol{n})^2 \\
& + (\boldsymbol{\chi}_1\cdot\boldsymbol{n})(\boldsymbol{\chi}_2\cdot\boldsymbol{n})\boldsymbol{p}^2 - \left(2 + \frac{m_1}{m_2}\right)(\boldsymbol{\chi}_1\cdot\boldsymbol{p})(\boldsymbol{\chi}_2\cdot\boldsymbol{n})(\boldsymbol{p}\cdot\boldsymbol{n}) - \left(2 + \frac{m_2}{m_1}\right)(\boldsymbol{\chi}_1\cdot\boldsymbol{n})(\boldsymbol{\chi}_2\cdot\boldsymbol{p})(\boldsymbol{p}\cdot\boldsymbol{n}) \\
& - \frac{1}{6}(\boldsymbol{\chi}_1\cdot\boldsymbol{p})(\boldsymbol{\chi}_2\cdot\boldsymbol{p}) - \frac{1}{6}(\boldsymbol{\chi}_1\cdot\boldsymbol{\chi}_2)\boldsymbol{p}^2 + \left(1 + \frac{m_2}{m_1} + \frac{m_1}{m_2}\right)(\boldsymbol{\chi}_1\cdot\boldsymbol{\chi}_2)(\boldsymbol{p}\cdot\boldsymbol{n})^2\Bigg] \\
& + \frac{6\nu}{c^6 r^4}\Big[(\boldsymbol{\chi}_1\cdot\boldsymbol{\chi}_2) - 2(\boldsymbol{\chi}_1\cdot\boldsymbol{n})(\boldsymbol{\chi}_2\cdot\boldsymbol{n})\Big].
\end{aligned} \tag{4.9b}$$

The Hamiltonian $H^{\rm NLO}_{\rm S_2^2}$ can be obtained from Eq. (4.9a) by simply exchanging the particle labels 1 and 2.

If we are interested in the special case where the angular momentum is aligned with both spins, we can set $(\boldsymbol{\chi}_a\cdot\boldsymbol{p}) = (\boldsymbol{\chi}_a\cdot\boldsymbol{n}) = 0$. Then, the sum of the above Hamiltonians reduces to

$$\begin{aligned}
\hat{H}^{\rm NLO}_{\rm ss,aligned} = \frac{1}{c^6}\frac{\nu}{8r^3}\Bigg\{ & \frac{m_1}{m_2}\left[- 6\nu\left(1 + \frac{m_1}{m_2}\right)\boldsymbol{p}^2 + \left(3 - 12\nu - 3\nu\frac{m_1}{m_2}\right)(\boldsymbol{n}\cdot\boldsymbol{p})^2 + \left(24 - 4\nu - 4\nu\frac{m_1}{m_2}\right)\frac{1}{r}\right]\boldsymbol{\chi}_1^2 \\
& + \frac{m_2}{m_1}\left[- 6\nu\left(1 + \frac{m_2}{m_1}\right)\boldsymbol{p}^2 + \left(3 - 12\nu - 3\nu\frac{m_2}{m_1}\right)(\boldsymbol{n}\cdot\boldsymbol{p})^2 + \left(24 - 4\nu - 4\nu\frac{m_2}{m_1}\right)\frac{1}{r}\right]\boldsymbol{\chi}_2^2 \\
& + \left[- \nu\left(32 + 12\left(\frac{m_1}{m_2} + \frac{m_2}{m_1}\right)\right)\boldsymbol{p}^2 + \nu\left(42 + 24\left(\frac{m_1}{m_2} + \frac{m_2}{m_1}\right)\right)(\boldsymbol{n}\cdot\boldsymbol{p})^2 + \frac{6}{r}\right](\boldsymbol{\chi}_1\cdot\boldsymbol{\chi}_2)\Bigg\}.
\end{aligned} \tag{4.10}$$

4.3 Transformation from ADM to EOB coordinates

In order to translate the ADM Hamiltonians into the EOB formalism, some appropriate coordinate transformations have to be performed. A first step is the purely orbital canonical transformation $G_o(\boldsymbol{r},\boldsymbol{p})$ [65]. Moreover, since this work should be consistent with previous ones [64, 68, 70], we also have to take into account the canonical transformations that have been applied there.

A generating function $G(\boldsymbol{r},\boldsymbol{p}')$ transforms the coordinates according to

$$\boldsymbol{r}' = \boldsymbol{r} + \{\boldsymbol{r}, G(\boldsymbol{r},\boldsymbol{p}')\} \tag{4.11a}$$
$$\boldsymbol{p}' = \boldsymbol{p} + \{\boldsymbol{p}', G(\boldsymbol{r},\boldsymbol{p}')\}, \tag{4.11b}$$

where the derivatives inside the Poisson Brackets are taken with respect to $\boldsymbol{r}$ and $\boldsymbol{p}'$. The time independence of G ensures that the transformed Hamiltonian is numerically invariant, i.e. $H'(\boldsymbol{q}') = H(\boldsymbol{q})$. Provided that G can be treated as a small, perturbative factor, one can obtain the transformed Hamiltonian H' by inserting Eq. (4.11) into the numerical invariance condition. At linear order in G one has then

$$H'(\boldsymbol{q}') = H(\boldsymbol{q}') + \{G(\boldsymbol{q}'), H(\boldsymbol{q}')\}. \tag{4.12}$$

The 1PN orbital generating function

$$\hat{G}_{\mathrm{o}}^{\mathrm{1PN}} = \frac{1}{c^2}(\boldsymbol{r}\cdot\boldsymbol{p}')\left(-\frac{\nu}{2}\boldsymbol{p}'^2 + \left(1+\frac{\nu}{2}\right)\frac{1}{r}\right) \tag{4.13}$$

transforms $\hat{H}_{\mathrm{ss}}^{\mathrm{NLO}}$ according to

$$\hat{H}_{\mathrm{ss}}^{\mathrm{NLO}\prime}(\boldsymbol{r}',\boldsymbol{p}',\boldsymbol{\chi}_1,\boldsymbol{\chi}_2) = \hat{H}_{\mathrm{ss}}^{\mathrm{NLO}}(\boldsymbol{r}',\boldsymbol{p}',\boldsymbol{\chi}_1,\boldsymbol{\chi}_2) + \{\hat{G}_{\mathrm{o}}^{\mathrm{1PN}}, \hat{H}_{\mathrm{ss}}^{\mathrm{LO}}\}(\boldsymbol{r}',\boldsymbol{p}',\boldsymbol{\chi}_1,\boldsymbol{\chi}_2). \tag{4.14}$$

As a second step, we need the canonical transformation that has been employed to obtain the LO, spin-spin Hamiltonian in EOB coordinates [68]. As pointed out in Ref. [77], the corresponding generating function is given by

$$\hat{G}_{\mathrm{ss}}^{\mathrm{LO}}(\boldsymbol{r},\boldsymbol{p}',\boldsymbol{\chi}_1,\boldsymbol{\chi}_2) = -\frac{1}{c^4}\frac{1}{2r^2}\left\{\left[\boldsymbol{\chi}_0^2 - (\boldsymbol{\chi}_0\cdot\boldsymbol{n})^2\right](\boldsymbol{r}\cdot\boldsymbol{p}') + \left(\boldsymbol{\chi}_0\cdot\boldsymbol{n}\right)(\boldsymbol{r}\times\boldsymbol{p}')\cdot\left(\boldsymbol{\chi}_0\times\boldsymbol{n}\right)\right\}, \tag{4.15}$$

where χ_0 has already been defined in Eq. (4.8). When applied onto the transformed orbital Hamiltonian

$$\hat{H}_{\mathrm{o}}^{\mathrm{1PN}\prime} = \hat{H}_{\mathrm{o}}^{\mathrm{1PN}} + \{\hat{G}_{\mathrm{o}}^{\mathrm{1PN}}, \hat{H}_{\mathrm{o}}^{\mathrm{N}}\}, \tag{4.16}$$

$\hat{G}_{\mathrm{ss}}^{\mathrm{LO}}$ gives rise to some additional NLO, spin-spin terms:

$$\hat{H}_{\mathrm{ss}}^{\mathrm{NLO}\prime\prime}(\boldsymbol{r}'',\boldsymbol{p}'',\boldsymbol{\chi}_1,\boldsymbol{\chi}_2) = \hat{H}_{\mathrm{ss}}^{\mathrm{NLO}\prime}(\boldsymbol{r}'',\boldsymbol{p}'',\boldsymbol{\chi}_1,\boldsymbol{\chi}_2) + \{\hat{G}_{\mathrm{ss}}^{\mathrm{LO}}, \hat{H}_{\mathrm{o}}^{\mathrm{1PN}\prime}\}(\boldsymbol{r}'',\boldsymbol{p}'',\boldsymbol{\chi}_1,\boldsymbol{\chi}_2). \tag{4.17}$$

Now, we perform an additional NLO coordinate transformation $\hat{G}_{\mathrm{ss}}^{\mathrm{NLO}}$ which is quadratic in the spins. The Hamiltonian is transformed according to

$$\hat{H}^{\mathrm{NLO}'''}_{\mathrm{ss}}(\boldsymbol{r}''',\boldsymbol{p}''',\boldsymbol{\chi}_1,\boldsymbol{\chi}_2)=\hat{H}^{\mathrm{NLO}''}_{\mathrm{ss}}(\boldsymbol{r}''',\boldsymbol{p}''',\boldsymbol{\chi}_1,\boldsymbol{\chi}_2)+\{\hat{G}^{\mathrm{NLO}}_{\mathrm{ss}},\hat{H}^{\mathrm{N}}_{\mathrm{o}}\}(\boldsymbol{r}''',\boldsymbol{p}''',\boldsymbol{\chi}_1,\boldsymbol{\chi}_2). \tag{4.18}$$

Notice that the orbit, spin-orbit and LO spin-spin terms are not affected by this transformation, which can thus be safely used without compromising the results obtained by the previous papers. When taking into account the alignment constraint $(\boldsymbol{\chi}_a\cdot\boldsymbol{p})=(\boldsymbol{\chi}_a\cdot\boldsymbol{n})=0$, the most general form of $\hat{G}^{\mathrm{NLO}}_{\mathrm{ss}}$ is simply

$$\begin{aligned}\hat{G}^{\mathrm{NLO}}_{\mathrm{ss,al}}=\frac{1}{c^6 r}\Bigg\{&\left[\alpha_{11}\boldsymbol{p}^2(\boldsymbol{n}\cdot\boldsymbol{p})+\beta_{11}(\boldsymbol{n}\cdot\boldsymbol{p})^3+\gamma_{11}\frac{(\boldsymbol{n}\cdot\boldsymbol{p})}{r}\right]\boldsymbol{\chi}_1^2\\&+\left[\alpha_{12}\boldsymbol{p}^2(\boldsymbol{n}\cdot\boldsymbol{p})+\beta_{12}(\boldsymbol{n}\cdot\boldsymbol{p})^3+\gamma_{12}\frac{(\boldsymbol{n}\cdot\boldsymbol{p})}{r}\right](\boldsymbol{\chi}_1\cdot\boldsymbol{\chi}_2)\\&+\left[\alpha_{22}\boldsymbol{p}^2(\boldsymbol{n}\cdot\boldsymbol{p})+\beta_{22}(\boldsymbol{n}\cdot\boldsymbol{p})^3+\gamma_{22}\frac{(\boldsymbol{n}\cdot\boldsymbol{p})}{r}\right]\boldsymbol{\chi}_2^2\Bigg\},\end{aligned} \tag{4.19}$$

where α_{ab}, β_{ab} and γ_{ab} are gauge parameters.

This third transformation is the last step necessary to translate the ADM formalism into the EOB one. The EOB model correctly reproduces the NLO spin-spin effects if $\hat{H}^{\mathrm{NLO}'''}_{\mathrm{ss}}$ is formally equal to the corresponding contribution $\hat{H}^{\mathrm{NLO}}_{\mathrm{EOB,ss}}$ from the PN expansion of the "real" EOB Hamiltonian $\hat{H}_{\mathrm{EOB}}$ (see Sec. 4.4). In order to simplify the notation, we omit the triple prime so that $\boldsymbol{r}$, $\boldsymbol{p}$ now denote the new (rescaled) EOB coordinates appearing in Eq. (4.18). This notation will be adopted until the end of the paper.

4.4 PN expansion of the EOB Hamiltonian with leading-order spin-spin coupling

We remember that this paper closely follows the lineage of Refs. [64, 68, 70]. We shortly review the basic structure of the formalism that has been employed there. The EOB Hamiltonian takes the form

$$H_{\mathrm{EOB}}=Mc^2\sqrt{1+2\nu\left(\frac{H_{\mathrm{eff}}}{\mu c^2}-1\right)}, \tag{4.20}$$

where

$$H_{\mathrm{eff}}=H_{\mathrm{eff},0}+\Delta H_{\mathrm{eff,so}} \tag{4.21}$$

is the so-called effective Hamiltonian. The term $\Delta H_{\mathrm{eff,so}}$ (see Eq. (4.16) of Ref. [70]) has been introduced in order to correctly reproduce spin-orbit interaction up to NNLO. It has a linear dependence on the "test-spin"

$$\boldsymbol{\sigma}=\frac{1}{2}\left(g_S^{\mathrm{eff}}\boldsymbol{S}+g_{S^*}^{\mathrm{eff}}\boldsymbol{S}^*\right)-\boldsymbol{S}_0, \tag{4.22}$$

that is defined through the linear combinations of spins $\boldsymbol{S}\equiv\boldsymbol{S}_1+\boldsymbol{S}_2$ and $\boldsymbol{S}^*\equiv(m_2/m_1)\boldsymbol{S}_1+(m_1/m_2)\boldsymbol{S}_2$, and through the "gyro-gravitomagnetic" ratios g_S^{eff} and $g_{S^*}^{\mathrm{eff}}$ [64, 70].

The Hamiltonian $H_{\text{eff},0}$ describes the motion of a test particle of mass μ in an external metric g_{eff}. It can be written as

$$H_{\text{eff},0} = N^i P_i\, c + N\, c\sqrt{\mu^2 c^2 + \gamma^{ij} P_i P_j + Q_4(P_i)}, \tag{4.23}$$

where $Q_4(P_i)$ is a quartic-in-momenta term [67, 68] and where N, N^i and γ^{ij} are the lapse, shift and 3-metric of g_{eff}, i.e.

$$N = \frac{1}{\sqrt{-g^{00}_{\text{eff}}}}, \qquad N^i = \frac{g^{0i}_{\text{eff}}}{g^{00}_{\text{eff}}}, \qquad \gamma^{ij} = g^{ij}_{\text{eff}} - \frac{g^{0i}_{\text{eff}}\, g^{0j}_{\text{eff}}}{g^{00}_{\text{eff}}}. \tag{4.24a}$$

The metric g_{eff} is a ν-deformed Kerr metric for a central mass M and effective Kerr parameter

$$a_0 = \left|\left(1+\frac{m_2}{m_1}\right)\frac{\boldsymbol{S}_1}{M\,c} + \left(1+\frac{m_1}{m_2}\right)\frac{\boldsymbol{S}_2}{M\,c}\right|. \tag{4.25}$$

In Ref. [68], g_{eff} was first written in Boyer-Linquist-like coordinates and successively transformed into Cartesian-like coordinates, in order to allow the spins to rotate in any direction. Since we will finally keep the spins fixed along the $\boldsymbol{e}_3$ axis, however, a Boyer-Lindquist-like coordinate system is appropriate for our purposes. Using the index notation $0 = t$, $i = R, \theta, \varphi$ and with the additional notation

$$\rho = \sqrt{R^2 + a_0^2 \cos^2(\theta)}, \tag{4.26}$$

the effective metric reads

$$g^{tt}_{\text{eff}} = \frac{1}{\rho^2}\left(a_0^2\sin^2(\theta) - \frac{\left(a_0^2+R^2\right)^2}{\Delta_t(R)}\right) \tag{4.27a}$$

$$g^{RR}_{\text{eff}} = \frac{\Delta_R(R)}{\rho^2} \tag{4.27b}$$

$$g^{\theta\theta}_{\text{eff}} = \frac{1}{\rho^2} \tag{4.27c}$$

$$g^{\varphi\varphi}_{\text{eff}} = \frac{1}{\rho^2}\left(\frac{1}{\sin^2(\theta)} - \frac{a_0^2}{\Delta_t(R)}\right) \tag{4.27d}$$

$$g^{t\varphi}_{\text{eff}} = \frac{a_0}{\rho^2}\left(1 - \frac{a_0^2+R^2}{\Delta_t(R)}\right). \tag{4.27e}$$

The functions Δ_t and Δ_R encode, according to the EOB philosophy, the (Padï¿½-resummed) PN terms in a ν-dependent way. They are defined through

$$\Delta_t = R^2 P_m^n\left[A(u) + u^2\frac{c^4\, a_0^2}{M^2}\right] \tag{4.28a}$$

$$\Delta_R = \Delta_t\, D^{-1}, \tag{4.28b}$$

where P^n_m denotes the action of taking the (n,m)-Padé approximant with respect to the variable $u = M/(c^2 R)$. Finally, A and D^{-1} are Schwarzschild-like metric coefficients, which at 3PN accuracy are given by

$$A(u) = 1 - 2u + 2\nu\, u^3 + \left(\frac{94}{3} - \frac{41}{32}\pi^2\right)\nu\, u^4 \tag{4.29a}$$

$$D^{-1}(u) = 1 + 6\nu\, u^2 + 2(26 - 3\nu)\nu\, u^3. \tag{4.29b}$$

For $\nu = 0$ both Δ_t and Δ_R reduce to $\Delta = R^2 - 2MR/c^2 + a_0^2$, so that the exact Kerr metric is recovered. When expanded in PN orders, the elements of $g_{\rm eff}$ form a series in powers of $M/(c^2 R)$. The expansion has to be performed with respect to the Kerr parameter a_0 too. This is done writing

$$a_0 \equiv \frac{M}{c^2}\chi_0. \tag{4.30}$$

Notice that χ_0 is defined consistently with respect to Eq. (4.8). For completeness, we write the expansion of the lapse, shift and 3-metric up to 3PN:

$$N = 1 - \frac{M}{c^2 R} - \frac{1}{2}\left(\frac{M}{c^2 R}\right)^2 + \left((\boldsymbol{n}\cdot\boldsymbol{\chi}_0)^2 - \frac{1}{2} + \nu\right)\left(\frac{M}{c^2 R}\right)^3 + \mathcal{O}\left(\frac{1}{c^8}\right) \tag{4.31a}$$

$$N^\varphi = \frac{2\chi_0}{R}\left(\frac{M}{c^2 R}\right)^2 + \mathcal{O}\left(\frac{1}{c^8}\right) \tag{4.31b}$$

$$\begin{aligned}\gamma^{RR} = {}& 1 - 2\left(\frac{M}{c^2 R}\right) + \left(6\nu + \chi_0^2 - (\boldsymbol{n}\cdot\boldsymbol{\chi}_0)^2\right)\left(\frac{M}{c^2 R}\right)^2 \\ & + \left(42\nu - 6\nu^2 + 2(\boldsymbol{n}\cdot\boldsymbol{\chi}_0)^2\right)\left(\frac{M}{c^2 R}\right)^3 + \mathcal{O}\left(\frac{1}{c^8}\right)\end{aligned} \tag{4.31c}$$

$$\gamma^{\theta\theta} = \frac{1}{R^2}\left[1 - (\boldsymbol{n}\cdot\boldsymbol{\chi}_0)^2\left(\frac{M}{c^2 R}\right)^2 + \mathcal{O}\left(\frac{1}{c^8}\right)\right] \tag{4.31d}$$

$$\gamma^{\varphi\varphi} = \frac{1}{\sin^2(\theta) R^2}\left[1 - \chi_0^2\left(\frac{M}{c^2 R}\right)^2 - 2\left(\chi_0^2 - (\boldsymbol{n}\cdot\boldsymbol{\chi}_0)^2\right)\left(\frac{M}{c^2 R}\right)^3 + \mathcal{O}\left(\frac{1}{c^8}\right)\right]. \tag{4.31e}$$

We do not write explicitly the whole, straightforward expansion of $H_{\rm eff}$ up to 3PN, but just the spin-spin terms. At first we redefine the variables, introducing a notation compatible with the calculations of Sec. 4.3:

$$\boldsymbol{p}^2 \equiv \frac{1}{\mu^2}\left(P_R^2 + \frac{P_\theta^2}{R^2} + \frac{P_\varphi^2}{R^2\sin^2(\theta)}\right), \qquad (\boldsymbol{n}\cdot\boldsymbol{p}) \equiv \frac{P_R}{\mu}, \qquad r \equiv \frac{R}{M}. \tag{4.32a}$$

We then have

$$\hat{H}^{\rm LO}_{\rm eff,ss} = \frac{1}{c^4}\left[\left(\frac{(\boldsymbol{n}\cdot\boldsymbol{p})^2}{r^2} - \frac{1}{2}\frac{\boldsymbol{p}^2}{r^2}\right)\boldsymbol{\chi}_0^2 + \frac{1}{2}\frac{(\boldsymbol{p}\cdot\boldsymbol{\chi}_0)^2}{r^2} - \frac{(\boldsymbol{n}\cdot\boldsymbol{p})(\boldsymbol{p}\cdot\boldsymbol{\chi}_0)(\boldsymbol{n}\cdot\boldsymbol{\chi}_0)}{r^2} + \frac{(\boldsymbol{n}\cdot\boldsymbol{\chi}_0)^2}{r^3}\right] \tag{4.33}$$

$$\begin{aligned}\hat{H}^{\rm NLO}_{\rm eff,ss} = {}& \frac{1}{c^6}\left[\left(\frac{1}{4}\frac{\boldsymbol{p}^4}{r^2} - \frac{1}{2}\frac{(\boldsymbol{n}\cdot\boldsymbol{p})^2\boldsymbol{p}^2}{r^2} - \frac{1}{2}\frac{\boldsymbol{p}^2}{r^3} + \frac{2}{r^4}\right)\boldsymbol{\chi}_0^2 + \left(\frac{3}{2}\frac{\boldsymbol{p}^2}{r^3} + \frac{(\boldsymbol{n}\cdot\boldsymbol{p})^2}{r^3} - \frac{1}{r^4}\right)(\boldsymbol{n}\cdot\boldsymbol{\chi}_0)^2 \right. \\ & \left. + \left(-\frac{1}{4}\frac{\boldsymbol{p}^2}{r^2} + \frac{1}{2r^3}\right)(\boldsymbol{p}\cdot\boldsymbol{\chi}_0)^2 + \left(\frac{1}{2}\frac{\boldsymbol{p}^2(\boldsymbol{n}\cdot\boldsymbol{p})}{r^2} - \frac{(\boldsymbol{n}\cdot\boldsymbol{p})}{r^3}\right)(\boldsymbol{p}\cdot\boldsymbol{\chi}_0)(\boldsymbol{n}\cdot\boldsymbol{\chi}_0)\right].\end{aligned} \tag{4.34}$$

It is worth mentioning that the (rescaled) spin-spin contributions turn out to be independent of the deformation parameter ν, and can therefore be directly compared with the PN expanded Kerr Hamiltonian. Actually, one can check that Eq. (4.33) corresponds to Eq. (5.55) of Ref. [77].

Finally, the "effective" dynamics has to be mapped, according to Eq. (4.20), to the "real" dynamics described by $\hat{H}_{\rm EOB}$. From the inverse relation

$$\hat{H}_{\rm eff} = \frac{\mu^2 c^2 \hat{H}^2_{\rm EOB} - m_1^2 c^4 - m_2^2 c^4}{2 m_1 m_2 c^4} \tag{4.35}$$

it is easily found that

$$\hat{H}^{\rm NLO}_{\rm eff,ss} = \hat{H}^{\rm NLO}_{\rm EOB,ss} + \frac{\nu}{c^2} \hat{H}^{\rm N}_{\rm EOB,o} \hat{H}^{\rm LO}_{\rm EOB,ss}, \tag{4.36}$$

where $\hat{H}^{\rm N}_{\rm EOB,o}$ and $\hat{H}^{\rm LO}_{\rm EOB,ss}$ are left unmodified by the above mapping and can thus be obtained directly from the PN expansion of $\hat{H}_{\rm eff}$. The first one is simply the Newtonian Hamiltonian

$$\hat{H}^{\rm N}_{\rm EOB,o} = \frac{\boldsymbol{p}^2}{2} - \frac{1}{r}, \tag{4.37}$$

while $\hat{H}^{\rm LO}_{\rm EOB,ss}$ is given by Eq. (4.33). As a consistence check of the mapping between ADM and EOB coordinates, $\hat{H}^{\rm LO}_{\rm EOB,ss}$ can also be obtained by adding to (4.7) the Poisson Bracket formed by the terms given in Eqs. (5.24) and (4.3).

4.5 Including next-to-leading order spin-spin effects for equatorial orbits and aligned spins

Let us denote the EOB Hamiltonian of Sec. 4.4 with an additional label "old", stressing the fact that we are now searching a new Hamiltonian $\hat{H}_{\rm EOB}$ that correctly reproduces the NLO spin-spin terms. The correspondence between ADM and EOB coordinates that has been worked out in Sec. 4.3 requires that $\hat{H}^{\rm NLO}_{\rm EOB,ss}$ must be equal to $\hat{H}^{\rm NLO'''}_{\rm ss}$ (4.18). Writing

$$\hat{H}^{\rm NLO}_{\rm EOB,ss} = \hat{H}^{\rm NLO,old}_{\rm EOB,ss} + \Delta\hat{H}^{\rm NLO}_{\rm eff,ss} \tag{4.38}$$

one thus finds the relation

$$\hat{H}^{\rm NLO,old}_{\rm eff,ss} + \Delta\hat{H}^{\rm NLO}_{\rm eff,ss} \equiv \hat{H}^{\rm NLO'''}_{\rm ss} + \frac{\nu}{c^2} \hat{H}^{\rm N}_{\rm EOB,o} \hat{H}^{\rm LO}_{\rm EOB,ss}. \tag{4.39}$$

Remember that $\hat{H}^{\rm NLO'''}_{\rm ss}$ is determined up to some free gauge parameters associated to the generating function $\hat{G}^{\rm NLO}_{\rm ss}$. Clearly, the choice of $\hat{G}^{\rm NLO}_{\rm ss}$ uniquely defines $\Delta\hat{H}^{\rm NLO}_{\rm eff,ss}$. For a better understanding, we place the terms that are not yet fixed on the left hand side of the equation:

$$\Delta\hat{H}^{\rm NLO}_{\rm eff,ss} - \left\{\hat{G}^{\rm NLO}_{\rm ss}, \hat{H}^{\rm N}_{\rm o}\right\} = \hat{H}^{\rm NLO''}_{\rm ss} - \hat{H}^{\rm NLO,old}_{\rm eff,ss} + \frac{\nu}{c^2} \hat{H}^{\rm N}_{\rm EOB,o} \hat{H}^{\rm LO}_{\rm EOB,ss}. \tag{4.40}$$

We recall that the EOB dynamics can be explicitly written as a deformation, in the "small" parameter ν, of the well-known dynamics of a test particle in the Schwarzschild metric (for non

spinning systems) or in the Kerr metric (for spinning systems). In order to preserve this central feature, $\Delta\hat{H}^{\rm NLO}_{\rm eff,ss}$ must thus vanish for $\nu = 0$. A straightforward calculation shows that this is satisfied if

$$\hat{G}^{\rm NLO}_{\rm ss} = \frac{1}{c^6 r^2}\left[-\frac{1}{2}\Big(\boldsymbol{\chi_1}^2 + (\boldsymbol{n}\cdot\boldsymbol{\chi_1})^2\Big)(\boldsymbol{n}\cdot\boldsymbol{p}) + (\boldsymbol{p}\cdot\boldsymbol{\chi_1})(\boldsymbol{n}\cdot\boldsymbol{\chi_1})\right], \tag{4.41}$$

where χ_1 denotes the (dimensionless) spin of the largest body, i.e. of the Kerr black hole. $\hat{G}^{3PN}_{\rm ss}$ is not uniquely defined, since it can contain arbitrary terms that vanish in the Kerr limit. The existence of this canonical transformation is not surprising. Indeed, we expect the dynamics of the Kerr metric, when expanded in PN orders, to be equivalent to the test-mass limit of the ADM Hamiltonian (4.1). Notice that the effects of the smaller spin are of order $\mathcal{O}(\nu^2)$, and are thus completely suppressed in the limit $\nu \to 0$.

At this point, we turn the discussion to the special case of equatorial orbits and aligned spins. This is simply done by inserting the conditions $(\boldsymbol{\chi}_a\cdot\boldsymbol{p}) = (\boldsymbol{\chi}_a\cdot\boldsymbol{n}) = 0$ into Eq. (4.40). The consistency of this simplification is discussed in the Appendix. The generating function $\hat{G}^{\rm NLO}_{\rm ss}$ takes the general form

$$\begin{aligned}\hat{G}^{\rm NLO}_{\rm ss,al} = \frac{1}{c^6 r}\Bigg\{&\left[\alpha_{11}\boldsymbol{p}^2(\boldsymbol{n}\cdot\boldsymbol{p}) + \beta_{11}(\boldsymbol{n}\cdot\boldsymbol{p})^3 + \left(\gamma_{11} - \frac{1}{2}\right)\frac{(\boldsymbol{n}\cdot\boldsymbol{p})}{r}\right]\boldsymbol{\chi}_1^2\\ &+\left[\alpha_{12}\boldsymbol{p}^2(\boldsymbol{n}\cdot\boldsymbol{p}) + \beta_{12}(\boldsymbol{n}\cdot\boldsymbol{p})^3 + \gamma_{12}\frac{(\boldsymbol{n}\cdot\boldsymbol{p})}{r}\right](\boldsymbol{\chi}_1\cdot\boldsymbol{\chi}_2)\\ &+\left[\alpha_{22}\boldsymbol{p}^2(\boldsymbol{n}\cdot\boldsymbol{p}) + \beta_{22}(\boldsymbol{n}\cdot\boldsymbol{p})^3 + \left(\gamma_{22} - \frac{1}{2}\right)\frac{(\boldsymbol{n}\cdot\boldsymbol{p})}{r}\right]\boldsymbol{\chi}_2^2\Bigg\},\end{aligned} \tag{4.42}$$

where the free gauge parameters $\alpha_{ab}(\nu)$, $\beta_{ab}(\nu)$ and $\gamma_{ab}(\nu)$ must vanish for $\nu = 0$. Notice that, in order to guarantee a symmetric treatment of both spins, we have introduced a term of $-1/2$ to the $\boldsymbol{\chi}_2^2$-dependent part of the generating function too. Eq. (4.40) is solved by

$$\begin{aligned}\Delta\hat{H}^{\rm NLO}_{\rm eff,ss} = \quad &\frac{1}{c^6}\Bigg[\alpha_{11}\frac{\boldsymbol{p}^4}{r^2} - 4\beta_{11}\frac{(\boldsymbol{n}\cdot\boldsymbol{p})^4}{r^2} + (3\beta_{11} - 2\alpha_{11})\frac{(\boldsymbol{n}\cdot\boldsymbol{p})^2\boldsymbol{p}^2}{r^2}\\ &+\frac{1}{4}\left(-2 + 4\gamma_{11} - 4\alpha_{11} + 5\nu^2 + 2\nu^3 + \frac{m_1}{m_2}(7\nu^2 + 4\nu^3) + \left(\frac{m_1}{m_2}\right)^2(2\nu^2 + 2\nu^3)\right)\frac{\boldsymbol{p}^2}{r^3}\\ &+\frac{1}{8}\Bigg(12 - 24\gamma_{11} - 24\beta_{11} - 16\alpha_{11} - 12\nu^2 + 12\nu^3 + \frac{m_1}{m_2}(3\nu - 36\nu^2 + 24\nu^3)\\ &\quad+\left(\frac{m_1}{m_2}\right)^2(-15\nu^2 + 12\nu^3)\Bigg)\frac{(\boldsymbol{n}\cdot\boldsymbol{p})^2}{r^3}\\ &+\frac{1}{4}\left(2 - 4\gamma_{11} - 12\nu^2 - \nu^3 + \frac{m_1}{m_2}(12\nu - 26\nu^2 - 2\nu^3) + \left(\frac{m_1}{m_2}\right)^2(-14\nu^2 - \nu^3)\right)\frac{1}{r^4}\Bigg]\boldsymbol{\chi}_1^2\\ &+\frac{1}{c^6}\Bigg[\alpha_{22}\frac{\boldsymbol{p}^4}{r^2} - 4\beta_{22}\frac{(\boldsymbol{n}\cdot\boldsymbol{p})^4}{r^2} + (3\beta_{22} - 2\alpha_{22})\frac{(\boldsymbol{n}\cdot\boldsymbol{p})^2\boldsymbol{p}^2}{r^2}\\ &+\frac{1}{4}\left(-2 + 4\gamma_{22} - 4\alpha_{22} + 5\nu^2 + 2\nu^3 + \frac{m_2}{m_1}(7\nu^2 + 4\nu^3) + \left(\frac{m_2}{m_1}\right)^2(2\nu^2 + 2\nu^3)\right)\frac{\boldsymbol{p}^2}{r^3}\\ &+\frac{1}{8}\Bigg(12 - 24\gamma_{22} - 24\beta_{22} - 16\alpha_{22} - 12\nu^2 + 12\nu^3 + \frac{m_2}{m_1}(3\nu - 36\nu^2 + 24\nu^3)\end{aligned}$$

$$
\begin{aligned}
&+\left(\frac{m_2}{m_1}\right)^2(-15\nu^2+12\nu^3)\Big)\frac{(\boldsymbol{n}\cdot\boldsymbol{p})^2}{r^3}\\
&+\frac{1}{4}\left(2-4\gamma_{22}-12\nu^2-\nu^3+\frac{m_2}{m_1}(12\nu-26\nu^2-2\nu^3)+\left(\frac{m_2}{m_1}\right)^2(-14\nu^2-\nu^3)\right)\frac{1}{r^4}\Bigg]\chi_2^2\\
&+\frac{1}{c^6}\Bigg[\alpha_{12}\frac{\boldsymbol{p}^4}{r^2}-4\beta_{12}\frac{(\boldsymbol{n}\cdot\boldsymbol{p})^4}{r^2}+(3\beta_{12}-2\alpha_{12})\frac{(\boldsymbol{n}\cdot\boldsymbol{p})^2\boldsymbol{p}^2}{r^2}\\
&+\left(\gamma_{12}-\alpha_{12}+\nu^2+2\nu^3+\left(\frac{m_1}{m_2}+\frac{m_2}{m_1}\right)(\nu^2+\nu^3)\right)\frac{\boldsymbol{p}^2}{r^3}\\
&+\frac{1}{4}\left(-12\gamma_{12}-12\beta_{12}-8\alpha_{12}-3\nu^2+24\nu^3+\left(\frac{m_1}{m_2}+\frac{m_2}{m_1}\right)12\nu^3\right)\frac{(\boldsymbol{n}\cdot\boldsymbol{p})^2}{r^3}\\
&\left(-\gamma_{12}+6\nu-12\nu^2-\nu^3+\left(\frac{m_1}{m_2}+\frac{m_2}{m_1}\right)\left(-6\nu^2-\frac{\nu^3}{2}\right)\right)\frac{1}{r^4}\Bigg](\boldsymbol{\chi}_1\cdot\boldsymbol{\chi}_2).
\end{aligned}
\tag{4.43}
$$

The simplest way of including these terms may be to add them to the whole effective Hamiltonian,

$$
\hat{H}_{\rm eff}^{\rm old}\to\hat{H}_{\rm eff}\equiv\hat{H}_{\rm eff,old}^{\rm old}+\Delta\hat{H}_{\rm eff,ss}^{\rm NLO}. \tag{4.44}
$$

Of course, adding PN terms to EOB Hamiltonians can eventually lead to bad behaviors in the phase space region where the PN expansion fails, but the additional degrees of freedom given by the gauge parameters α_{ab}, β_{ab} and γ_{ab} can in principle be used to calibrate the model. In this case, one would get something similar to Ref. [87], where an adjustable NLO spin-spin term $\propto(\nu S^2)/r^4$ was added to the effective Hamiltonian for calibration purposes. However, we do not believe an inclusion of the new terms according to (4.44) to be satisfying. First of all, this would break the Kerr-like structure of the effective Hamiltonian. Secondly, the treatment of the spin would be made in a very different and non-straightforward way than in Refs. [64, 68, 70]. Thirdly, one can verify that the existence of an ISCO would not be preserved for all choices of the gauge parameters. For these reasons, we propose another approach. Instead of adding a new term to the effective Hamiltonian, we try to redefine the effective squared spin parameter χ_0^2 entering the deformed Kerr metric, adding an appropriate NLO term. By contrast, we leave unmodified the "linear" spin χ_0 appearing in the metric element $g_{\rm eff}^{t\varphi}$ (4.27e). Notice, in passing, that the introduction of the "test spin" σ in Ref. [70] is equivalent to a redefinition of the "linear" spin χ_0 in $g_{\rm eff}^{t\varphi}$, while leaving all squared spins untouched. For this reason, the spin modification we are proposing is a very natural continuation of this philosophy. We replace all squared spins χ_0^2 entering $g_{\rm eff}$ (4.27) according to

$$
\chi_0^2\to\overline{\chi_{\rm eff}^2}\equiv\chi_0^2+\Delta\chi_{\rm eff}^2, \tag{4.45}
$$

where

$$
\begin{aligned}
\Delta\chi_{\rm eff}^2\equiv\frac{1}{c^2}\Bigg[&\left(a_{11}\boldsymbol{p}^2+b_{11}(\boldsymbol{n}\cdot\boldsymbol{p})^2+\frac{c_{11}}{r}\right)\chi_1^2\quad+\left(a_{22}\boldsymbol{p}^2+b_{22}(\boldsymbol{n}\cdot\boldsymbol{p})^2+\frac{c_{22}}{r}\right)\chi_2^2\\
&+\left(a_{12}\boldsymbol{p}^2+b_{12}(\boldsymbol{n}\cdot\boldsymbol{p})^2+\frac{c_{12}}{r}\right)\chi_1\chi_2\Bigg]+\Delta\chi_{\rm eff,NNLO}^2.
\end{aligned}
\tag{4.46}
$$

The (yet undetermined) term $\Delta\chi_{\rm eff,NNLO}^2$ has been inserted for calibration purposes in order to avoid bad behaviors of the new effective squared spin $\overline{\chi_{\rm eff}^2}$ (see Sec. 4.6). The function Δ_t becomes

$$\Delta_t = M^2 r^2 P_m^n\Big[A(u) + u^2 \overline{\chi^2_{\rm eff}}(r, \boldsymbol{p}^2, \boldsymbol{n}\cdot\boldsymbol{p})\Big], \tag{4.47}$$

where the variable u has to be set equal to $c^{-2}r^{-1}$ only after Padéing. This ensures that the radial variable entering the effective squared spin does not gets resummed too (else, one would "break" the spin as a whole, treating the variables it depends on in different ways). Of course, Δ_R has to be modified correspondingly (4.28b).

The new effective squared spin, together with (4.33), gives rise to the additional contribution

$$\Delta\hat{H}^{\rm NLO}_{\rm eff,ss} = \frac{1}{c^6 r^2}\left((\boldsymbol{n}\cdot\boldsymbol{p})^2 - \frac{\boldsymbol{p}^2}{2}\right)\Delta\chi^2_{\rm eff}. \tag{4.48}$$

A correct choice of the coefficients a_{ab}, b_{ab}, c_{ab} and of the gauge parameters α_{ab}, β_{ab}, γ_{ab} solves Eq. (4.40). The result is

$$a_{11} = \frac{\nu}{16}\left(-32\nu - 22\nu^2 + \frac{m_1}{m_2}(21 - 44\nu - 44\nu^2) + \left(\frac{m_1}{m_2}\right)^2(-21\nu - 22\nu^2)\right) \tag{4.49a}$$

$$b_{11} = 0 \tag{4.49b}$$

$$c_{11} = \frac{\nu}{16}\left(88\nu + 14\nu^2 + \frac{m_1}{m_2}(-117 + 196\nu + 28\nu^2) + \left(\frac{m_1}{m_2}\right)^2(117\nu + 14\nu^2)\right) \tag{4.49c}$$

$$a_{12} = \frac{\nu}{8}\left(24 - 53\nu - 44\nu^2 + \left(\frac{m_1}{m_2} + \frac{m_2}{m_1}\right)(-32\nu - 22\nu^2)\right) \tag{4.49d}$$

$$b_{12} = 0 \tag{4.49e}$$

$$c_{12} = \frac{\nu}{8}\left(-120 + 229\nu + 28\nu^2 + \left(\frac{m_1}{m_2} + \frac{m_2}{m_1}\right)(112\nu + 14\nu^2)\right). \tag{4.49f}$$

The coefficients a_{22}, b_{22} and c_{22} can be obtained from a_{11}, b_{11} and c_{11}, just exchanging the particle label 1 and 2. The gauge coefficients are

$$\alpha_{11} = \frac{\nu}{32}\left(32\nu + 22\nu^2 + \frac{m_1}{m_2}(-21 + 44\nu + 44\nu^2) + \left(\frac{m_1}{m_2}\right)^2(21\nu + 22\nu^2)\right) \tag{4.50a}$$

$$\beta_{11} = 0 \tag{4.50b}$$

$$\gamma_{11} = \frac{1}{4}\left(2 - 12\nu^2 - \nu^3 + \frac{m_1}{m_2}(12\nu - 26\nu^2 - 2\nu^3) + \left(\frac{m_1}{m_2}\right)^2(-14\nu^2 - \nu^3)\right) \tag{4.50c}$$

$$\alpha_{12} = \frac{\nu}{16}\left(-24 + 53\nu + 44\nu^2 + \left(\frac{m_1}{m_2} + \frac{m_2}{m_1}\right)(32\nu + 22\nu^2)\right) \tag{4.50d}$$

$$\beta_{12} = 0 \tag{4.50e}$$

$$\gamma_{12} = \frac{\nu}{2}\left(12 - 24\nu - 2\nu^2 + \left(\frac{m_1}{m_2} + \frac{m_2}{m_1}\right)(-12\nu - \nu^2)\right). \tag{4.50f}$$

It is remarkable that all b_{ab} and β_{ab} vanish, thereby eliminating one third of the newly involved coefficients.

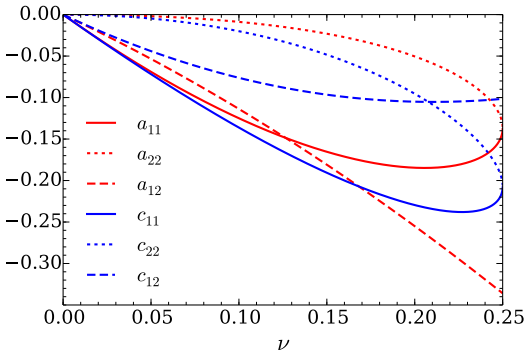

Figure 4.1: *Plot of the coefficients a_{ab} and c_{ab} as a function of ν.*

4.6 Discussion

In this section, the consistency and some properties of the proposed EOB Hamiltonian are discussed.

At first, it is easy to check that for $\nu \to 0$ all a_{ab}, b_{ab} and c_{ab} vanish. Because of the notation involving the non-symmetric ratios m_1/m_2 and m_2/m_1, the ν-dependence is not very explicit. However, the above statement follows from the simple fact that $\lim_{\nu\to 0} \nu\, m_1/m_2 = 1$. The Kerr limit

$$H_{\mathrm{EOB}} \to H_{\mathrm{Kerr}} \quad \text{for } \nu \to 0 \tag{4.51}$$

is therefore still valid, consistently with the usual interpretation of the EOB Hamiltonian as a ν-dependent deformation of the Kerr (or Schwarzschild) metric.

In this section, we limit the discussion to the equal masses ($m_1 = m_2$) and equal, aligned spins ($\chi_1 = \chi_2 = \chi_0$) case. Indeed, we expect the most relevant discrepancies from the Kerr case to occur for both mass and spin ratios of the order of one, and thus we believe this particular choice of parameters to be representative for the whole "non-Kerr" behavior of the EOB dynamics.

Since χ_0 can be either aligned or anti-aligned with the angular momentum $\boldsymbol{l}$, we use the notation $\chi_0 \equiv |\boldsymbol{l}|^{-1}\, \boldsymbol{l} \cdot \boldsymbol{\chi}_0$. We take into account the spin-orbit effects up to NNLO, using the gyro-gravitomagnetic ratios as given by Eqs. (55)-(56) of Ref. [64]. Moreover, we calculate Δ_t with the Padé approximant P^1_3 (4.47) and include the orbital dynamics up to 3PN (4.29). A numerical implementation of the new Hamiltonian shows that the existence of an innermost stable circular orbit (ISCO) is preserved. This is *a priori* not obvious, since the strong-field properties are significantly influenced by adding non resummed PN terms.

Before doing explicit calculations, however, it is necessary to fix the NNLO term $\Delta\chi^2_{\mathrm{eff,NNLO}}$. The motivation of inserting it lies in the fact that, while the original effective spin χ_0 has the great advantage of preserving the Kerr Bound $|\chi_0| \leq 1$ by construction, this is not necessarily true for the modified $\overline{\chi^2_{\mathrm{eff}}}$ anymore, because of its dependence on the dynamical variables. Moreover, $\overline{\chi^2_{\mathrm{eff}}}$ is not the square of any real function, and thus we also have to make sure that it never takes negative values. In the far-field limit ($1/r \sim \boldsymbol{p}^2 \to 0$), the original value $\overline{\chi^2_{\mathrm{eff}}} \to \chi_0^2$ is recovered. By contrast, the strong-field behavior can eventually lead to inconsistencies such as the violation of the Kerr bound or a negative effective spin squared. The most natural thing to do is to correct these possible bad behaviors with an appropriate NNLO term. Of course, an accurate determination of it can only be done by a comparison with numerical relativity or with the inclusion of

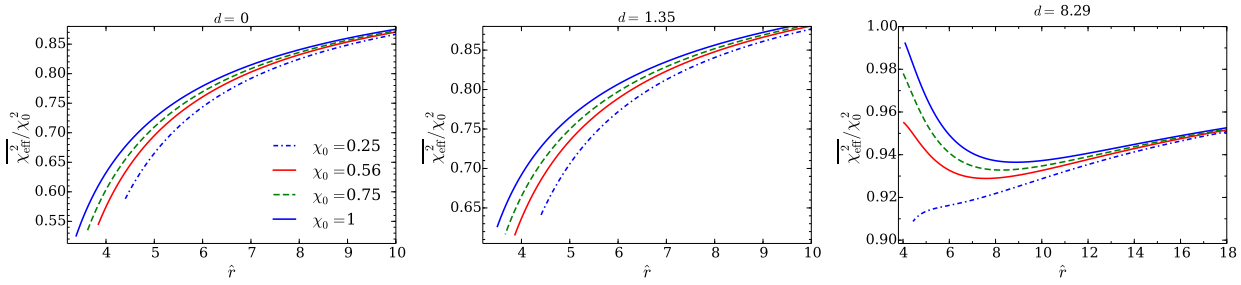

Figure 4.1: *Effective squared spin $\overline{\chi^2_{eff}}/\chi_0^2$ for circular orbits plotted as a function of the dimensionless orbital radius $\hat{r} = c^2\, r$. Each line stops at its corresponding ISCO.*

higher order spin-spin terms. Here we just require consistency in the following, restricted way. With the simple ansatz

$$\Delta\chi^2_{\rm eff,NNLO} = \frac{d\,\nu}{c^4\, r^2}\Big[\chi_1^2 + \chi_2^2 + \chi_1\,\chi_2\Big], \tag{4.52}$$

we try to give a reasonable lower and upper bound for d so that

$$0 \leq \overline{\chi^2_{\rm eff}} \leq 1 \tag{4.53}$$

along stable and unstable circular orbits. A complete analysis of all orbits relevant for GW detection would of course require a numerical evaluation of a large portion of the phase space. Anyway, we believe that restricting the analysis to circular orbits does not influence significantly the estimation of d. Indeed, unstable circular orbits lie on the light ring, which corresponds to the smallest separation radius that can be reached by an eccentric orbit with given angular momentum. Since $\boldsymbol{p}^2$ is expected to increase with $1/r$, and since a_{ab} and c_{ab} have the same sign (see Fig. 4.1), it is reasonable to think that the effective squared spin $\overline{\chi^2_{\rm eff}}$ is most likely to assume an unphysical value when the separation radius lies on the light ring.

The dynamics of circular orbits is obtained setting the radial momentum $(\boldsymbol{n}\cdot\boldsymbol{p}) = 0$ and solving

$$\frac{\partial}{\partial r} H_{\rm EOB}(r,l) = 0, \tag{4.54}$$

where $l = r\sqrt{\boldsymbol{p}^2 - (\boldsymbol{n}\cdot\boldsymbol{p})^2}$ denotes the (rescaled) angular momentum. Among the solutions, the stable circular orbits correspond to the local minima of the effective potential $H_{\rm EOB}(r,l)$, while the light ring $r_{LR}(l)$ corresponds to the local maxima. The ISCO is located at the turning point, and is thus determined by the additional condition

$$\frac{\partial^2}{\partial r^2} H_{\rm EOB}(r,l) = 0. \tag{4.55}$$

Evaluating the effective radial potential $H_{\rm EOB}(r,l)$ for χ_0 ranging from -1 to 1, we found the estimation $1.35 \lesssim d \lesssim 8.29$. This means that, if we want $\overline{\chi^2_{\rm eff}}$ to always be a positive number, the introduction of a non-zero $\Delta\chi^2_{\rm eff,NNLO}$ is necessary. The effective squared spin $\overline{\chi^2_{\rm eff}}$ is plotted in Fig. 4.1 for stable circular orbits and in Fig. 4.2 in the correspondence of the light ring. There, the light ring is interpreted as the smallest separation radius of an orbit with eccentricity

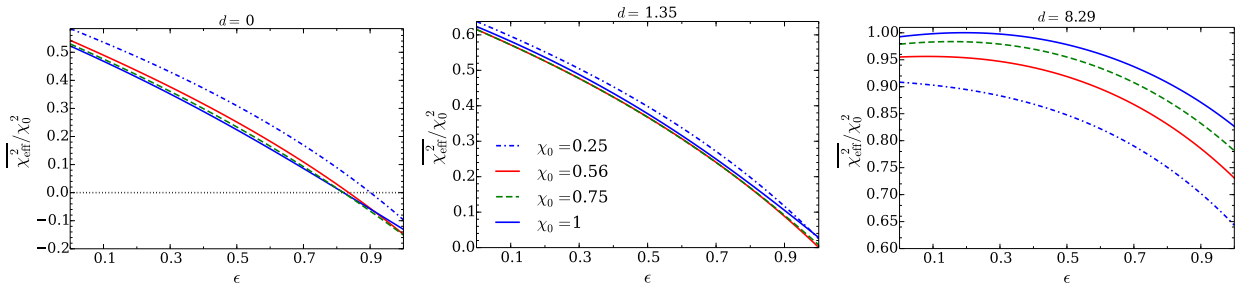

Figure 4.2: *Effective squared spin* $\overline{\chi^2_{eff}}/\chi_0^2$ *evaluated at the lightring* r_{LR} *for eccentric orbits as a function of the eccentricity* ϵ.

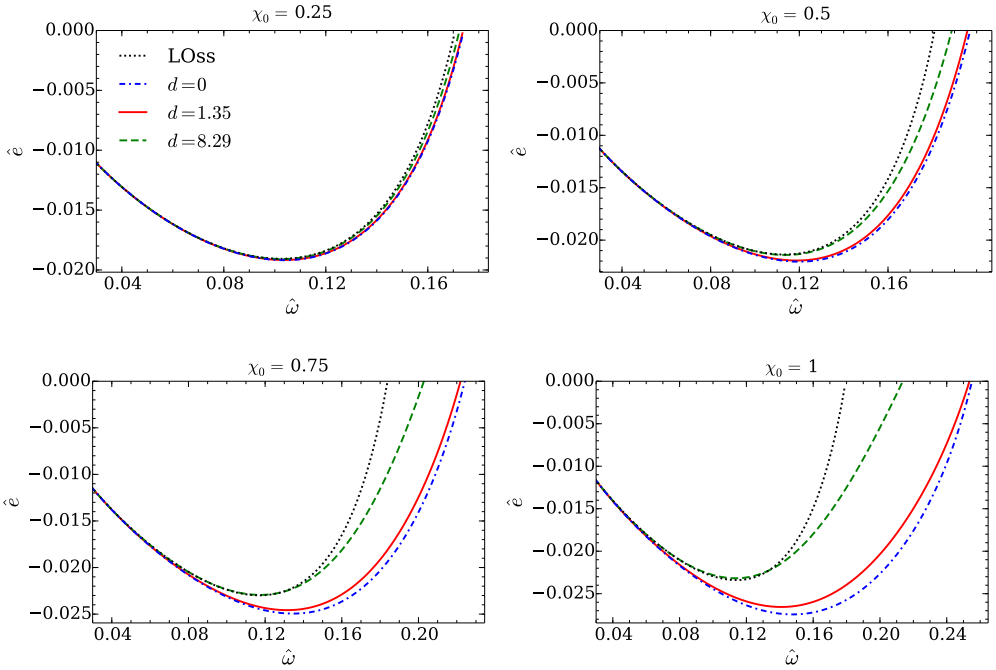

Figure 4.3: *Binding energy curve for circular orbits for different values of* χ_0. *The black dotted line denotes the EOB Hamiltonian with LO spin-spin coupling and NNLO spin-orbit coupling, as given by Ref. [64]. Equal masses and equal spins are assumed.*

$$\epsilon = \frac{r_{max} - r_{LR}}{r_{max} + r_{LR}}, \tag{4.56}$$

where r_{max} is the largest separation radius. In addition to the limiting cases $d = 1.35$ and $d = 8.29$, we also consider the "purely analytical" case where the positivity requirement for $\overline{\chi^2_{\rm eff}}$ is dropped off by removing the corrective term $\Delta\chi^2_{\rm eff,NNLO}$, which is equivalent to set $d = 0$. As shown in Fig. 4.2, the limiting value $\overline{\chi^2_{\rm eff}} = 0$ is reached for $d \approx 1.35$, $\chi_0 \approx 0.56$ and $\epsilon \to 1$, while $\overline{\chi^2_{\rm eff}} = 1$ for $d \approx 8.29$, $\chi_0 = 1$ and $\epsilon \approx 0.2$. It is also visible that $d = 8.29$ is responsible for a non-monotonic dependency of $\overline{\chi^2_{\rm eff}}$ on r for large spin values. On the other hand, setting $d = 0$ does not actually seem an unreasonable choice, unless one is interested in highly eccentric "zoom-whirl" orbits: indeed, for all stable circular orbits $\overline{\chi^2_{\rm eff}}/\chi_0^2 > 1/2$, while for eccentric orbits $\overline{\chi^2_{\rm eff}} > 0$ up to $\epsilon \sim 0.8$.

As in Ref. [70], we also investigate the binding energy of the system along circular orbits. In Fig. 4.3, the dimensionless, non relativistic energy

$$\hat{e} = \frac{H_{\rm EOB}}{M c^2} - 1 \tag{4.57}$$

is plotted as a function of the dimensionless frequency

$$\hat{\omega} = \frac{1}{c^3 \mu} \frac{\partial}{\partial l} H_{\rm EOB}. \tag{4.58}$$

Notice that the ISCO corresponds to the curve minima. For comparison, we also show the binding energy for LO spin-spin coupling, according to Ref. [64].

As already mentioned, the presence of larger spins aligned with the angular momentum is responsible for more bounded orbits. As shown in Fig. 4.3, the inclusion of NLO spin-spin terms strengthens this effect, leading to a binding energy increase up to $\sim 15\%$ (for the $\chi_0 = 1$ and $d = 0$ case). Notice that there is a subtlety which may be a source of confusion: since the effective Kerr parameter squared gets smaller after the NLO spin-spin inclusion ($\overline{\chi^2_{\rm eff}} \leq \chi_0^2$, see Figs. 4.1 and 4.2), one might have wrongly expected smaller binding energies. Instead, this simply suggests that in the Kerr-like metric the relation "a larger effective spin implies a more bounded orbit" is essentially a spin-orbit feature, while the quadratic appearances of the Kerr parameter seem to act in the opposite way.

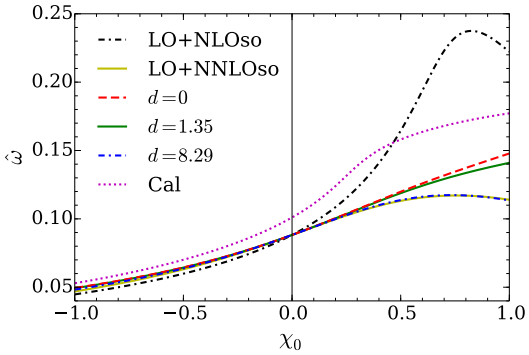

Figure 4.4: *Frequency $\hat{\omega}$ at the ISCO as a function of χ_0. Equal masses and equal spins are assumed.*

A second thing that can be observed from Fig. 4.3 is that the curve for the "'maximal" $d \approx 8.29$ is very similar (at least in the range of stable orbits) to the curve with LO spin-spin effects. Thus, the actual role of the maximal d becomes clear: restoring, in the ISCO region, an effective spin squared close to the LO one, χ_0^2 (see also Fig. 4.1), it acts almost compensating the NLO spin-spin effects. For this reason, we believe that a large d may be a bad choice. On the other hand, a "purely analytical" implementation (i.e., with $d = 0$) does not show any particular problem up to large eccentricities, and may therefore be a reasonable choice for an uncalibrated EOB model.

This argument is supported by Fig. 4.4, that shows (as in Ref. [75]) the orbital frequency $\hat{\omega}_{\rm ISCO}$ at the ISCO. The curve called "LO+NLOso" corresponds to the prediction of Ref [70], and thus includes LO spin-spin effects and just NLO spin-orbit effects, while "LO+NNLOso" includes LO spin-spin and NNLO spin-orbits effects (according to Ref. [64]). Spin-spin effects at NLO are implemented in the three lowest curves (that correspond to the model discussed up to now, and thus reproduce spin-orbit effects at NNLO accuracy). As a further comparison, we also have included the curve predicted by Ref. [89], that we denote by "Cal". The corresponding EOB Hamiltonian is based on the model developed in Refs. [74, 75, 77]. It includes spin-orbit effects at NNLO and spin-spin effects at LO, and has been calibrated inserting appropriate 3PN spin-spin and 4.5PN

spin-orbit terms. "Cal" generates reliable waveforms up to $\chi_0 \sim 0.7$. Because of a different resummation of the orbital part, the non spinning behavior differs quite significantly from our model. In particular, in "Cal" the functions Δ_t and Δ_R depend on an adjustable parameter K [75], which determines the radii where the horizons of the effective metric are located. The calibration of K is responsible for the discrepancy at $\chi_0 = 0$ between "Cal" and our model. This can be understood by looking at Fig. 1 of Ref. [75], that corresponds to a choice of K different from the one used in "Cal". For $\chi_0 = 0$, one reads a value $\omega_{\rm ISCO} \approx 0.90$, which is quite close to the value $\omega_{\rm ISCO} \approx 0.88$ predicted by our model. In the EOB Hamiltonian of this paper, there is no parameter analogous to K that can be calibrated against numerical relativity. However, since K appears in the expansion starting from 4PN, the discrepancy at $\chi_0 = 0$ might be reduced or even disappear when including higher order (and eventually calibrated) terms in the functions Δ_t and Δ_R. We remark that the exact radial potential $A(u)$ is known at linear order in the symmetric mass-ratio [102]. Moreover, radial potentials at full 4PN [79], or with some "fiducial values" up to 5PN (obtained through gravitational self-force calculations), see e.g. Ref. [91], have already been inserted into an EOB model, however only for the non spinning case.

Fig. 4.4 shows that the system gets "speeded up" by the action of the NLO spin-spin coupling. The most interesting point is that the the system is moved into the right direction (assumed to be the one shown by "Cal"), especially for the purely analytical $d = 0$ case.

4.7 Conclusion

We have shown that, by adding a term of fractional 1PN order to the effective Kerr parameter squared of the effective-one-body model developed in Refs. [64, 68, 70], it is possible to reproduce the next-to-leading order, spin-spin contribution of the PN expanded Hamiltonian for two black holes with spins aligned with the angular momentum. In particular, this is possible thanks to a specific canonical transformation quadratic in the spins that has to be added to all transformations already found in the above references. The additional spin-squared term vanishes whenever the mass-ratio tends to zero, so as to correctly reproduce the exact Kerr dynamics.

We have then evaluated the dynamics of circular orbits in the case of equal masses and spins. As a significant result, the effective radial potential still preserves the usual structure, reproducing local minima and maxima (corresponding to stable and unstable orbits, respectively) and also showing the existence of an ISCO. We recall that the location of the ISCO is of particular relevance for GW detection, since it describes the amount of energy that has been released during the inspiralling.

The general effect of the additional terms is to reduce the effective Kerr parameter squared. The problem is that, in the strong-field region, it can even vanish or become negative, thus breaking e.g. the horizon structure of the effective metric. In order to avoid this, it is possible to further modify the effective Kerr parameter squared inserting an additional term of fractional 2PN order, that should possibly be calibrated with numerical relativity. We have proposed a simple radial-dependent ansatz for the term in question, giving an estimation for his coefficient in order to preserve not only the positivity, but also the Kerr bound. Such bad behaviors, however, only happen in the regime of highly eccentric orbits ($\epsilon \sim 0.8$). In addition, a comparison with an EOB model calibrated with numerical relativity shows that the inclusion of NLO spin-spin terms leads to an improvement in the description of the frequency at the ISCO, which is most relevant right in the case where no bound-preserving NNLO additional terms have been inserted. For these reasons, we believe that an EOB model with just NLO spin-spin terms is sufficiently self-consistent.

In general, the effect of the NLO spin-spin coupling is that of increasing the binding energy and the frequency at the ISCO. The need for further improvements still remains, yet it is clear that the inclusion of NLO spin-spin effects points in the right direction.

Acknowledgments

We thank Thibault Damour for a very fruitful discussion, which helped to clarify many important points. Moreover, we benefitted from discussions with Jan Steinhoff, Enrico Barausse and Alessandro Nagar. S.B. is supported by the Swiss National Science Foundation. We thank the referee for useful comments.

4.8 Appendix: Existence of equatorial orbits

In this section we want to briefly motivate that constraining the orbital evolution to the equatorial plane, while holding the spins $\boldsymbol{S}_1$ and $\boldsymbol{S}_2$ fixed along the e_3 direction, is consistent with the conservative dynamics up to NLO in the spin-spin coupling. It has already been proved [125] that the conservative 2.5PN dynamics of maximally rotating compact binaries does not allow the spins to precess, if they are both initially aligned with the total angular momentum $\boldsymbol{J}$. In Ref. [125], this statement is shown using an approach which dates back to Dirac. The idea is to express the parallelism of $\boldsymbol{S}_1$, $\boldsymbol{S}_2$ and $\boldsymbol{J}$ as a set of constraints

$$C_a(x, p, S) = 0 \tag{4.59}$$

and to show that their time derivative can be written in the form

$$\dot{C}_a(x, p, S) = \sum_b D_{ab}(x, p, S)\, C_b. \tag{4.60}$$

This implies that all time derivatives of the constraints are a linear combination of the constraints themselves, and thus vanish at an initial time $t = 0$ when all C_a's are set to zero. This in turn guarantees that the parallelism is conserved even at later times. Denoting the (rescaled) orbital angular momentum as

$$\boldsymbol{l} = r\, \boldsymbol{n} \times \boldsymbol{p}, \tag{4.61}$$

the constraints can be written as

$$C_a := \boldsymbol{S}_a - \lambda_a \boldsymbol{l} = 0, \tag{4.62}$$

where $\lambda_a := |\boldsymbol{S}_a||\boldsymbol{l}|^{-1}$. Ref. [125] shows that Eq. (4.60) is valid if one can express the time derivative $\dot{\boldsymbol{S}}_b$ of the spins as a linear combination of the constraints. The generalization to the NLO spin-spin coupling turns out to be straightforward. Without loss of generality, consider only the spin $\boldsymbol{S}_1$. One has to keep into account the two additional terms $\left\{\boldsymbol{S}_1, H^{\mathrm{NLO}}_{\mathrm{S}_1^2}\right\}$ and $\left\{\boldsymbol{S}_1, H^{\mathrm{NLO}}_{\mathrm{S}_1\mathrm{S}_2}\right\}$ appearing in its first time derivative. Formally, $H^{\mathrm{NLO}}_{\mathrm{S}_1^2}$ only contains terms of type $A\, \boldsymbol{S}_1^2$ and $A_{vw}\, (\boldsymbol{S}_1 \cdot \boldsymbol{v})(\boldsymbol{S}_1 \cdot \boldsymbol{w})$, where the vectors $\boldsymbol{v}$ and $\boldsymbol{w}$ can either denote $\boldsymbol{n}$ or $\boldsymbol{p}$. Analogously, the terms appearing in $H^{\mathrm{NLO}}_{\mathrm{S}_1\mathrm{S}_2}$ are of type $B\, (\boldsymbol{S}_1 \cdot \boldsymbol{S}_2)$ and $B_{vw}\, (\boldsymbol{S}_1 \cdot \boldsymbol{v})(\boldsymbol{S}_2 \cdot \boldsymbol{w})$. Notice that the coefficients A, A_{vw}, B, and B_{vw} are

functions of $\boldsymbol{r}$ and $\boldsymbol{p}$, and are independent of the spins. The evaluation of the Poisson brackets leads to the following terms:

$$\left\{\boldsymbol{S}_1, A\,\boldsymbol{S}_1^2\right\} = 0 \tag{4.63a}$$

$$\begin{aligned}\{\boldsymbol{S}_1, A_{vw}\,(\boldsymbol{S}_1\cdot\boldsymbol{v})(\boldsymbol{S}_1\cdot\boldsymbol{w})\} &= A_{vw}\Big((\boldsymbol{S}_1\cdot\boldsymbol{w})(\boldsymbol{v}\times\boldsymbol{S}_1)+(\boldsymbol{S}_1\cdot\boldsymbol{v})(\boldsymbol{w}\times\boldsymbol{S}_1)\Big)\\ &= A_{vw}\Big(\big[(\boldsymbol{S}_1\cdot\boldsymbol{w})-\lambda_1\,(\boldsymbol{l}\cdot\boldsymbol{w})\big](\boldsymbol{v}\times\boldsymbol{S}_1)\\ &\quad+\big[(\boldsymbol{S}_1\cdot\boldsymbol{v})-\lambda_1\,(\boldsymbol{l}\cdot\boldsymbol{v})\big](\boldsymbol{w}\times\boldsymbol{S}_1)\Big)\end{aligned} \tag{4.63b}$$

$$\begin{aligned}\{\boldsymbol{S}_1, B\,(\boldsymbol{S}_1\cdot\boldsymbol{S}_2)\} &= B(\boldsymbol{S}_2\times\boldsymbol{S}_1)\\ &= B[(\boldsymbol{S}_2\times\boldsymbol{S}_1)-\lambda_1\,(\boldsymbol{S}_2\times\boldsymbol{l})]+B\lambda_1[(\boldsymbol{S}_2\times\boldsymbol{l})-\lambda_2\,(\boldsymbol{l}\times\boldsymbol{l})]\end{aligned} \tag{4.63c}$$

$$\begin{aligned}\{\boldsymbol{S}_1, B_{vw}\,(\boldsymbol{S}_1\cdot\boldsymbol{v})(\boldsymbol{S}_2\cdot\boldsymbol{w})\} &= B_{vw}\,(\boldsymbol{S}_2\cdot\boldsymbol{w})(\boldsymbol{v}\times\boldsymbol{S}_1)\\ &= B_{vw}[(\boldsymbol{S}_2\cdot\boldsymbol{w})-\lambda_2\,(\boldsymbol{l}\cdot\boldsymbol{w})](\boldsymbol{v}\times\boldsymbol{S}_1).\end{aligned} \tag{4.63d}$$

The last step of Eqs. (4.63b), (4.63c), and (4.63d) uses the fact that, by construction, $(\boldsymbol{l}\cdot\boldsymbol{n}) = (\boldsymbol{l}\cdot\boldsymbol{p}) = 0$. This, together with the result of Ref. [125], shows that the $\dot{\boldsymbol{S}}_b$ can be expressed as a linear combination of the constraints C_a, and therefore Eq. (4.60) also holds at NLO.

At last, we wish to argue that the alignment constraint is invariant under the transformation from ADM to EOB coordinates. First of all, it is clear that all canonical transformations that do not involve spin variables preserve the alignment. Indeed, the only vectors building up their respective generating functions are the vectors $\boldsymbol{r}$ and $\boldsymbol{p}$, which are therefore transformed (according to Eq. (4.11)) into linear combinations of themselves, thereby remaining on the plane perpendicular to the spin. The same argument is valid for the canonical transformation $\hat{G}^{\mathrm{NLO}}_{\mathrm{ss,al}}$, since the spins variables appearing there just have scalar character. By contrast, this might not seem obvious in the case of $\hat{G}^{\mathrm{LO}}_{\mathrm{ss}}$, and thus we resolved to perform an explicit calculation. The transformation reads, after inserting the alignment constraint for $\boldsymbol{r}$ and $\boldsymbol{p}$:

$$\boldsymbol{r}' = \boldsymbol{r}\left(1-\frac{1}{c^4}\frac{\chi_0^2}{2r^2}\right)\boldsymbol{p}' = \boldsymbol{p}+\frac{1}{2c^2\,r^2}\left[\boldsymbol{p}'\,\chi_0^2-2\boldsymbol{n}\,(\boldsymbol{n}\cdot\boldsymbol{p}')\chi_0^2+\boldsymbol{\chi}_0\Big((\boldsymbol{n}\times\boldsymbol{p}')\cdot(\boldsymbol{\chi}_0\times\boldsymbol{n})\Big)\right]. \tag{4.64}$$

The first equation already shows that $(\boldsymbol{r}'\cdot\boldsymbol{\chi}_0) = 0$. Using the fact that $(\boldsymbol{n}\times\boldsymbol{p})\cdot(\boldsymbol{\chi}_0\times\boldsymbol{n}) = 0$, we insert the second equation into the expression $(\boldsymbol{\chi}_0\times\boldsymbol{n})\cdot(\boldsymbol{n}\times\boldsymbol{p}')$ obtaining

$$(\boldsymbol{\chi}_0\times\boldsymbol{n})\cdot(\boldsymbol{n}\times\boldsymbol{p}')\left(1-\frac{1}{2c^4\,r^2}\left(\chi_0^2-(\boldsymbol{\chi}_0\times\boldsymbol{n})^2\right)\right) = 0, \tag{4.65}$$

from which immediately follows that $(\boldsymbol{n}\times\boldsymbol{p}')\cdot(\boldsymbol{\chi}_0\times\boldsymbol{n}) = 0$. This means that $\boldsymbol{p}'$ is again a linear combination of $\boldsymbol{r}$ and $\boldsymbol{p}$ and lies therefore on the plane perpendicular to $\boldsymbol{\chi}_0$. Very similar arguments can be used for the spin-orbit effects, as well as for their corresponding canonical transformation into EOB coordinates.

CHAPTER 5

Effective-one-body Hamiltonian with next-to-leading order spin-spin coupling

S. Balmelli, Ph. Jetzer. *Published in Physical Review D, Volume* **91**, *064011 (2015)*

Abstract

We propose a way of including the next-to-leading (NLO) order spin-spin coupling into an effective-one-body (EOB) Hamiltonian. This work extends [S. Balmelli and P. Jetzer, Phys. Rev. D **87**, 124036 (2013)], which is restricted to the case of equatorial orbits and aligned spins, to general orbits with arbitrary spin orientations. This is done applying appropriate canonical phase-space transformations to the NLO spin-spin Hamiltonian in Arnowitt-Deser-Misner (ADM) coordinates, and systematically adding "effective" quantities at NLO to all spin-squared terms appearing in the EOB Hamiltonian. As required by consistency, the introduced quantities reduce to zero in the test-mass limit. We expose the result both in a general gauge and in a gauge-fixed form. The last is chosen such as to minimize the number of new coefficients that have to be inserted into the effective spin squared. As a result, the 25 parameters that describe the ADM NLO spin-spin dynamics get condensed into only 12 EOB terms.

5.1 Introduction

Thanks to the LIGO/Virgo network of second-generation ground based interferometers, a first direct detection of gravitational waves (GW) is expected to occur in few years [126]. Furthermore, in the next decades, space-born GW detectors [127] (such as the planned eLISA) will open an entire new window to astrophysics, and allow tests of General Relativity at an unprecedented level [128]. Both types of detectors rely on coalescing (and possible spinning) black hole binaries as a primary GW source.

In order to extract the GW signal from the noise, very precise waveform templates need to be constructed. Currently, the most accurate description of coalescing black holes is provided by numerical relativity (NR) (see e.g. [109, 129–131] for some recent advances). However, the full parameter space is too large (especially in the case of nonzero spins) for being densely covered by NR simulations . This is the main reason why semi-analytical methods, by far less computationally expensive, can turn out to be very useful. At the present time, the effective-one-body (EOB) approach (we refer to [121] for a general review) is the only semi-analytical method that has been able to accurately describe the complete waveform of a coalescing process. After years of constant development [4, 65–67, 71–73, 82–85, 108, 132–135] the EOB has now reached an excellent agreement with NR waveforms in the case of nonspinning binaries [91, 131]. A lot of effort has also been put into the modeling of spins [64, 68, 70, 74–77, 80, 81, 87–90, 115], leading to a good overlap with NR waveforms in the case of nonprecessing (aligned or anti-aligned) spins [81, 90, 131]. By contrast, the description of precessing spins still needs some work before reaching a comparable performance [80], and is currently one of the most urgent tasks. In view of this, it may be crucial to incorporate more analytical information from the spin-orbit and spin-spin Hamiltonian computed within the post-newtonian (PN) theory.

In Ref. [115], a possible way of including the next-to-leading (NLO) spin-spin coupling [49, 50] (see also [46, 47, 56, 123]) into the spinning EOB model of Refs. [64, 68, 70] has been exposed for the special case of equatorial orbits and nonprecessing spins. A general inclusion of NLO spin-spin effects for fully precessing orbits would be a necessary step for extending the reliability of EOB waveforms to a significantly larger portion of the parameter space. The present paper aims at filling this gap, providing a possible implementation of the missing terms.

Recently, an improved (and calibrated) EOB model for spinning binaries has been proposed [81], where the NLO spin-spin coupling is only incorporated for the case of circular orbits. The present paper could be a first step for developing, at a next stage, a more general version of that improved model.

The paper has the following structure: in Sec. (5.2) we summarize the main concepts and the formalism of Ref. [115]. In Sec. (5.3), which is the central part of the paper, we propose a way of including the NLO spin-spin terms and show the explicit result, both in a general form (with a given number of free gauge parameters) and in a gauge-fixed formulation. Finally, Sec. (5.4) discusses a second, slightly different way of incorporating the wished spin-spin terms. Both approaches are compared plotting the (gauge invariant) angular frequency and binding energy at the last stable orbit (LSO). The plot also shows the prediction of the calibrated models of Refs. [89, 90].

Throughout the paper, we use geometric units with $G \equiv c \equiv 1$. When writing formulae in a PN expanded form, however, we will reintroduce the usage of c, prepending a factor $(1/c)^{2n}$ with the mere purpose of labeling the PN order n.

5.2 Summary of the previous work

In this section, we outline the method followed in Ref. [115], which forms the basis of the current paper. We work in EOB coordinates, with R being the radial coordinate, $\boldsymbol{n}$ the unit radial vector and $\boldsymbol{P}$ the momentum vector. We will often use the rescaled variables $r \equiv R/M$ and $\boldsymbol{p} \equiv \boldsymbol{P}/\mu$. Here, $M \equiv m_1 + m_1$ is the central EOB mass (m_1 and m_2 being the individual masses of the two black holes), and $\mu \equiv m_1 m_2/M$ is the reduced mass. Moreover, we denote by $\nu \equiv \mu/M$ the symmetric mass ratio.

The starting point is the EOB model of Ref. [68] (which includes both spin-spin and spin-orbit coupling at leading order (LO)), together with its extensions to the NLO [70] and to the next-to-next-to leading order (NNLO) [64] spin-orbit coupling. As already mentioned, in Ref. [115] the NLO spin-spin Hamiltonian in ADM coordinates has been reformulated and inserted into this EOB model for the special case of two black holes whose spins are aligned (or anti-aligned) with the orbital angular momentum. In particular, it has been shown that it is sufficient to replace the spin parameter a_0 of the effective metric (see for instance Eqs. (4.7) and (4.8) of Ref. [115]), whenever it appears as a second power, by a new, effective *squared* spin parameter. Using the dimensionless notation $\chi_0 = a_0/M$, this prescription takes the form

$$\chi_0^2 \to (\chi^2)_{\rm eff} = \chi_0^2 + \Delta\chi^2_{\rm eff}. \tag{5.1}$$

We recall that χ_0 is a combination of the dimensionless spin parameters χ_1 and χ_2 ($\chi_a = S_a/m_a^2$) of the two bodies:

$$\chi_0 = \frac{m_1}{M}\chi_1 + \frac{m_2}{M}\chi_2. \tag{5.2}$$

The additional term $\Delta\chi^2_{\rm eff}$ is of fractional 1PN order with respect to χ_0^2 and carries the information for reproducing the correct NLO spin-spin coupling. It reads as

$$\Delta\chi^2_{\rm eff} = \frac{1}{c^2}\left[\left(a_{11}\boldsymbol{p}^2 + \frac{c_{11}}{r}\right)\chi_1^2 \quad + \left(a_{22}\boldsymbol{p}^2 + \frac{c_{22}}{r}\right)\chi_2^2 \quad + \left(a_{12}\boldsymbol{p}^2 + \frac{c_{12}}{r}\right)\chi_1\chi_2\right]. \tag{5.3}$$

The calculation of the coefficients a_{ab} and c_{ab} is the main result of Ref. [115], given by Eq. (5.12) there. All of them vanish in the test mass limit $\nu \to 0$, consistently with the requirement that the EOB metric must reduce to the Kerr one.

PN results in ADM coordinates can be included into an EOB model after suitable canonical transformations. We denote here by $G_{\rm o}^{\rm PN}$ and $G_{\rm ss}^{\rm PN}$ the generating functions of the corresponding purely orbital and spin-spin transformation, respectively. The procedure for transforming the NLO spin-spin Hamiltonian from ADM into EOB coordinates is made of three steps:[1]

1) A purely orbital transformation

$$H_{\rm ss}^{\rm NLO\prime} = H_{\rm ss}^{\rm NLO(ADM)} + \left\{G_{\rm o}^{\rm 1PN}, H_{\rm ss}^{\rm LO(ADM)}\right\}. \tag{5.4}$$

[1] Here, we treat the PN expansion under the assumption of rapidly rotating black holes ($S_a = \frac{m_a^2}{c}\chi_a$, with $|\chi_a| \lesssim 1$), which assigns a well-defined PN order to the spin-dependent terms. As a consequence, throughout this paper, $G_{\rm ss}$ and $H_{\rm ss}$ are of 2PN order when labeled with "LO", of 3PN order when labeled with "NLO", and so on.

2) A LO spin-spin transformation

$$H_{\rm ss}^{\rm NLO\prime\prime} = H_{\rm ss}^{\rm NLO\prime} + \left\{G_{\rm ss}^{\rm LO}, H_{\rm o}^{\rm 1PN\prime}\right\}, \tag{5.5}$$

where

$$H_{\rm o}^{\rm 1PN\prime} = H_{\rm o}^{\rm 1PN(ADM)} + \left\{G_{\rm o}^{\rm 1PN}, H_{\rm o}^{\rm N(ADM)}\right\}. \tag{5.6}$$

3) A NLO spin-spin transformation

$$H_{\rm ss}^{\rm NLO\prime\prime\prime} = H_{\rm ss}^{\rm NLO\prime\prime} + \left\{G_{\rm ss}^{\rm NLO}, H_{\rm o}^{\rm N(ADM)}\right\}. \tag{5.7}$$

Notice that, for consistency, the transformations must be performed in a well-defined order. As indicated above, we make *first* use of the orbital transformation $G_{\rm o}$, and *then* of the spin-spin transformation $G_{\rm ss}$ [2]. Notice that, in Ref. [64], the spin-orbit generating function $G_{\rm so}$ is also applied after $G_{\rm o}$. By contrast, an evaluation order prescription between spin-orbit and spin-spin transformation would first be necessary when taking into account contributions that are cubic in the spins.

The final Hamiltonian must be equal to the corresponding term arising from the PN expansion of the EOB Hamiltonian. Since, for the moment, this is only true in the spin-aligned case, we are just allowed to write:

$$H_{\rm ss,al}^{\rm NLO\prime\prime\prime} = H_{\rm ss,al}^{\rm NLO(EOB)}. \tag{5.8}$$

The NLO spin-spin transformation $\hat{G}_{\rm ss,al}^{\rm NLO} \equiv G_{\rm ss,al}^{\rm NLO}/\mu$ is given by

$$\hat{G}_{\rm ss,al}^{\rm NLO} = \frac{(\boldsymbol{n}\cdot\boldsymbol{p})}{c^6\, r}\left\{\left[\alpha_{11}\,\boldsymbol{p}^2 + \left(\gamma_{11} - \frac{1}{2}\right)\frac{1}{r}\right]\boldsymbol{\chi}_1^2 + \left[\alpha_{22}\,\boldsymbol{p}^2 + \left(\gamma_{22} - \frac{1}{2}\right)\frac{1}{r}\right]\boldsymbol{\chi}_2^2 + \left[\alpha_{12}\,\boldsymbol{p}^2 + \gamma_{12}\frac{1}{r}\right](\boldsymbol{\chi}_1\cdot\boldsymbol{\chi}_2)\right\}.$$

Notice that, in view of a generalization to precessing orbits, we have written the individual dimensionless spins $\boldsymbol{\chi}_a = \boldsymbol{S}_a/m_a^2$ as vectors. The coefficients α_{ab} and γ_{ab} can be found in Eq. (5.13) of Ref. [115]. It is also provided an expression for $\hat{G}_{\rm ss}^{\rm NLO}$ in the test mass limit (assuming $m_1 > m_2$):

$$\lim_{\nu\to 0}\hat{G}_{\rm ss}^{\rm NLO} = \frac{1}{c^6 r^2}\left[-\frac{1}{2}\Big(\boldsymbol{\chi_1}^2 + (\boldsymbol{n}\cdot\boldsymbol{\chi_1})^2\Big)(\boldsymbol{n}\cdot\boldsymbol{p}) + (\boldsymbol{p}\cdot\boldsymbol{\chi_1})(\boldsymbol{n}\cdot\boldsymbol{\chi_1})\right]. \tag{5.9}$$

The purpose of this paper is that of generalizing the prescription (5.1) to the case of general orbits, i.e., when the scalar products $(\boldsymbol{n}\cdot\boldsymbol{\chi}_a)$ and $(\boldsymbol{p}\cdot\boldsymbol{\chi}_a)$ $(a = 1, 2)$ cannot be set to zero.

[2] Since the set of canonical transformations carries a group structure, the successive evaluation of $G_{\rm o}(\mathbf{r},\mathbf{p}')$ and of $G_{\rm ss}(\mathbf{r}',\mathbf{p}'')$ is a canonical transformation itself (with generating function $G_{\rm ss,o}(\mathbf{r},\mathbf{p}'') = \mathbf{G}_{\rm o}(\mathbf{r},\mathbf{p}') + \mathbf{G}_{\rm ss}(\mathbf{r}',\mathbf{p}'') - \mathbf{r}'\cdot\mathbf{p}'$). Despite taking a unique generating function would avoid the necessity of fixing an evaluation order prescription, we prefer here to use two separated transformations, so as to maintain the continuity with respect to Ref. [115]. As a second reason, the transformation of the Hamiltonian is more easily calculated here than for a single generating function, since in that last case effects quadratic in the transformation must be considered (see e.g. Eq. (6.9) of Ref. [65]).

5.3 Including NLO spin-spin terms into the EOB for general orbits

5.3.1 The prescription

In Ref [115], the EOB metric is written in Boyer-Lindquist-like coordinates. When spin precessions must be taken into account, however, it is necessary to switch to another system of coordinates. Following Ref. [68] (and reformulating the angular variable θ according to $a_0\cos(\theta) \equiv (\boldsymbol{n}\cdot\boldsymbol{a}_0)$), we can write the effective metric in Cartesian-like coordinates,

$$g^{00}_{\rm eff} = \frac{1}{\rho^2}\left(\boldsymbol{a}_0^2 - (\boldsymbol{n}\cdot\boldsymbol{a}_0)^2 - \frac{\left(R^2+a_0^2\right)^2}{\Delta_t}\right) \tag{5.10}$$

$$g^{0i}_{\rm eff} = \frac{R}{\rho^2}\left(1 - \frac{R^2+a_0^2}{\Delta_t}\right)(\boldsymbol{a_0}\times\boldsymbol{n})^i \tag{5.11}$$

$$g^{ij}_{\rm eff} = \frac{1}{\rho^2}\left(\Delta_R n^i n^j + R^2\left(\delta^{ij} - n^i n^j\right) - R^2\frac{(\boldsymbol{a}_0\times\boldsymbol{n})^i(\boldsymbol{a}_0\times\boldsymbol{n})^j}{\Delta_t}\right), \tag{5.12}$$

where $\rho^2 = R^2 + (\boldsymbol{n}\cdot\boldsymbol{a}_0)^2$. Δ_t and Δ_R can be found e.g. in Eq. (4.9) of Ref. [115] (notice that they both depend on the spin through a term $\sim a_0^2$). The effective Hamiltonian (that we denote here as "old", in order to avoid confusion with the modified version that is presented in this paper) takes the form

$$H^{\rm old}_{\rm eff} = \Delta H_{\rm so} + N^i P_i + N\sqrt{\mu^2 + \gamma^{ij}P_iP_j + Q_4(P_i)}, \tag{5.13}$$

with a quartic-in-momenta term $Q_4(P_i)$ [67, 68] and with

$$N = \frac{1}{\sqrt{-g^{00}_{\rm eff}}}, \qquad N^i = \frac{g^{0i}_{\rm eff}}{g^{00}_{\rm eff}} \qquad \gamma^{ij} = g^{ij}_{\rm eff} + \frac{\beta^i\beta^j}{\alpha^2}. \tag{5.14a}$$

$\Delta H_{\rm so}$ has been introduced to describe higher-order spin-orbit couplings. It is defined in terms of the gyro-gravitomagnetic ratios $g_S^{\rm eff}$ and $g_{S^*}^{\rm eff}$, see Eqs. (4.15) and (4.16) of Ref. [70].

With the reduced quantities $\boldsymbol{\chi}_0 = \boldsymbol{a}_0/M = (m_1\boldsymbol{\chi}_1 + m_2\boldsymbol{\chi}_2)/M$, $\hat{H} = H/\mu$, $\hat{\Delta}_r = \Delta_R/M$ and $\hat{\Delta}_t = \Delta_t/M$, we can write, more explicitly:

$$\Delta\hat{H}_{\rm so} + N^i p_i = \frac{r\nu}{2\tilde{r}^4}(r^2 + \boldsymbol{\chi}_0^2 - \hat{\Delta}_t)\left(\left(\frac{m_1}{m_2}g_S^{\rm eff} + g_{S^*}^{\rm eff}\right)(\boldsymbol{n}\times\boldsymbol{p})\cdot\boldsymbol{\chi}_1 + \left(\frac{m_2}{m_1}g_S^{\rm eff} + g_{S^*}^{\rm eff}\right)(\boldsymbol{n}\times\boldsymbol{p})\cdot\boldsymbol{\chi}_2\right) \tag{5.15a}$$

$$N = \left(\frac{\hat{\Delta}_t\left(r^2 + (\boldsymbol{n}\cdot\boldsymbol{\chi}_0)^2\right)}{\tilde{r}^4}\right)^{1/2} \tag{5.15b}$$

$$\gamma^{ij}p_ip_j = \frac{r^2}{r^2 + (\boldsymbol{n}\cdot\boldsymbol{\chi}_0)^2}\left[\boldsymbol{p}^2 + \left(\frac{\hat{\Delta}_r}{r^2} - 1\right)(\boldsymbol{n}\cdot\boldsymbol{p})^2 - \frac{1}{\tilde{r}^4}\left(2r^2 - \hat{\Delta}_t + \boldsymbol{\chi}_0^2 + (\boldsymbol{n}\cdot\boldsymbol{\chi}_0)^2\right)((\boldsymbol{n}\times\boldsymbol{p})\cdot\boldsymbol{\chi}_0)^2\right], \tag{5.15c}$$

where

$$\tilde{r}^4 = \left(r^2 + \boldsymbol{\chi}_0^2\right)^2 - \hat{\Delta}_t\left(\boldsymbol{\chi}_0^2 - (\boldsymbol{n}\cdot\boldsymbol{\chi}_0)^2\right). \tag{5.16}$$

The spin-squared term $((\boldsymbol{n}\times\boldsymbol{p})\cdot\boldsymbol{\chi}_0)^2$, generated by the contraction of $\gamma^{ij}p_ip_j$, can be expressed through the simple scalars $\boldsymbol{p}^2$, $(\boldsymbol{n}\cdot\boldsymbol{p})$, $\boldsymbol{\chi}_0^2$, $(\boldsymbol{n}\cdot\boldsymbol{\chi}_0)$ and $(\boldsymbol{p}\cdot\boldsymbol{\chi}_0)$ according to

$$((\boldsymbol{n}\times\boldsymbol{p})\boldsymbol{\chi}_0)^2 = \Big(\boldsymbol{p}^2-(\boldsymbol{n}\cdot\boldsymbol{p})^2\Big)\Big(\boldsymbol{\chi}_0^2-(\boldsymbol{n}\cdot\boldsymbol{\chi}_0)^2\Big)-\big((\boldsymbol{p}\cdot\boldsymbol{\chi}_0)-(\boldsymbol{n}\cdot\boldsymbol{p})(\boldsymbol{n}\cdot\boldsymbol{\chi}_0)\big)^2. \tag{5.17}$$

Let us now do some considerations:

i) The prescription (5.1) acts selectively - leaving all non-squared spins untouched - and cannot be truly considered as a redefinition of the effective spin of the EOB metric. It is, rather, a direct modification of the effective Hamiltonian.

   One can say the same for the inclusions of spin-orbit terms done in Refs. [64, 68, 70]. Adding the spin-orbit coupling requires a modification of all terms in the metric that are linear in the spin - or, equivalently, a direct modification of the Hamiltonian through an additional quantity $\Delta H_{\rm so}$ (Eq. (4.16) of Ref. [70]).

ii) Changing the Hamiltonian itself rather than the metric is of course not unreasonable. Since the motion of a spinning particle is non-geodesic, there is no reason to believe that the dynamics of spinning bodies can be accurately described by geodesics in an effective metric. One should in principle not worry about intervening on the structure of the effective Hamiltonian itself.

In view of these remarks, and noting, in addition, that the effective Hamiltonian depends on the spin squared only through the scalars $\boldsymbol{\chi}_0^2$, $(\boldsymbol{n}\cdot\boldsymbol{\chi}_0)^2$, $(\boldsymbol{p}\cdot\boldsymbol{\chi}_0)^2$ and $(\boldsymbol{n}\cdot\boldsymbol{\chi}_0)(\boldsymbol{p}\cdot\boldsymbol{\chi}_0)$, we see a natural way to generalize (5.1). We treat the spin differently whether it is contracted with itself, $\boldsymbol{n}$ or $\boldsymbol{p}$, and propose the following type of replacements in Eq. (5.15):

$$\boldsymbol{\chi}_0^2 \to \big(\boldsymbol{\chi}^2\big)_{\rm eff} = \boldsymbol{\chi}_0^2+\frac{1}{c^2}\Big[z_{11}^{(\chi)}\boldsymbol{\chi}_1^2+z_{22}^{(\chi)}\boldsymbol{\chi}_2^2+z_{12}^{(\chi)}\boldsymbol{\chi}_1\cdot\boldsymbol{\chi}_2\Big] \tag{5.18a}$$

$$(\boldsymbol{n}\cdot\boldsymbol{\chi}_0)^2 \to (\boldsymbol{n}\cdot\boldsymbol{\chi})^2_{\rm eff} = (\boldsymbol{n}\cdot\boldsymbol{\chi}_0)^2+\frac{1}{c^2}\Big[z_{11}^{(n)}(\boldsymbol{n}\cdot\boldsymbol{\chi}_1)^2+z_{22}^{(n)}(\boldsymbol{n}\cdot\boldsymbol{\chi}_2)^2+z_{12}^{(n)}(\boldsymbol{n}\cdot\boldsymbol{\chi}_1)(\boldsymbol{n}\cdot\boldsymbol{\chi}_2)\Big] \tag{5.18b}$$

$$(\boldsymbol{p}\cdot\boldsymbol{\chi}_0)^2 \to (\boldsymbol{p}\cdot\boldsymbol{\chi})^2_{\rm eff} = (\boldsymbol{p}\cdot\boldsymbol{\chi}_0)^2+\frac{1}{c^2}\Big[z_{11}^{(p)}(\boldsymbol{p}\cdot\boldsymbol{\chi}_1)^2+z_{22}^{(p)}(\boldsymbol{p}\cdot\boldsymbol{\chi}_2)^2+z_{12}^{(p)}(\boldsymbol{p}\cdot\boldsymbol{\chi}_1)(\boldsymbol{p}\cdot\boldsymbol{\chi}_2)\Big] \tag{5.18c}$$

$$\begin{aligned}(\boldsymbol{n}\cdot\boldsymbol{\chi}_0)(\boldsymbol{p}\cdot\boldsymbol{\chi}_0) \to ((\boldsymbol{n}\cdot\boldsymbol{\chi})(\boldsymbol{p}\cdot\boldsymbol{\chi}))_{\rm eff} &= (\boldsymbol{n}\cdot\boldsymbol{\chi}_0)(\boldsymbol{p}\cdot\boldsymbol{\chi}_0)+\frac{1}{c^2}\Big[z_{11}^{(np)}(\boldsymbol{n}\cdot\boldsymbol{\chi}_1)(\boldsymbol{p}\cdot\boldsymbol{\chi}_1)+z_{22}^{(np)}(\boldsymbol{n}\cdot\boldsymbol{\chi}_2)(\boldsymbol{p}\cdot\boldsymbol{\chi}_2)\\ &\quad+\frac{1}{2}\Big(z_{12}^{(np)}(\boldsymbol{n}\cdot\boldsymbol{\chi}_1)(\boldsymbol{p}\cdot\boldsymbol{\chi}_2)+z_{21}^{(np)}(\boldsymbol{p}\cdot\boldsymbol{\chi}_1)(\boldsymbol{n}\cdot\boldsymbol{\chi}_2)\Big)\Big],\end{aligned} \tag{5.18d}$$

where

$$z_{ab}^{(\rm x)} \equiv \left(a_{ab}^{(\rm x)}\boldsymbol{p}^2+b_{ab}^{(\rm x)}(\boldsymbol{n}\cdot\boldsymbol{p})^2+\frac{c_{ab}^{(\rm x)}}{r}\right), \tag{5.19}$$

the symbol (x) corresponding to (χ), (n), (p) or (np). Recall that the functions $\hat{\Delta}_r$ and $\hat{\Delta}_t$ depend on χ_0^2, and thus need to be transformed according to (5.18a). The effective Hamiltonian that results applying (5.18) onto $\hat{H}_{\rm eff}^{\rm old}$ will be simply denoted as $\hat{H}_{\rm eff}$.

The coefficients $a_{ab}^{(\chi)}$, $b_{ab}^{(\chi)}$ and $c_{ab}^{(\chi)}$ are already known, their explicit expression being given by Eq. (5.12) of Ref. [115] (where the label (χ) had not been used). In particular, since the $b_{ab}^{(\chi)}$'s vanish, (5.18a) is consistent with Eq. (5.3).

Determining the $z_{ab}^{(\rm x)}$'s from the Hamiltonian in ADM coordinates cannot be done without finding, simultaneously, the generating function $\hat{G}_{\rm ss}^{\rm NLO}$ of the corresponding canonical transformation (see Eq. (6.30)). We are looking for a sufficiently general ansatz that implements its already known test-mass limit (5.9), and that mantains, in addition, the symmetry under exchange of the labels 1 and 2. The searched canonical tranformation may have the following form:

$$\begin{aligned}\hat{G}_{\rm ss}^{\rm NLO} = \frac{1}{c^6 r}\Bigg\{ & (\boldsymbol{n}\cdot\boldsymbol{p})\left[\left(\zeta_{11}^{(\chi)}-\frac{1}{2r}\right)\boldsymbol{\chi}_1^2+\left(\zeta_{11}^{(n)}-\frac{1}{2r}\right)(\boldsymbol{n}\cdot\boldsymbol{\chi}_1)^2+\delta_{11}^{(p)}(\boldsymbol{p}\cdot\boldsymbol{\chi}_1)^2\right]+\left(\zeta_{11}^{(np)}+\frac{1}{r}\right)(\boldsymbol{n}\cdot\boldsymbol{\chi}_1)(\boldsymbol{p}\cdot\boldsymbol{\chi}_1)\\ & +(\boldsymbol{n}\cdot\boldsymbol{p})\left[\left(\zeta_{22}^{(\chi)}-\frac{1}{2r}\right)\boldsymbol{\chi}_2^2+\left(\zeta_{22}^{(n)}-\frac{1}{2r}\right)(\boldsymbol{n}\cdot\boldsymbol{\chi}_2)^2+\delta_{22}^{(p)}(\boldsymbol{p}\cdot\boldsymbol{\chi}_2)^2\right]+\left(\zeta_{22}^{(np)}+\frac{1}{r}\right)(\boldsymbol{n}\cdot\boldsymbol{\chi}_2)(\boldsymbol{p}\cdot\boldsymbol{\chi}_2)\\ & +(\boldsymbol{n}\cdot\boldsymbol{p})\left[\zeta_{12}^{(\chi)}(\boldsymbol{\chi}_1\cdot\boldsymbol{\chi}_2)+\zeta_{12}^{(n)}(\boldsymbol{n}\cdot\boldsymbol{\chi}_1)(\boldsymbol{n}\cdot\boldsymbol{\chi}_2)+\delta_{12}^{(p)}(\boldsymbol{p}\cdot\boldsymbol{\chi}_1)(\boldsymbol{p}\cdot\boldsymbol{\chi}_2)\right]\\ & +\frac{1}{2}\left(\zeta_{12}^{(np)}(\boldsymbol{n}\cdot\boldsymbol{\chi}_1)(\boldsymbol{p}\cdot\boldsymbol{\chi}_2)+\zeta_{21}^{(np)}(\boldsymbol{p}\cdot\boldsymbol{\chi}_1)(\boldsymbol{n}\cdot\boldsymbol{\chi}_2)\right)\Bigg\},\end{aligned} \tag{5.20}$$

where

$$\zeta_{ab}^{(\rm x)} \equiv \left(\alpha_{ab}^{(\rm x)}\boldsymbol{p}^2+\beta_{ab}^{(\rm x)}(\boldsymbol{n}\cdot\boldsymbol{p})^2+\frac{\gamma_{ab}^{(\rm x)}}{r}\right) \tag{5.21}$$

for (x) = (χ),(n) and (np). The $\delta_{ab}^{(p)}$'s are, instead, constant coefficients. Notice that a canonical transformation of this type applies an infinitesimal rotation on the spins according to

$$\boldsymbol{\chi}_a' = \boldsymbol{\chi}_a + \left(\frac{\partial G}{\partial \boldsymbol{\chi}_a}\times\boldsymbol{\chi}_a\right).$$

In our specific case, the spins are left invariant under the constraint of aligned spins and equatorial orbits:

$$\left(\frac{\partial G_{\rm ss}^{\rm NLO}}{\partial \boldsymbol{\chi}_a}\times\boldsymbol{\chi}_a\right)\Bigg|_{\rm al} = 0.$$

Thus, nonprecessing orbits are preserved under the transformation given by (6.34), which is a consistency requirement for the approach we are following.

5.3.2 The general solution

In order to determine all coefficients, we first explicitly calculate the transformations given by Eqs. (6.27)-(6.30). All needed expressions are already collected in Ref. [115], and specifically: $\hat{H}_{\rm o}^{\rm N(ADM)}$ can be found in Eq. (2.3) there, $\hat{H}_{\rm o}^{\rm 1PN(ADM)}$ in Eq. (2.4); $\hat{H}_{\rm ss}^{\rm LO(ADM)}$ in Eq. (2.7), $\hat{H}_{\rm ss}^{\rm NLO(ADM)}$

in Eq. (2.9); $\hat{G}_{\rm o}^{\rm 1PN}$ in Eq. (3.3), and $\hat{G}_{\rm ss}^{\rm LO}$ in Eq. (3.5). We need to rearrange two of these formulae, namely $\hat{H}_{\rm ss}^{\rm NLO(ADM)}$ and $\hat{G}_{\rm ss}^{\rm LO}$, that had been originally written in a form that is not suitable for our purpose. In Eq. (2.9b) of Ref. [115], it appears the scalar $((\boldsymbol{p}\times\boldsymbol{\chi}_1)\cdot\boldsymbol{n})((\boldsymbol{p}\times\boldsymbol{\chi}_2)\cdot\boldsymbol{n})$. Using the identity (5.17) (but with the vector $\boldsymbol{\chi}_1+\boldsymbol{\chi}_2$ instead of $\boldsymbol{\chi}_0$) it is easy to show that it can be decomposed as

$$\begin{aligned}\Big((\boldsymbol{p}\times\boldsymbol{\chi}_1)\cdot\boldsymbol{n}\Big)\Big((\boldsymbol{p}\times\boldsymbol{\chi}_2)\cdot\boldsymbol{n}\Big) &= \Big(\boldsymbol{p}^2-(\boldsymbol{n}\cdot\boldsymbol{p})^2\Big)(\boldsymbol{\chi}_1\cdot\boldsymbol{\chi}_2)-\boldsymbol{p}^2(\boldsymbol{n}\cdot\boldsymbol{\chi}_1)(\boldsymbol{n}\cdot\boldsymbol{\chi}_2)-(\boldsymbol{p}\cdot\boldsymbol{\chi}_1)(\boldsymbol{p}\cdot\boldsymbol{\chi}_2)\\ &\quad+(\boldsymbol{n}\cdot\boldsymbol{p})\Big((\boldsymbol{p}\cdot\boldsymbol{\chi}_1)(\boldsymbol{n}\cdot\boldsymbol{\chi}_2)+(\boldsymbol{n}\cdot\boldsymbol{\chi}_1)(\boldsymbol{p}\cdot\boldsymbol{\chi}_2)\Big).\end{aligned} \tag{5.22}$$

Eq. (2.9b) of Ref. [115] then becomes

$$\begin{aligned}\hat{H}_{\rm S_1S_2}^{\rm NLO} =&\frac{3\nu}{r^3}\Bigg[-\left(\frac{1}{2}+\frac{\nu}{3}\right)\boldsymbol{p}^2(\boldsymbol{\chi}_1\cdot\boldsymbol{\chi}_2)+\left(1-\frac{\nu}{4}\right)(\boldsymbol{n}\cdot\boldsymbol{p})^2(\boldsymbol{\chi}_1\cdot\boldsymbol{\chi}_2)\\ &+\left(\frac{1}{2}+\frac{3}{4}\nu\right)\boldsymbol{p}^2(\boldsymbol{n}\cdot\boldsymbol{\chi}_1)(\boldsymbol{n}\cdot\boldsymbol{\chi}_2)+\frac{5}{2}\nu(\boldsymbol{n}\cdot\boldsymbol{p})^2(\boldsymbol{n}\cdot\boldsymbol{\chi}_1)(\boldsymbol{n}\cdot\boldsymbol{\chi}_2)\\ &+\left(\frac{1}{2}+\frac{\nu}{6}\right)(\boldsymbol{p}\cdot\boldsymbol{\chi}_1)(\boldsymbol{p}\cdot\boldsymbol{\chi}_2)-\left(1+\frac{\nu}{4}-\frac{\nu}{2}\frac{m_1}{m_2}\right)(\boldsymbol{n}\cdot\boldsymbol{p})(\boldsymbol{n}\cdot\boldsymbol{\chi}_1)(\boldsymbol{p}\cdot\boldsymbol{\chi}_2)\\ &-\left(1+\frac{\nu}{4}-\frac{\nu}{2}\frac{m_2}{m_1}\right)(\boldsymbol{n}\cdot\boldsymbol{p})(\boldsymbol{p}\cdot\boldsymbol{\chi}_1)(\boldsymbol{n}\cdot\boldsymbol{\chi}_2)\Bigg]+\frac{\nu}{r^4}\Big[6(\boldsymbol{\chi}_1\cdot\boldsymbol{\chi}_2)-12(\boldsymbol{n}\cdot\boldsymbol{\chi}_1)(\boldsymbol{n}\cdot\boldsymbol{\chi}_2)\Big].\end{aligned} \tag{5.23}$$

Furthermore, using basic vector identities, Eq. (3.5) of Ref. [115] is simplified as follows:

$$\hat{G}_{\rm ss}^{\rm LO} = -\frac{1}{c^4}\frac{1}{2r^2}\Big\{\Big[\boldsymbol{\chi}_0^2-(\boldsymbol{\chi}_0\cdot\boldsymbol{n})^2\Big](\boldsymbol{r}\cdot\boldsymbol{p})+\Big(\boldsymbol{\chi}_0\cdot\boldsymbol{n}\Big)(\boldsymbol{r}\times\boldsymbol{p})\cdot\Big(\boldsymbol{\chi}_0\times\boldsymbol{n}\Big)\Big\} \tag{5.24}$$

$$= -\frac{1}{c^4}\frac{1}{2r}\Big[(\boldsymbol{n}\cdot\boldsymbol{p})\boldsymbol{\chi}_0^2-(\boldsymbol{n}\cdot\boldsymbol{\chi}_0)(\boldsymbol{p}\cdot\boldsymbol{\chi}_0)\Big]. \tag{5.25}$$

After all transformations (6.27)-(6.30), the resulting $H_{\rm ss}^{\rm NLO'''}$ must be equated to the corresponding term $H_{\rm ss}^{\rm NLO(EOB)}$ obtained by a PN expansion of the EOB Hamiltonian

$$\hat{H}_{\rm EOB} = \frac{1}{\nu}\sqrt{1+2\nu\left(\frac{\hat{H}_{\rm eff}}{\mu}-1\right)}. \tag{5.26}$$

The expansion can be done simply replacing $r\to\overline{r}/\varepsilon^2$, $\boldsymbol{p}\to\varepsilon\,\overline{\boldsymbol{p}}$ and performing a Taylor series in the small number ε. $H_{\rm ss}^{\rm NLO(EOB)}$ is then defined as the part proportional to ε^8 which is quadratic in the spins. Finding a solution for the equation

$$H_{\rm ss}^{\rm NLO'''}(\boldsymbol{r},\boldsymbol{p}) = H_{\rm ss}^{\rm NLO(EOB)}(\boldsymbol{r},\boldsymbol{p}) \tag{5.27}$$

is equivalent to solving an inhomogeneous system of 57 linear equations (18 for the spin(1)-spin(1) combination, 18 for the spin(2)-spin(2) and 21 for the spin(1)-spin(2) one), with 72 variables. This means that, if the system admits a solution, there will be at least 15 undetermined variables, that, as we shall see, will play the role of gauge coefficients. Notice that, because of the symmetry under exchange of the particle label 1 and 2, the system can be reduced to 39 equations and 50 variables. The general set of equations is solved by:

$$
\begin{aligned}
\alpha_{11}^{(\chi)} &= \frac{11\nu^2}{32} + \frac{3\nu^2}{4}\frac{m_1}{m_2} & \alpha_{12}^{(\chi)} &= \frac{11\nu^2}{16} + \frac{\nu}{2} \\
\beta_{11}^{(\chi)} &= 0 & \beta_{12}^{(\chi)} &= 0 \\
\gamma_{11}^{(\chi)} &= \frac{5\nu}{4} + \left(\frac{\nu}{2} - \frac{\nu^2}{4}\right)\frac{m_2}{m_1} & \gamma_{12}^{(\chi)} &= -\frac{\nu^2}{2} \\
\\
\alpha_{11}^{(n)} &= 0 & \alpha_{12}^{(n)} &= 0 \\
\beta_{11}^{(n)} &= 0 & \beta_{12}^{(n)} &= 0.
\end{aligned}
\tag{5.28}
$$

$$
\begin{aligned}
a_{11}^{(\chi)} &= -\frac{11\nu^2}{16} - \frac{3\nu^2}{2}\frac{m_1}{m_2} & a_{11}^{(n)} &= -\frac{19\nu}{4} + \frac{39\nu^2}{8} + \left(-\frac{\nu}{2} + \frac{15\nu^2}{4}\right)\frac{m_2}{m_1} + \gamma_{11}^{(n)} - \alpha_{11}^{(np)} \\
b_{11}^{(\chi)} &= 0 & b_{11}^{(n)} &= \frac{5\nu}{4} + \frac{15\nu^2}{2} + \left(\frac{5\nu}{2} + \frac{15\nu^2}{4}\right)\frac{m_2}{m_1} - 5\gamma_{11}^{(n)} - \beta_{11}^{(np)} \\
c_{11}^{(\chi)} &= -\frac{29\nu^2}{16} - \frac{3\nu^2}{2}\frac{m_1}{m_2} & c_{11}^{(n)} &= -\frac{11\nu}{4} + \nu^2 + \left(-\frac{\nu}{2} + \frac{7\nu^2}{4}\right)\frac{m_2}{m_1} - \gamma_{11}^{(n)} - \gamma_{11}^{(np)} \\
a_{12}^{(\chi)} &= -\nu - \frac{11\nu^2}{8} & a_{12}^{(n)} &= -2\nu - \frac{3\nu^2}{4} + \gamma_{12}^{(n)} - \frac{1}{2}\left(\alpha_{21}^{(np)} + \alpha_{12}^{(np)}\right) \\
b_{12}^{(\chi)} &= 0 & b_{12}^{(n)} &= -5\nu - \frac{15\nu^2}{2} - 5\gamma_{12}^{(n)} - \frac{1}{2}\left(\beta_{21}^{(np)} + \beta_{12}^{(np)}\right) \\
c_{12}^{(\chi)} &= -\nu + \frac{19\nu^2}{8} & c_{12}^{(n)} &= -2\nu + \frac{3\nu^2}{2} - \gamma_{12}^{(n)} - \frac{1}{2}\left(\gamma_{21}^{(np)} + \gamma_{12}^{(np)}\right)
\end{aligned}
$$

$$
\begin{aligned}
a_{11}^{(p)} &= 2(\alpha_{11}^{(np)} + \delta_{11}^{(p)}) & a_{12}^{(p)} &= \alpha_{21}^{(np)} + \alpha_{12}^{(np)} + 2\delta_{12}^{(p)} \\
b_{11}^{(p)} &= 2(\beta_{11}^{(np)} - 2\delta_{11}^{(p)}) & b_{12}^{(p)} &= \beta_{21}^{(np)} + \beta_{12}^{(np)} - 4\delta_{12}^{(p)} \\
c_{11}^{(p)} &= 4\nu + 2\frac{m_2}{m_1}\nu + \frac{\nu^2}{2} + 2(\gamma_{11}^{(np)} - \delta_{11}^{(p)}) & c_{12}^{(p)} &= -\nu + \nu^2 + \gamma_{21}^{(np)} + \gamma_{12}^{(np)} - 2\delta_{12}^{(p)} \\
a_{11}^{(np)} &= 2(\alpha_{11}^{(np)} - \beta_{11}^{(np)}) & b_{11}^{(np)} &= 4\beta_{11}^{(np)} \\
a_{12}^{(np)} &= 2(\alpha_{12}^{(np)} - \beta_{12}^{(np)}) & b_{12}^{(np)} &= 4\beta_{12}^{(np)} \\
a_{21}^{(np)} &= 2(\alpha_{21}^{(np)} - \beta_{21}^{(np)}) & b_{21}^{(np)} &= 4\beta_{21}^{(np)}
\end{aligned}
$$

$$
\begin{aligned}
c_{11}^{(np)} &= \frac{13\nu}{2} + \frac{15\nu^2}{4} + \left(4\nu + \frac{3\nu^2}{2}\right)\frac{m_2}{m_1} + \frac{1}{4}(-8\gamma_{11}^{(n)} + 8\alpha_{11}^{(np)} + 8\beta_{11}^{(np)} + 12\gamma_{11}^{(np)} + 8\delta_{11}^{(p)}) \\
c_{12}^{(np)} &= -\frac{5\nu^2}{2} - 12\nu^3 - \left(5\nu^2 + 6\nu^3\right)\frac{m_1}{m_2} - \left(2\nu^2 + 6\nu^3\right)\frac{m_2}{m_1} - 2\gamma_{12}^{(n)} + 2\alpha_{12}^{(np)} + 2\beta_{12}^{(np)} + 3\gamma_{12}^{(np)} + 2\delta_{12}^{(p)} \\
c_{21}^{(np)} &= -\frac{5\nu^2}{2} - 12\nu^3 - \left(5\nu^2 + 6\nu^3\right)\frac{m_2}{m_1} - \left(2\nu^2 + 6\nu^3\right)\frac{m_1}{m_2} - 2\gamma_{12}^{(n)} + 2\alpha_{21}^{(np)} + 2\beta_{21}^{(np)} + 3\gamma_{21}^{(np)} + 2\delta_{12}^{(p)}.
\end{aligned}
\tag{5.29}
$$

As already mentioned, the coefficients α_{22}, β_{22}, γ_{22}, a_{22}, b_{22} and c_{22} directly follow from the solution above exchanging the particle labels 1 and 2. In regard to this point, it is worth discussing

the Kerr limit $\nu \to 0$. In this case, indeed, one has to choose which one of the two spins vanishes - thus somehow breaking the symmetry between them. For $\nu \to 0$ (and $m_2/m_1 \to 0$) all coefficients α, β and γ must vanish, with the only exception of $\gamma_{22}^{(\chi)}$, $\gamma_{22}^{(n)}$ and $\gamma_{22}^{(np)}$. The reason of that lies in the form of the canonical transformation (6.34) and its limit (5.9). The price of having enforced the formal symmetry between spin(1) and spin(2), by adding ν-independent terms also to the spin(2)-spin(2) contribution of $\hat{G}_{ss}^{\rm NLO}$, is that of generating coefficients γ_{22} that do not tend to zero in the Kerr limit (and specifically: $\gamma_{22}^{(\chi)} \to 1/2$, $\gamma_{22}^{(n)} \to 1/2$ and $\gamma_{22}^{(np)} \to -1$, which can be easily verified taking into account that $\nu\, m_1/m_2 \to 1$).

By contrast, all coefficients a, b and c vanish for $\nu \to 0$, as required by consistency. In particular, the non-zero limit of $\gamma_{22}^{(\chi)}$, $\gamma_{22}^{(n)}$ and $\gamma_{22}^{(np)}$ is responsible for the convergence towards zero of $a_{22}^{(n)}$, $b_{22}^{(n)}$, $c_{22}^{(n)}$, $c_{22}^{(p)}$ and $c_{22}^{(np)}$, which might not have seemed immediately obvious from Eq. (5.29). Alternatively, to make this convergence more explicit, one could redefine

$$\tilde{\gamma}_{22}^{(\chi)} \equiv \gamma_{22}^{(\chi)} - \frac{1}{2} = \frac{\nu^2}{2} + \frac{m_2}{m_1}\left(-\frac{\nu}{2} + \frac{\nu^2}{4}\right), \qquad \tilde{\gamma}_{22}^{(n)} \equiv \gamma_{22}^{(n)} - \frac{1}{2}, \qquad \tilde{\gamma}_{22}^{(np)} \equiv \gamma_{22}^{(np)} + 1, \tag{5.30}$$

which absorb the ν-independent terms in the spin(2)-spin(2) part of (6.34), and satisfy $\tilde{\gamma}_{22}^{(\chi)}$, $\tilde{\gamma}_{22}^{(n)}$,$\tilde{\gamma}_{22}^{(np)} \to 0$. Now we can do the following reformulation:

$$\begin{aligned}
a_{22}^{(n)} &= -\frac{21\nu^2}{8} + \left(\frac{\nu}{2} - \frac{15\nu^2}{4}\right)\frac{m_2}{m_1} + \tilde{\gamma}_{22}^{(n)} - \alpha_{22}^{(np)} \\
b_{22}^{(n)} &= -\left(\frac{5\nu}{2} + \frac{15\nu^2}{4}\right)\frac{m_2}{m_1} - 5\tilde{\gamma}_{22}^{(n)} - \beta_{22}^{(np)} \\
c_{22}^{(n)} &= -\frac{5\nu^2}{2} + \left(\frac{\nu}{2} - \frac{7\nu^2}{4}\right)\frac{m_2}{m_1} - \tilde{\gamma}_{22}^{(n)} - \tilde{\gamma}_{22}^{(np)} \\
c_{22}^{(p)} &= \frac{\nu^2}{2} - 2\nu\frac{m_2}{m_1} + 2\tilde{\gamma}_{22}^{(np)} - 2\delta_{22}^{(p)} \\
c_{22}^{(np)} &= \frac{3\nu^2}{4} - \left(4\nu + \frac{3\nu^2}{2}\right)\frac{m_2}{m_1} - 2\tilde{\gamma}_{22}^{(n)} \\
&\quad + 2\alpha_{22}^{(np)} + 2\beta_{22}^{(np)} + 3\tilde{\gamma}_{22}^{(np)} + 2\delta_{22}^{(p)}.
\end{aligned} \tag{5.31}$$

We stress that, in this case, the formal symmetry with respect to the corresponding a_{11} , b_{11} and c_{11} is not directly visible.

5.3.3 Gauge fixing

The general solution (5.29) contains 18 gauge parameters, namely $\gamma_{11}^{(n)}$, $\delta_{11}^{(p)}$, $\alpha_{11}^{(np)}$, $\beta_{11}^{(np)}$, $\gamma_{11}^{(np)}$; $\gamma_{22}^{(n)}$, $\delta_{22}^{(p)}$, $\alpha_{22}^{(np)}$, $\beta_{22}^{(np)}$, $\gamma_{22}^{(np)}$; and $\gamma_{12}^{(n)}$, $\delta_{12}^{(p)}$, $\alpha_{12}^{(np)}$, $\alpha_{21}^{(np)}$, $\beta_{12}^{(np)}$, $\beta_{21}^{(np)}$, $\gamma_{12}^{(np)}$, $\gamma_{21}^{(np)}$. An appropriate choice of them can be used to simplify the 30 coefficients $a_{ab}^{(\rm x)}$, $b_{ab}^{(\rm x)}$ and $c_{ab}^{(\rm x)}$ (for (x) = $(n),(p),(np)$), that are not uniquely determined. One could try to impose the so-called Damour-Jaranowski-Schäfer (DJS) gauge (see e.g. Refs. [64, 70]) which would consist in eliminating those new terms proportional to $\boldsymbol{p}^2$, i.e., all coefficients $a_{ab}^{(\rm x)}$. We cannot, however, make all of them vanish: there is no way, within the method we have followed, to impose the DJS gauge. Notice that this does not mean

that the DJS gauge is a bad choice in general: in the spin-orbit sector, it is a very useful gauge, independently of how the spin-spin sector looks like. Moreover, the impossibility of imposing it in this paper is strictly related with the type of prescription we have followed. It would be interesting to investigate, in a future work, if a different method for including NLO spin-spin terms would allow to impose a DJS gauge in the spin-spin sector too.

Here, we nevertheless wish to give an example of gauge fixing, and choose an alternative approach. We can, for example, search a gauge for which the maximal number of coefficients can be set to zero. One finds that at most 24 of them can vanish, the remarkable fact being that this happens for a unique gauge choice, and namely when the non-zero coefficients are $a_{11}^{(n)}$, $c_{11}^{(n)}$, $a_{22}^{(n)}$, $c_{22}^{(n)}$, $a_{12}^{(n)}$ and $c_{12}^{(n)}$. In this case, the gauge coefficients are fixed as follows:

$$
\begin{aligned}
&\gamma_{11}^{(n)} = \frac{\nu}{4} + \frac{3}{2}\nu^2 + \left(\frac{\nu}{2} + \frac{3}{4}\nu^2\right)\frac{m_2}{m_1} && \gamma_{12}^{(n)} = -\nu - \frac{3\nu^2}{2} && \\
&\delta_{11}^{(p)} = 0 && \delta_{12}^{(p)} = 0 && \\
&\alpha_{11}^{(np)} = 0 && \alpha_{12}^{(np)} = 0 && \alpha_{21}^{(np)} = 0 \\
&\beta_{11}^{(np)} = 0 && \beta_{12}^{(np)} = 0 && \beta_{21}^{(np)} = 0 \\
&\gamma_{11}^{(np)} = -2\nu - \frac{\nu^2}{4} - \nu\frac{m_2}{m_1} && \gamma_{12}^{(np)} = \frac{\nu^2}{2} + \nu^2\frac{m_1}{m_2} && \gamma_{21}^{(np)} = \frac{\nu^2}{2} + \nu^2\frac{m_2}{m_1}.
\end{aligned}
$$

We may also write

$$
\tilde{\gamma}_{22}^{(n)} = -\left(\frac{\nu}{2} + \frac{3}{4}\nu^2\right)\frac{m_2}{m_1}, \qquad \tilde{\gamma}_{22}^{(np)} = -\frac{\nu^2}{4} + \frac{m_2}{m_1}\nu. \tag{5.32}
$$

The coefficients of the effective spin squared take the following, remarkably simple form:

$$
\begin{aligned}
a_{11}^{(\chi)} &= -\left(\frac{11}{16} + \frac{3}{2}\frac{m_1}{m_2}\right)\nu^2 & a_{11}^{(n)} &= -\left(\frac{21}{8} + \frac{9}{2}\frac{m_1}{m_2}\right)\nu^2 \\
c_{11}^{(\chi)} &= -\left(\frac{29}{16} + \frac{3}{2}\frac{m_1}{m_2}\right)\nu^2 & c_{11}^{(n)} &= -\left(\frac{9}{4} + \frac{m_1}{m_2}\right)\nu^2 \\
a_{12}^{(\chi)} &= -\nu - \frac{11\nu^2}{8} & a_{12}^{(n)} &= -3\nu - \frac{9\nu^2}{4} \\
c_{12}^{(\chi)} &= -\nu + \frac{19\nu^2}{8} & c_{12}^{(n)} &= -\frac{3\nu}{2} + \frac{7\nu^2}{2},
\end{aligned} \tag{5.33}
$$

which is the main result of this paper. For clarity purposes, we summarize the whole, new effective Hamiltonian:

$$
\begin{aligned}
\hat{H}_{\rm eff} = \;& \frac{\nu r}{2\tilde{r}_{\rm eff}^4}\left(r^2 + \left(\boldsymbol{\chi}^2\right)_{\rm eff} - \hat{\Delta}_t^{\rm eff}\right)\left[\left(\frac{m_1}{m_2}g_S^{\rm eff} + g_{S^*}^{\rm eff}\right)(\boldsymbol{n}\times\boldsymbol{p})\cdot\boldsymbol{\chi}_1 + \left(\frac{m_2}{m_1}g_S^{\rm eff} + g_{S^*}^{\rm eff}\right)(\boldsymbol{n}\times\boldsymbol{p})\cdot\boldsymbol{\chi}_2\right] \\
+ \;& \left(\frac{\hat{\Delta}_t^{\rm eff}}{\tilde{r}_{\rm eff}^4}\right)^{1/2}\left(r^2 + (\boldsymbol{n}\cdot\boldsymbol{\chi})_{\rm eff}^2\right)^{1/2}\left[1 + \frac{1}{\left(1 + \frac{(\boldsymbol{n}\cdot\boldsymbol{\chi})_{\rm eff}^2}{r^2}\right)}\left(\boldsymbol{p}^2 + \left(\frac{\hat{\Delta}_r^{\rm eff}}{r^2} - 1\right)(\boldsymbol{n}\cdot\boldsymbol{p})^2\right.\right. \\
- \;& \left.\left.\frac{1}{\tilde{r}_{\rm eff}^4}\left(2r^2 - \hat{\Delta}_t^{\rm eff} + \left(\boldsymbol{\chi}^2\right)_{\rm eff} + (\boldsymbol{n}\cdot\boldsymbol{\chi})_{\rm eff}^2\right)((\boldsymbol{n}\times\boldsymbol{p})\cdot\boldsymbol{\chi})_{\rm eff}^2\right) + Q_4(\boldsymbol{p})\right]^{1/2},
\end{aligned} \tag{5.34}
$$

with

$$\tilde{r}^4_{\rm eff} = \left(r^2 + \left(\chi^2\right)_{\rm eff}\right)^2 - \hat{\Delta}^{\rm eff}_t \left(\left(\chi^2\right)_{\rm eff} - (\boldsymbol{n}\cdot\boldsymbol{\chi})^2_{\rm eff}\right), \tag{5.35}$$

and with

$$((\boldsymbol{n}\times\boldsymbol{p})\cdot\boldsymbol{\chi})^2_{\rm eff} = 2(\boldsymbol{n}\cdot\boldsymbol{p})(\boldsymbol{n}\cdot\boldsymbol{\chi}_0)(\boldsymbol{p}\cdot\boldsymbol{\chi}_0) - \boldsymbol{p}^2(\boldsymbol{n}\cdot\boldsymbol{\chi})^2_{\rm eff} - (\boldsymbol{p}\cdot\boldsymbol{\chi}_0) + \left(\boldsymbol{p}^2 - (\boldsymbol{n}\cdot\boldsymbol{p})^2\right)\left(\chi^2\right)_{\rm eff}.$$

The Δ-potentials are

$$\begin{aligned}
\hat{\Delta}^{\rm eff}_t &= r^2 P^1_3\left[1 - 2u + 2\nu u^3 + \left(\frac{94}{3} - \frac{41}{32}\pi^2\right)\nu u^4 + \left(\chi^2\right)_{\rm eff} u^2\right] \\
\hat{\Delta}^{\rm eff}_r &= \hat{\Delta}^{\rm eff}_t\left(1 + 6\nu u^2 + 2(26 - 3\nu)\nu u^3\right),
\end{aligned}$$

where P^1_3 denotes the (1,3)-Padé approximant taken with respect to the variable $u \equiv r^{-1}$. Notice that, as in Ref. [115], we do *not* take the Padé with respect to the variable r contained in $\left(\chi^2\right)_{\rm eff}$.

We recall that the LO effective spin is defined as $\boldsymbol{\chi}_0 = \frac{m_1}{M}\boldsymbol{\chi}_1 + \frac{m_2}{M}\boldsymbol{\chi}_2$, while the implementation of NLO spin-spin effects reads as follows:

$$\begin{aligned}
\left(\chi^2\right)_{\rm eff} = \chi_0^2 - \frac{1}{c^2}\Bigg\{&\left[\left(\frac{11}{16} + \frac{3}{2}\frac{m_1}{m_2}\right)\nu^2\boldsymbol{p}^2 + \left(\frac{29}{16} + \frac{3}{2}\frac{m_1}{m_2}\right)\frac{\nu^2}{r}\right]\boldsymbol{\chi}_1^2 \\
&+ \left[\left(\frac{11}{16} + \frac{3}{2}\frac{m_2}{m_1}\right)\nu^2\boldsymbol{p}^2 + \left(\frac{29}{16} + \frac{3}{2}\frac{m_2}{m_1}\right)\frac{\nu^2}{r}\right]\boldsymbol{\chi}_2^2 \\
&+ \left[\left(\nu + \frac{11\nu^2}{8}\right)\boldsymbol{p}^2 + \left(\nu - \frac{19\nu^2}{8}\right)\frac{1}{r}\right]\boldsymbol{\chi}_1\boldsymbol{\chi}_2\Bigg\}
\end{aligned} \tag{5.36a}$$

$$\begin{aligned}
(\boldsymbol{n}\cdot\boldsymbol{\chi})^2_{\rm eff} = (\boldsymbol{n}\cdot\boldsymbol{\chi}_0)^2 - \frac{1}{c^2}\Bigg\{&\left[\left(\frac{21}{8} + \frac{9}{2}\frac{m_1}{m_2}\right)\nu^2\boldsymbol{p}^2 + \left(\frac{9}{4} + \frac{m_1}{m_2}\right)\frac{\nu^2}{r}\right](\boldsymbol{n}\cdot\boldsymbol{\chi}_1)^2 \\
&+ \left[\left(\frac{21}{8} + \frac{9}{2}\frac{m_2}{m_1}\right)\nu^2\boldsymbol{p}^2 + \left(\frac{9}{4} + \frac{m_2}{m_1}\right)\frac{\nu^2}{r}\right](\boldsymbol{n}\cdot\boldsymbol{\chi}_2)^2 \\
&+ \left[\left(3\nu + \frac{9\nu^2}{4}\right)\boldsymbol{p}^2 + \left(\frac{3\nu}{2} - \frac{7\nu^2}{2}\right)\frac{1}{r}\right](\boldsymbol{n}\cdot\boldsymbol{\chi}_1)(\boldsymbol{n}\cdot\boldsymbol{\chi}_2)\Bigg\}.
\end{aligned} \tag{5.36b}$$

The 25 coefficients that build the rather complex NLO spin-spin Hamiltonian in ADM coordinates get condensed into 12 new contributions in the EOB. This result is maybe not as striking as in the nonspinning sector (where, at 3PN order, the 11 ADM coefficients are reduced to 3 EOB terms only), still it confirms the notable ability of the EOB in reproducing higher-order effects.

5.4 Discussion: "full" and "partial" inclusion

One of the basic ideas behind the EOB is that of defining a map between real and effective quantities. The complicated PN dynamics of spinning bodies, however, has forced a splitting of the concept of "effective spin" in the EOB. Instead of having one single map between (S_1, S_2) and $S_{\rm eff}$, one has to distinguish between linear and squared spin, and even, as shown in this paper, between different contractions of the spin vector with the dynamical variables, and map each component

in a different way. Having thus lost, so to say, the concept of an unique effective spin, one might ask up to which point are we allowed to split the handling of it. The inclusion of NLO spin-spin effects we have presented in this paper obeys a simple rule: the spin mapping is only diversified when strictly necessary, in other words, the spin terms are as much as possible equally treated. We may call this the "full" approach, because of its formal and intuitive simplicity. One could also have followed another line of thought, pursuing the computational efficiency rather than the conceptual unity. Such an alternative approach would consist in leaving untouched some spin terms of the effective Hamiltonian that actually don't contribute to the NLO spin-spin part of the PN expanded EOB. For example, the spin-orbit contribution $H_{so} = \Delta H_{\rm so} + \beta^i p_i$ of the effective Hamiltonian only generates terms that are odd in the spins, and is thus unrelated to the spin-spin coupling. We may therefore apply the prescription (5.18) only to the orbital (even in the spins) part $H_{\rm orb} = \alpha\sqrt{1+\gamma^{ij}p_i p_j}$, leaving $H_{\rm so}$ as given by the "old" formulation (5.15a). We denote this kind of inclusion as "partial". It is clear that this way of proceeding leads to an explicit expression for $H_{\rm eff}$ which is shorter and simpler than in the "full" case, but it implies, at the same time, an additional and unnecessary fragmentation of the effective spin. In addition, a problem related to this approach is the fact that the "partial" Hamiltonian contains two different Delta potentials, Δ_t and $\Delta_t^{\rm eff}$. Since these potentials are defined through a Padé approximant, which may contain poles, the "partial" Hamiltonian will in principle show twice as many poles than the "full" one, if the spin is nonzero.

Let us finally remark that the "full" and "partial" Hamiltonians differ by terms that are odd (and at least cubic) in the spins, and therefore comparing them may help to distinguish the effects intrinsically related to the pure NLO spin-spin coupling from higher-order terms that get automatically resummed into the EOB after the NLO spin-spin inclusion.

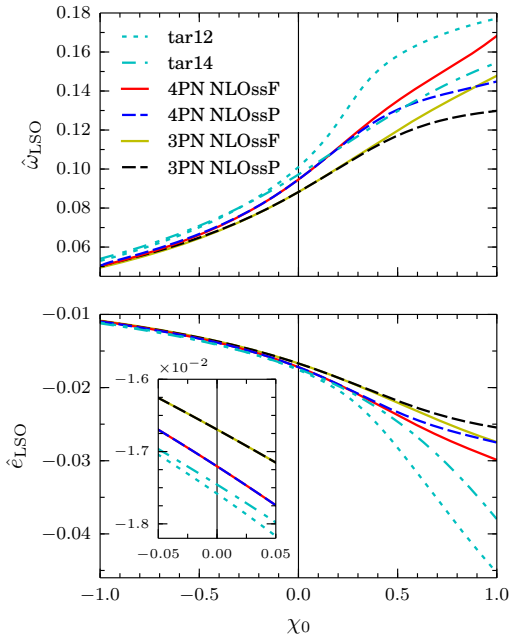

Figure 5.1: *Reduced angular frequency (top) and binding energy (bottom) at the LSO as a function of the effective spin parameter χ_0, in the case of equal masses and equal spins, for different EOB models.*

Fig. 6.3 shows the angular freguency $\hat{\omega}_{\rm LSO}$ and the binding energy $\hat{e}_{\rm LSO}$ at the LSO (see also Refs. [115]) as a function of the spin parameter χ_0 for different EOB models, in the case of equal masses ($\nu = 1/4$). The curves "3PN NLOssF","3PN NLOssP", "4PN NLOssF" and "4PN NLOssP"

denote the purely analytical EOB model discussed in this paper and in Ref. [115], with NLO spin-spin coupling ("F" and "P"indicating the "full" or "partial" inclusion) and with next-to-next-to-leading order (NNLO) spin-orbit coupling (that is reproduced by the gyro-gravitomagnetic factors calculated in Refs. [64, 70]). The label "3PN" or "4PN" refers to the purely orbital order, resummed with Padé P^1_3 or P^1_4, respectively. The 4PN orbital order needs an additional term $\nu\left(a_5^c(\nu)+a_5^{\ln}(\nu)\ln u\right)u^5$ (Eq. (5) of Ref. [79]) inside of $\hat{\Delta}_t$. The figure clearly shows that the effect of the 4PN terms at the LSO is repulsive, since the frequency and the binding energy get increased.

In Ref. [115], it has already been pointed out that a smaller effective spin squared leads to more bounded orbits. It is thus not surprising that the "partial" inclusion is less bounded than the "full" one, as it can be seen in the figure.

For completeness, Fig. 6.3 also shows two curves generated by a different EOB model. Here, "tar12" and "tar14" denote the calibrated model of Refs. [89, 90]. They both contain analytical information up to LO in the spin squared sector, with a calibration at the NLO level, and to NNLO in the spin-orbit sector, with calibration at next-to-next-to-next-to-leading order (NNNLO). The main difference between the two models is that "tar14" reproduces the 4PN purely orbital order and is calibrated for a varying mass-ratio, while "tar12" only contains the 3PN orbital order, and is calibrated for equal masses.

Since the calibration is done at the waveform level, together with the tuning of some parameters related to the dissipative part, it is difficult to have a precise guess about the real accuracy of the curves "tar12" and "tar14". Hoping that the deviation from reality is not so large as to compromise a qualitative discussion of the plot, we can observe that the "partial" approach does not seem to show any particular advantage with respect to the "full" one. On the contrary, the "full" curves are generally closer to the corresponding calibrated ones. This might be interpreted as a further argument in favour of the "full" approach. Systematically replacing, everywhere in the EOB Hamiltonian, terms by their "effective" equivalent is thus not only conceptually robust, but seems even to behave well numerically.

A second interesting point is that the difference between our EOB model and the calibrated "tar" models is significantly smaller at the 4PN level than at the 3PN. In particular, the frequency $\hat{\omega}_{\rm LSO}$ predicted by "tar14" roughly follows the curves "4PN LSOssF"and "4PN LSOssP", and lies in the gap between the two for $\chi_0 \geq 0.5$. The maximal deviation between "4PN" and "tar14" is 6.2% ("P") and 8.7% ("F"), while between "3PN" and "tar12" is 24.6% ("F") and 26.7% ("P"). The same is true in the nonspinning regime. For $\chi_0 = 0$, the "4PN" value of $\hat{\omega}_{\rm LSO}$ deviates from "tar14" by only 2.6%, whereas the difference between "tar12" and "3PN" is of 12.7%.

In the case of the binding energy, there is a good correspondence for spin equal to zero (the deviations are 1.4% at 4PN and 5.0% at 3PN). However, for large spins, the difference is quite large (up to 39.2% ("F") and 43.5% ("P") at the 3PN level, and up to 20.9% ("F") and 27.1% ("P") at 4PN). Nevertheless, from 3PN to 4PN there is still an improvement up to a factor ~ 2. This fact may strengthen the hope that the need for a calibration becomes less urgent when higher-order analytical terms are included.

5.5 Conclusion

We have proposed a prescription for modifying the EOB Hamiltonian of Ref. [70], so that, when expanded in PN terms, it reproduces the correct NLO spin-spin coupling for general precessing orbits. This is a generalization of the result of Ref. [115], where only equatorial orbits with aligned spins had been taken into account. The implementation of the correct spin-spin terms is possible

after a suitable canonical phase-space transformation of the ADM Hamiltonian. We have first shown the result in a rather general gauge, with 18 free gauge parameters (that actually reduce to 10 if we require symmetry under exchange of the particles). Then, a specific gauge is chosen. Being impossible, under the type of prescription we have considered, to impose a DJS-type gauge (i.e., to remove all new inclusions of type $\boldsymbol{p}^2\chi^2$), we have done the simple choice of looking for a gauge for which the maximal number of the coefficients entering the effective spin squared can be set to zero. It turned out that there is a unique gauge satisfying this criterion.

In the end, a slightly different approach is taken into account, where the effective spin squared is left at LO in the spin-orbit sector of the effective Hamiltonian. This partial inclusion is less repulsive than the full one, and has the unpleasant feature of increasing the number of poles of the Padé approximant by a factor 2. A comparison of the (gauge invariant) angular frequency and binding energy, taken at the LSO, with the calibrated EOB models of Refs. [89, 90], leads to the conclusion that the "partial" approach do not show any particular advantage with respect to the "full" one. By an Occam's razor-like argument, the "full" approach, which is conceptually more consistent, may thus be preferable. As a last thing, the plot also brings the encouraging evidence that, as higher order terms are included, the purely analytical EOB approaches more and more a calibrated model even in the strong field.

Acknowlodgements

We are thankful to Thibault Damour for a very useful discussion. Moreover, we would also like to thank Andrea Taracchini for having provided us some information. S.B. is supported by the Swiss National Science Foundation.

CHAPTER 6

A new effective-one-body Hamiltonian with next-to-leading order spin-spin coupling

S. Balmelli, T. Damour. *Accepted for publication on Physical Review D*

We present a new effective-one-body (EOB) Hamiltonian with next-to-leading order (NLO) spin-spin coupling for black hole binaries endowed with arbitrarily oriented spins. The Hamiltonian is based on the model for parallel spins and equatorial orbits developed in [Physical Review D **90**, 044018 (2014)], but differs from it in several ways. In particular, the NLO spin-spin coupling is not incorporated by a redefinition of the centrifugal radius r_c, but by separately modifying certain sectors of the Hamiltonian, which are identified according to their dependence on the momentum vector. The gauge-fixing procedure we follow allows us to reduce the 25 different terms of the NLO spin-spin Hamiltonian in Arnowitt-Deser-Misner coordinates to only 9 EOB terms. This is an improvement with respect to the EOB model recently proposed in [Physical Review D **91**, 064011 (2015)], where 12 EOB terms were involved. Another important advantage is the remarkably simple momentum structure of the spin-spin terms in the effective Hamiltonian, which is simply quadratic up to an overall square root. Moreover, a Damour-Jaranowski-Schäfer-type gauge could be established, thus allowing one to concentrate, in the case of circular and equatorial orbits, the whole spin-spin interaction in a single radial potential.

6.1 Introduction

The increasing interest in the modeling of gravitational waveforms from coalescing binaries, strongly motivated by the construction of ground-based detectors such as Virgo [136] or the now operating advanced LIGO [137] instruments, has led in the last decade to a significant effort in calculating spin effects in the post-Newtonian (PN) two-body problem beyond the leading order (LO). The spin-orbit coupling at the next-to-leading-order (NLO) was first derived in harmonic coordinates [33, 34], and then within an Arnowitt-Deser-Misner (ADM) formalism [22].

The ADM approach (see especially the formalism developed in Ref. [35]) has been quite fruitful, since it has also allowed the calculation of the next-to-next-to-leading order (NNLO) spin-orbit coupling [36, 37] and of the NLO spin-spin[1] coupling [48–50]. A method based on Effective Field Theory techniques [38] has also been able to derive the same results (see e.g. [42]), and is expected to complete soon the (full, physically relevant) spin-spin coupling at the NNLO accuracy [55].

Past work has shown that the most efficient way of using PN-expanded results to describe the dynamics of coalescing binaries is to encode them into an effective-one-body (EOB) model [65–68, 73]. This objective has been pursued in different versions of the EOB [64, 68–70, 74–77, 80] for both the spin-orbit coupling (up to NNLO) and the spin-spin coupling (up to LO).

More recently, an EOB Hamiltonian reproducing the correct NLO spin-spin coupling has been proposed [115, 138], where the terms in question are included by a subleading-order modification of various squared-spin terms. An unpleasant feature of this approach is that the so-obtained effective squared-spin acquires a momentum dependence that cannot be removed by any gauge tuning, and that greatly complicates the analytic form of the Hamiltonian. In addition, the momentum-dependent terms in question are non-zero even in the most simple case of circular and equatorial orbits, which prevents one from having a direct insight into the dynamics by means of a radial potential A, as is the case for the models with just LO spin-spin coupling (see e.g. [64, 68–70]).

Recently, Ref. [81] has proposed a new EOB description of binary black holes with parallel spins, moving along equatorial orbits. The EOB Hamiltonian of Ref. [81] incorporates a reformulation of the NLO spin-spin terms of Ref. [115], but presents some basic structural differences with respect to Refs. [68, 70, 115, 138]. The most important ones are the introduction of a new variable (the centrifugal radius r_c), which plays a central role for the description of quadratic spin effects, and a simplification of the spin-orbit structure.

The present work is meant as an improvement of both Ref. [138] and Ref. [81]. It will overcome the problematic features of Ref. [138] discussed above, while staying as close as possible to the new formalism and ideas introduced in Ref. [81]. Our final result will be an EOB Hamiltonian describing arbitrarily oriented spinning black holes whose structure is physically transparent and quite close to that of the Hamiltonian describing the dynamics of a test-particle in a Kerr background. As a bonus, our Hamiltonian will make manifest six hidden symmetries of the NLO spin-spin coupling, thereby allowing one to describe the latter coupling by means of only 9 terms (instead of the 25 terms present in their ADM formulation).

In Sec 6.2, which is the core of the paper, our whole procedure is sequentially presented until the main results are obtained; in particular, Sec 6.2.1 revisits the Kerr Hamiltonian and develops, from this limiting case, the basic ideas to be applied in the EOB case; Sec. 6.2.2 introduces the EOB model from which we start, and Sec 6.2.3 defines the transformation between the ADM and EOB coordinates; Sec. 6.2.4 discusses two possible gauge choices, eventually opting for a single one, which leads to an identification of some forms quadratic in the spins that must be inserted into the EOB model to reproduce the NLO spin-spin coupling; Sec. 6.2.5 proposes a resummation of the results into a final EOB Hamiltonian; Sec. 6.2.6 provides a more detailed description of the quadratic forms, with some details about their eigenvalue decomposition and their positivity properties. In Sec 6.3, the spin-orbit sector is discussed with some emphasis about the resummation choices of the gyro-gravitomagnetic factors. The physical characteristics of the last stable orbit (LSO) for equal masses and equal, aligned spins, are then computed and compared with the predictions of other EOB models. Finally, the Appendix briefly discusses some

[1] In this paper, "spin-spin" refers to any interaction quadratic in the spins, i.e., $\propto S_1^2$, S_2^2 and $S_1 S_2$.

unexpected "symmetries" in the coefficients of the quadratic forms. Througout the paper we use geometrical units with $G \equiv c \equiv 1$.

6.2 A new effective-one-body description of the next-to-leading order spin-spin coupling

Let us recall that one of the basic features of the EOB formalism is to represent the Hamiltonian of a (comparable-mass and comparable-spin) two-body system in the form

$$H_{\rm EOB} = M\sqrt{1+2\nu\left(\frac{H^{\rm eff}}{\mu}-1\right)}, \tag{6.1}$$

where the "effective" Hamiltonian $H^{\rm eff}$ is a *deformed version* of the Hamiltonian describing the dynamics of a (spinning) test-particle in a Kerr background. The EOB effective Hamiltonian is decomposed as

$$H^{\rm eff} = H_{\rm orb} + H_{\rm so}, \tag{6.2}$$

where the spin-orbit part $H_{\rm so}$ gathers the contributions that are odd in the spins (i.e. linear, cubic, etc.), while the orbital part $H_{\rm orb}$ those that are even in the spins (i.e. spin-independent, and then quadratic, quartic, etc.).

6.2.1 Structure of the Kerr Hamiltonian in Cartesian-like coordinates

As an orientation towards defining a new EOB Hamiltonian incorporating NLO spin-quadratic effects, let us reexamine the structure of the limiting case (to which $H^{\rm eff}$ should reduce in the extreme mass ratio limit) of the Hamiltonian of a (non spinning) test-particle in a Kerr background. For this Kerr dynamics, and for the special case of equatorial orbits, Ref. [81] has highlighted the role played by the *centrifugal* radius

$$r_c = \sqrt{r^2 + a^2 + \frac{2Ma^2}{r}}, \tag{6.3}$$

where r is the Boyer-Lindquist radial coordinate. In Eq. (6.3), M denotes the mass of the considered Kerr black hole, and a its Kerr parameter. The *orbital* sector of the test-particle Kerr Hamiltonian (after setting apart, similarly to Eq. (6.2), its spin-orbit sector) takes the form (in polar coordinates)

$$H^{\rm Kerr}_{\rm orb,eq} = \sqrt{A^{\rm eq}(r_c,a)\left(\mu^2 + \frac{p_r^2}{B^{\rm eq}(r_c,a)} + \frac{p_\varphi^2}{r_c^2}\right)}. \tag{6.4}$$

Here, μ denotes the mass of the test-particle[2]. We see in Eq. (6.4) that the angular momentum dependence is encoded in the centrifugal term p_φ^2/r_c^2, involving the centrifugal radius r_c. The construction of the EOB model of Ref. [81] is based upon the idea of exploiting the role of r_c. In

[2]One of the features of the EOB formalism is that, after suitably deforming the Kerr Hamiltonian, it will be possible to replace μ by the reduced mass of the binary system, $\mu \equiv m_1 m_2/(m_1+m_2)$, to describe the two-body effective Hamiltonian $H^{\rm eff}$ entering Eq. (6.1).

addition, it was suggested to incorporate NLO spin-spin effects (though only for circular orbits) by redefining the relation between r_c and the Boyer-Lindquist-like coordinate r, by adding to a a new, radial dependent spin-quadratic term $\delta a^2(r)$. This model can be extended without particular problems to equatorial, noncircular orbits. For example, the missing NLO spin-spin terms can be reproduced by a p_r-dependent term of the type

$$\left(1+\frac{M\delta a^2_{p_r}}{r^3}\right)\frac{p_r^2}{B^{\rm eq}}$$

(where $\delta a^2_{p_r}$ is an appropriate quadratic combination of the individual spin parameters a_1 and a_2), or alternatively, by a modification of the r-r_c relation inside of $B^{\rm eq}$.

In the present work, our aim is to define an EOB dynamics which is able to give the simplest possible description of general, *precessing* spinning binary systems with arbitrarily oriented spins. When both spins, as well as the orbital plane, precess, there no longer exist useful analogs of the z-axis, and associated structures (equatorial plane, angular momentum p_φ) that motivated the emphasis on the centrifugal radius (6.3) and the associated form (6.4) of the Kerr Hamiltonian. This motivates us to reexamine the structure of the Kerr Hamiltonian when it is written in (Boyer-Lindquist-based) Cartesian-like coordinates $\boldsymbol{r}=(x,y,z)$, with $x=r\sin\theta\cos\varphi$, $y=r\sin\theta\sin\varphi$, $z=r\cos\theta$, namely:

$$H^{\rm Kerr}_{\rm orb}=\sqrt{\frac{\Delta\,(r^2+(\boldsymbol{n}\cdot\boldsymbol{a})^2)}{\mathcal{R}^4+\Delta(\boldsymbol{n}\cdot\boldsymbol{a})^2}\left(\mu^2+\frac{1}{1+\frac{(\boldsymbol{n}\cdot\boldsymbol{a})^2}{r^2}}\left[\boldsymbol{p}^2+\left(\frac{\Delta}{r^2}-1\right)(\boldsymbol{n}\cdot\boldsymbol{p})^2-\frac{(r^2+2r+(\boldsymbol{n}\cdot\boldsymbol{a})^2)}{\mathcal{R}^4+\Delta(\boldsymbol{n}\cdot\boldsymbol{a})^2}\left((\boldsymbol{n}\times\boldsymbol{p})\cdot\boldsymbol{a}\right)^2\right]\right)}, \tag{6.5}$$

where $\boldsymbol{r}\equiv r\,\boldsymbol{n}$ and

$$\Delta=r^2-2Mr+\boldsymbol{a}^2 \tag{6.6}$$

$$\mathcal{R}^4=r^4+r^2\boldsymbol{a}^2+2Mr\boldsymbol{a}^2=r^2r_c^2. \tag{6.7}$$

In this reformulation, the centrifugal term p_φ^2/r_c^2 has been split in two parts. It is now contained in both the $\boldsymbol{p}^2$-contribution (with $\boldsymbol{p}^2\equiv p_r^2+p_\theta^2/r^2+p_\varphi^2/(r^2\sin^2\theta)$), and in the term $((\boldsymbol{n}\times\boldsymbol{p})\cdot\boldsymbol{a})^2$ (which is equal to $\boldsymbol{a}^2p_\varphi^2/r^2$ because $\boldsymbol{a}=|\boldsymbol{a}|\partial/\partial z$). Bringing these two parts together, and considering for simplicity equatorial orbits[3] $(\boldsymbol{n}\cdot\boldsymbol{a})=0$, the centrifugal radius r_c emerges from the identity

$$\frac{1}{r^2}\left(1-\frac{\boldsymbol{a}^2}{\mathcal{R}^4}\left(r^2+2r\right)\right)=\frac{1}{r_c^2}. \tag{6.8}$$

The Kerr Hamiltonian written as in Eq. (6.5) will be the starting point of the new EOB model, i.e., we will look for an EOB effective, orbital Hamiltonian $H^{\rm eff}_{\rm orb}$ which is the simplest possible deformation of Eq. (6.5). Let us introduce specific notations for the coefficients of the various contributions as they appear in Eq. (6.5), namely:

$$H^{\rm Kerr}_{\rm orb}=\left[A^{\rm Kerr}\left(\mu^2+B^{\rm Kerr}_p\,\boldsymbol{p}^2+B^{\rm Kerr}_{np}\,(\boldsymbol{n}\cdot\boldsymbol{p})^2+B^{\rm Kerr}_{\varepsilon np}\,((\boldsymbol{n}\times\boldsymbol{p})\cdot\boldsymbol{a})^2\right)\right]^{1/2}. \tag{6.9}$$

[3] Let us, however, recall in passing that r_c, Eq. (6.3), continues to play a central role even for non equatorial orbits, modulo the introduction of a "$\cos\theta$-dressing factor", see Eq. (2.2) in Ref. [81].

We have thereby distinguished four principal sectors in $H^{\rm Kerr}_{\rm orb}$. The first sector, described by the overall factor $A^{\rm Kerr}(\boldsymbol{r},\boldsymbol{a})$, is an anisotropic (spin-dependent) gravitational potential which generalizes the Schwarzschild (isotropic) potential $1-2M/r$. It reads

$$A^{\rm Kerr}(\boldsymbol{r},\boldsymbol{a}) = \frac{\Delta\left(r^2+(\boldsymbol{n}\cdot\boldsymbol{a})^2\right)}{\mathcal{R}^4+\Delta(\boldsymbol{n}\cdot\boldsymbol{a})^2} = A^{\rm Kerr,\,eq}(r_c)\frac{1+\frac{(\boldsymbol{n}\cdot\boldsymbol{a})^2}{r^2}}{1+\frac{\Delta(\boldsymbol{n}\cdot\boldsymbol{a})^2}{r^2 r_c^2}}, \tag{6.10}$$

where $A^{\rm Kerr,\,eq}$ denotes the equatorial Kerr radial potential, given by

$$A^{\rm Kerr,\,eq}(r_c) = \left(1-\frac{2M}{r_c}\right)\frac{1+\frac{2M}{r_c}}{1+\frac{2M}{r}}. \tag{6.11}$$

As emphasized in [81], $A^{\rm Kerr,\,eq}(r_c)$ is a small deformation of $1-\frac{2M}{r_c}$, even for large spins. The explicit expression of the remaining functions $B_p^{\rm Kerr}$, $B_{np}^{\rm Kerr}$ and $B_{\varepsilon np}^{\rm Kerr}$ can be deduced by a straightforward comparison with Eq. (6.5), for instance $B_p^{\rm Kerr} = 1/\left(1+(\boldsymbol{n}\cdot\boldsymbol{a})^2/r^2\right)$.

We now take the square $\left(H^{\rm Kerr}_{\rm orb}\right)^2$ of the Kerr Hamiltonian, which is a quadratic function of the momenta, and investigate the momentum dependence of the spin-quadratic terms generated by each sector (without specifying the radial behavior $\sim 1/r^n$, $n\geq 3$). More precisely, we formally expand the four separate building blocks $A^{\rm Kerr}$, $B_p^{\rm Kerr}$, $B_{np}^{\rm Kerr}$ and $B_{\varepsilon np}^{\rm Kerr}$ in powers of $\boldsymbol{a}$ (keeping $\boldsymbol{r}$ fixed), and retain only the terms quadratic in spin (spin-spin terms). We immediately observe that

i) All momentum-independent terms $\boldsymbol{a}^2$ and $(\boldsymbol{n}\cdot\boldsymbol{a})^2$ are encoded in the radial potential $A^{\rm Kerr}(\mathbf{r},\mathbf{a})$.

ii) The spin-spin terms contained in $B_p^{\rm Kerr}\boldsymbol{p}^2$ and $B_{np}^{\rm Kerr}(\boldsymbol{n}\cdot\boldsymbol{p})^2$ can only be of the types $\boldsymbol{p}^2\boldsymbol{a}^2$, $\boldsymbol{p}^2(\boldsymbol{n}\cdot\boldsymbol{a})^2$, and $(\boldsymbol{n}\cdot\boldsymbol{p})^2\boldsymbol{a}^2$, $(\boldsymbol{n}\cdot\boldsymbol{p})^2(\boldsymbol{n}\cdot\boldsymbol{a})^2$, respectively.

iii) As the last contribution $B_{\varepsilon np}^{\rm Kerr}\,((\boldsymbol{n}\times\boldsymbol{p})\cdot\boldsymbol{a})^2$ includes, as second factor, a term quadratic in $\boldsymbol{a}$, its spin-spin contribution only comes from the latter factor, namely $((\boldsymbol{n}\times\boldsymbol{p})\cdot\boldsymbol{a})^2$. When decomposed in elementary scalar product factors, $((\boldsymbol{n}\times\boldsymbol{p})\cdot\boldsymbol{a})^2$ is found to be a combination of six different terms: the four terms $\boldsymbol{p}^2\boldsymbol{a}^2$, $\boldsymbol{p}^2(\boldsymbol{n}\cdot\boldsymbol{a})^2$, $(\boldsymbol{n}\cdot\boldsymbol{p})\boldsymbol{a}^2$, $(\boldsymbol{n}\cdot\boldsymbol{p})^2(\boldsymbol{n}\cdot\boldsymbol{a})^2$ that appeared in ii), together with two new couplings $(\boldsymbol{p}\cdot\boldsymbol{a})^2$ and $(\boldsymbol{n}\cdot\boldsymbol{p})(\boldsymbol{n}\cdot\boldsymbol{a})(\boldsymbol{p}\cdot\boldsymbol{a})$ (see Eq. (3.9) of Ref. [138]).

The fact that every sector plays a rather individual role suggests a natural procedure for including the NLO spin-spin coupling into a new EOB Hamiltonian. This will be the topic of the next subsection.

6.2.2 The Effective-One-Body orbital Hamiltonian

The idea at the basis of our new EOB Hamiltonian is to write the orbital part of the EOB effective Hamiltonian $H^{\rm eff}_{\rm orb}$ in the same form as Eq. (6.9), but with (momentum-independent) coefficients $A(\boldsymbol{r},\nu,\boldsymbol{a}_1,\boldsymbol{a}_2)$, $B_p(\boldsymbol{r},\nu,\boldsymbol{a}_1,\boldsymbol{a}_2)$, $B_{np}(\boldsymbol{r},\nu,\boldsymbol{a}_1,\boldsymbol{a}_2)$ and $B_{\varepsilon np}(\boldsymbol{r},\nu,\boldsymbol{a}_1,\boldsymbol{a}_2)$ that are appropriate deformations of the coefficients $A^{\rm Kerr}(\boldsymbol{r},\boldsymbol{a})$, $B_p^{\rm Kerr}(\boldsymbol{r},\boldsymbol{a})$, $B_{np}^{\rm Kerr}(\boldsymbol{r},\boldsymbol{a})$ and $B_{\varepsilon np}^{\rm Kerr}(\boldsymbol{r},\boldsymbol{a})$.
To be fully explicit, the structure of our new EOB Hamiltonian is given by Eq (6.1), with $H^{\rm eff}$ of the form Eq (6.2). In the latter equation, the spin-orbit part is taken of the general form

$$H_{\rm so} = G_S\, \boldsymbol{L}\cdot\boldsymbol{S} + G_{S^*}\, \boldsymbol{L}\cdot\boldsymbol{S}^*, \tag{6.12}$$

in terms of the following symmetric combinations of the two spin vectors

$$\boldsymbol{S} \equiv \boldsymbol{S}_1 + \boldsymbol{S}_2 \equiv m_1\boldsymbol{a}_1 + m_2\boldsymbol{a}_2, \tag{6.13}$$

$$\boldsymbol{S}^* \equiv \frac{m_2}{m_1}\boldsymbol{S}_1 + \frac{m_1}{m_2}\boldsymbol{S}_2 \equiv m_2\boldsymbol{a}_1 + m_1\boldsymbol{a}_2. \tag{6.14}$$

The factors G_S and G_{S^*} in Eq. (6.12) are functions of $\boldsymbol{r}$, $\boldsymbol{p}$, $\boldsymbol{a}_1$ and $\boldsymbol{a}_2$, and are even in the spin vectors. They are not the focus of the present work (see, however, below for more discussion of them).

In the present paper, we focus on a new definition of the spin-quadratic contribution of an effective orbital EOB Hamiltonian $H^{\rm eff}_{\rm orb}$ having the following structure:

$$H^{\rm eff}_{\rm orb} = \Big[A\,(\boldsymbol{r},\nu,\boldsymbol{a}_1,\boldsymbol{a}_2)\Big(\mu^2 + B_p\,(\boldsymbol{r},\nu,\boldsymbol{a}_1,\boldsymbol{a}_2)\,\boldsymbol{p}^2 + B_{np}\,(\boldsymbol{r},\nu,\boldsymbol{a}_1,\boldsymbol{a}_2)\,(\boldsymbol{n}\cdot\boldsymbol{p})^2 + B_{\varepsilon np}\,((\boldsymbol{n}\times\boldsymbol{p})\cdot\boldsymbol{a})^2\text{-like terms} + Q_4\Big)\Big]^{1/2}, \tag{6.15}$$

where the structure of the last-indicated contribution on the right-hand-side (rhs) of Eq. (6.15) will be discussed below.

Let us start by specifying the structure that we shall require for the dependence of the EOB potentials A, B_p and B_{np} on the mass-ratio[4] ν and the two individual vectorial Kerr parameters of the two black holes $\boldsymbol{a}_1 \equiv \boldsymbol{S}_1/m_1$, $\boldsymbol{a}_2 \equiv \boldsymbol{S}_2/m_2$. We recall [68] that an effective orbital Hamiltonian with the correct LO spin-spin coupling is simply obtained by replacing the Kerr spin vector $\boldsymbol{a}$ entering Eq. (6.5) by the following effective spin vector

$$\boldsymbol{a}_0 \equiv \boldsymbol{a}_1 + \boldsymbol{a}_2. \tag{6.16}$$

In addition to the replacement (6.16), the two masses, M and μ, entering the Kerr dynamics are replaced by

$$M = m_1 + m_2, \qquad \mu = \frac{m_2\, m_2}{m_2 + m_2}. \tag{6.17}$$

This suggests to look for EOB potentials A, B_p, B_{np} of the form

$$A(\boldsymbol{r},\nu,\boldsymbol{a}_1,\boldsymbol{a}_2) = A^{\nu K_0}(\boldsymbol{r},\nu,\boldsymbol{a}_0) + \delta A, \tag{6.18}$$

$$B_p(\boldsymbol{r},\nu,\boldsymbol{a}_1,\boldsymbol{a}_2) = B_p^{\nu K_0}(\boldsymbol{r},\nu,\boldsymbol{a}_0) + \delta B_p, \tag{6.19}$$

$$B_{np}(\boldsymbol{r},\nu,\boldsymbol{a}_1,\boldsymbol{a}_2) = B_{np}^{\nu K_0}(\boldsymbol{r},\nu,\boldsymbol{a}_0) + \delta B_{np}, \tag{6.20}$$

where $A^{\nu K_0}$, $B_p^{\nu K_0}$, $B_{np}^{\nu K_0}$ are some ν-deformed versions of the Kerr-like potentials defined by replacing $\boldsymbol{a}$ by $\boldsymbol{a}_0$ in the potentials $A^{\rm Kerr}$, $B_p^{\rm Kerr}$, $B_{np}^{\rm Kerr}$ entering Eq. (6.9), and where δA, δB_p, δB_{np} are

[4] We shall use here the convention $m_1 \geq m_2$ so that all the mass-ratios can be expressed in terms of $\nu = m_1 m_2/(m_1+m_2)^2$. E.g., $X_1 \equiv m_1/(m_1+m_2) = (1+\sqrt{1-4\nu})/2$, $X_2 \equiv m_2/(m_1+m_2) = (1-\sqrt{1-4\nu})/2$.

additional NLO spin-spin contributions. Explicitly, we shall (following Ref. [81], except for the treatment of NLO spin-spin effects) take as ν-deformed[5] , LO spin-spin, Kerr-like A potential

$$A^{\nu K_0}(\boldsymbol{r},\nu,\boldsymbol{a}_0) = A^{\rm eq}(r_c,\nu,a_0)\frac{1+\frac{(\boldsymbol{n}\cdot\boldsymbol{a}_0)^2}{r^2}}{1+\frac{\Delta(r,\boldsymbol{a}_0)(\boldsymbol{n}\cdot\boldsymbol{a}_0)^2}{r^2 r_c^2}}, \tag{6.21}$$

where

$$A^{\rm eq}(r_c,\nu,a_0) = A_{\rm orb}(r_c,\nu)\frac{1+\frac{2M}{r_c}}{1+\frac{2M}{r}}, \tag{6.22}$$

with

$$A_{\rm orb}(r_c,\nu) \equiv P^1_5\left[A^{\rm PN}_{\rm orb}\left(\frac{M}{r_c},\nu\right)\right], \tag{6.23}$$

where $P^1_5[A^{\rm PN}_{\rm orb}]$ denotes the (1,5)-Padé resummation of the 5PN-level, Taylor-expanded orbital radial potential. More precisely, we use Eqs. (28)-(29) in [81] together with the exact value of $a^c_5(\nu)$ [79] and the recent calibration $a^c_6(\nu) = 3097.3\nu^2 - 1330.6\nu + 81.38$ [92] (instead of the values for a^c_5 and a^6_5 that were employed in Ref. [81]).

Here, and in the following, r_c is defined as being the following function of r and $\boldsymbol{a}_0$,

$$r_c \equiv \sqrt{r^2 + \boldsymbol{a}_0^2 + \frac{2M}{r}\boldsymbol{a}_0^2}. \tag{6.24}$$

As for the other Kerr-like EOB potentials, we take

$$B_p^{\nu K_0} = \frac{1}{1+\frac{(\boldsymbol{n}\cdot\boldsymbol{a}_0)^2}{r^2}}, \tag{6.25}$$

$$B_{np}^{\nu K_0} = \frac{1}{1+\frac{(\boldsymbol{n}\cdot\boldsymbol{a}_0)^2}{r^2}}\left(\frac{A^{\rm eq}(r_c,\nu,a_0)}{D_{\rm orb}(r_c,\nu)}\frac{r_c^2}{r^2} - 1\right), \tag{6.26}$$

where $A^{\rm eq}(r_c,\nu,a_0)$ was defined in Eq. (6.22) above, and where $D_{\rm orb}(r_c,\nu)$ is defined by Eq. (33) of [81] with $u_c \equiv M/r_c$. Finally, the quartic-in-momenta term Q_4 that has to be added to the four main summands inside the effective Hamiltonian is defined by Eq. (35) in Ref. [81].

6.2.3 Canonical transformation from ADM to EOB

In order to determine the additional, NLO spin-spin terms δA, δB_p, δB_{np} in Eqs. (6.18)-(6.20) (as well as the NLO-accurate $B_{\varepsilon np}\,((\boldsymbol{n}\times\boldsymbol{p})\cdot\boldsymbol{a})^2$-like terms in Eq. (6.15)) we need to transform the ADM NLO spin-spin Hamiltonian $H^{\rm NLO(ADM)}_{\rm ss}$ [42, 48–50] into a corresponding EOB Hamiltonian by means of a suitable canonical transformation. As in Refs. [115, 138], this will be done by composing three successive canonical transformations. The first transformation $G^{\rm 1PN}_{\rm o}(\boldsymbol{r},\boldsymbol{p})$ (given

[5] For the purpose of this article, it is not necessary to be careful about the ν-deformations of A and B_{np}, since the NLO spin-spin coupling is not affected by them. Indeed, neither A nor B_{np} contain ν-dependent terms at the 1PN level, and thus there is no coupling of this type with the LO spin-spin part leading to NLO spin-spin terms. However, an influence of the purely orbital ν-deformation on the spin-spin sector is still present in the transformation between ADM and EOB coordinates, and also in the transformation between the effective and EOB Hamiltonians.

by Eqs. (6.15)-(6.16) in Ref. [65]) is of a purely orbital type, and has the following effect on spin-spin terms:

$$H_{\rm ss}^{\rm NLO\prime} = H_{\rm ss}^{\rm NLO(ADM)} + \left\{G_{\rm o}^{\rm 1PN}, H_{\rm ss}^{\rm LO(ADM)}\right\}. \tag{6.27}$$

It is followed by a LO spin-spin canonical transformation $G_{\rm ss}^{\rm LO}(\boldsymbol{r},\boldsymbol{p},\boldsymbol{S}_1,\boldsymbol{S}_2)$ (given by Eq. (5.15) in Ref. [75], see also Eq. (3.16) of Ref. [138]) yielding a further modification of spin-spin terms:

$$H_{\rm ss}^{\rm NLO\prime\prime} = H_{\rm ss}^{\rm NLO\prime} + \left\{G_{\rm ss}^{\rm LO}, H_{\rm o}^{\rm 1PN\prime}\right\}, \tag{6.28}$$

where

$$H_{\rm o}^{\rm 1PN\prime} = H_{\rm o}^{\rm 1PN(ADM)} + \left\{G_{\rm o}^{\rm 1PN}, H_{\rm o}^{\rm N(ADM)}\right\}. \tag{6.29}$$

Finally, we perform a NLO spin-spin canonical transformation $G_{\rm ss}^{\rm NLO}(\boldsymbol{r},\boldsymbol{p},\boldsymbol{S}_1,\boldsymbol{S}_2)$ (whose structure will be discussed below) yielding a last modification of spin-spin terms

$$H_{\rm ss}^{\rm NLO\prime\prime\prime} = H_{\rm ss}^{\rm NLO\prime\prime} + \left\{G_{\rm ss}^{\rm NLO}, H_{\rm N}\right\}. \tag{6.30}$$

$H_{\rm ss}^{\rm NLO\prime\prime\prime}$ must then be equal to the corresponding term in the PN expansion of the EOB Hamiltonian we are seeking. It is convenient to focus the attention onto the squared effective orbital Hamiltonian $\left(H_{\rm orb}^{\rm eff}\right)^2$, which has an intuitive structure. Because of the relation

$$\hat{H}^{\rm eff} = 1 + \hat{H}_{\rm EOB}^{\rm NR} + \frac{\nu}{2}\left(\hat{H}_{\rm EOB}^{\rm NR}\right)^2, \tag{6.31}$$

where $H_{\rm EOB}^{\rm NR} \equiv H_{\rm EOB} - M$ is the "non relativistic" EOB Hamiltonian, and where the hat denotes a μ-scaling $\hat{H} \equiv H/\mu$, $\hat{G} \equiv G/\mu$ we are left with the condition

$$\left(\hat{H}_{\rm orb}^{\rm eff}\right)^2\Big|_{\rm NLOss} = 2\left(\hat{H}_{\rm ss}^{\rm NLO\prime\prime\prime} + (1+\nu)\,\hat{H}_{\rm N}\left(\hat{H}_{\rm ss}^{\rm LO(ADM)} + \{\hat{G}_{\rm ss}^{\rm LO}, \hat{H}_{\rm N}\}\right)\right), \tag{6.32}$$

where the notation on the left hand side simply denotes the NLO spin-spin part of the PN expansion of $\left(\hat{H}_{\rm orb}^{\rm eff}\right)^2$. In other words, our problem is to find a suitable $G_{\rm ss}^{\rm NLO}$ such that the rhs of Eq. (6.32) is equal to the NLO spin-spin contribution to the expression

$$\begin{aligned}\left(H_{\rm orb}^{\rm eff}\right)^2 = \Big[&\left(A^{\nu K_0} + \delta A\right)\left(\mu^2 + \left(B_p^{\nu K_0} + \delta B_p\right)\boldsymbol{p}^2 + \left(B_{np}^{\nu K_0} + \delta B_{np}\right)(\boldsymbol{n}\cdot\boldsymbol{p})^2\right.\\ &\left. + B_{\varepsilon np}\left((\boldsymbol{n}\times\boldsymbol{p})\cdot\boldsymbol{a}\right)^2\text{-like terms} + Q_4\right)\Big]^{1/2},\end{aligned} \tag{6.33}$$

with appropriate NLO spin-spin terms δA, δB_p, δB_{np}, and with a suitable NLO-accurate EOB version of the $((\boldsymbol{n}\times\boldsymbol{p})\cdot\boldsymbol{a})^2$ term in the Kerr Hamiltonian (6.5).

We introduce at this point a change in the notation. Since NLO spin-spin terms are more conveniently expressed by dimensionless quantities, we will from now on only make use of the dimensionless rescaled variables $\hat{r} \equiv r/M$, $\hat{r}_c \equiv r_c/M$, $\hat{\boldsymbol{p}} \equiv \boldsymbol{p}/\mu$, $\boldsymbol{\chi}_1 \equiv \boldsymbol{a}_1/m_1$, $\boldsymbol{\chi}_2 \equiv \boldsymbol{a}_2/m_2$, $\boldsymbol{\chi}_0 \equiv \boldsymbol{a}_0/M$, $\hat{H} \equiv H/\mu$ and $\hat{G} \equiv G/\mu$. However, in order to lighten the notation, we will omit to display the hats on the dynamical variables r, r_c and $\boldsymbol{p}$.

Before evaluating Eq. (6.32), it is necessary to specify the form of the canonical transformation (6.30). In Ref. [138], the generating function $\hat{G}_{\rm ss}^{\rm NLO}$ had been chosen in a rather general way, which involved terms cubic in the momenta. The latter terms gave rise, in the Hamiltonian, to NLO

spin-spin terms that were quartic in the momenta. The presence of such terms is a feature not shared by the ADM Hamiltonian, but was related to the idea of defining, in the EOB formalism, an "effective spin" that may also depend on $\boldsymbol{p}^2$ and $(\boldsymbol{n}\cdot\boldsymbol{p})^2$, thereby introducing higher powers of the momenta.

In this paper, by contrast, we want to hold the dependence on the momenta as simple as possible. We found it possible to end up with a squared effective EOB Hamiltonian involving only quadratic-in-momenta spin-spin terms by choosing an NLO spin-spin generating function $\hat{G}^{\rm NLO}_{\rm ss}$ which is only linear in momenta (rather than cubic as in Ref. [138]). [This fact relies on the combined structure of the LO spin-spin canonical transformation $G^{\rm LO}_{\rm ss}$ [75] (going from ADM coordinates to Boyer-Lindquist coordinates) and of the nonlinear transformation relating the effective Hamiltonian to the real one.] Among the 33 gauge coefficients taken into account in Ref. [138] for $\hat{G}^{\rm NLO}_{\rm ss}$, we only need to maintain 10 of them.[6] We thus consider a generating function of the following form:[7]

$$\hat{G}^{\rm NLO}_{\rm ss} = \frac{(\boldsymbol{n}\cdot\boldsymbol{p})}{r^2}\Big(\alpha_{ij}(\boldsymbol{\chi}_i\cdot\boldsymbol{\chi}_j)+\beta_{ij}(\boldsymbol{n}\cdot\boldsymbol{\chi}_i)(\boldsymbol{n}\cdot\boldsymbol{\chi}_j)\Big)+\frac{1}{r^2}\gamma_{ij}(\boldsymbol{n}\cdot\boldsymbol{\chi}_i)(\boldsymbol{p}\cdot\boldsymbol{\chi}_j), \tag{6.34}$$

where we use the summation convention on the spin labels $i,j=1,2$, and where the coefficients α_{ij} and β_{ij} are assumed to be symmetric, while $\gamma_{ij}\neq\gamma_{ji}$.

The change induced by $\hat{G}^{\rm NLO}_{\rm ss}$ in the Hamiltonian is

$$\begin{aligned}\Big\{\hat{G}^{\rm NLO}_{\rm ss},\hat{H}_{\rm N}\Big\} = \frac{1}{r^3}\Bigg[&\left(\alpha_{ij}\boldsymbol{p}^2-3\alpha_{ij}(\boldsymbol{n}\cdot\boldsymbol{p})^2-\frac{\alpha_{ij}}{r}\right)(\boldsymbol{\chi}_i\cdot\boldsymbol{\chi}_j)+\left(\beta_{ij}\boldsymbol{p}^2-5\beta_{ij}(\boldsymbol{n}\cdot\boldsymbol{p})^2-\frac{\beta_{ij}+\gamma_{(ij)}}{r}\right)(\boldsymbol{n}\cdot\boldsymbol{\chi}_i)(\boldsymbol{n}\cdot\boldsymbol{\chi}_j)\\&+\gamma_{(ij)}(\boldsymbol{p}\cdot\boldsymbol{\chi}_i)(\boldsymbol{p}\cdot\boldsymbol{\chi}_j)+\Big(2\beta_{ij}-3\gamma_{ij}\Big)(\boldsymbol{n}\cdot\boldsymbol{p})(\boldsymbol{n}\cdot\boldsymbol{\chi}_i)(\boldsymbol{p}\cdot\boldsymbol{\chi}_j)\Bigg],\end{aligned} \tag{6.35}$$

where we have introduced the symmetrized coefficients $\gamma_{(ij)}\equiv(\gamma_{ij}+\gamma_{ji})/2$ in order to point out that the only term which is not symmetric under exchange of the indices i and j is the last one, i.e., $-3\gamma_{ij}r^{-3}(\boldsymbol{n}\cdot\boldsymbol{p})(\boldsymbol{n}\cdot\boldsymbol{\chi}_i)(\boldsymbol{p}\cdot\boldsymbol{\chi}_j)$. We will show in the next subsection why γ_{ij} must contain an antisymmetric part $\gamma_{[ij]}$, and how $\gamma_{[ij]}$ can be used to yield a simple $H^{\rm eff}_{\rm orb}$.

6.2.4 Gauge choice

One of the useful features of the EOB formalism is to use canonical transformations as gauge transformations able (after some gauge choice) to simplify the structure of PN-expanded Hamiltonians. Here, we shall apply this philosophy to the NLO spin-spin Hamiltonian. The original NLO spin-spin Hamiltonian, obtained in ADM gauge in Refs. [48–50], contains 25 different terms

[6] The 23 coefficients that we discard here are all those cubic in $\boldsymbol{p}$. Each of them leads, after the Poisson Bracket with the Newtonian Hamiltonian, to terms quartic in the momenta. An explicit calculation easily shows that the so obtained 23 quartic expressions are linearly independent in the 32-dimensional space of NLO spin-spin polynomials that are quartic in the momenta, whose basis is defined by scalars of the type $\boldsymbol{p}^4(\boldsymbol{\chi}_i\cdot\boldsymbol{\chi}_j)/r^2$, $(\boldsymbol{n}\cdot\boldsymbol{p})^4(\boldsymbol{\chi}_i\cdot\boldsymbol{\chi}_j)/r^2$, and so on. There is therefore no way of tuning these 23 coefficients, apart from setting all of them to zero, that prevents the transformed Hamiltonian from being quartic in the momenta.

[7] We warn the reader that the nomenclature of the gauge coefficients differs significantly from the one used in Refs. [115, 138]. In particular, the coefficients α, β and γ used here correspond to $\gamma^{(\chi)}$, $\gamma^{(n)}$ and $\gamma^{(np)}$ in Ref. [138]. The reason beyond these choices has been that of favoring the readability and self-consistence of this paper over the continuity with respect to Ref. [138].

in the center-of-mass frame (see Eq. (2.9a) of Ref. [115], which accounts for both spin(1)-spin(1) and spin(2)-spin(2) terms, and Eq. (3.15) of Ref. [138] (spin(1)-spin(2)) for a center-of-mass formulation). [This is the generic number of terms for an NLO spin-spin Hamiltonian which is at most quadratic in momenta, as the ADM spin-spin Hamiltonian happens to be.] As we have introduced in Eq. (6.34) a NLO spin-spin transformation involving 10 arbitrary parameters ($\alpha_{(ij)}$, $\beta_{(ij)}$, $\gamma_{(ij)}$ and $\gamma_{[12]}$), we expect to be able to end up with a simplified EOB NLO spin-spin Hamiltonian containing at most 15 different terms. In particular, we wish to simplify the *a priori* most complicated sector of the ADM Hamiltonian (and of its generic EOB counterpart), namely the sector comprising the seven different terms

$$(\boldsymbol{p}\cdot\boldsymbol{\chi}_i)(\boldsymbol{p}\cdot\boldsymbol{\chi}_j) \quad \text{and} \quad (\boldsymbol{n}\cdot\boldsymbol{p})(\boldsymbol{n}\cdot\boldsymbol{\chi}_i)(\boldsymbol{p}\cdot\boldsymbol{\chi}_j) \tag{6.36}$$

appearing in the last two contributions on the rhs of Eq. (6.35). As discussed above, in the Kerr case (with only one $\boldsymbol{\chi}$), these couplings came out of the decomposition of the Kerr coupling $B_{\varepsilon np}\left((\boldsymbol{n}\times\boldsymbol{p})\cdot\boldsymbol{a}\right)^2$ into elementary product factors. We found convenient to use the freedom of $\hat{G}^{\rm NLO}_{\rm ss}$ to impose that the EOB sector containing the seven different terms (6.36) take the following maximally simplified form:

$$B^{\rm Kerr}_{\varepsilon np}(\boldsymbol{r},\boldsymbol{a}_0)\left((\boldsymbol{n}\times\boldsymbol{p})\cdot\boldsymbol{a}_0\right)^2 \tag{6.37}$$

differing by its Kerr counterpart (last terms on the rhs of Eq. (6.5)) only by the replacement $\boldsymbol{a}\to\boldsymbol{a}_0\equiv\boldsymbol{a}_1+\boldsymbol{a}_2$. It is easily checked that this requirement uniquely fixes 7 degrees of freedom in $\hat{G}^{\rm NLO}_{\rm ss}$, in determining the gauge parameters $\beta_{(ij)}$ and γ_{ij} (which, as exhibited in Eq. (6.35), entered the gauge variation of the seven terms (6.36)).

More precisely, these 7 gauge parameters must take the values

$$\beta_{11} = -\left(\frac{1}{2}+\frac{3}{4}\nu\right)(X_1-\nu) \tag{6.38a}$$

$$\beta_{22} = -\left(\frac{1}{2}+\frac{3}{4}\nu\right)(X_2-\nu) \tag{6.38b}$$

$$\beta_{12} = \beta_{21} = -\left(\frac{1}{2}+\frac{3}{4}\nu\right)\nu \tag{6.38c}$$

and

$$\gamma_{11} = X_1-\nu-\frac{\nu^2}{4} \tag{6.39a}$$

$$\gamma_{22} = X_2-\nu-\frac{\nu^2}{4} \tag{6.39b}$$

$$\gamma_{12} = \frac{\nu}{2}X_1-\frac{\nu^2}{4} \tag{6.39c}$$

$$\gamma_{21} = \frac{\nu}{2}X_2-\frac{\nu^2}{4}. \tag{6.39d}$$

Note that, in the limit $m_2\ll m_1$ (under which $X_2\to 0$, $X_1\to 1$, $\nu\to 0$) we have $\beta_{11}\to-\frac{1}{2}$ and $\gamma_{11}\to 1$, which is a necessary requirement for the structure of $\hat{G}^{\rm NLO}_{\rm ss}$ (as discussed in Refs. [115, 138]). Note also that the antisymmetric part of γ_{ij} is fixed to the value

$$\gamma_{[ij]} = \frac{\nu}{4}\left(X_i-X_j\right). \tag{6.40}$$

It is easily checked (using Eq. (6.35)) that this value allows one to gauge away the antisymmetric-looking[8] ADM term [50]

$$\hat{H}^{\rm NLO(ADM)}_{\rm ss,\,antis.} = \frac{3}{4}\nu\frac{(\boldsymbol{n}\cdot\boldsymbol{p})}{r^3}(X_1-X_2)\Big((\boldsymbol{n}\cdot\boldsymbol{\chi}_1)(\boldsymbol{p}\cdot\boldsymbol{\chi}_2)-(\boldsymbol{n}\cdot\boldsymbol{\chi}_2)(\boldsymbol{p}\cdot\boldsymbol{\chi}_1)\Big), \tag{6.41}$$

so as to end up with a symmetric contribution $\propto(\boldsymbol{n}\cdot\boldsymbol{\chi}_1)(\boldsymbol{p}\cdot\boldsymbol{\chi}_2)+(\boldsymbol{n}\cdot\boldsymbol{\chi}_2)(\boldsymbol{p}\cdot\boldsymbol{\chi}_1)$ of the type contained in the expansion of the term $((\boldsymbol{n}\times\boldsymbol{p})\cdot\boldsymbol{a}_0)^2$.

Having fixed the $B_{\varepsilon np}\,((\boldsymbol{n}\times\boldsymbol{p})\cdot\boldsymbol{a})^2$ sector by using the 7 gauge parameters $\beta_{(ij)}\,\gamma_{ij}$, we are left with the 3 gauge parameters $\alpha_{(ij)}$ to simplify the NLO contributions δA, δB_p and δB_{np} to the remaining physical sectors of the NLO spin-spin EOB Hamiltonian. As we started from 25 different contributions and used only 7 gauge parameters, we would expect δA, δB_p and δB_{np} to involve $25-7=18$ different contributions, in the form of 6 different quadratic forms in the two spin vectors. More specifically, one can *a priori* decompose δA, δB_p and δB_{np} in the form

$$\delta A = \frac{1}{r^4}\left(A^Q_\chi - A^Q_{n\chi}\right) \tag{6.42}$$

$$\delta B_p = \frac{1}{r^3}\left(B^Q_{p,\chi} - B^Q_{p,n\chi}\right) \tag{6.43}$$

$$\delta B_{np} = \frac{1}{r^3}\left(B^Q_{np,\chi} - B^Q_{np,n\chi}\right), \tag{6.44}$$

(where the minus signs are introduced for later convenience) with six (symmetric) quadratic forms

$$A^Q_\chi = a^\chi_{ij}(\boldsymbol{\chi}_i\cdot\boldsymbol{\chi}_j) \tag{6.45}$$

$$A^Q_{n\chi} = a^{n\chi}_{ij}(\boldsymbol{n}\cdot\boldsymbol{\chi}_i)(\boldsymbol{n}\cdot\boldsymbol{\chi}_j) \tag{6.46}$$

$$B^Q_{p,\chi} = b^{p,\chi}_{ij}(\boldsymbol{\chi}_i\cdot\boldsymbol{\chi}_j) \tag{6.47}$$

$$B^Q_{p,n\chi} = b^{p,n\chi}_{ij}(\boldsymbol{n}\cdot\boldsymbol{\chi}_i)(\boldsymbol{n}\cdot\boldsymbol{\chi}_j) \tag{6.48}$$

$$B^Q_{np,\chi} = b^{np,\chi}_{ij}(\boldsymbol{\chi}_i\cdot\boldsymbol{\chi}_j) \tag{6.49}$$

$$B^Q_{np,n\chi} = b^{np,n\chi}_{ij}(\boldsymbol{n}\cdot\boldsymbol{\chi}_i)(\boldsymbol{n}\cdot\boldsymbol{\chi}_j). \tag{6.50}$$

[Note that the summation convention on the indices i,j means that, e.g., $A^Q_\chi = a^\chi_{11}\boldsymbol{\chi}_1^2 + 2a^\chi_{12}(\boldsymbol{\chi}_1\cdot\boldsymbol{\chi}_2) + a^\chi_{22}\boldsymbol{\chi}_2^2$.] A first remarkable finding is that our request of having the simple, Kerr-like form (6.37) implies another simplification for free. Namely, we find that the 3 coefficients

$$b^{np,n\chi}_{ij} = 0, \tag{6.51}$$

so that the second quadratic form, $B^Q_{np,n\chi}$, entering δB_{np} simply vanishes. We also find that the coefficients of the second quadratic forms $A^Q_{n\chi}$ and $B^Q_{p,n\chi}$ entering δA and δB_p are uniquely fixed

[8] Note, however, that this term is symmetric under the combined permutation $X_1\leftrightarrow X_2$, $\boldsymbol{\chi}_1\leftrightarrow\boldsymbol{\chi}_2$.

to the values

$$a_{11}^{n\chi} = \left(2\nu X_1 + \frac{5}{2}\nu^2\right) \tag{6.52a}$$
$$a_{22}^{n\chi} = \left(2\nu X_2 + \frac{5}{2}\nu^2\right) \tag{6.52b}$$
$$a_{12}^{n\chi} = a_{21}^{n\chi} = \left(\frac{3}{2}\nu - \frac{7}{2}\nu^2\right) \tag{6.52c}$$

$$b_{11}^{p,n\chi} = \left(9\nu X_1 - \frac{15}{4}\nu^2\right) \tag{6.53a}$$
$$b_{22}^{p,n\chi} = \left(9\nu X_2 - \frac{15}{4}\nu^2\right) \tag{6.53b}$$
$$b_{12}^{p,n\chi} = b_{21}^{p,n\chi} = \left(3\nu + \frac{9}{4}\nu^2\right). \tag{6.53c}$$

Let us now consider the three remaining quadratic forms (linear in $(\boldsymbol{\chi}_i \cdot \boldsymbol{\chi}_j)$) A_χ^Q, $B_{p,\chi}^Q$ and $B_{np,\chi}^Q$. These three forms are not fixed by our previous request, because they depend on the three gauge parameters $\alpha_{(ij)}$, which are still free at this stage. In view of Eq. (6.35) (keeping in mind the factor 2 in Eq. (6.32)) the effect of a gauge shift $\delta\alpha_{ij}$ on the three quadratic forms A_χ^Q, $B_{p,\chi}^Q$ and $B_{np,\chi}^Q$ is

$$\delta A_\chi^Q = -2\,\delta\alpha_{ij}(\boldsymbol{\chi}_i \cdot \boldsymbol{\chi}_j) \tag{6.54}$$
$$\delta B_{p,\chi}^Q = 2\,\delta\alpha_{ij}(\boldsymbol{\chi}_i \cdot \boldsymbol{\chi}_j) \tag{6.55}$$
$$\delta B_{np,\chi}^Q = -6\,\delta\alpha_{ij}(\boldsymbol{\chi}_i \cdot \boldsymbol{\chi}_j). \tag{6.56}$$

In view of these transformation properties we could use the α_{ij}-freedom to set to zero any of the three forms A_χ^Q, $B_{p,\chi}^Q$ and $B_{np,\chi}^Q$. Setting to zero A_χ^Q does not seem physically appealing because A_χ^Q has a relatively simple and intuitive meaning as a higher-order contribution to the already present spin-spin contribution to the radial potential $A^{\nu K_0}$, Eq. (6.21). This leaves us with two natural options: setting either $B_{p,\chi}^Q$ or $B_{np,\chi}^Q$ to zero.

Let us first briefly discuss the latter option, i.e. using α_{ij} to set $b_{ij}^{np,\chi} \equiv 0$. Explicit calculations then show that a simple link emerges between the resulting gauge-fixed $B_{p,\chi}^Q$ and the form $B_{p,n\chi}^Q$ which was already fixed (and given by Eq. (6.53)). Indeed, we find in this case that the following relation holds

$$b_{ij}^{p,\chi} = \frac{1}{3} b_{ij}^{p,n\chi}. \tag{6.57}$$

This relation means that the momentum-dependent part of the NLO spin-spin contribution to $\left(H^{\rm eff}\right)^2$ takes the simple form

$$\frac{\boldsymbol{p}^2}{r^3} b_{ij}^{p,\chi} \left((\boldsymbol{\chi}_i \cdot \boldsymbol{\chi}_j) - 3(\boldsymbol{n} \cdot \boldsymbol{\chi}_i)(\boldsymbol{n} \cdot \boldsymbol{\chi}_j)\right),$$

where we recognize a coupling between $\boldsymbol{p}^2$ and a spin-spin structure akin to the LO quadrupole potential present in the ADM Hamiltonian

$$\hat{H}_{\rm ss}^{\rm LO(ADM)} = -\frac{1}{2r^3}\left(\boldsymbol{\chi}_0^2 - 3(\boldsymbol{n}\cdot\boldsymbol{\chi}_0)^2\right) = \frac{\boldsymbol{\chi}_0^2}{r^3}P_2(\cos\vartheta). \tag{6.58}$$

In the last equality, ϑ is the angle between $\boldsymbol{n}$ and $\boldsymbol{\chi}_0$, and P_2 is the second Legendre polynomial. Notice that a coupling of the type $\hat{H}_{\rm N}\hat{H}_{\rm ss}^{\rm LO(ADM)}$ (which involves $\boldsymbol{p}^2\hat{H}_{\rm ss}^{\rm LO(ADM)}$) is explicitly visible in Eq. (6.32).

The other option is to use the α_{ij} freedom to set, instead, the form $B^Q_{p,\chi}$ to zero, i.e.

$$b_{ij}^{p,\chi} \equiv 0. \tag{6.59}$$

In analogy to Refs. [64, 70], this choice can be called a Damour-Jaranowski-Schäfer gauge. When the orbits are circular and equatorial, the gauge-choice (6.59) leads to a very simple spin-spin structure, since in that case A^Q_χ becomes the only quadratic form that does not vanish. Consequently, all new NLO spin-spin information is contained in the radial potential A. We will adopt this gauge for the rest of the paper.

To satisfy Eq. (6.59), the α_{ij} gauge parameters must be taken to be

$$\alpha_{11} = -\left(\frac{1}{2}+\frac{5}{4}\nu\right)X_1 + \frac{\nu}{2} + \frac{\nu^2}{2} \tag{6.60a}$$

$$\alpha_{22} = -\left(\frac{1}{2}+\frac{5}{4}\nu\right)X_2 + \frac{\nu}{2} + \frac{\nu^2}{2} \tag{6.60b}$$

$$\alpha_{12} = \alpha_{21} = -\frac{\nu}{2}. \tag{6.60c}$$

In the limit $m_2 \ll m_1$, we have $\alpha_{11} \to -\frac{1}{2}$, which is a necessary requirement for the structure of $\hat{G}_{\rm ss}^{\rm NLO}$ [115, 138]. Solving Eq. (6.32) then leads first to

$$a_{11}^\chi = 3\nu X_1 - \frac{\nu^2}{2} \tag{6.61a}$$

$$a_{22}^\chi = 3\nu X_2 - \frac{\nu^2}{2} \tag{6.61b}$$

$$a_{12}^\chi = a_{21}^\chi = \nu - \frac{\nu^2}{2} \tag{6.61c}$$

and then to a remarkable result for the coefficients of $B^Q_{np,\chi}$. Namely, we find that they turn out to coincide with the coefficients of the above-determined quadratic form $B^Q_{p,n\chi}$, i.e.

$$b_{ij}^{np,\chi} = b_{ij}^{p,n\chi}. \tag{6.62}$$

Here, as in the case of the other possible gauge $b_{ij}^{np,\chi} \equiv 0$, a symmetry becomes visible between b_{ij}-type coefficients belonging to different quadratic forms.

The final result is remarkable: the information stored in the 9 coefficients a_{ij}^χ, $a_{ij}^{n\chi}$ and $b_{ij}^{p,n\chi}$ is sufficient, once inserted in the EOB Hamiltonian, to reproduce the whole NLO spin-spin coupling (which initially involved 25 different terms). The EOB has not only exploited the full power of the gauge transformations, involving 10 parameters, but has also revealed 6 additional and

unexpected symmetries (see the Appendix for a further discussion of these symmetries). Notice that the EOB Hamiltonian proposed in Ref. [138] involved 12 different terms. A symmetry similar to (6.51) was present, but there was no equivalent to (6.57) or (6.62).

To summarize the results so far, the effective orbital Hamiltonian has the form

$$\hat{H}^{\rm eff}_{\rm orb} = \sqrt{A\left(1 + B_p\,\boldsymbol{p}^2 + B_{np}\,(\boldsymbol{n}\cdot\boldsymbol{p})^2 - \frac{1}{1+\frac{(\boldsymbol{n}\cdot\boldsymbol{\chi}_0)^2}{r^2}}\frac{(r^2+2r+(\boldsymbol{n}\cdot\boldsymbol{\chi}_0)^2)}{\mathcal{R}^4+\Delta(\boldsymbol{n}\cdot\boldsymbol{\chi}_0)^2}((\boldsymbol{n}\times\boldsymbol{p})\cdot\boldsymbol{\chi}_0)^2 + Q_4\right)}. \tag{6.63}$$

Here, the quantities entering the $((\boldsymbol{n}\times\boldsymbol{p})\cdot\boldsymbol{a}_0)^2$ term are

$$\Delta = r^2 - 2r + \boldsymbol{\chi}_0^2 \tag{6.64}$$

$$\mathcal{R}^4 = r^4 + r^2\boldsymbol{\chi}_0^2 + 2r\,\boldsymbol{\chi}_0^2, \tag{6.65}$$

with the dimensionless effective spin

$$\boldsymbol{\chi}_0 = X_1\boldsymbol{\chi}_1 + X_2\boldsymbol{\chi}_2. \tag{6.66}$$

On the other hand, we obtained above explicit, but non-resummed, expressions for the NLO-spin-spin accurate potentials A, B_p and B_{np}. In our preferred ($B^Q_{p,\chi}=0$) gauge, and in view of the remarkable cancellation of $B^Q_{np,n\chi}$, they have the form

$$A(\boldsymbol{r},\nu,\boldsymbol{\chi}_1,\boldsymbol{\chi}_2) = A^{\nu K_0} + \frac{1}{r^4}\left(A^Q_\chi - A^Q_{n\chi}\right), \tag{6.67}$$

$$B_p(\boldsymbol{r},\nu,\boldsymbol{\chi}_1,\boldsymbol{\chi}_2) = B_p^{\nu K_0} - \frac{1}{r^3}B^Q_{n\chi}, \tag{6.68}$$

$$B_{np}(\boldsymbol{r},\nu,\boldsymbol{\chi}_1,\boldsymbol{\chi}_2) = B_{np}^{\nu K_0} + \frac{1}{r^3}B^Q_{\chi}. \tag{6.69}$$

Here, $A^{\nu K_0}$, $B_p^{\nu K_0}$, $B_{np}^{\nu K_0}$ have been defined in Eqs. (6.21), (6.25), (6.26), while the four remaining NLO spin-spin quadratic forms entering our results (here and henceforth we simplify the notation by suppressing the index p on $B^Q_{p,n\chi}$ and the index np on $B^Q_{np,\chi}$) take the following explicit form:

$$A^Q_\chi = \left(3\nu X_1 - \frac{\nu^2}{2}\right)\boldsymbol{\chi}_1^2 + \left(3\nu X_2 - \frac{\nu^2}{2}\right)\boldsymbol{\chi}_2^2 + \left(2\nu - \nu^2\right)(\boldsymbol{\chi}_1\cdot\boldsymbol{\chi}_2) \tag{6.70}$$

$$A^Q_{n\chi} = \left(2\nu X_1 + \frac{5}{2}\nu^2\right)(\boldsymbol{n}\cdot\boldsymbol{\chi}_1)^2 + \left(2\nu X_2 + \frac{5}{2}\nu^2\right)(\boldsymbol{n}\cdot\boldsymbol{\chi}_2)^2 + \left(3\nu - 7\nu^2\right)(\boldsymbol{n}\cdot\boldsymbol{\chi}_1)(\boldsymbol{n}\cdot\boldsymbol{\chi}_2) \tag{6.71}$$

$$B^Q_\chi = \left(9\nu X_1 - \frac{15}{4}\nu^2\right)\boldsymbol{\chi}_1^2 + \left(9\nu X_2 - \frac{15}{4}\nu^2\right)\boldsymbol{\chi}_2^2 + \left(6\nu + \frac{9}{2}\nu^2\right)(\boldsymbol{\chi}_1\cdot\boldsymbol{\chi}_2) \tag{6.72}$$

$$B^Q_{n\chi} = \left(9\nu X_1 - \frac{15}{4}\nu^2\right)(\boldsymbol{n}\cdot\boldsymbol{\chi}_1)^2 + \left(9\nu X_2 - \frac{15}{4}\nu^2\right)(\boldsymbol{n}\cdot\boldsymbol{\chi}_2)^2 + \left(6\nu + \frac{9}{2}\nu^2\right)(\boldsymbol{n}\cdot\boldsymbol{\chi}_1)(\boldsymbol{n}\cdot\boldsymbol{\chi}_2). \tag{6.73}$$

Note again the remarkable fact, found above, Eq. (6.62), that the coefficients of $B^Q_{n\chi}$ coincide with the coefficients of B^Q_χ (i.e. $B^Q_{n\chi}$ is obtained from B^Q_χ simply by replacing $(\boldsymbol{\chi}_i\cdot\boldsymbol{\chi}_j)\to(\boldsymbol{n}\cdot\boldsymbol{\chi}_i)(\boldsymbol{n}\cdot\boldsymbol{\chi}_j)$).

6.2.5 Resummation options

We wish to discuss now various options for incorporating the NLO spin-spin contributions $r^{-4}\left(A^Q_\chi - A^Q_{n\chi}\right)$, $-r^{-3}B^Q_{n\chi}$ and $r^{-3}B^Q_\chi$ in a somewhat resummed manner, within the ν-deformed Kerr-like basic contributions $A^{\nu K_0}$, $B_p^{\nu K_0}$ and $B_{np}^{\nu K_0}$. Let us first consider the contributions $\propto A^Q_{n\chi}$ and $B^Q_{n\chi}$, which are quadratic in $(\boldsymbol{n}\cdot\boldsymbol{\chi}_i)$. The presence in $A^{\nu K_0}$, Eq. (6.21), of a factor $1+(\boldsymbol{n}\cdot\boldsymbol{\chi}_0)^2/r^2$ and in $B_p^{\nu K_0}$, Eq. (6.25), of a factor $\left(1+(\boldsymbol{n}\cdot\boldsymbol{\chi}_0)^2/r^2\right)^{-1}$ suggests to incorporate the quadratic forms $r^{-4}A^Q_{n\chi}$ and $r^{-3}B^Q_{n\chi}$ as additive modifications of the term $r^{-2}(\boldsymbol{n}\cdot\boldsymbol{\chi}_0)^2$. This leads to the forms

$$A(\boldsymbol{r},\nu,\boldsymbol{\chi}_1,\boldsymbol{\chi}_2) \equiv A^{\rm eq}(r_c,\nu,(\boldsymbol{\chi}_i\cdot\boldsymbol{\chi}_j))\frac{1+\frac{(\boldsymbol{n}\cdot\boldsymbol{\chi}_0)^2}{r^2}-\frac{A^Q_{n\chi}}{r^4}}{1+\frac{\Delta(\boldsymbol{n}\cdot\boldsymbol{\chi}_0)^2}{r^2r_c^2}}, \tag{6.74}$$

and

$$B_p(\boldsymbol{r},\nu,\boldsymbol{\chi}_1,\boldsymbol{\chi}_2) \equiv \frac{1}{1+\frac{(\boldsymbol{n}\cdot\boldsymbol{\chi}_0)^2}{r^2}+\frac{B^Q_{n\chi}}{r^3}}. \tag{6.75}$$

We recall that, in this work, the centrifugal radius is defined as

$$r_c = \sqrt{r^2+\boldsymbol{\chi}_0^2+\frac{2\boldsymbol{\chi}_0^2}{r}}. \tag{6.76}$$

In Eq. (6.74) we have introduced the notation $A^{\rm eq}(r_c,\nu,(\boldsymbol{\chi}_i\cdot\boldsymbol{\chi}_j))$ for an equatorial potential (remaining in the limit $(\boldsymbol{n}\cdot\boldsymbol{\chi}_i)\to 0$) which should incorporate, in a combined manner, both the Kerr-like equatorial potential (6.22) and the purely radial NLO spin-spin correction $r^{-4}A^Q_\chi$. There are two main possibilities for doing so:

i) A full factorization

$$A^{\rm eq}(r_c,\nu,(\boldsymbol{\chi}_i\cdot\boldsymbol{\chi}_j)) \equiv A_{\rm orb}(r_c,\nu)\frac{1+\frac{2}{r_c}}{1+\frac{2}{r}}\left(1+\frac{A^Q_\chi}{r_c^4}\right). \tag{6.77}$$

ii) A semi-additive inclusion

$$A^{\rm eq}(r_c,\nu,(\boldsymbol{\chi}_i\cdot\boldsymbol{\chi}_j)) \equiv A_{\rm orb}(r_c,\nu)\frac{1+\frac{2}{r_c}+\frac{A^Q_\chi}{r_c^4}}{1+\frac{2}{r}}. \tag{6.78}$$

Here, $A_{\rm orb}(r_c,\nu)$ denotes the Padé-resummed orbital potential (6.23), which entered the Kerr-like equatorial potential (6.22). Note that the option ii) is equivalent to replacing the factor $1+A^Q_\chi/r_c^4$ of option i) by $1+A^Q_\chi/(r_c^4+2r_c^3)$. As a consequence, the second option reduces the effect of A^Q_χ compared to the first option. In addition, let us recall that the factor $(1+2/r_c)/(1+2/r)$ in $A^{\rm eq}(r_c)$ is smaller than 1 and embodies the attractive nature of the extra coupling linked to the combined effect of the quadrupole deformations and of the spin(1)-spin(2) interaction

$$\frac{1+\frac{2}{r_c}}{1+\frac{2}{r}} \approx 1-\frac{\boldsymbol{\chi}_0^2}{r_c^3}+... \tag{6.79}$$

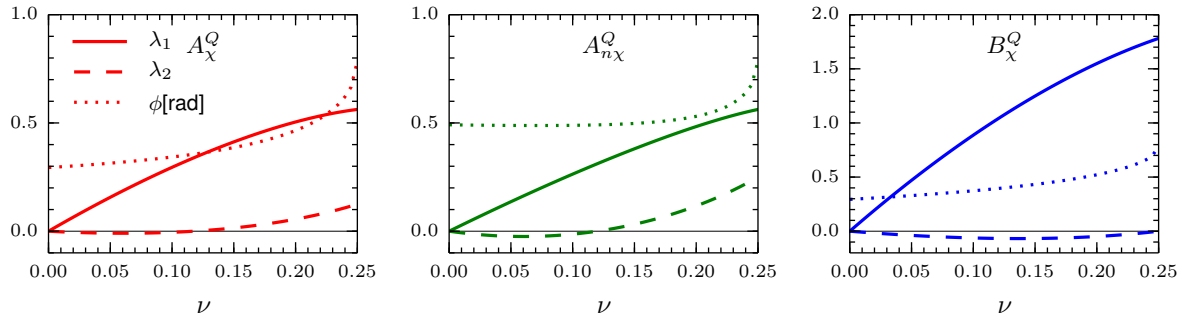

Figure 6.1: *The eigenvalues λ_1, λ_2 and the rotation angle ϕ are plotted as a function of ν for the quadratic forms A^Q_χ, $A^Q_{n\chi}$ and B^Q_χ. The information relative to the form $B^Q_{n\chi}$ is equivalent to the one provided by the plot of B^Q_χ. Notice that $\phi(1/4) = \pi/4 \approx 0.79$ for all forms.*

We then see that the main effect, for equatorial orbits, of NLO spin-spin effects is to reduce the attractive character of the LO spin-spin coupling by adding a *repulsive* coupling $\propto +A^Q_\chi/r^4$. [We will see in the next subsection that, in most cases, A^Q_χ is positive.]

Alternative versions ib) and iib) of the above options can be obtained by using the Boyer-Lindquist radius instead of the centrifugal one, thus substituting A^Q_χ/r_c^4 with A^Q_χ/r^4. Among these four options, we choose in the following the semi-additive inclusion ii), given by Eq. (6.78), as our standard one.

Let us finally consider various ways of incorporating the correction $r^{-3}B^Q_\chi$ in the Kerr-like basic potential $B^{\nu K_0}_{np}$, Eq. (6.26). A simple way is to modify the fraction r_c^2/r^2 as it appears in Eq. (6.26). We choose here to do it by defining

$$B_{np} \equiv \frac{1}{1+\frac{(\boldsymbol{n}\cdot\boldsymbol{\chi}_0)^2}{r^2}} \left(\frac{A^{\rm eq}_B(r_c)}{D_{\rm orb}} \frac{r_c^2 + \frac{B^Q_\chi}{r}}{r^2} - 1 \right), \tag{6.80}$$

where we used a "bare" version $A^{\rm eq}_B(r_c)$ of the equatorial radial potential (i.e., a version which does not contain the insertion of A^Q_χ), namely

$$A^{\rm eq}_B(r_c,\nu,a_0) \equiv A_{\rm orb}(r_c,\nu) \frac{1+\frac{2M}{r_c}}{1+\frac{2M}{r}}. \tag{6.81}$$

6.2.6 The quadratic forms

To have a feeling for the physical effects of the various NLO spin-spin quadratic forms A^Q_χ, $A^Q_{n\chi}$, B^Q_χ entering our results, we investigate here their magnitudes and their signs as functions of the two spins. The structure of each of the three quadratic forms A^Q_χ, $A^Q_{n\chi}$, B^Q_χ is described by a *symmetric* 2×2 matrix, say q_{ij}. Let us first mention that all the matrix elements q_{ij} happen to be positive (which does not, however, imply the positive-definite character of the corresponding quadratic form). By considering the (orthogonal) eigendirections and the eigenvalues of q_{ij}, we see that, in the case of a form of the type

$$Q(\boldsymbol{\chi}_1,\boldsymbol{\chi}_2) = q_{ij}(\boldsymbol{\chi}_i\cdot\boldsymbol{\chi}_j), \tag{6.82}$$

there must be an angle $\phi \in [-\frac{\pi}{2}, \frac{\pi}{2})$ such that

$$Q = \lambda_1 \left(\boldsymbol{\chi}_1 \cos\phi + \boldsymbol{\chi}_2 \sin\phi\right)^2 + \lambda_2 \left(-\boldsymbol{\chi}_1 \sin\phi + \boldsymbol{\chi}_2 \cos\phi\right)^2 \tag{6.83}$$

(and analogously for a form of the type $q_{ij}(\boldsymbol{n}\cdot\boldsymbol{\chi}_i)(\boldsymbol{n}\cdot\boldsymbol{\chi}_j)$). Here, for definiteness, λ_1 denotes the larger eigenvalue, i.e. $\lambda_1 \geq \lambda_2$. When $\nu = 1/4$, because of the symmetry under exchange of the spins $\boldsymbol{\chi}_1$ and $\boldsymbol{\chi}_2$, the only allowed combinations are $\cos\phi = \pm\sin\phi$, thus $\phi(\nu = 1/4) = \pm\pi/4$ in the interval $[-\pi/2, \pi/2)$. By contrast, the behavior of ϕ in the test-mass limit $\nu \to 0$ does not follow a general rule.

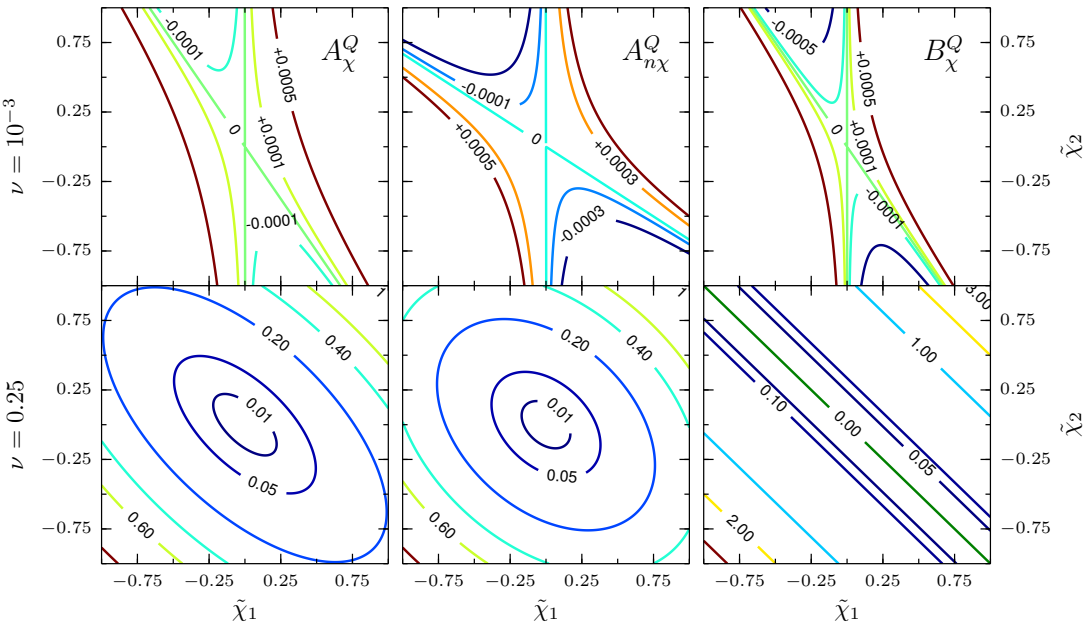

Figure 6.2: *Contour plots of A^Q_χ, $A^Q_{n\chi}$ and B^Q_χ, each quadratic form corresponding to a column. The two rows correspond to the values $\nu = 10^{-3}$ and $\nu = 0.25$ for which the forms are evaluated. In the case of A^Q_χ and B^Q_χ, aligned or anti-aligned spins are assumed, and the scalar parameters $\tilde{\chi}_i$ have to be interpreted as $\tilde{\chi}_i \equiv \pm|\boldsymbol{\chi}_i|$, with $\tilde{\chi}_1\tilde{\chi}_2 = (\boldsymbol{\chi}_1 \cdot \boldsymbol{\chi}_2)$. On the other hand, $\tilde{\chi}_i \equiv (\boldsymbol{n}\cdot\boldsymbol{\chi}_i)$ in the contour plots of $A^Q_{n\chi}$. The figures appear to be inclined with respect to a configuration symmetric under reflection of the coordinate axes. The measure of such a rotation (in the anti-clockwise direction) is nothing but the angle ϕ introduced in Eq. (6.83) and plotted in Figure 6.1.*

As shown in Figure 6.1, the eigenvalues λ_1, λ_2 of the EOB quadratic forms A^Q_χ, $A^Q_{n\chi}$ (and therefore the forms themselves) are positive in most of the range of interest. For sufficiently small ν, the smaller eigenvalues λ_2 are negative, and the forms are indefinite. On the other hand, for larger values of ν, A^Q_χ and $A^Q_{n\chi}$ are both positive definite.

More specifically, the eigenvalues of A^Q_χ are given by

$$\lambda_{1,2} = \frac{\nu}{2}\left(3 - \nu \pm \sqrt{13 - 40\nu + \nu^2}\right), \tag{6.84}$$

with λ_2 crossing zero at $\nu_0 = 2/17 \approx 0.12$, which corresponds to a mass ratio $m_1/m_2 \approx 6.34$. For circular, equatorial orbits, $\nu > \nu_0$ implies that the new NLO spin-spin terms are always repulsive.

By contrast, for $\nu < \nu_0$ there are special configurations of the spins where their effect is slightly attractive.

The smallest eigenvalue of $A^Q_{n\chi}$ crosses zero when $\nu = (13 - \sqrt{145})/8 \approx 0.12$. By contrast with A^Q_χ and $A^Q_{n\chi}$, B^Q_χ is never positive definite. However, its largest eigenvalue is always positive, and, most of the time, much larger than λ_2. As we shall see later, this implies that B^Q_χ is positive for most spin configurations. Note also that B^Q_χ becomes degenerate ($\lambda_2 = 0$) exactly in the case of equal masses ($\nu = 1/4$).

In the two-dimensional parameter space measuring either the projected spins ($\boldsymbol{n}\cdot\boldsymbol{\chi}_i$), or the algebraic magnitudes of two parallel spins $\boldsymbol{\chi}_1 \parallel \boldsymbol{\chi}_2$, the contour lines of Q define ellipses, hyperbolas or straight lines, depending on whether λ_2 is positive, negative or equal to zero, respectively. A graphical visualization of them is given in Figure 6.2.

The eigenvalue decomposition (6.83) does not provide a direct handle on the extremal points of the quadratic forms. In order to investigate them, one must resort to other arguments. Since all coefficients in Eqs. (6.70)-(6.72) are positive for every $\nu \in (0, 1/4]$, it is clear that the global maxima $Q^{\max}(\nu)$ are reached when $\boldsymbol{\chi}_1^2 = \boldsymbol{\chi}_2^2 = (\boldsymbol{\chi}_1\cdot\boldsymbol{\chi}_2) = 1$, or $(\boldsymbol{n}\cdot\boldsymbol{\chi}_1) = (\boldsymbol{n}\cdot\boldsymbol{\chi}_2) = 1$, respectively.

For investigating the minima, let us rewrite

$$Q(\boldsymbol{\chi}_1, \boldsymbol{\chi}_2) = q_{11}\left(\boldsymbol{\chi}_1 + \frac{q_{12}}{q_{11}}\boldsymbol{\chi}_2\right)^2 + \left(q_{22} - \frac{q_{12}^2}{q_{11}}\right)\boldsymbol{\chi}_2^2. \tag{6.85}$$

If $\lambda_2 < 0$, then also $\left(q_{22} - q_{12}^2/q_{11}\right) < 0$. In this case, provided that $q_{12}/q_{11} \leq 1$ (which is indeed true for all quadratic forms (6.70)-(6.72)), the global minimum $Q^{\min}(\nu)$ is reached for the anti-aligned configuration

$$\boldsymbol{\chi}_1 = -\frac{q_{12}}{q_{11}}\boldsymbol{\chi}_2 \text{ , and } \boldsymbol{\chi}_2^2 = 1. \tag{6.86}$$

Otherwise, if $\lambda_2 \geq 0$, the minimum is met in the trivial case $\boldsymbol{\chi}_1 = \boldsymbol{\chi}_2 = 0$. Analogous spin configurations, obtained substituting $\boldsymbol{\chi}_i$ with $(\boldsymbol{n}\cdot\boldsymbol{\chi}_i)$ in Eq. (6.86), define the minima of the forms of the type $q_{ij}(\boldsymbol{n}\cdot\boldsymbol{\chi}_i)(\boldsymbol{n}\cdot\boldsymbol{\chi}_j)$. As a consequence, the extremal values of B^Q_χ and of $B^Q_{n\chi}$ coincide.

Figure 6.3 provides a complete information about the range of values that can be taken by each quadratic form. Let us remark, in passing, a peculiar feature: although the coefficients of A^Q_χ and of $A^Q_{n\chi}$ could have seemed to be unrelated, they satisfy the identity

$$\sum_{ij} a^\chi_{ij} = \sum_{ij} a^{n\chi}_{ij} = (5 - 2\nu)\,\nu. \tag{6.87}$$

Consequently, as is visible on the figure, the maximal curves $A^{Q,\max}_\chi(\nu)$ and $A^{Q,\max}_{n\chi}(\nu)$ are exactly the same. Among the whole range of ν, their overall maximum is given by $A^{Q,\max}_\chi(1/4) = A^{Q,\max}_{n\chi}(1/4) = 9/8$. The overall minimum of A^Q_χ is approximately equal to -0.011 and is reached at $\nu \approx 0.061$, while for $A^Q_{n\chi}$ it is reached at $\nu \approx 0.059$ and is nearly equal to -0.033. Moreover, $B^{Q,\max}_\chi(1/4) = 57/16$, while the overall minimum $B^{Q,\min}_\chi \approx -0.083$ corresponds to $\nu \approx 0.146$.

An order-of-magnitude estimate of the maximal change introduced in $A^{\rm eq}$ by A^Q_χ (see Eq. (6.78)) can be made by setting $r_c \sim 2$ and $A^{Q,\max}_\chi \sim 0.6$, leading to a deviation of $+0.04$ with respect to the LO term $2/r_c \sim 1$. By contrast, the change in the special configurations where A^Q_χ is negative is smaller (in absolute value) than 10^{-3} , since in this case $A^{Q,\min}_\chi \sim -1/100$.

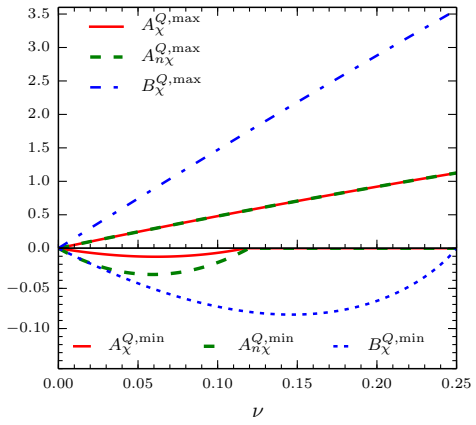

Figure 6.3: *The curves $Q^{max}(\nu)$ and $Q^{min}(\nu)$ are plotted for the quadratic forms A_χ^Q, $A_{n\chi}^Q$ and B_χ^Q. The region between the two curves represents all possible values that can be taken by the corresponding quadratic form.*

6.3 The spin-orbit sector and the last stable circular orbit

In this last section, we investigate some predictions of the new EOB Hamiltonian proposed here concerning the characteristics of the last stable circular orbit (LSO), considered for parallel spins, and circular, equatorial orbits.

At first, it is necessary to fix the spin-orbit sector $H_{\rm so}^{\rm eff}$, that enters the whole effective Hamiltonian as an additive contribution

$$\hat{H}^{\rm eff} = \hat{H}^{\rm eff}_{\rm orb} + \hat{H}^{\rm eff}_{\rm so}. \tag{6.88}$$

Several different versions of the EOB spin-orbit effective coupling $\hat{H}^{\rm eff}_{\rm so}$ have been proposed in the literature [64, 68–70, 74, 75, 77, 81]. Here we shall follow the recent approach [81], generalizing it to the general, non-equatorial case. Explicitly, we take

$$\hat{H}^{\rm eff}_{\rm so} = \frac{1}{r\, r_c^2}\left(1+\frac{\Delta(\boldsymbol{n}\cdot\boldsymbol{\chi}_0)^2}{r^2\, r_c^2}\right)^{-1} g_S^{\rm eff}\boldsymbol{l}\cdot\boldsymbol{\chi} + \frac{1}{r_c^3} g_{S^*}^{\rm eff}\boldsymbol{l}\cdot\boldsymbol{\chi}^*. \tag{6.89}$$

Here, $\boldsymbol{l}\equiv\boldsymbol{r}\times\boldsymbol{p}\equiv\boldsymbol{L}/(\mu M)$ is the (dimensionless) rescaled orbital angular momentum, and $\boldsymbol{\chi}$ and $\boldsymbol{\chi}^*$ are the symmetric spin combinations (6.13)-(6.14), namely

$$\boldsymbol{\chi} \equiv \frac{\boldsymbol{S}_1+\boldsymbol{S}_2}{(m_1+m_2)^2} = X_1^2\boldsymbol{\chi}_1 + X_2^2\boldsymbol{\chi}_2 \tag{6.90}$$

$$\boldsymbol{\chi}^* \equiv \frac{\frac{m_2}{m_1}\boldsymbol{S}_1+\frac{m_1}{m_2}\boldsymbol{S}_2}{(m_1+m_2)^2} = \nu\,(\boldsymbol{\chi}_1+\boldsymbol{\chi}_2), \tag{6.91}$$

while $g_S^{\rm eff}$ and $g_{S^*}^{\rm eff}$ are two dimensionless gyro-gravitomagnetic factors[9]. The post-Newtonian expansions of $g_S^{\rm eff}$ and $g_{S^*}^{\rm eff}$ are fully known up to NNLO order [64, 68, 70, 77], and one knows both the test-mass limit of $g_{S^*}^{\rm eff}$ [75] and its first gravitational self-force correction [114].

[9]The gyro-gravitomagnetic factors $g_S^{\rm eff}$ and $g_{S_*}^{\rm eff}$ used here correspond to $2\,\hat{G}_S$ and $\frac{3}{2}\,\hat{G}_{S^*}$ in Ref. [81].

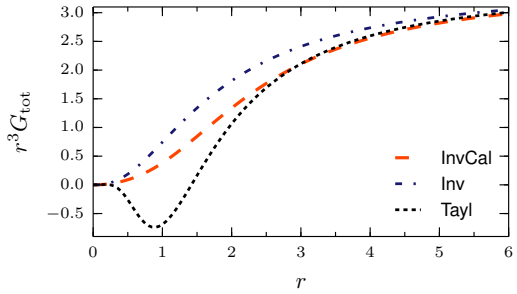

Figure 6.1: *The quantity $r^3 G_{tot}$ is plotted against r for circular orbits. Equal masses and equal spins $\chi_1 \equiv \chi_2 \equiv 0.65$ are assumed. The curve InvCal corresponds to the model described in Ref. [81], with the NNNLO calibration of c_3 described in Ref. [92]. The curve Inv makes use of the same (inverse) resummation of InvCal, but only includes terms up to NNLO (i.e., it does neither contain the calibrated term c_3, nor the two purely Schwarzschild, spinning-particle coefficients that enter into c^*_{30} and c^*_{40}, see Eqs. (46), (53), (54) in Ref. [81]). Finally, Tayl expands the gyro-gravitomagnetic factors of Inv in a Taylor series. In other words, Tayl is built with the factors g_S^{eff} and $g_{S^*}^{eff}$ as given by Ref. [64], but with r_c^{DN14} (the centrifugal radius defined in Ref. [81]) instead of the Boyer-Lindquist-like radius r. The usage of r_c^{DN14} for Tayl has the only goal of allowing a more straightforward comparison against Inv and InvCal.*

Here, we shall use, as fiducial spin-orbit coupling, the non-resummed, Taylor-expanded NNLO-accurate expansions of $g_S^{\rm eff}$ and $g_{S^*}^{\rm eff}$ [64, 77], expressed in the Damour-Jaranowski-Schäfer gauge, and (following Ref. [81]) using r_c as radial variable. This means that we use

$$g_S^{\rm eff} = 2 - \frac{27}{8}\nu(\boldsymbol{n}\cdot\boldsymbol{p})^2 - \frac{5\nu}{8}\frac{1}{r_c} + \frac{5}{8}\nu(1+7\nu)(\boldsymbol{n}\cdot\boldsymbol{p})^4 + \left(-\frac{21}{2}\nu + \frac{23}{8}\nu^2\right)\frac{(\boldsymbol{n}\cdot\boldsymbol{p})^2}{r_c} - \left(\frac{51}{4}\nu + \frac{\nu^2}{8}\right)\frac{1}{r_c^2} \tag{6.92}$$

$$g_{S^*}^{\rm eff} = \frac{3}{2} - \left(\frac{9}{4}\nu + \frac{15}{8}\right)(\boldsymbol{n}\cdot\boldsymbol{p})^2 - \left(\frac{9}{8} + \frac{3}{4}\nu\right)\frac{1}{r_c} + \left(\frac{35}{16} + \frac{5}{2}\nu + \frac{45}{16}\nu^2\right)(\boldsymbol{n}\cdot\boldsymbol{p})^4 + \left(\frac{69}{16} - \frac{9}{4}\nu + \frac{57}{16}\nu^2\right)\frac{(\boldsymbol{n}\cdot\boldsymbol{p})^2}{r_c} - \left(\frac{27}{16} + \frac{39}{4}\nu + \frac{3}{16}\nu^2\right)\frac{1}{r_c^2}. \tag{6.93}$$

We are aware of the fact that such Taylor-expanded gyro-gravitomagnetic factors have the property of changing sign in the strong-field region, thereby turning the repulsive (for spins parallel to the orbital angular momentum) spin-orbit interaction into an attractive coupling. In order to avoid this change of sign, Ref. [81] used an *inverse* Taylor resummation of the gyro-gravitomagnetic factors (of the type $g_s^{\rm eff} = 2/(1 + \frac{\tilde{c}_1}{r_c} + ...)$ etc.).

We compare in Fig 6.1 the radial behavior of the total dimensionless effective gyro-gravitomagnetic factors $r^3 G_{\rm tot} \equiv r^3\left(\frac{1}{r\,r_c^2} g_S^{\rm eff} + \frac{1}{r_c^3} g_{S^*}^{\rm eff}\right)$ defined by using either Taylor-expanded $g_S^{\rm eff}$, $g_{S^*}^{\rm eff}$ or inverse Taylor-expanded ones. As the main purpose of this subsection is to compare the effect of our new way to incorporate NLO spin-spin coupling to previous suggestions [92, 115, 138], it will be convenient for us to use the simple Taylor-expanded prescriptions (6.92)-(6.93) because they ensure the existence of an LSO for arbitrary values of the spins. By contrast, when using inverse-resummed gyro-gravitomagnetic factors the constantly repulsive character of the spin-orbit interaction allows (for large, parallel spins) the sequence of circular orbits to continue existing as the angular momentum decreases, without encountering a loss of stability at some radius.

This is illustrated in Fig 6.2 which displays the effective Hamiltonian as a function of radius, for parallel spins equal to $\chi_1 = \chi_2 = 0.65$, and for three different values of the orbital angular

momentum: $l = 2.7$ (left panel), $l = 2.55$ (central panel) and $l = 2.4$ (right panel). This figure contrasts models which exhibit an LSO for large spins (such as tar14 [90] and models using Taylor-expanded gyro-gravitomagnetic factors, such as our present model, Eq. (6.78), or a version of nag15 [92] in which $g_S^{\rm eff}$ and $g_{S^*}^{\rm eff}$ are replaced by their Taylor-expanded form) with models that do not, because there exists a continuous sequence of shrinking circular orbits of smaller and smaller radii (such as nag15 [92]). In particular, it is instructive to compare in Fig 6.2 the three different versions of the model nag15: (i) the version nag15_TaylSO (with Taylor-expanded $g_S^{\rm eff}$ and $g_{S^*}^{\rm eff}$) has an LSO and is quite close to our model (Eq. (6.78)); (ii) the version nag15_NoCal (which differs from [92] by turning off the Numerical-Relativity-calibrated NNLO spin-orbit parameters) displays the strongly repulsive character of the spin-orbit coupling at small radii; and (iii) the original model nag15, which contains extra spin-orbit parameters having the property of reducing (without cancelling) the strongly repulsive character of the spin-orbit coupling.

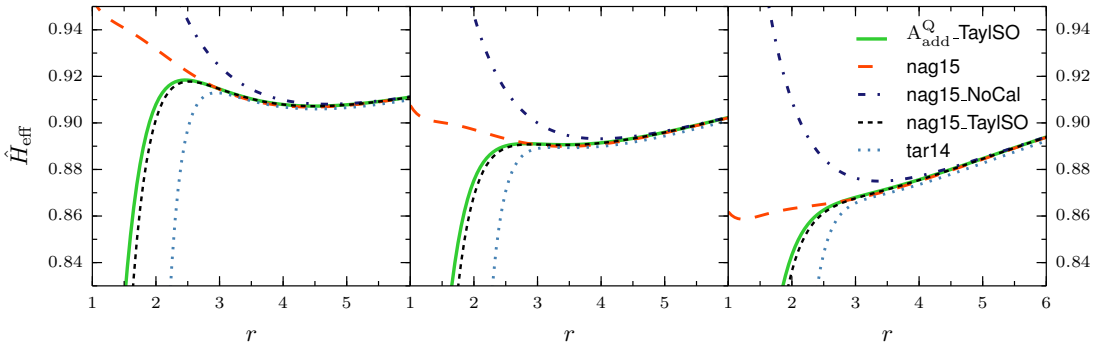

Figure 6.2: *The effective Hamiltonian is plotted as a function of r for circular, equatorial orbits, for parallel spins equal to $\chi_1 = \chi_2 = 0.65$, and for three different values of the orbital angular momentum: $l = 2.7$ (left panel), $l = 2.55$ (central panel) and $l = 2.4$ (right panel). The curves tar14 and nag15 denote the calibrated Hamiltonians of Ref. [90] and of Ref. [92], respectively (see the discussion about Fig 6.3 for some more details); nag15_NoCal is obtained from nag15 setting to zero the spin-orbit calibration, as well as the two purely Schwarzschild, spinning-particle coefficients that enter into c^*_{30} and c^*_{40}, see Eqs. (46), (53), (54) in Ref. [81]. Moreover, nag15_TaylSO is obtained from nag15_NoCal by Taylor-expanding its (NNLO) gyro-gravitomagnetic factors. Notice that the spin-orbit sector of nag15, nag15_NoCal and nag15_TaylSO exactly corresponds to the curves InvCal, Inv and Tayl of Fig 6.1, respectively. Finally, A^{Q}_{add}_TaylSO corresponds to the spin-spin model developed in this paper, with a Taylor expanded NNLO spin-orbit sector, and with the same purely orbital terms of nag15.*

As a consequence, the effective potential of nag15 exhibits (especially for $l = 2.4$) a small "bump", as if the system would still be trying to develop an LSO. After this pseudo-LSO, the system rolls down to a further stable minimum, whose existence is ensured by the strong positive spin-orbit barrier. For sufficiently large spins, the bump ceases to show up, leading therefore to a continuous sequence of circular orbits. In that case, as for the uncalibrated curve nag15_NoCal in Fig 6.2, the strength of the spin-orbit barrier is such as to completely absorb the region where the LSO would have formed.

The top panels of Fig 6.3 display a plot of the dimensionless Kerr parameter of the binary system

$$\chi_J \equiv \frac{1}{\nu}\frac{j_{\rm tot}}{\hat{H}^2_{\rm EOB}}, \tag{6.94}$$

evaluated at the LSO, where

$$j_{\rm tot} \equiv l + \frac{m_1}{m_2}\chi_1 + \frac{m_2}{m_1}\chi_2 \tag{6.95}$$

is the dimensionless total angular momentum.

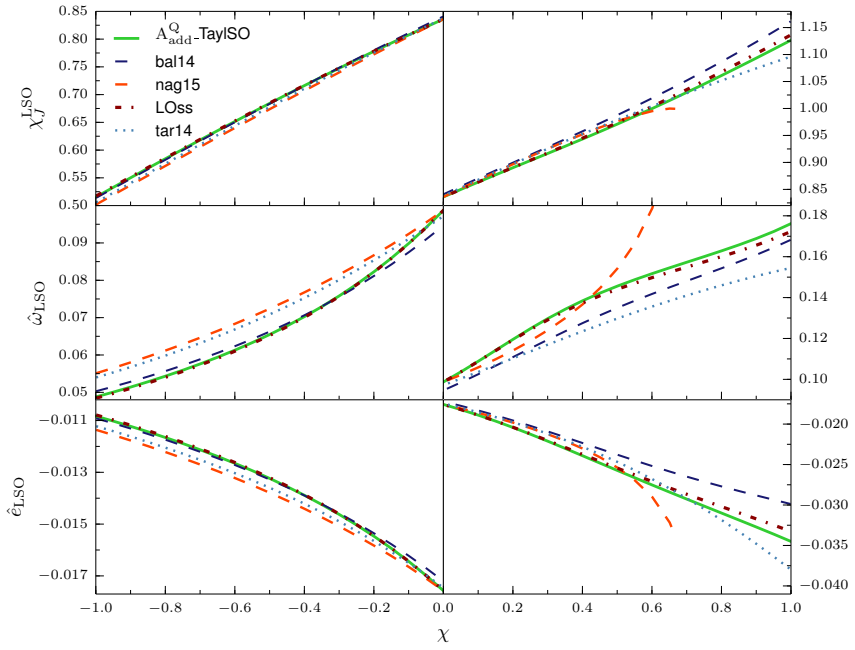

Figure 6.3: *Gauge invariant quantities (top panels: dimensionless total Kerr parameter χ_J; central panels: dimensionless orbital frequency $\hat{\omega}$; bottom panels: dimensionless binding energy $\hat{e}$) at the LSO are plotted as a function of the spin $\chi \equiv \chi_1 \equiv \chi_2$. Equal masses are assumed.*

If it were measured after the whole merger-ringdown process, χ_J would correspond to the dimensionless spin of the final black hole, and would therefore be expected to stay always smaller than one. At the LSO, however, the system still has to radiate away energy and angular momentum. It is therefore not worrying to find values $\chi_J^{\rm LSO}$ that (slightly) exceed 1 for large spins $\chi \gtrsim 0.6$.

The central panels plot the dimensionless angular frequency

$$\hat{\omega} \equiv \frac{\partial}{\partial l}\hat{H}_{\rm EOB}, \tag{6.96}$$

and the bottom panels the dimensionless binding energy[10]

$$\hat{e} = \nu\,\hat{H}_{\rm EOB} - 1, \tag{6.97}$$

both evaluated at the LSO. As in Fig 6.2, nag15 denotes the calibrated Hamiltonian of Ref. [92]. We recall that, in this model, the spin orbit sector is complete up to NNLO and calibrated at the NNNLO level, together with the inclusion of two additional, purely Schwarzschild spinning-particle terms. Furthermore, the purely orbital coupling is complete at 4PN, and is calibrated at 5PN. Among all models shown in the figure, this is the only one for which the gyro-gravitomagnetic

[10]Notice that $\hat{e} = H_{\rm EOB}/M - 1$ when expressed in terms of the non-reduced EOB Hamiltonian $H_{\rm EOB}$ given by Eq. (6.1).

Table 6.1: *Dimensionless total Kerr parameter χ_J, orbital frequency ω and binding energy $\hat{e}$ at the LSO for some values of the spins. Both semi-additive (Add) and factorized (Fact) resummations of A^Q_χ are shown, together with the case where A^Q_χ is set to zero (LO).*

	χ	χ_J	$\hat{\omega}$	$\hat{e}$
LO	-1	0.5169	0.04841	-0.01078
Add		0.5154	0.04877	-0.01083
Fact		0.5148	0.04893	-0.01085
LO	0.5	0.9735	0.1441	-0.02544
Add		0.9709	0.1456	-0.02572
Fact		0.9689	0.1472	-0.02598
LO	1	1.136	0.1723	-0.03326
Add		1.127	0.1762	-0.03450
Fact		1.118	0.1812	-0.03587

factors are inversely resummed. The interruption of the nag15 curves (near $\chi \simeq 0.65$) marks the end of the region where an LSO exists. Just before reaching that point, a rather strong deviation from the Taylor-spin-orbit curves is clearly visible.

The curves labeled by $A^Q_{\rm add}$_TaylSO denote the spin-spin model developed in this paper, with Taylor expanded, NNLO, r_c-dependent gyro-gravitomagnetic factors, while the orbital order is the same as in nag15. Moreover, LOss represents the curves that are obtained from $A^Q_{\rm add}$_TaylSO by setting A^Q_χ to zero. The $A^Q_{\rm add}$_TaylSO and LOss curves are always quite close to each other. This shows that the difference introduced by the NLO spin-spin coupling is therefore rather small, and by far less important than the effects due to the type of spin-orbit resummation. The repulsive character of the NLO spin-spin terms, already remarked in Sec 6.2.6, is clearly visible on all plots. Indeed, the total Kerr parameter is smaller than in the LOss, which means that the system radiates away more angular momentum before reaching the end of the inspiral. Similarly, a larger orbital frequency and binding energy are the signs of a more bound system, and thus imply the existence of an additional repulsive effect preventing the plunge to happen too early.

For completeness, we also show the prediction of the uncalibrated NLO spin-spin Hamiltonian bal14 described in Ref. [138]. It is important to remark that bal14 differs from the model of this paper in various aspects, and in particular, it involves a different resummation of both spin-orbit and spin-spin couplings.

Finally, tar14 represents the calibrated model of Ref. [90], that encodes the NNLO spin-orbit and LO spin-spin couplings, with a calibration at the NNNLO and NLO level, respectively. The orbital order is included up to 4PN. A first aspect to be noticed is the proximity of tar14 with nag15 in the range of negative spins, that can be considered as a qualitative check of the effectiveness of two different calibrations. For positive spins, the comparison is affected by the different behavior of nag15 for what concerns the LSO.

In Table 6.1 we complement the information contained in Fig 6.3 by giving a quantitative comparison of the two different resummation options (6.77)-(6.78) of the A potential, for several values of the spin (namely -1, $+0.5$ and $+1$). The table confirms the expectation (see Sec 6.2.5) that the factorized (Fact) resummation is stronger than the semi-additive (Add) one. For example, for extremal spins, the increase in the angular frequency at the LSO due to A^Q_χ is $\simeq +2\%$ for Add, and $\simeq +5\%$ for Fact, while the binding energy increase is $\simeq +4\%$ (in agreement with the order-of-magnitude estimation done in Sec 6.2.6) and $\simeq +8\%$, respectively.

6.4 Conclusions

In this paper, we have proposed a new EOB Hamiltonian for spinning, precessing black hole binaries. Explicitly, our Hamiltonian is of the form (6.1)-(6.2), with an orbital part of the effective Hamiltonian obtained by combining Eqs. (6.63), (6.70)-(6.76), (6.77) (or (6.78)), (6.80), (6.81), and a spin-orbit part defined by combining Eqs. (6.89)-(6.93). In particular, we have included spin-spin effects at NLO accuracy by quadratic-in-spin modifications of the building blocks $A(\boldsymbol{r},\nu,\boldsymbol{a}_1,\boldsymbol{a}_2)$, $B_p(\boldsymbol{r},\nu,\boldsymbol{a}_1,\boldsymbol{a}_2)$, $B_{np}(\boldsymbol{r},\nu,\boldsymbol{a}_1,\boldsymbol{a}_2)$ that are present in the Hamiltonian as coefficients of (part of the) momentum-dependent terms. Our new approach has several simplifying features with respect to previous works. First, it maintains a momentum dependence of the squared effective orbital Hamiltonian $\left(H^{\rm eff}_{\rm orb}\right)^2$ which is no more than quadratic (for the spin-spin terms). Second, we found that it was possible to choose a spin-gauge where the most complicated NLO spin-spin couplings $\propto (\boldsymbol{p}\cdot\boldsymbol{a}_i)(\boldsymbol{p}\cdot\boldsymbol{a}_j)$ and $(\boldsymbol{n}\cdot\boldsymbol{p})(\boldsymbol{n}\cdot\boldsymbol{a}_i)(\boldsymbol{p}\cdot\boldsymbol{a}_j)$ could be absorbed in a simple Kerr-like coupling $\propto((\boldsymbol{n}\times\boldsymbol{p})\cdot\boldsymbol{a}_0)^2$, where $\boldsymbol{a}_0\equiv\boldsymbol{a}_1+\boldsymbol{a}_2$ (with $\boldsymbol{a}_1\equiv\boldsymbol{S}_1/m_1$ and $\boldsymbol{a}_2=\boldsymbol{S}_2/m_2$) denotes the spin combination describing the LO spin-spin coupling in a Kerr way. This feature should lead to a simple description of the general precessing spin (and precessing orbital angular momentum) dynamics because of the privileged role of the single basic Kerr-like vectorial spin parameter $\boldsymbol{a}_0\equiv\boldsymbol{a}_1+\boldsymbol{a}_2$.

A further tuning allowed us to impose a Damour-Jaranowski-Schäfer-type gauge, that has the useful property of confining all new spin-spin terms into the radial potential $A(\boldsymbol{r},\nu,\boldsymbol{a}_1,\boldsymbol{a}_2)$ as soon as the spins are aligned and the orbits circular. The NLO spin-spin deformation of the above mentioned sectors is then encoded into quadratic-in-spin forms A^Q_χ, $A^Q_{n\chi}$, B^Q_χ and $B^Q_{n\chi}$, see Eq. (6.70)-(6.73), which are our main results. A remarkable fact is that the coefficients of B^Q_χ and of $B^Q_{n\chi}$ are exactly the same. Therefore, the 25 independent coefficients that define the NLO spin-spin Hamiltonian in ADM coordinates shrink down to only 9 in the EOB description. A further, minor symmetry property lies in the fact that the *sum* of all the coefficients of A^Q_χ and of $A^Q_{n\chi}$ are equal. These features correspond to a notable improvement with respect to the model developed in Ref. [138], where the momentum structure of spin-dependent terms is by far less simple (for instance, the squared effective orbital Hamiltonian of Ref. [138] does not show a polynomial dependence on the momenta, and furthermore no Damour-Jaranowski-Schäfer-type gauge could be imposed) and where the number of independent NLO spin-spin coefficients to be inserted in the EOB description amounts to 12.

The quadratic forms we have found here have positive coefficients only. However, as quadratic forms, they are either indefinite (with a positive eigenvalue and a negative one), degenerate (with one eigenvalue being strictly positive and the other zero) or positive definite, depending on the value of the symmetric mass ratio ν. For sufficiently low ν, the smaller eigenvalue is negative, and the form is negative-valued for particular configurations of anti-aligned, or nearly anti-aligned spins. By contrast, aligned configurations always lead to positive values, that are moreover much larger (by a factor $\sim$ 50-100) than the negative minima. For what concerns circular, equatorial orbits, one can conclude that the NLO spin-spin effects are repulsive in most cases, apart from very small, attractive effects that only show up for mass ratios $m_1/m_2\geq 6.34$ and for (nearly) anti-aligned spins. This repulsive character is clearly visible when comparing the total angular momentum, angular frequency and binding energy at the LSO with the corresponding prediction of the Hamiltonian without the NLO spin-spin inclusion. We propose two different options for resumming the quadratic form A^Q_χ, a semi-additive and a factorized one. The ultimate choice of the best resummation option can only be done with a systematic comparison against Numerical Relativity simulations. We expect our new Hamiltonian, once calibrated, to mark a new step

towards an accurate description of the coalescence of two precessing, spinning black holes.

Acknowledgments

S.B. thanks IHES for hospitality during the development of the main part of this work. He is supported by the Swiss National Science Foundation.

6.5 Appendix: On the hidden "symmetry" of the NLO spin-spin coupling

We have seen in the text that the (effective) EOB Hamiltonian was exhibiting six remarkable cancellations and/or coincidences among the spin-quadratic forms describing the NLO spin-spin coupling. Namely, in our preferred gauge-fixing, these six remarkable "symmetries" amounted to the equations $(i,j=1,2)$

$$b_{ij}^{np,n\chi}\equiv 0, \qquad b_{ij}^{np,\chi}\equiv b_{ij}^{p,n\chi}. \tag{6.98}$$

These 6 symmetries, together with the appropriate use of the 10 NLO gauge parameters contained in $\hat{G}_{\rm ss}^{\rm NLO}$, has allowed us to end up with a final EOB Hamiltonian containing only 9 different coefficients to describe the NLO spin-spin sector, when starting from the ADM spin-spin Hamiltonian which contained 25 different NLO spin-spin coefficients. In this Appendix, we trace the origin of these six symmetries in the original ADM Hamiltonian. Let us denote the momentum-dependent part of a NLO spin-spin Hamiltonian as

$$\begin{aligned}\hat{H}_{\rm ss}^{\rm NLO}|_{p\text{-dep}} =& \frac{1}{r^3}\Big[\Big(c_1^{ij}\boldsymbol{p}^2+c_2^{ij}(\boldsymbol{n}\cdot\boldsymbol{p})^2\Big)(\boldsymbol{\chi}_i\cdot\boldsymbol{\chi}_j)+\Big(c_3^{ij}\boldsymbol{p}^2+c_4^{ij}(\boldsymbol{n}\cdot\boldsymbol{p})^2\Big)(\boldsymbol{n}\cdot\boldsymbol{\chi}_i)(\boldsymbol{n}\cdot\boldsymbol{\chi}_j)\\ &+c_5^{ij}(\boldsymbol{p}\cdot\boldsymbol{\chi}_i)(\boldsymbol{p}\cdot\boldsymbol{\chi}_j)+c_6^{ij}(\boldsymbol{n}\cdot\boldsymbol{p})(\boldsymbol{p}\cdot\boldsymbol{\chi}_i)(\boldsymbol{n}\cdot\boldsymbol{\chi}_j)\Big].\end{aligned} \tag{6.99}$$

Because of the variation structure described by Eq. (6.35), under a canonical transformation

$$\hat{\tilde{H}}_{\rm ss}^{\rm NLO}=\hat{H}_{\rm ss}^{\rm NLO(ADM)}+\Big\{\hat{G}_{\rm ss}^{\rm NLO},\hat{H}_{\rm N}\Big\}, \tag{6.100}$$

one can easily check that the combinations $3c_1^{ij}+c_2^{ij}$, $5c_3^{ij}+c_4^{ij}$ and $-2c_3^{ij}+3c_5^{ij}+c_6^{(ij)}$ are gauge invariant. We can further check (from the explicit expressions of the ADM coefficients) that the 6 following gauge-invariant combinations of coefficients happen to vanish:

$$3c_1^{ij}+c_2^{ij}+c_3^{ij}+\frac{c_4^{ij}}{5}=0 \tag{6.101a}$$

$$3c_1^{ij}+c_2^{ij}+c_3^{ij}-\frac{3}{2}c_5^{ij}-\frac{c_6^{(ij)}}{2}=0. \tag{6.101b}$$

One can consider that the six identities (6.101) constitute the hidden origin of the six (more manifest) relations (6.98) found in their EOB transcription. In that sense, one can say that the EOB formulation is useful in revealing, and making manifest, symmetries that existed, in a hidden way, as 6 relations between the 25 original ADM coefficients. So that, finally, there is, as expected, a conservation of linearly independent NLO spin-spin coefficients, with 9 = 25 – 10(gauge) – 6(relations).

CHAPTER 7

A few things about neutron stars

Together with small-mass coalescing black holes, neutron star (or black hole-neutron star) binaries are the most important class of coalescing objects whose gravitational radiation is expected to be measured with the currently operating network of ground-based interferometric detectors. For neutron stars, an accurate description of the two-body dynamics is therefore as crucial as it is for black holes. However, the two-body problem is made even more difficult by the non-negligible internal structure of neutron stars, which involves very complicated physics. In particular, the equation of state for matter is essentially unknown at the incredibly high densities (probably above nuclear density) that are characteristic of these type of objects. From this point of view, neutron stars are not only an excellent laboratory for general relativity, but also for nuclear physics under extreme conditions. The information carried by the gravitational wave signal emitted during coalescence might be very useful to constrain the equation of state. In particular, recent studies highlight the importance of the *late stages* of the coalescing process, where the effects linked to the internal are strongest (see e.g. [139]). As in the case of coalescing black holes, the only methods being able to provide a sufficiently accurate description of the merger of two neutron stars are, at the present time, Numerical Relativity (see [140–144] for some recent advances) and the EOB approach (see, in particular, Ref. [145]). The aim of the present chapter is to introduce some basic elements concerning the neutron star's equation of state and its description in the EOB framework. This prepares the ground for Chapter 8 (Ref. [146]) which is an application of the (spinning) EOB formalism to infer some properties of the neutron star's equation of state, and which may be considered as a kind of corollary to the present thesis.

7.0.1 Equation of state and maximal mass of degenerate matter

In the first decades of last century, the discoveries of unusual characteristics of Sirius B (which exhibited a nearly white spectrum together with a very low luminosity, that could not fit with the stellar structure models of the time), led to the first modelization of a degenerate star as a macroscopic quantum system occupying (in the ideal case) the lowest quantum level. The uncertainty principle

$$\Delta P \, \Delta R \geq \hbar \tag{7.1}$$

provides a very basical equation of state, since it allows to estimate the minimal momentum (and thus kinetic energy) density ΔP^3 that can be contained in a volume ΔR^3. Taking P as a representative average momentum of the particles (with mass m) composing the star (having mass M), an approximate balance between kinetic and potential energy may be of the type

$$E \sim \alpha_1 \frac{M}{m}\sqrt{P^2+m^2} - \alpha_2 \left(\frac{M}{m}\right)^2 P, \tag{7.2}$$

for some positive coefficients a_1 and a_2, where the linear momentum on the second term is obtained applying the uncertainty principle on the Newtonian energy $\sim -M/R_{\rm N}$, where $R_{\rm N}$ is the radius of the star. In order for the configuration to be stable, the average momentum P must of course correspond to a minimal total energy E. If $\alpha_2 M/m < \alpha_1$, a minimum is certainly reached for some $P \geq 0$, since in this case $E \to \infty$ for $P \to \infty$. With increasing M/m, also the equilibrium momentum P becomes larger, which means that the stable configuration is shifted towards the relativistic regime. As soon as $\alpha_2 M/m > \alpha_1$, however, the attractive gravitational term wins for P large enough, with a dramatic consequence: the total energy is no longer bounded by below, and gravitational collapse occur. This defines a maximal mass for degenerate stars.

In the Fermi-gas approximation, which is nothing but a more rigorous application of the above arguments, the degenerate gas composing the star is modeled with Fermi-Dirac statistics. The ground-state degenerate pressure $\mathcal{P}$ is a function of the density ρ, and is of the polytropic type $\mathcal{P} \propto \rho^{(\gamma+1)/\gamma}$, where $\gamma = 3/2$ in the non relativistic regime $P \ll m$, and $\gamma = 2$ in the relativistic regime $P \gg m$. This defines the *equation of state*. The balance between pressure and gravity is obtained, for a Newtonian gravitational field, with the hydrostatic equilibrium equation

$$\frac{d\mathcal{P}}{dR} = -\rho \frac{M(R)}{R^2}, \tag{7.3}$$

where $M(R)$ is the mass contained in a shell of radius R. In analogy with the toy model above, stability is los as soon as the relativistic regime is reached. The corresponding limiting mass is known as the Chandrasekar mass $M_{\rm Ch}$. Taking into consideration a star made of degenerate neutrons with mass $m \equiv m_N$, it is given by

$$M_{\rm Ch} \approx 3.1 \frac{M_{\rm pl}^3}{m_N^2} \approx 5.73 M_\odot. \tag{7.4}$$

where $M_{\rm pl}$ is Planck's mass. Chandrasekhar's formula is very accurate when applied to white dwarfs (that are a mixture of degenerate electrons and non-degenerate helium nuclei), in which case $M_{\rm Ch} \approx 3.1 M_\odot$. However, for neutron stars, there are two important differences, that make the Chandrasekar limit inappropriate:

i) While the gravitational field of a white dwarf only differs from a Newtonian field by a factor $\sim 10^{-6}$, neutron stars are in the relativistic strong-field regime, with compactnesses $C = M/R_{\rm NS} \sim 0.12 - 0.2$. Relativistic corrections are therefore needed.

ii) For the same reasons, the density of a neutron star is extremely high, even above nuclear density $\rho = 1.8\times 10^{14}{\rm g/cm}^3$. By contrast, the density of a white dwarf is $\sim 10^6{\rm g/cm}^3$. Therefore, also the approximation of purely gravitationally interacting particle is inaccurate. To build reliable neutron stars model, particle physics effects cannot be neglected.

A relativistic generalization of the hydrostatic equilibrium formula for the pressure $\mathcal{P}$ is given by the Tolman-Oppenheimer-Volkoff formula [147, 148]

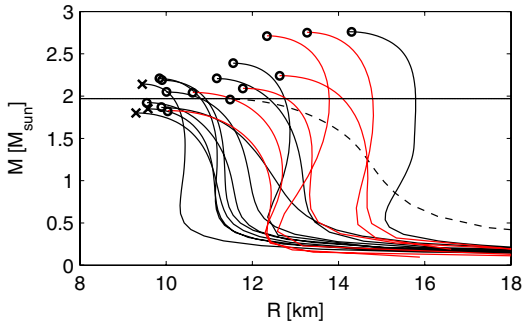

Figure 7.1: *Mass-radius relations for realistic equations of state. The figure is taken from Ref. [152].*

$$\frac{d\mathcal{P}}{dR} = -(\rho + \mathcal{P})\frac{M(R) + 4\pi\mathcal{P}R^3}{R^2\left(1 - \frac{2M(R)}{R}\right)}. \tag{7.5}$$

Being part of the relativistic stress-energy tensor, the pressure $\mathcal{P}$ contributes to the gravitational field and is subjected to it, thereby entering the right-hand-side of the equation. Moreover, notice the Schwarzschild-type correction $1 - 2M(R)/R$ to the Newtonian gravitational field. Due to the stronger gravitational attraction, the TOV formula adds instability to the star. Applying this result to a Fermi-model for degenerate neutrons, the maximal neutron star's mass reduces to

$$M_{\text{Max}} \approx 0.7 M_\odot, \tag{7.6}$$

thus 8 times smaller than the non relativistic result.

Since these early contributions, models for the equation of state have become much more complex. In particular, the internal of a neutron star is now modelled as a multi-layer structure, composed of electrons, and superfluid neutrons and protons, where nuclear interaction cannot be disregarded (as an example, see [149] for the SLy equation of state). At the present time, there remains a large uncertainty among realistic equations of state. In Fig 7.1 we show a plot of the mass-versus-radius relation for a sample of equations of state, bringing into evidence the variety of the current models. We can notice that the maximal mass is now at an intermediate value between the predictions of the (Fermi-gas) Newtonian and TOV models. The horizontal line corresponds to the observational evidence of a $\sim 2M_\odot$ neutron star [150, 151]. All equations of state predicting a lower maximal mass might therefore be discarded.

7.0.2 Tidal effects in the EOB

The main effect of the neutron star's equation of state on the two-body dynamics lies in its *tidal polarizability*. The star deforms under the influence of the inhomogeneous gravitational field of the companion, deviating from sphericity, and in turn generating a multipolar gravitational field. The electric-type polarizability coefficient μ_l (carrying the dimension of a length to the $2l+1$-th power) is a measure of the mass-multipole moment $M_{i_1,\dots,i_l}$ induced on the neutron star by an l-th order external gravitational field $G_{i_1,\dots,i_l}$, in the sense that

$$M_{i_1,\dots,i_l} = \mu_l G_{i_1,\dots,i_l}. \tag{7.7}$$

Similarly, magnetic-type polarizability coefficients measure the induced current multipole moment. However, it has been shown [153, 154] that their effect on the neutron star's dynamics is

only a small fraction ($\sim 5\%$) of the electric-type tidal effects. They will thus be neglected here. Moreover, for the sake of simplicity, we only consider Newtonian (LO) external fields. Tidal effects are described by the Lagrangian [155]

$$L_{\rm tid} = \sum_{l\geq 2} L^{\rm LO}_{\mu_l}, \tag{7.8}$$

with

$$L^{\rm LO}_{\mu_l} = \sum_{a=1,2} \frac{1}{2}\frac{\mu_l^a}{l!}\left(\frac{\partial}{\partial z_a^{i_1}}\cdots\frac{\partial}{\partial z_a^{i_l}}\frac{m_b}{|\boldsymbol{z}_a-\boldsymbol{z}_b|}\right)^2 = \sum_{a=1,2}\frac{(2l-1)!!}{2}\,\mu_l^a\,\frac{m_b^2}{R^{2l+2}}. \tag{7.9}$$

Notice that the leading-order tidal effects are as small as $\sim 1/R^6$. In the above equation $a,b=1,2$ ($a\neq b$) are labels for the two neutron stars, while $\boldsymbol{z}_a$ and $\boldsymbol{z}_b$ denote the positions of the two bodies, with $R\equiv|\boldsymbol{z}_a-\boldsymbol{z}_b|$. Introducing the (dimensionless) second Love number

$$k_l^a \equiv \frac{(2l-1)!!}{2}\,\frac{\mu_l^a}{R_a^{2l+1}}, \tag{7.10}$$

where R_a is the neutron star's individual radius, the tidal Lagrangian can be reformulated as

$$L^{\rm N}_{\mu_l} = \sum_{a=1,2} k_l^a m_b^2\left(\frac{R_a}{R}\right)^{2l+1}. \tag{7.11}$$

Ref. [156] discussed a proposal for including the tidal coupling into the EOB formalism. The EOB Hamiltonian should accordingly exhibit a tidal sector $H_{\rm EOB}|_{\rm rid} = -L_{\rm tid}$ when PN expanded. Because of the purely radial dependency of the above result, the most natural place to look at is the EOB radial potential $A(u,\nu)$. Denoting by $A^0(u,\nu)$ the usual, non-tidal effective radial potential, the EOB model developed in [156] consists of a modification

$$A(u,\nu)\equiv A^0(u,\nu)+A^{\rm tid}_{\rm LO}(u,\nu), \qquad A^{\rm tid}_{\rm LO}(u,\nu)\equiv -\sum_{l\geq 2}\kappa_l^T\,u^{2l+2}. \tag{7.12}$$

In the above equation, the radial dependence of tidal effects is expressed through the inverse dimensionless radius $u=M/R$, where we recall that $M\equiv m_1+m_2$ is the total mass of the system. On the other hand, all quantities that are intrinsic of the neutron star's equation of state are fully encoded in the *tidal coupling constants*

$$\kappa_l^T \equiv \sum_{a=1,2} 2\,k_l^a\,\frac{m_b}{m_a}\left(\frac{R_a}{M}\right)^{2l+1}. \tag{7.13}$$

Notice that Ref. [156] goes beyond the LO field, also including tidal effects of fractional 1PN order. Moreover, fractional 2PN tidal corrections are calculated in Ref. [166].

Let us remark that the equation of state does not define neither the love number k_l^a nor κ_l^T in an unique way, since also the mass of the star(s) contribute determining their value. But the fact that the dominant tidal effect is uniquely parametrized by κ_2^T allows to establish a quasi-universal relation in the dynamics: when κ_2^T is the same, also the tidal dynamics is the same, no matter what is the equation of state. Chapter 8 is devoted to a detailed discussion of this interesting property.

CHAPTER 8

Quasiuniversal properties of neutron star mergers

S. Bernuzzi, A. Nagar, S. Balmelli, T. Dietrich, M. Ujevic.

Published in Physical Review Letters, Volume **112**, *201101 (2014)*

Binary neutron star mergers are studied using nonlinear 3+1 numerical relativity simulations and the analytical effective-one-body (EOB) model. The EOB model predicts quasiuniversal relations between the mass-rescaled gravitational wave frequency and the binding energy at the moment of merger, and certain dimensionless binary tidal coupling constants depending on the stars Love numbers, compactnesses and the binary mass ratio. These relations are quasiuniversal in the sense that, for a given value of the tidal coupling constant, they depend significantly neither on the equation of state nor on the mass ratio, though they do depend on stars spins. The spin dependence is approximately linear for small spins aligned with the orbital angular momentum. The quasiuniversality is a property of the conservative dynamics; nontrivial relations emerge as the binary interaction becomes tidally dominated. This analytical prediction is qualitatively consistent with new, multi-orbit numerical relativity results for the relevant case of equal-mass irrotational binaries. Universal relations are thus expected to characterize neutron star mergers dynamics. In the context of gravitational wave astronomy, these universal relations may be used to constrain the neutron star equation of state using waveforms that model the merger accurately.

8.1 Introduction

Binary neutron star (BNS) inspirals are among the most promising sources for the advanced configurations of the ground based gravitational wave (GW) detector network [157]. Advanced configurations of LIGO and Virgo detectors are expected to listen to $\sim 0.4 - 400\ \mathrm{yr}^{-1}$ events starting from 2016-19 [126]. Direct GW observations will then probe such systems in the near future. In particular, because the late–inspiral–merger phase depends crucially on the stars internal structure, the measurement of the tidal polarizablity parameters from GWs will put the strongest constraints on the unknown nuclear equation of state (EOS) [139, 158–160].

An accurate modeling of neutron star mergers requires numerical relativity (NR). In recent years simulations have become fairly robust, but exploring the physical parameter space remains a challenge out of reach. Furthermore, the interpretation of simulation data can be nontrivial: meaningful quantities must be gauge invariant and possibly have well-defined post-Newtonian (PN) limits. The GW phasing analysis for multi-orbits (~ 10) simulations was performed by some groups, e.g. [161–163]. The BNS dynamics, expressed via the gauge-invariant relation between binding energy and angular momentum [90, 108], was recently analyzed in both the nonspinning and spinning case [122, 164]. For both observables a solid analytical framework, although approximate, is essential for extracting information from the simulations.

Despite these detailed studies, simple, and fundamental questions about the merger physics still lack of quantitative answers. For instance, a test-mass in the Schwarzschild metric of mass M has a last stable orbit (LSO) at $R_{\rm LSO} = 6M$, (we use units with $G = c = 1$) with dimensionless (or mass-reduced) orbital frequency $M\Omega_{\rm LSO}^{\rm Schw} = 6^{-3/2} \approx 0.06804$. The associated GW frequency $2M\Omega_{\rm LSO}^{\rm Schw} \approx 0.13608$ is commonly used to mark the end of the quasiadiabatic BNS inspiral, setting M equal to the total mass of the binary. Similarly, the specific LSO binding energy $E_{b\,\rm LSO}^{\rm Schw} = (8/9)^{1/2} - 1 \approx -0.0572$ is used to estimate the total amount of GW energy emitted during the coalescence process. These numbers appear ubiquitously in BNS-related studies, e.g., [160], but are, in principle, no more then an order of magnitude estimates as they neglect both finite mass ratio and finite size effects. Some questions arise: How to model/include these effects? How does the merger frequency and binding energy depend on the main parameters of the binary (EOS, mass ratio and individual spins)? How accurate are the Schwarzschild LSO estimates? In this work we use new multi-orbit NR data and the analytical effective-one-body (EOB) approach problem to put forward some answers. We find that the GW frequency and binding energy at the moment of merger are characterized only by certain dimensionless tidal coupling constants (a fact also empirically observed in [159] for the frequency) and the stars spins as a consequence of a fundamental property of the underlying conservative dynamics.

8.2 EOB and the LSO

The EOB formalism [65–68] maps the relativistic 2-body problem, with masses M_A and M_B, into the motion of an effective particle of mass $\mu = M_A M_B/M$, with $M = M_A + M_B$, moving into an effective metric. It employs standard PN results (e.g., [165]) in a *resummed* form, and it is robust and predictive also in the strong-field and fast-motion regime. The EOB model can be completed with NR information; complete (inspiral-merger-ringdown) binary black hole waveforms for GW astronomy can be produced for general mass-ratio and spin configurations [90, 91]. Tidal effects can also be included in the model [139, 156]. The EOB model consists of three building blocks: (i) a Hamiltonian $H_{\rm EOB}$; (ii) a factorized gravitational waveform; and (iii) a radiation reaction force $\mathcal{F}_\varphi$. The EOB Hamiltonian is $H_{\rm EOB} = M\sqrt{1 + 2\nu(\hat{H}_{\rm eff} - 1)}$ where, in the nonspinning case, $\hat{H}_{\rm eff}(u, p_{r_*}, p_\varphi) \equiv H_{\rm eff}/\mu = \sqrt{A(u;\nu)(1 + p_\varphi^2 u^2 + 2\nu(4-3\nu)u^2 p_{r*}^4) + p_{r*}^2}$, with $\nu \equiv \mu/M$, $u \equiv 1/r \equiv GM/Rc^2$, $p_\varphi \equiv P_\varphi/(M\mu)$ is the dimensionless orbital angular momentum and $p_{r_*} \equiv \sqrt{A/B}p_r = P_r/\mu$ is a dimensionless radial momentum, $A(u;\nu)$ and $B(u;\nu)$ are the EOB potentials. The conservative dynamics ($\mathcal{F}_\varphi = 0$) along circular orbits ($p_{r_*} = 0$) is determined only by $A(u;\nu)$. Finite-size effects are formally 5PN. They are included in $A(u;\nu)$ by adding a tidal term $A^T(u;\nu)$ to the point-mass $A^0(u;\nu)$ contribution, i.e. $A(u) \equiv A^0(u;\nu) + A^T(u;\nu)$ [156]. The $A^0(u)$ function is analytically known at 4PN accuracy and formally reads $A^0_{\rm 4PN}(u;\nu) = 1 - 2u + \nu\hat{a}_{\rm 4PN}(u;\nu)$, where $\hat{a}_{\rm 4PN}(u;\nu) \equiv a_3 u^3 + a_4 u^4 + (a_5^c(\nu) + a_5^{\ln}\ln u)u^5$ [79]. We use here *only* the 4PN-accurate an-

alytical information and we do not add any "flexibility parameter" calibrated to NR data. The Taylor-expanded function $A^0_{\rm 4PN}$ is resummed using a (1,4) Padé approximant, i.e. $A^0(u;\nu) \equiv P^1_4[A^0_{\rm 4PN}(u;\nu)]$, with the logarithmic term treated as a constant in the Padé. The tidal part of the interaction potential is known at next-to-next-to-leading order (NNLO, fractional 2PN) and reads $A^T(u) = -\sum_{\ell=2}^4 \kappa^T_\ell u^{2\ell+2}(1+\bar{\alpha}^{(\ell)}_1 u + \bar{\alpha}^{(\ell)}_2 u^2)$, with only $\bar{\alpha}^{(2),(3)}_{1,2}$ known analytically [166]. For $\ell \geq 2$, the dimensionless tidal coupling constants are [156]

$$\kappa^T_\ell \equiv 2\left[\frac{1}{q}\left(\frac{X_A}{C_A}\right)^{2\ell+1} k^A_\ell + q\left(\frac{X_B}{C_B}\right)^{2\ell+1} k^B_\ell\right], \tag{8.1}$$

where $q = M_A/M_B \geq 1$, $X_A \equiv M_A/M = q/(1+q)$, $X_B \equiv M_B/M = 1/(1+q)$, $k^{A,B}_\ell$ and $C_{A,B}$ are the dimensionless Love numbers and compactness of star A and B. All the information about the EOS is encoded in the κ^T_ℓ's. For typical compactnesses $C \sim 0.12-0.2$, $\kappa^T_2 \sim \mathcal{O}(10^2)$ and $\kappa^T_{3,4} \sim \mathcal{O}(10^3)$.

Stable circular orbits correspond to minima in u of $\hat{H}_{\rm eff}$ for a given value of p_φ. For any u, the condition $\hat{H}_{\rm eff}(u)' = 0$ yields $j^2(u) = -A'(u)/(u^2 A(u))'$ for the angular momentum along circular orbits $j \equiv p_\varphi$ ($' \equiv \partial_u$). The orbital frequency reads $M\Omega(u;\nu) = \mu^{-1}\boldsymbol{p}_j H_{\rm EOB} = j(u)A(u;\nu)u^2/(H_{\rm EOB}\hat{H}_{\rm eff})$. The end of the adiabatic (circular) dynamics is marked by the LSO, i.e., the inflection point of $\hat{H}_{\rm eff}$, that yields $(u_{\rm LSO}, j_{\rm LSO})$ and in turn the LSO orbital frequency $M\Omega_{\rm LSO}(\nu)$. The Schwarzschild LSO frequency is recovered by construction $M\Omega_{\rm LSO}(\nu=0) = M\Omega^{\rm Schw}_{\rm LSO}$. The ν-dependent, nontidal, corrections to A are globally repulsive, i.e., $M\Omega_{\rm LSO}(\nu) > M\Omega^{\rm Schw}_{\rm LSO}$ [65]. The tidal contribution A^T is, instead, always attractive, and moves $M\Omega_{\rm LSO}$ to lower frequencies. The LSO frequency results then as a balance between repulsive and attractive effects.

Spin effects are included following Ref. [68], which is robust enough for BNS realistic spin values (dimensionless magnitude $\chi_{A,B} \lesssim 0.1$). The spin-orbit interaction is taken at NNLO [64], the spin-spin at leading-order [115]. The spin gauge freedom is fixed according to [64, 70]. To have circular orbits, we only consider spins parallel (or antiparallel) to the orbital angular momentum. The LSO computation is analogous to the nonspinning case. $M\Omega_{\rm LSO}$ is larger (smaller) than the nonspinning case for parallel (antiparallel) spins, i.e., the system is less (more) bound [68, 164].

The complete nonadiabatic EOB model ($\mathcal{F}_\varphi \neq 0$) allows one to go beyond the adiabatic-circular-LSO analysis and to examine the model quantitatively with NR data. For the radiation reaction $\mathcal{F}_\varphi$ we use the tidal extension of the point-mass prescriptions of [139], and also include a radial component [1]. The point-mass dynamics is taken at 4PN in both the $A(u;\nu)$ and $\bar{D}^0(u;\nu) \equiv [A(u;\nu)B(u;\nu)]^{-1}$ functions, using in the latter linear-in-ν 4PN coefficient obtained numerically [102, 167]. Note that the formal regime of validity of the model may break when the dynamics is evaluated for $u \gtrsim u_{\rm LSO}$ since the two stars may be already in contact at those radial separations [156].

8.3 κ^T_ℓ-universal relations

We studied the dependence of $2M\Omega_{\rm LSO}$ and the binding energy per reduced mass at LSO, $E_{b\,\rm LSO} = (H_{\rm EOB} - M)/\mu$, when varying EOS, compactness, mass ratio and spin. For each EOS in a sample of 12 realistic ones, we vary the mass of each star between $1.3M_\odot$ and the maximum mass allowed, $M_{\rm max} \gtrsim 2M_\odot$. We found that both $2M\Omega_{\rm LSO}$ and $E_{b\,\rm LSO}$ are essentially independent of the choice of EOS when expressed versus any of the tidal coupling constant κ^T_ℓ. For example, Fig. 8.1 displays $2M\Omega_{\rm LSO}$ and $E_{b\,\rm LSO}$ versus the dominant coupling constant κ^T_2 for $q=1$ and no spins. From the

[1] Contrarily to [122, 161], NR-determined next-to-quasicircular corrections to the waveform and to $\mathcal{F}_\varphi$ are not included.

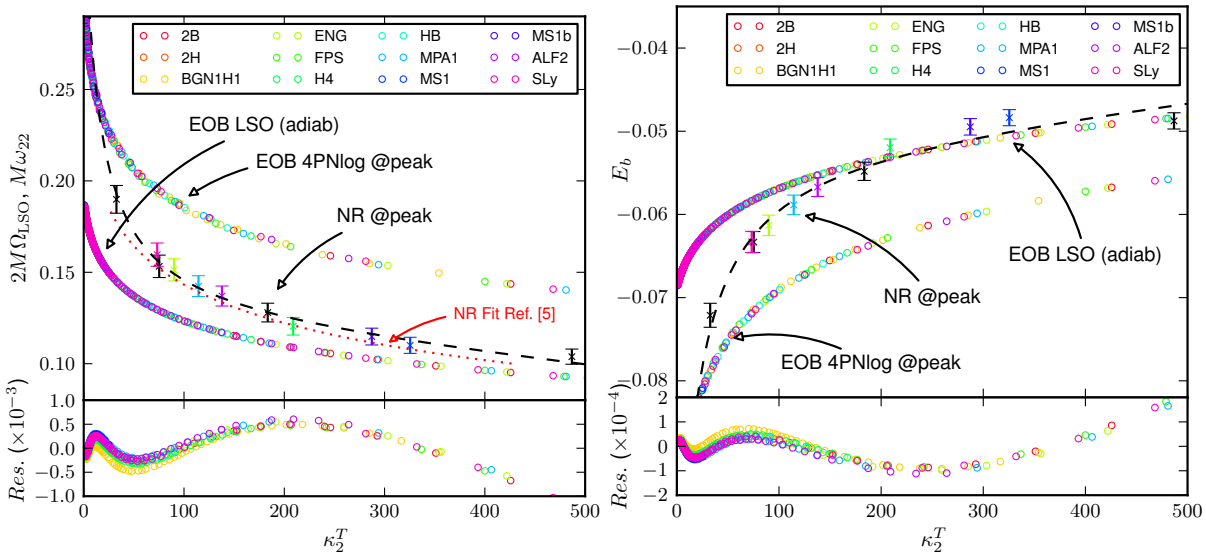

Figure 8.1: *GW frequency (left) and binding energy (right) versus the coupling constant κ_2^T for equal-masses, irrotational mergers. Main panels: Circles refer to EOB quantities computed at either the adiabatic LSO ($2M\Omega_{\rm LSO}$, $E_{b\,\rm LSO}$) or the moment of merger ($M\omega^{\rm EOB}_{22\,mrg}$, $E^{\rm EOB}_{b\,mrg}$). Different colors refer to different EOS. crosses (with error bars) refer to NR quantities at the moment of merger, ($M\omega^{\rm NR}_{22\,mrg}$, $E^{\rm NR}_{b\,mrg}$). Among these, the black crosses refer to polytropic EOS. The dashed black lines are the fits given in the text. The dotted red line in the left panel is the phenomenological fit of [159]. Bottom panels: Differences in $2M\Omega_{\rm LSO}$ and $E_{b\,\rm LSO}$ with respect the fits of the LSO data. An analogue result holds for the nonadiabatic EOB quantities at the moment of merger. The EOS dependence is negligible: all quantities (EOB LSO, 4PNlog EOB, and NR) show κ_ℓ^T-universality.*

residuals (bottom panels) one sees that deviations from universality are below the 0.2%. The same quasiuniversal behavior is found also for unequal-mass, spinning BNS. Varying $1 \leq q \leq 2$ does not lead to curves significantly different from those in Fig. 8.1, the only difference being a narrower interval of variability of κ_2^T. By contrast, the spin-orbit coupling, significantly changes the EOB LSO frequency and binding energy already at spin magnitudes $\chi \sim 0.01 - 0.1$. An example is given by Fig. 8.1, restricted to EOS ENG for clarity. The dimensionless spin value is chosen to be $\chi = \pm 0.1$. The difference between $q = 2$ and $q = 1$ curves is $\lesssim 0.5\%$. The spin dependence is linear for spins $\chi \lesssim 0.1$, as expected for the spin-orbit interaction. Note that the functional dependence $2M\Omega_{\rm LSO}(\kappa_2^T)$ (and similarly $E_{b\,\rm LSO}(\kappa_2^T)$), is algebraically complicated already for the simplest choice of the $A(u)$ function and cannot be made explicit. Both quantities can be robustly fitted to a low-order rational polynomial of the form $f(\kappa) = f(0)(1 + n_1\kappa + n_2\kappa^2)/(1 + d_1\kappa + d_2\kappa^2)$, where $f(0)$ is the point-mass LSO value $(2M\Omega_{\rm LSO}(0), E_{b\,\rm LSO}(0)) \approx (0.1892, -0.0688)$.

As merger is approached, the dynamics enters a tidally dominated regime: the values of $2M\Omega_{\rm LSO}$ and $E_{b\,\rm LSO}$ are strongly influenced by tidal effects. Close to the LSO the tidal potential $A^T(u;\nu)$ may become comparable or larger than $\nu\hat{a}(u;\nu) \equiv A^0(u;\nu) - (1 - 2u)$, that determines point-mass (ν-dependent) effects. One can see this comparing the various contributions to the "radial force" $dA/dr = -u^2\left[-2 + \nu\hat{a}'(u;\nu) + A'_T(u;\nu)\right]$. For example, at LSO (EOS SLy, $\nu = 1/4$) one has: for $C = 0.14$ and $\kappa_2^T = 274.51$, $u_{\rm LSO} \approx 0.1366$, which yield $\nu\hat{a}'(u) \approx 0.0703$ and $A'_T(u;\nu) \approx -0.1168$; for $C = 0.18$ and $\kappa_2^T = 58.52$, $u_{\rm LSO} \approx 0.1645$, which yield $\nu\hat{a}'(u) \approx 0.1127$ and $A'_T(u;\nu) \approx -0.0669$. Concerning the LSO frequency, one gets $M\Omega_{\rm LSO} = 0.0517$ for $C = 0.14$ and $M\Omega_{\rm LSO} = 0.06674$ for $C = 0.18$ [2]. The values of $M\Omega_{\rm LSO}$ and $E_{b\,\rm LSO}$ are rather close to the Schwarzschild ones,

[2] We stress that the result is qualitatively and quantitatively robust when changing the PN order of A^0 from 3PN to the 5PN (the latter employs NR-tuned flexibility parameters [91]). We observe monotonic behavior with the various PN order. The fractional difference between 5PN and 4PN is between 0.3 to 1% for $\kappa_2^T \gtrsim 50$, and up to 3% for $\kappa_2^T \in [10, 50]$.

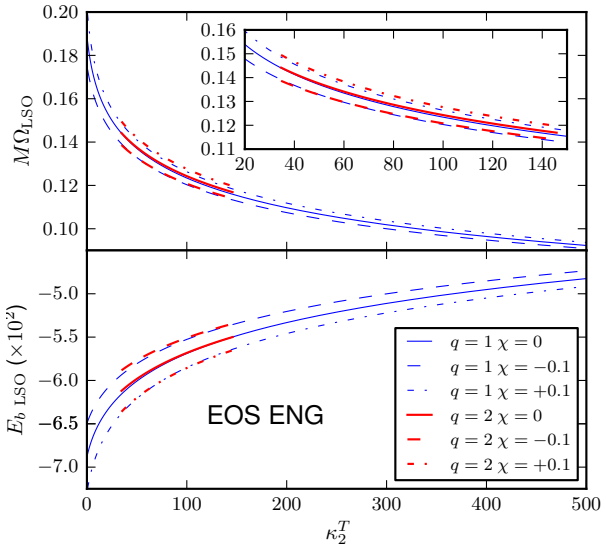

Figure 8.1: *GW frequency (top) and binding energy (bottom) versus the coupling constant κ_2^T at EOB LSO: varying mass ratio and spin magnitude. Only the ENG EOS is plotted for simplicity. The effect of mass ratio is almost negligible. The effect of spin is dominated by spin-orbit coupling.*

being the latter determined by $A(u;\nu=0)=1-2u$. The behavior is *not* a property of the LSO, but it is expected to hold also for $u>u_{\rm LSO}$, since $A^T(u)\propto u^6$; i.e. it holds during the whole merger process. By contrast, the universal curves extracted at separations larger then the LSO progressively flatten (the κ_ℓ^T-dependency weakens) and approach the degenerate point-mass case as the tidal interaction becomes negligible.

The complete nonadiabatic EOB dynamics can be continued also after the LSO crossing and the orbital frequency $M\Omega(t)$ develops a local maximum [122], likewise the point-mass case. The analytical time-domain $\ell=m=2$ EOB waveform is characterized by a peak in the modulus and a peak in the frequency $M\omega_{22}^{\rm EOB}$, reproducing the well-known qualitative structure of the NR waveforms, e.g. [159, 168]. In this sense, the complete tidal EOB waveform qualitatively implements "the merger", already at the analytical level, i.e. without NR-tuning. We define the *moment of merger* (in both EOB and NR) as the peak of the amplitude of the $\ell=m=2$ mode of the GW. This is an idealization since the actual merger process takes place during the last few orbits of the coalescence. As shown in Fig. 8.1, the EOB wave frequency $M\omega_{22\,mrg}^{\rm EOB}$ and the binding energy $E_{b\,mrg}^{\rm EOB}$ at the moment of merger are also characterized by a κ_ℓ^T-universality.

8.4 Comparison with NR

The adiabatic tidal EOB analysis captures the relevant qualitative features of the merger dynamics. Specifically, the quasiuniversal properties of $M\Omega$ and E_b close to the EOB LSO hold also for the actual NR merger frequency and binding energy. We stress that we do *not* advocate a formal link between the EOB LSO and NR quantities, but rather give a suggestive argument for the existence of these universal structures.

We performed new NR simulations of coalescing BNS, employing the BAM code and the method described in [168, 169], though: (i) we use the Z4c formulation of Einstein's equations [170]; (ii) GWs are extracted from an extended wavezone [171]. The binaries are equal-mass, irrotational configurations with different EOSs. A $\Gamma=2$ polytropic EOS model is employed to simulate

different compactnesses $C_A = C_B = (0.12, 0.14, 0.16, 0.18)$; EOS MS1, MS1b, H4, ALF2, MPA1, ENG, SLy are employed for simulations with fixed isolation mass $M = 2 \times 1.35 M_\odot$. The evolutions covers about ten orbits up to merger. These are among the longest BNS simulations ever performed, and some of the few where an error analysis is available [122, 162]. For each NR data set, we compute the binding energy per reduced mass, $E_b^{\rm NR}$, subtracting the GW energy loss from the initial ADM mass, following [108, 122, 164]. Here, differently from previous works, all the multipoles are included. GW frequency and binding energy are extracted at the moment of merger. We estimate error bars due to truncation errors and waveform finite extraction uncertainties from resolution tests for fewer configurations. More details on these simulations will be given elsewhere.

Recently, Ref. [159] proposed a phenomenological linear relation between the log of $M\omega_{22\,mrg}^{\rm NR}$ and the quantity $\Lambda^{1/5} = (\frac{2}{3}k_2)^{1/5}C^{-1} = (\frac{16}{3}\kappa_2^T(q=1))^{1/5}$ inspecting an independent sample of equal-mass, irrotational NR waveforms for six different EOS. We believe the effectiveness of that empirical fit is explained by the κ_ℓ^T-universality.

The NR GW frequency $M\omega_{22\,mrg}^{\rm NR}$ and binding energy $E_{b\,mrg}^{\rm NR}$ at the moment of merger are plotted as functions of κ_2^T in Fig. 8.1. The fit of [159] complements our numerical data, with which is perfectly consistent. As indicated by the figure, the NR points are compatible with the κ_ℓ^T-universality. Similarly to the EOB quantities, the NR data can be fitted to rational polynomials. We constrain the fit to the "black-hole limit" by factoring out the values $E_{b\,mrg}^{\rm NR}(\kappa_\ell^T = 0) \approx -0.120$ and $M\omega_{22\,mrg}^{\rm NR}(\kappa_\ell^T = 0) \approx 0.360$ as given by equal-mass binary black hole simulations [108]. The fitting fuction is $f(\kappa) = f(0)(1+n_1\kappa+n_2\kappa^2)/(1+d_1\kappa)$, with $(n_1, n_2, d_1) = (2.59\cdot10^{-2}, -1.28\cdot10^{-5}, 7.49\cdot10^{-2})$ for the frequency and $(n_1, n_2, d_1) = (2.62\cdot10^{-2}, -6.32\cdot10^{-6}, 6.18\cdot10^{-2})$ for the binding energy. Considering $E_b(\kappa)$ and $M\omega_{22}(\kappa)$ as a parametric curve, one obtains a relation between the binding energy and the frequency at the moment of merger that is essentially linear,

$$E_{b\,mrg}^{\rm NR} \approx -0.284\, M\omega_{22\,mrg}^{\rm NR} - 0.0182\,, \tag{8.2}$$

with $M\omega_{22\,mrg}^{\rm NR} \in [0.1, 0.360]$. Also in this case the black hole limit is incorporated in the fit. Quantitatively, there are differences between the NR merger quantities $(M\omega_{22\,mrg}^{\rm NR}, E_{b\,mrg}^{\rm NR})$, and the corresponding EOB ones, $(M\omega_{22\,mrg}^{\rm EOB}, E_{b\,mrg}^{\rm EOB})$, see Fig. 8.1. The relative difference on the relevant interval $\kappa_2^T \in [50, 350]$ is between $20-30\%$ for the frequency and $10-20\%$ for the binding energy. This quantitative disagreement is not surprising: hydrodynamics effects and nonlinear tidal interactions are not modeled in $A^T(u)$. At an effective level, the (uncalibrated) EOB 4PN tidal dynamics basically underestimates attractive effects and gives a larger (smaller) frequency (binding energy) at merger. Coincidentally, the adiabatic EOB LSO gives a rather good numerical approximation, especially for $\kappa_2^T \gtrsim 200$. The key, remarkable point here is that the adiabatic model already captures the κ_ℓ^T-universality, indicating the latter emerges fundamentally from the conservative dynamics. Furthermore, the simple LSO analysis gives reasonable estimates of merger relations for any EOS, mass ratio and (aligned) spins!

8.5 Outlook

Modeling GWs from neutron star mergers is a challenging open problem (see e.g., [172] for very recent work) that can be tackled interfacing accurate nonlinear simulations with the EOB analytical framework. While pursuing this approach we have identified κ_ℓ^T as fundamental "coupling constants" of the binary tidal interactions, together with κ^T-universal relations and their physical origin. Extension of the present work needs more multi-orbit and precise NR simulation

including, in particular, spins [164]. Future work will be devoted to explore effective extensions of the nonadiabatic EOB model, e.g., the use of flexibility parameters or different resummations of A^T [166]. Ultimately, a NR-tuned tidal EOB model is expected to deliver accurate merger waveforms for BNS GW detection, similar to the black hole binary case [90, 91].

The κ^T-universality has consequences for GW astronomy. For example, using EOB-based merger templates (containing the characteristic peak) in match filtered searches one might be able to accurately extract the value of κ_2^T from the template's peak [139]. A single measure of the frequency at the moment of merger would thus constrain both the EOS and the binding energy. The actual possibility to pursue this strategy deserves a study on its own. In this respect, the κ^T-universality characterizing the merger has similarities with the findings of [152] and with the universal relations found for single neutron star properties [173]. Also, we propose to use the value of the merger frequency, as given by our fits, to mark the end of inspiral templates; this will improve the simple Schwarzschild LSO criterion, e.g. [160]. Interestingly, due to the coincidental "compensation" of finite mass effects in the tidally dominated regime, the Schwarzschild LSO values give very good estimates to the GW frequency and binding energy at BNS merger for irrotational binaries with $\kappa_2^T \sim 200$.

Acknowledgments

We thank B. Brügmann, T. Damour, C. Van den Broeck for useful comments. This work was supported in part by DFG grant SFB/Transregio 7 "Gravitational Wave Astronomy" and the Graduiertenakademie Jena. S.B. and Si.B. thank IHES for hospitality during the development of part of this work. Si.B. is supported by the Swiss National Science Foundation. M.U. is supported by CAPES under BEX 10208/12-7, and thanks TPI Jena for hospitality during the development of this work. Simulation were performed on the LRZ cluster in Münich.

CHAPTER 9

Conclusions

The Arnowitt-Deser-Misner (ADM) formalism provides a powerful framework for describing the dynamics of General Relativity. Following its prescriptions, the gauge-freedom due to diffeomophism covariance can be constrained, leading for instance to a 3+1 splitting of spacetime, where a class of spacelike surfaces, as well as a time direction, are selected to describe the dynamics. The result is an Hamiltonian expressed in terms of a minimal set of phase-space variables. For what concerns the general relativistic two-body problem, both matter and spin degrees of freedom can be described as canonical variables within the ADM formalism. The current knowledge of the post-Newtonian (PN) expanded ADM Hamiltonian has reached the 4PN order for what concerns the orbital dynamics, the 3.5PN order (NNLO) for the spin-orbit coupling and the 3PN order (NLO) for the spin-spin coupling.

The knowledge of high-order relativistic effects in the two-body dynamics is crucial for gravitational wave detection prospects. Past work has shown that, to this purpose, the Effective-One-Body approach is the most efficient way to incorporate PN results. In the EOB formalism, PN terms are transformed according to suitable canonical transformations, and then resummed in a new Hamiltonian. The most notable features are i) an analytical formulation of the dynamics which is much more simple than in the PN-expanded case; but especially ii) the capability of building accurate complete waveforms (thus beyond the reach of PN theory), in particular when the model is completed with some parameters that are calibrated with Numerical Relativity waveforms.

Building on already existing EOB Hamiltonians for spinning black holes, we have proposed two different ways to include the NLO spin-spin coupling into the EOB. In the first method (Chapters 4 and 5), the proposal is that of introducing a subleading-order modification of the spin variables. In particular, for arbitrarily oriented spins, it is necessary to distinguish between different combinations of the spin with the phase space variables, and to introduce a different subleading-order modification for each of them. This procedure, although intuitively quite natural, leads to an EOB Hamiltonian with some unwished features. As a first thing, the Damour-Jaranowski-Schäfer gauge could not be imposed, which means that the NLO spin-spin inclusion does not reduces to a momentum-independent potential in the most simple (and most important) case of aligned spins and circular orbits. More generally, the momentum depency of the (NLO modified) effective spin squared makes the EOB Hamiltonian a very complicated function of the momenta,

which are resummed in non-polynomial structures. This is a clear worsening with respect to the previous EOB Hamiltonian without NLO spin-spin terms, whose quasi-geodesic character had the nice property of making the squared effective orbital Hamiltonian a polynomial (and quadratic, with the only exception of a quartic 3PN term) function of the momenta. Despite these problems, the inclusion proposed here also highlights a notable ability of the EOB in reproducing the NLO spin-spin terms. In particular, the 25 independent coefficients defining the NLO spin-spin Hamiltonian in ADM coordinates are reduced to only 12 EOB coefficients.

The second way to include the NLO spin-spin coupling overcomes the problems discussed above. Here, the idea was rather that of isolating different sectors inside of the EOB Hamiltonian, according to their dependency on the momenta. As a result, four forms quadratic in the spins had to be inserted into an appropriate sector. In particular, this procedure did not destroy the simple momentum dependency of the effective Hamiltonain. Furthermore, it was possible to impose a Damour-Jaranowski-Schäfer-type gauge, and more specifically, in accordance with the EOB philosophy, all circular-orbits terms could be collected into the radial potential $A(u, \nu, a_1, a_2)$. This allows, for instance, to understand that NLO spin-spin effects are essentially repulsive (apart from special configurations of aligned, or nearly anti-aligned spins), and lead to a $\sim 5\%$ change in the energy of circular orbits. Finally, an additional "hidden" relation between the coefficients of ADM NLO spin-spin Hamiltonian, that was not explicit in the model of Chapter 6, allowed to further reduce the number of independent parameters from 12 to 9.

As an application of the spinning EOB model, we have also considered, in Chapter 8, the case of spinning neutron star binaries. In particular, we have recognized the dominant role of the tidal coupling constant κ_2^T in the description of tidal effects; this led to quasi-universal properties at the merger, that have been confirmed by Numerical Relativity simulations, and that might be useful to constrain the neutron star's equation of state. However, the inclusion of spin effects introduces a degeneracy in the universality, so that a separate measurement of the spin may be necessary.

We believe that the analytical results of Chapter 6 provide an important starting point for future calibrated EOB models. For instance, the circular-orbits NLO spin-spin terms derived in Chapter 4 have been reformulated and inserted in the calibrated models of Refs. [81, 92], which has proven to be at least as accurate as the "Maryland" EOB model [90]. We shall remark that, however, [92] involves less calibration parameters than [90], where, for instance, the NLO spin-spin coupling is calibrated.

The most urgent prospect for future work may be that of recalibrating the EOB model for circular orbits with the NLO spin-spin inclusion as proposed in Chapter 6. The next step would be an extension of the whole EOB model to the case of precessing spins. In view of this, we notice that a strategy for evaluating precessing waveforms in an EOB framework has been recently elaborated by Pan *et al* [80]. Moreover, EFT calculations are expected to derive soon NNLO spin-spin effects [55]. It would be interesting to verify whether the ideas developed in Chapter 6 can be extended to the next level of accuracy in the spin-spin sector.

The synergy between EOB and Numerical Relativity is currently the most powerful method for generating complete waveform templates. We are confident that the EOB will be at the forefront of research when the doors of gravitational wave astronomy will finally be disclosed.

References

[1] A. Einstein, *Ideas and Opinions*. Carl Seelig ed., 1954.

[2] A. Einstein, "Über Gravitationswellen," *Sitzungsberichte der Königlich Preußischen Akademie der Wissenschaften (Berlin)*, pp. 154–167, 1918.

[3] M. Maggiore, *Gravitational Waves. Volume 1: Theory and experiments*. Oxford University Press, 2008.

[4] A. Buonanno, Y. Pan, H. P. Pfeiffer, M. A. Scheel, L. T. Buchman, and L. E. Kidder, "Effective-one-body waveforms calibrated to numerical relativity simulations: Coalescence of non-spinning, equal-mass black holes," *Phys. Rev. D*, vol. 79, p. 124028, Jun 2009.

[5] T. Bogdanović, C. S. Reynolds, and M. C. Miller, "Alignment of the spins of supermassive black holes prior to coalescence," *The Astrophysical Journal Letters*, vol. 661, no. 2, p. L147, 2007.

[6] C. Reisswig, S. Husa, L. Rezzolla, E. N. Dorband, D. Pollney, and J. Seiler, "Gravitational-wave detectability of equal-mass black-hole binaries with aligned spins," *Phys. Rev. D*, vol. 80, p. 124026, Dec 2009.

[7] A. Einstein, L. Infeld, and B. Hoffmann, "The Gravitational equations and the problem of motion," *Annals Math.*, vol. 39, pp. 65–100, 1938.

[8] R. A. Hulse and J. H. Taylor, "Discovery of a pulsar in a binary system," *Astrophys. J.*, vol. 195, pp. L51–L53, 1975.

[9] T. Damour and N. Deruelle, "Radiation Reaction and Angular Momentum Loss in Small Angle Gravitational Scattering," *Phys. Lett.*, vol. A87, p. 81, 1981.

[10] P. Jaranowski and G. Schäfer, "Third post-newtonian higher order adm hamilton dynamics for two-body point-mass systems," *Phys. Rev. D*, vol. 57, pp. 7274–7291, Jun 1998.

[11] L. Blanchet and G. Faye, "General relativistic dynamics of compact binaries at the third postNewtonian order," *Phys. Rev. D*, vol. 63, p. 062005, 2001.

[12] T. Damour, P. Jaranowski, and G. Schaefer, "Poincare invariance in the ADM Hamiltonian approach to the general relativistic two-body problem," *Phys. Rev. D*, vol. 62, p. 021501, 2000. [Erratum: Phys. Rev.D63,029903(2001)].

[13] T. Damour, P. Jaranowski, and G. Schaefer, "Dimensional regularization of the gravitational interaction of point masses," *Phys. Lett.*, vol. B513, pp. 147–155, 2001.

[14] P. Jaranowski and G. Schäfer, "Dimensional regularization of local singularities in the fourth post-newtonian two-point-mass hamiltonian," *Phys. Rev. D*, vol. 87, p. 081503, Apr 2013.

[15] T. Damour, P. Jaranowski, and G. Schäfer, "Nonlocal-in-time action for the fourth post-newtonian conservative dynamics of two-body systems," *Phys. Rev. D*, vol. 89, p. 064058, Mar 2014.

[16] R. L. Arnowitt, S. Deser, and C. W. Misner, "The Dynamics of general relativity," *Gen. Rel. Grav.*, vol. 40, pp. 1997–2027, 2008.

[17] T. Regge and C. Teitelboim, "Role of Surface Integrals in the Hamiltonian Formulation of General Relativity," *Annals Phys.*, vol. 88, p. 286, 1974.

[18] R. L. Arnowitt, S. Deser, and C. W. Misner, "Canonical variables for general relativity," *Phys. Rev.*, vol. 117, pp. 1595–1602, 1960.

[19] J. Steinhoff, "Canonical formulation of spin in general relativity," *Annalen Phys.*, vol. 523, pp. 296–353, 2011.

[20] G. Schäfer, "The general relativistic two-body problem. Theory and experiment," in *Symposia Gaussiana, Proc. 2nd Gauss Symposium, Conf. A: Mathematical and Theoretical Physics, Munich, 1993*, pp. 667–679, 1995.

[21] L. Blanchet and G. Faye, "Hadamard regularization," *J. Math. Phys.*, vol. 41, pp. 7675–7714, 2000.

[22] T. Damour, P. Jaranowski, and G. Schäfer, "Hamiltonian of two spinning compact bodies with next-to-leading order gravitational spin-orbit coupling," *Phys. Rev. D*, vol. 77, p. 064032, Mar 2008.

[23] M. Mathisson, "Neue mechanik materieller systemes," *Acta Phys. Polon.*, vol. 6, pp. 163–2900, 1937.

[24] A. Papapetrou, "Spinning test particles in general relativity. 1.," *Proc. Roy. Soc. Lond.*, vol. A209, pp. 248–258, 1951.

[25] F. A. E. Pirani, "On the Physical significance of the Riemann tensor," *Acta Phys. Polon.*, vol. 15, pp. 389–405, 1956. [Gen. Rel. Grav.41,1215(2009)].

[26] W. M. Tulczyjew, "Equations of motion of rotating bodies in general relativity theory," *Acta Phys. Polon.*, vol. 18, p. 393, 1959.

[27] W. G. Dixon, "A covariant multipole formalism for extended test bodies in general relativity," *Nuovo Cim.*, vol. 34, no. 2, pp. 317–339, 1964.

[28] B. M. Barker, S. N. Gupta, and R. D. Haracz, "One-Graviton Exchange Interaction of Elementary Particles," *Phys. Rev.*, vol. 149, pp. 1027–1032, 1966.

[29] B. M. Barker and R. F. O'Connell, "Derivation of the equations of motion of a gyroscope from the quantum theory of gravitation," *Phys. Rev. D*, vol. 2, pp. 1428–1435, 1970.

[30] B. M. Barker and R. F. O'Connell, "Gravitational Two-Body Problem with Arbitrary Masses, Spins, and Quadrupole Moments," *Phys. Rev. D*, vol. 12, pp. 329–335, 1975.

[31] B. M. Barker and R. F. O'Connell, "The gravitational interaction: Spin, rotation, and quantum effects - a review," *Gen. Relativ. Gravit.*, vol. 11, pp. 149–175, 1979.

[32] P. D. D'Eath, "Interaction of two black holes in the slow-motion limit," *Phys. Rev. D*, vol. 12, pp. 2183–2199, 1975.

[33] G. Faye, L. Blanchet, and A. Buonanno, "Higher-order spin effects in the dynamics of compact binaries. i. equations of motion," *Phys. Rev. D*, vol. 74, p. 104033, Nov 2006.

[34] L. Blanchet, A. Buonanno, and G. Faye, "Higher-order spin effects in the dynamics of compact binaries. II. Radiation field," *Phys. Rev. D*, vol. 74, p. 104034, 2006. [Erratum: Phys. Rev.D81,089901(2010)].

[35] J. Steinhoff, G. Schäfer, and S. Hergt, "Adm canonical formalism for gravitating spinning objects," *Phys. Rev. D*, vol. 77, p. 104018, May 2008.

[36] J. Steinhoff and G. Schaefer, "Canonical formulation of self-gravitating spinning-object systems," *Europhys. Lett.*, vol. 87, p. 50004, 2009.

[37] J. Hartung and J. Steinhoff, "Next-to-next-to-leading order post-Newtonian spin-orbit Hamiltonian for self-gravitating binaries," *Annalen Phys.*, vol. 523, pp. 783–790, 2011.

[38] W. D. Goldberger and I. Z. Rothstein, "Effective field theory of gravity for extended objects," *Phys. Rev. D*, vol. 73, p. 104029, May 2006.

[39] R. A. Porto, "Next to leading order spin-orbit effects in the motion of inspiralling compact binaries," *Class. Quant. Grav.*, vol. 27, p. 205001, 2010.

[40] M. Levi, "Next to Leading Order gravitational Spin-Orbit coupling in an Effective Field Theory approach," *Phys. Rev. D*, vol. 82, p. 104004, 2010.

[41] D. L. Perrodin, "Subleading Spin-Orbit Correction to the Newtonian Potential in Effective Field Theory Formalism," in *On recent developments in theoretical and experimental general relativity, astrophysics and relativistic field theories. Proceedings, 12th Marcel Grossmann Meeting on General Relativity, Paris, France, July 12-18, 2009. Vol. 1-3*, pp. 725–727, 2010.

[42] M. Levi and J. Steinhoff, "Spinning gravitating objects in the effective field theory in the post-Newtonian scheme," 2015.

[43] M. Levi and J. Steinhoff, "Next-to-next-to-leading order gravitational spin-orbit coupling via the effective field theory for spinning objects in the post-Newtonian scheme," 2015.

[44] R. A. Porto, "Post-Newtonian corrections to the motion of spinning bodies in NRGR," *Phys. Rev. D*, vol. 73, p. 104031, 2006.

[45] R. A. Porto and I. Z. Rothstein, "The Hyperfine Einstein-Infeld-Hoffmann potential," *Phys. Rev. Lett.*, vol. 97, p. 021101, 2006.

[46] R. A. Porto and I. Z. Rothstein, "Spin(1)Spin(2) Effects in the Motion of Inspiralling Compact Binaries at Third Order in the Post-Newtonian Expansion," *Phys. Rev. D*, vol. 78, p. 044012, 2008. [Erratum: Phys. Rev.D81,029904(2010)].

[47] R. A. Porto and I. Z. Rothstein, "Next to Leading Order Spin(1)Spin(1) Effects in the Motion of Inspiralling Compact Binaries," *Phys. Rev. D*, vol. 78, p. 044013, 2008. [Erratum: Phys. Rev.D81,029905(2010)].

[48] S. Hergt and G. Schaefer, "Higher-order-in-spin interaction Hamiltonians for binary black holes from Poincare invariance," *Phys. Rev. D*, vol. 78, p. 124004, 2008.

[49] J. Steinhoff, S. Hergt, and G. Schäfer, "Spin-squared hamiltonian of next-to-leading order gravitational interaction," *Phys. Rev. D*, vol. 78, p. 101503, Nov 2008.

[50] J. Steinhoff, S. Hergt, and G. Schäfer, "Next-to-leading order gravitational spin(1)-spin(2) dynamics in hamiltonian form," *Phys. Rev. D*, vol. 77, p. 081501, Apr 2008.

[51] R. A. Porto and I. Z. Rothstein, "Comment on 'On the next-to-leading order gravitational spin(1) - spin(2) dynamics' by J. Steinhoff et al," 2007.

[52] S. Hergt, J. Steinhoff, and G. Schaefer, "On the comparison of results regarding the post-Newtonian approximate treatment of the dynamics of extended spinning compact binaries," *J. Phys. Conf. Ser.*, vol. 484, p. 012018, 2014.

[53] S. Hergt, J. Steinhoff, and G. Schaefer, "Reduced Hamiltonian for next-to-leading order Spin-Squared Dynamics of General Compact Binaries," *Class. Quant. Grav.*, vol. 27, p. 135007, 2010.

[54] M. Levi, "Binary dynamics from spin1-spin2 coupling at fourth post-newtonian order," *Phys. Rev. D*, vol. 85, p. 064043, Mar 2012.

[55] M. Levi and J. Steinhoff, "Next-to-next-to-leading order gravitational spin-squared potential via the effective field theory for spinning objects in the post-Newtonian scheme," 2015.

[56] M. Levi and J. Steinhoff, "Equivalence of ADM Hamiltonian and Effective Field Theory approaches at next-to-next-to-leading order spin1-spin2 coupling of binary inspirals," *J. Cosmol. Astropart. Phys.*, vol. 12, p. 003, 2014.

[57] N. Straumann, *General Relativity*. Graduate Text in Physics, Springer Netherlands, 2013.

[58] J. Ehlers and E. Rudolph, "Dynamics of extended bodies in general relativity center-of-mass description and quasirigidity," *General Relativity and Gravitation*, vol. 8, no. 3, pp. 197–217, 1977.

[59] W. G. Dixon, "Dynamics of extended bodies in general relativity. I. Momentum and angular momentum," *Proc. Roy. Soc. Lond.*, vol. A314, pp. 499–527, 1970.

[60] W. G. Dixon, "Dynamics of extended bodies in general relativity. II. Moments of the charge-current vector," *Proc. Roy. Soc. Lond.*, vol. A319, pp. 509–547, 1970.

[61] J. Steinhoff and D. Puetzfeld, "Multipolar equations of motion for extended test bodies in General Relativity," *Phys. Rev. D*, vol. 81, p. 044019, 2010.

[62] M. H. L. Pryce, "The Mass center in the restricted theory of relativity and its connection with the quantum theory of elementary particles," *Proc. Roy. Soc. Lond.*, vol. A195, pp. 62–81, 1948.

[63] S. Weinberg, *The Quantum Theory of Fields, Volume 1: Foundations*. Cambridge University Press, 2005.

[64] A. Nagar, "Effective one-body hamiltonian of two spinning black holes with next-to-next-to-leading order spin-orbit coupling," *Phys. Rev. D*, vol. 84, p. 084028, Oct 2011.

[65] A. Buonanno and T. Damour, "Effective one-body approach to general relativistic two-body dynamics," *Phys. Rev. D*, vol. 59, p. 084006, Mar 1999.

[66] A. Buonanno and T. Damour, "Transition from inspiral to plunge in binary black hole coalescences," *Phys. Rev. D*, vol. 62, p. 064015, Aug 2000.

[67] T. Damour, P. Jaranowski, and G. Schäfer, "Determination of the last stable orbit for circular general relativistic binaries at the third post-newtonian approximation," *Phys. Rev. D*, vol. 62, p. 084011, Sep 2000.

[68] T. Damour, "Coalescence of two spinning black holes: An effective one-body approach," *Phys. Rev. D*, vol. 64, p. 124013, Nov 2001.

[69] A. Buonanno, Y. Chen, and T. Damour, "Transition from inspiral to plunge in precessing binaries of spinning black holes," *Phys. Rev. D*, vol. 74, p. 104005, Nov 2006.

[70] T. Damour, P. Jaranowski, and G. Schäfer, "Effective one body approach to the dynamics of two spinning black holes with next-to-leading order spin-orbit coupling," *Phys. Rev. D*, vol. 78, p. 024009, Jul 2008.

[71] T. Damour and A. Nagar, "Final spin of a coalescing black-hole binary: An effective-one-body approach," *Phys. Rev. D*, vol. 76, p. 044003, Aug 2007.

[72] T. Damour and A. Nagar, "Improved analytical description of inspiralling and coalescing black-hole binaries," *Phys. Rev. D*, vol. 79, p. 081503, Apr 2009.

[73] T. Damour, B. R. Iyer, and A. Nagar, "Improved resummation of post-newtonian multipolar waveforms from circularized compact binaries," *Phys. Rev. D*, vol. 79, p. 064004, Mar 2009.

[74] E. Barausse, E. Racine, and A. Buonanno, "Hamiltonian of a spinning test particle in curved spacetime," *Phys. Rev. D*, vol. 80, p. 104025, Nov 2009.

[75] E. Barausse and A. Buonanno, "Improved effective-one-body hamiltonian for spinning black-hole binaries," *Phys. Rev. D*, vol. 81, p. 084024, Apr 2010.

[76] Y. Pan, A. Buonanno, R. Fujita, E. Racine, and H. Tagoshi, "Post-newtonian factorized multipolar waveforms for spinning, nonprecessing black-hole binaries," *Phys. Rev. D*, vol. 83, p. 064003, Mar 2011.

[77] E. Barausse and A. Buonanno, "Extending the effective-one-body hamiltonian of black-hole binaries to include next-to-next-to-leading spin-orbit couplings," *Phys. Rev. D*, vol. 84, p. 104027, Nov 2011.

[78] D. Bini and T. Damour, "Gravitational radiation reaction along general orbits in the effective one-body formalism," *Phys. Rev. D*, vol. 86, p. 124012, Dec 2012.

[79] D. Bini and T. Damour, "Analytical determination of the two-body gravitational interaction potential at the fourth post-newtonian approximation," *Phys. Rev. D*, vol. 87, p. 121501, Jun 2013.

[80] Y. Pan, A. Buonanno, A. Taracchini, L. E. Kidder, A. H. Mroué, H. P. Pfeiffer, M. A. Scheel, and B. Szilágyi, "Inspiral-merger-ringdown waveforms of spinning, precessing black-hole binaries in the effective-one-body formalism," *Phys. Rev. D*, vol. 89, p. 084006, Apr 2014.

[81] T. Damour and A. Nagar, "New effective-one-body description of coalescing nonprecessing spinning black-hole binaries," *Phys. Rev. D*, vol. 90, p. 044018, Aug 2014.

[82] T. Damour and A. Nagar, "Faithful effective-one-body waveforms of small-mass-ratio coalescing black hole binaries," *Phys. Rev. D*, vol. 76, p. 064028, Sep 2007.

[83] T. Damour, A. Nagar, M. Hannam, S. Husa, and B. Brügmann, "Accurate effective-one-body waveforms of inspiralling and coalescing black-hole binaries," *Phys. Rev. D*, vol. 78, p. 044039, Aug 2008.

[84] T. Damour and A. Nagar, "Comparing effective-one-body gravitational waveforms to accurate numerical data," *Phys. Rev. D*, vol. 77, p. 024043, Jan 2008.

[85] T. Damour, A. Nagar, E. N. Dorband, D. Pollney, and L. Rezzolla, "Faithful effective-one-body waveforms of equal-mass coalescing black-hole binaries," *Phys. Rev. D*, vol. 77, p. 084017, Apr 2008.

[86] A. Buonanno, Y. Pan, H. P. Pfeiffer, M. A. Scheel, L. T. Buchman, and L. E. Kidder, "Effective-one-body waveforms calibrated to numerical relativity simulations: Coalescence of nonspinning, equal-mass black holes," *Phys. Rev. D*, vol. 79, p. 124028, Jun 2009.

[87] Y. Pan, A. Buonanno, L. T. Buchman, T. Chu, L. E. Kidder, H. P. Pfeiffer, and M. A. Scheel, "Effective-one-body waveforms calibrated to numerical relativity simulations: Coalescence of nonprecessing, spinning, equal-mass black holes," *Phys. Rev. D*, vol. 81, p. 084041, Apr 2010.

[88] Y. Pan, A. Buonanno, M. Boyle, L. T. Buchman, L. E. Kidder, H. P. Pfeiffer, and M. A. Scheel, "Inspiral-merger-ringdown multipolar waveforms of nonspinning black-hole binaries using the effective-one-body formalism," *Phys. Rev. D*, vol. 84, p. 124052, Dec 2011.

[89] A. Taracchini, Y. Pan, A. Buonanno, E. Barausse, M. Boyle, T. Chu, G. Lovelace, H. P. Pfeiffer, and M. A. Scheel, "Prototype effective-one-body model for nonprecessing spinning inspiral-merger-ringdown waveforms," *Phys. Rev. D*, vol. 86, p. 024011, Jul 2012.

[90] A. Taracchini, A. Buonanno, Y. Pan, T. Hinderer, M. Boyle, D. A. Hemberger, L. E. Kidder, G. Lovelace, A. H. Mroué, H. P. Pfeiffer, M. A. Scheel, B. Szilágyi, N. W. Taylor, and A. Zenginoglu, "Effective-one-body model for black-hole binaries with generic mass ratios and spins," *Phys. Rev. D*, vol. 89, p. 061502, Mar 2014.

[91] T. Damour, A. Nagar, and S. Bernuzzi, "Improved effective-one-body description of coalescing nonspinning black-hole binaries and its numerical-relativity completion," *Phys. Rev. D*, vol. 87, p. 084035, Apr 2013.

[92] T. Damour and A. Nagar, "New effective-one-body description of coalescing nonprecessing spinning black-hole binaries," *Phys. Rev. D*, vol. 90, p. 044018, Aug 2014.

[93] C. Huwyler, A. Klein, and P. Jetzer, "Testing general relativity with lisa including spin precession and higher harmonics in the waveform," *Phys. Rev. D*, vol. 86, p. 084028, Oct 2012.

[94] P. R. Brady, J. D. E. Creighton, and K. S. Thorne, "Computing the merger of black hole binaries: The IBBH problem," *Phys. Rev. D*, vol. 58, p. 061501, 1998.

[95] F. Pretorius, "Evolution of binary black hole spacetimes," *Phys. Rev. Lett.*, vol. 95, p. 121101, 2005.

[96] M. Campanelli, C. O. Lousto, P. Marronetti, and Y. Zlochower, "Accurate evolutions of orbiting black-hole binaries without excision," *Phys. Rev. Lett.*, vol. 96, p. 111101, 2006.

[97] J. G. Baker, J. Centrella, D.-I. Choi, M. Koppitz, and J. van Meter, "Gravitational wave extraction from an inspiraling configuration of merging black holes," *Phys. Rev. Lett.*, vol. 96, p. 111102, 2006.

[98] `http://www.black-holes.org/waveforms`.

[99] T. Damour and G. Schaefer, "Higher Order Relativistic Periastron Advances and Binary Pulsars," *Nuovo Cim. B*, vol. 101, p. 127, 1988.

[100] T. Damour, "Gravitational self-force in a schwarzschild background and the effective one-body formalism," *Phys. Rev. D*, vol. 81, p. 024017, Jan 2010.

[101] L. Blanchet, S. Detweiler, A. Le Tiec, and B. F. Whiting, "High-order post-newtonian fit of the gravitational self-force for circular orbits in the schwarzschild geometry," *Phys. Rev. D*, vol. 81, p. 084033, Apr 2010.

[102] E. Barausse, A. Buonanno, and A. Le Tiec, "Complete nonspinning effective-one-body metric at linear order in the mass ratio," *Phys. Rev. D*, vol. 85, p. 064010, Mar 2012.

[103] T. Damour, B. R. Iyer, and B. S. Sathyaprakash, "Improved filters for gravitational waves from inspiraling compact binaries," *Phys. Rev. D*, vol. 57, pp. 885–907, Jan 1998.

[104] A. Nagar, T. Damour, and A. Tartaglia, "Binary black hole merger in the extreme mass ratio limit," *Class. Quant. Grav.*, vol. 24, pp. S109–S124, 2007.

[105] T. Damour and A. Gopakumar, "Gravitational recoil during binary black hole coalescence using the effective one body approach," *Phys. Rev. D*, vol. 73, p. 124006, Jun 2006.

[106] T. Damour and B. R. Iyer, "Multipole analysis for electromagnetism and linearized gravity with irreducible cartesian tensors," *Phys. Rev. D*, vol. 43, pp. 3259–3272, May 1991.

[107] A. Nagar and S. Akcay, "Horizon-absorbed energy flux in circularized, nonspinning black-hole binaries, and its effective-one-body representation," *Phys. Rev. D*, vol. 85, p. 044025, Feb 2012.

[108] T. Damour, A. Nagar, D. Pollney, and C. Reisswig, "Energy versus angular momentum in black hole binaries," *Phys. Rev. Lett.*, vol. 108, p. 131101, Mar 2012.

[109] L. T. Buchman, H. P. Pfeiffer, M. A. Scheel, and B. Szilágyi, "Simulations of unequal-mass black hole binaries with spectral methods," *Phys. Rev. D*, vol. 86, p. 084033, Oct 2012.

[110] B. Carter, "Global structure of the kerr family of gravitational fields," *Phys. Rev.*, vol. 174, pp. 1559–1571, Oct 1968.

[111] D. C. Wilkins, "Bound geodesics in the kerr metric," *Phys. Rev. D*, vol. 5, pp. 814–822, Feb 1972.

[112] S. A. Hughes, "Evolution of circular, nonequatorial orbits of kerr black holes due to gravitational-wave emission," *Phys. Rev. D*, vol. 61, p. 084004, Mar 2000.

[113] K. S. Thorne, "Multipole Expansions of Gravitational Radiation," *Rev. Mod. Phys.*, vol. 52, pp. 299–339, 1980.

[114] D. Bini and T. Damour, "Two-body gravitational spin-orbit interaction at linear order in the mass ratio," *Phys. Rev. D*, vol. 90, p. 024039, Jul 2014.

[115] S. Balmelli and P. Jetzer, "Effective-one-body hamiltonian with next-to-leading order spin-spin coupling for two nonprecessing black holes with aligned spins," *Phys. Rev. D*, vol. 87, p. 124036, Jun 2013. [Erratum: Phys. Rev.D90,no.8,089905(2014)].

[116] L. E. Kidder, "Using full information when computing modes of post-Newtonian waveforms from inspiralling compact binaries in circular orbit," *Phys. Rev. D*, vol. 77, p. 044016, 2008.

[117] L. Blanchet, G. Faye, B. R. Iyer, and S. Sinha, "The Third post-Newtonian gravitational wave polarisations and associated spherical harmonic modes for inspiralling compact binaries in quasi-circular orbits," *Class. Quant. Grav.*, vol. 25, p. 165003, 2008. [Erratum: Class. Quant. Grav.29,239501(2012)].

[118] P. Amaro-Seoane, S. Aoudia, S. Babak, P. Binétruy, E. Berti, A. Bohé, C. Caprini, M. Colpi, N. J. Cornish, K. Danzmann, J.-F. çois Dufaux, J. Gair, O. Jennrich, P. Jetzer, A. Klein, R. N. Lang, A. Lobo, T. Littenberg, S. T. McWilliams, G. Nelemans, A. Petiteau, E. K. Porter, B. F. Schutz, A. Sesana, R. Stebbins, T. Sumner, M. Vallisneri, S. Vitale, M. Volonteri, and H. Ward, "Low-frequency gravitational-wave science with elisa/ngo," *Classical Quantum Gravity*, vol. 29, no. 12, p. 124016, 2012.

[119] G. M. Harry and the LIGO Scientific Collaboration, "Advanced ligo: the next generation of gravitational wave detectors," *Classical Quantum Gravity*, vol. 27, no. 8, p. 084006, 2010.

[120] T. Damour and A. Nagar, "The effective one body description of the two-body problem," *Fundam. Theor. Phys.*, vol. 162, p. 211, 2011.

[121] T. Damour, "The general relativistic two body problem and the effective one body formalism." Dec 2012.

[122] S. Bernuzzi, A. Nagar, M. Thierfelder, and B. Brügmann, "Tidal effects in binary neutron star coalescence," *Phys. Rev. D*, vol. 86, p. 044030, Aug 2012.

[123] M. Levi, "Next-to-leading order gravitational spin1-spin2 coupling with kaluza-klein reduction," *Phys. Rev. D*, vol. 82, p. 064029, Sep 2010.

[124] J. Hartung and J. Steinhoff, "Next-to-next-to-leading order post-newtonian spin(1)-spin(2) hamiltonian for self-gravitating binaries," *Annalen Phys.*, vol. 523, p. 919, 2011.

[125] M. Tessmer, J. Hartung, and G. Schäfer, "Motion and gravitational wave forms of eccentric compact binaries with orbital-angular-momentum-aligned spins under next-to-leading order in spin-orbit and leading order in spin(1)-spin(2) and spin-squared couplings," *Class. Quant. Grav.*, vol. 27, p. 165005, 2010.

[126] J. Aasi *et al.*, "Prospects for Localization of Gravitational Wave Transients by the Advanced LIGO and Advanced Virgo Observatories," 2013.

[127] S. Vitale, "Space-borne gravitational wave observatories," *Gen. Relativ. Gravit.*, vol. 46, 2014.

[128] P. A. Seoane *et al.*, "The Gravitational Universe," 2013.

[129] G. Lovelace, M. Boyle, M. A. Scheel, and B. Szilagyi, "Accurate gravitational waveforms for binary-black-hole mergers with nearly extremal spins," *Classical Quantum Gravity*, vol. 29, p. 045003, 2012.

[130] A. Mroué, M. Scheel, B. Szilágyi, H. Pfeiffer, M. Boyle, D. Hemberger, L. Kidder, G. Lovelace, S. Ossokine, N. Taylor, A. i. e. i. f. Zenginoğlu, L. Buchman, T. Chu, E. Foley, M. Giesler, R. Owen, and S. Teukolsky, "Catalog of 174 binary black hole simulations for gravitational wave astronomy," *Phys. Rev. Lett.*, vol. 111, p. 241104, Dec 2013.

[131] I. Hinder *et al.*, "Error-analysis and comparison to analytical models of numerical waveforms produced by the nrar collaboration," *Classical Quantum Gravity*, vol. 31, p. 025012, 2014.

[132] T. Damour, E. Gourgoulhon, and P. Grandclément, "Circular orbits of corotating binary black holes: Comparison between analytical and numerical results," *Phys. Rev. D*, vol. 66, p. 024007, Jun 2002.

[133] A. Buonanno, Y. Chen, and M. Vallisneri, "Detecting gravitational waves from precessing binaries of spinning compact objects: Adiabatic limit," *Phys. Rev. D*, vol. 67, p. 104025, May 2003.

[134] A. Buonanno, G. B. Cook, and F. Pretorius, "Inspiral, merger, and ring-down of equal-mass black-hole binaries," *Phys. Rev. D*, vol. 75, p. 124018, Jun 2007.

[135] A. Buonanno, Y. Pan, J. G. Baker, J. Centrella, B. J. Kelly, S. T. McWilliams, and J. R. van Meter, "Approaching faithful templates for nonspinning binary black holes using the effective-one-body approach," *Phys. Rev. D*, vol. 76, p. 104049, Nov 2007.

[136] `http://www.ego-gw.it/`.

[137] J. Aasi *et al.*, "Advanced LIGO," *Class. Quant. Grav.*, vol. 32, p. 074001, 2015.

[138] S. Balmelli and P. Jetzer, "Effective-one-body hamiltonian with next-to-leading order spin-spin coupling," *Phys. Rev. D*, vol. 91, p. 064011, Mar 2015.

[139] T. Damour, A. Nagar, and L. Villain, "Measurability of the tidal polarizability of neutron stars in late-inspiral gravitational-wave signals," *Phys. Rev. D*, vol. 85, p. 123007, Jun 2012.

[140] S. Bernuzzi, T. Dietrich, W. Tichy, and B. Brügmann, "Mergers of binary neutron stars with realistic spin," *Phys. Rev. D*, vol. 89, no. 10, p. 104021, 2014.

[141] D. Radice, L. Rezzolla, and F. Galeazzi, "High-Order Numerical-Relativity Simulations of Binary Neutron Stars," 2015.

[142] T. Dietrich, S. Bernuzzi, M. Ujevic, and B. Brügmann, "Numerical relativity simulations of neutron star merger remnants using conservative mesh refinement," *Phys. Rev. D*, vol. 91, no. 12, p. 124041, 2015.

[143] T. Dietrich, N. Moldenhauer, N. K. Johnson-McDaniel, S. Bernuzzi, C. M. Markakis, B. Brügmann, and W. Tichy, "Binary Neutron Stars with Generic Spin, Eccentricity, Mass ratio, and Compactness - Quasi-equilibrium Sequences and First Evolutions," 2015.

[144] K. Barkett *et al.*, "Gravitational waveforms for neutron star binaries from binary black hole simulations," 2015.

[145] S. Bernuzzi, A. Nagar, T. Dietrich, and T. Damour, "Modeling the Dynamics of Tidally Interacting Binary Neutron Stars up to the Merger," *Phys. Rev. Lett.*, vol. 114, no. 16, p. 161103, 2015.

[146] S. Bernuzzi, A. Nagar, S. Balmelli, T. Dietrich, and M. Ujevic, "Quasiuniversal properties of neutron star mergers," *Phys. Rev. Lett.*, vol. 112, p. 201101, May 2014.

[147] R. C. Tolman, "Static solutions of einstein's field equations for spheres of fluid," *Phys. Rev.*, vol. 55, pp. 364–373, Feb 1939.

[148] J. R. Oppenheimer and G. M. Volkoff, "On massive neutron cores," *Phys. Rev.*, vol. 55, pp. 374–381, Feb 1939.

[149] E. Chabanat, P. Bonche, P. Haensel, J. Meyer, and R. Schaeffer, "A Skyrme parametrization from subnuclear to neutron star densities. 2. Nuclei far from stablities," *Nucl. Phys.*, vol. A635, pp. 231–256, 1998.

[150] P. B. Demorest, T. Pennucci, S. M. Ransom, M. S. E. Roberts, and J. W. T. Hessels, "A two-solar-mass neutron star measured using shapiro delay," *Nature*, vol. 467, pp. 1081–1083, 10 2010.

[151] J. Antoniadis, P. C. C. Freire, and N. e. a. Wex, "A massive pulsar in a compact relativistic binary," *Science*, vol. 340, no. 6131, 2013.

[152] A. Bauswein and H.-T. Janka, "Measuring neutron-star properties via gravitational waves from binary mergers," *Phys. Rev. Lett.*, vol. 108, p. 011101, 2012.

[153] T. Damour and A. Nagar, "Relativistic tidal properties of neutron stars," *Phys. Rev. D*, vol. 80, p. 084035, Oct 2009.

[154] T. Binnington and E. Poisson, "Relativistic theory of tidal love numbers," *Phys. Rev. D*, vol. 80, p. 084018, Oct 2009.

[155] T. Damour, M. Soffel, and C. Xu, "General-relativistic celestial mechanics. i. method and definition of reference systems," *Phys. Rev. D*, vol. 43, pp. 3273–3307, May 1991.

[156] T. Damour and A. Nagar, "Effective one body description of tidal effects in inspiralling compact binaries," *Phys. Rev. D*, vol. 81, p. 084016, Apr 2010.

[157] J. Abadie *et al.*, "Predictions for the Rates of Compact Binary Coalescences Observable by Ground-based Gravitational-wave Detectors," *Classical Quantum Gravity*, vol. 27, p. 173001, 2010.

[158] J. S. Read, C. Markakis, M. Shibata, K. Uryu, J. D. Creighton, *et al.*, "Measuring the neutron star equation of state with gravitational wave observations," *Phys.Rev. D*, vol. 79, p. 124033, 2009.

[159] J. S. Read, L. Baiotti, J. D. E. Creighton, J. L. Friedman, B. Giacomazzo, K. Kyutoku, C. Markakis, L. Rezzolla, M. Shibata, and K. Taniguchi, "Matter effects on binary neutron star waveforms," *Phys. Rev. D*, vol. 88, p. 044042, Aug 2013.

[160] W. Del Pozzo, T. G. F. Li, M. Agathos, C. Van Den Broeck, and S. Vitale, "Demonstrating the feasibility of probing the neutron-star equation of state with second-generation gravitational-wave detectors," *Phys. Rev. Lett.*, vol. 111, p. 071101, Aug 2013.

[161] L. Baiotti, T. Damour, B. Giacomazzo, A. Nagar, and L. Rezzolla, "Analytic modeling of tidal effects in the relativistic inspiral of binary neutron stars," *Phys. Rev. Lett.*, vol. 105, p. 261101, Dec 2010.

[162] S. Bernuzzi, M. Thierfelder, and B. Brügmann, "Accuracy of numerical relativity waveforms from binary neutron star mergers and their comparison with post-Newtonian waveforms," *Phys. Rev. D*, vol. 85, p. 104030, 2012.

[163] K. Hotokezaka, K. Kyutoku, and M. Shibata, "Exploring tidal effects of coalescing binary neutron stars in numerical relativity," *Phys. Rev. D*, vol. 87, no. 4, p. 044001, 2013.

[164] S. Bernuzzi, T. Dietrich, W. Tichy, and B. Brügmann, "Mergers of binary neutron stars with realistic spin," *Phys. Rev. D*, vol. 89, no. 10, p. 104021, 2014.

[165] L. Blanchet, "Gravitational radiation from post-Newtonian sources and inspiralling compact binaries," *Living Rev. Rel.*, vol. 9, p. 4, 2006.

[166] D. Bini, T. Damour, and G. Faye, "Effective action approach to higher-order relativistic tidal interactions in binary systems and their effective one body description," *Phys. Rev. D*, vol. 85, p. 124034, 2012.

[167] L. Barack, T. Damour, and N. Sago, "Precession effect of the gravitational self-force in a Schwarzschild spacetime and the effective one-body formalism," *Phys. Rev. D*, vol. 82, p. 084036, 2010.

[168] M. Thierfelder, S. Bernuzzi, and B. Brügmann, "Numerical relativity simulations of binary neutron stars," *Phys.Rev. D*, vol. 84, p. 044012, 2011.

[169] B. Brügmann, J. A. Gonzalez, M. Hannam, S. Husa, U. Sperhake, *et al.*, "Calibration of Moving Puncture Simulations," *Phys. Rev. D*, vol. 77, p. 024027, 2008.

[170] S. Bernuzzi and D. Hilditch, "Constraint violation in free evolution schemes: Comparing BSSNOK with a conformal decomposition of Z4," *Phys. Rev. D*, vol. 81, p. 084003, 2010.

[171] D. Hilditch, S. Bernuzzi, M. Thierfelder, Z. Cao, W. Tichy, *et al.*, "Compact binary evolutions with the Z4c formulation," *Phys. Rev. D*, vol. 88, p. 084057, 2013.

[172] L. Wade, J. D. E. Creighton, E. Ochsner, B. D. Lackey, B. F. Farr, T. B. Littenberg, and V. Raymond, "Systematic and statistical errors in a bayesian approach to the estimation of the neutron-star equation of state using advanced gravitational wave detectors," *Phys. Rev. D*, vol. 89, no. 10, p. 103012, 2014.

[173] K. Yagi and N. Yunes, "I-Love-Q," *Science*, vol. 341, pp. 365–368, 2013.